

RETURNING MATERIALS:
Place in book drop to remove this checkout from your record. FINES will be charged if book is returned after the date stamped below.

# EVALUATION OF NOVEL AND EXISTING IONIZATION METHODS FOR COMPLEX MIXTURE ANALYSIS

by

Daniel B. Kassel

Submitted to

Michigan State University
in partial fulfillment of the requirements
for the degree of

**DOCTOR OF PHILOSOPHY** 

Department of Chemistry

1988

#### ABSTRACT

# EVALUATION OF NOVEL AND EXISTING IONIZATION METHODS FOR COMPLEX MIXTURE ANALYSIS

by

#### Daniel B. Kassel

A number of existing and novel ionization methods are evaluated as to their utility for enhancing the type and quantity of information that can be derived for the analysis of mixtures when used in conjunction with conventional mass spectrometric methods. Mixtures of organic acids isolated from urine are targeted for such analyses. A new desorption/ionization method, K<sup>+</sup> ionization of desorbed species (K<sup>+</sup>IDS), is shown to be an attractive method for analyses of these complex mixtures and is useful for differentiating between various disease states and healthy conditions, without the need for extensive work-up of physiological samples and gas chromatographic analysis. K<sup>+</sup>IDS is based on thermionic emission of alkali materials for the production of gas phase alkali ions. Adduct ion formation occurs as the species being analyzed is rapidly heated and desorbed into the gas phase. A dual filament K<sup>+</sup>IDS probe is described which has replaced a single-filament design and has led to a 30-40 fold improvement in sensitivity of the technique. Furthermore, the implementation of this design has resulted in better quantitative representations of complex mixtures of those compounds considered marginally volatile. Chemical ionization mass spectrometry (CIMS) using ammonia as

` ` } the reagent gas is evaluated as to its capacity for providing quantitative information for the analysis of complex mixtures of organic acids. This technique is found to be superior to conventional electron impact (EI) ionization for experiments involving the use of stable-isotope tracers to study various aspects of metabolism. Feasibility experiments are performed using stable-isotope tracers for a means of differentiating between disease-states that are clinically indistinguishable. A novel ionization method based on carbon tetrachloride pretreatment for electron capture negative ion mass spectrometry is described. The technique involves reactions that take place on ion source surfaces to generate free radical intermediates that exhibit very high cross-sections for electron attachment. Lower limits of detection are observed for several classes of compounds when this ionization method is employed. The production of molecular adduct ions having unique isotopic patterns allows for unequivocable determinations of molecular weights of unknowns and adduct ion formation is found not to be competitive with lowenergy fragmentation pathways observed under conventional electron capture-negative ion conditions.

In memory of my father, Fred L. Kassel, whose spirit continues to guide me towards excellence in clinical chemistry and all that I pursue in life.

#### **ACKNOWLEDGMENTS**

It has been a long, but truly enjoyable four and half years spent at Michigan State University in pursuit of my Ph.D. degree. Joe, Bob, and Mark, you guys have been truly great friends. How could I ever forget the sunglasses and scarf incident in our first term of analytical chemistry, late nights at PT O'Malleys, tubing, pre-games with are famous concoction, and of course, the Froggers! These times I will always remember, even the unpleasant ones, such as being buried by an avalanche of snow following my initiation to skiing at Crystal Mtn.!

I owe a great deal of thanks to members of the mass spectrometry facility (Brian, Mike, Mel, and Doug) for all their help and suggestions. Special thanks go to the members of both the Allison and Wastson groups. The commaraderie that existed in the laboratory made being in the chemistry building that much more pleasant. Karen and Kathleen, "old faithful" is now solely in your hands. Keep on milking it for everything its worth. I wish you both most successful careers in chemistry. Gary, what can I say. You've been a real good friend. Remember, Boston is only a short distance away (short enough even for week-end trips!). Jim, I'll never forget the trip to Florida, Dukbo, and the eye-opening experiences. Of course, I can't forget the kindness of all the graduate office personnel! To Val, Kelly, Anna, and Ellen, thanks for the friendship, conversation, lemon drops, and use of the copier.

My scientific development in the past years has been a result of the guidance and inspiration of my mentors and colleagues. I give a lot of credit to David Pinkston, whom I respect tremendously as a person and chemist, and of whom I have tried to model my graduate studies career. To my mentor John Allison, for whom I have the

utmost repect and admiration as both a person and and research advisor, I cannot thank enough. I attribute much of my growth as a scientist to your tremendous support and encouragement, the insightful discussions that we have had, and the confidence you have had in me. I will always be grateful for these things, and am hopeful that our paths will cross in the future. Dr. Watson, you have shown a lot of confidence in my abilities and for that I am grateful. I have enjoyed greatly my association with you and have learned much from you, not the least of which, the ability to write scientific documents. I appreciate your encouragement, and I hope my association with one of your mentors will be as fruitful for me as it was for you. Dr. Sweeley, you have been an incredible inspiration to me and I only hope that I can achieve as much success as you in bioanalytical chemistry. I honestly hope that we can, in the future, continue to collaborate on projects of mutual interest. I have learned a great deal from you and look forward to keeping in contact.

Most importantly, I am grateful to my family (Mom, J-Lo, Deb, and Paul) for all their encouragement, support, understanding, friendship, and love. The relationship that I have developed with my family over the past years is deeply cherished. It is ironic that the loss of a loved one is often the necessary energy for creating such strong bonds between family members. I hope the relationship between my family and its members continues to grow, and that success and happiness comes in all their endeavers.

# **TABLE OF CONTENTS**

	Page
List of Tables	x.
List of Figures	xi.
List of Schemes	xviii.
Chapter 1: Complex Mixture Analysi	is 1
Introduction	2
Metabolic profiling	
Chapter 2: Desorption/Ionization (DI)	and K <sup>+</sup> IDS Theory14
K <sup>+</sup> IDS theory	
Operative mechanism of l	K <sup>+</sup> IDS22
Experimental consideratio	ns24
Initial results utilizing K <sup>+</sup> ID	S for mixture analysis29
Chapter 3: A Novel DI method, K <sup>+</sup> IDS,	for the Rapid Screening of Urine for Organic
Acidemias	44
Introduction	44
Experimental	47

	Results of mixture analysis utilizing "dual-filament" probe	49
	K <sup>+</sup> IDS for urinary organic acid profiling	54
	Conclusions	68
Chapter 4:	Extension of the Utility and Applications of K <sup>+</sup> IDS	75
	Organic synthesis on K <sup>+</sup> IDS emitter surface	76
	K <sup>+</sup> IDS analyses of cardiac glycosides	86
	Utility of K <sup>+</sup> IDS for peptide mapping	91
	Future studies utilizing strengths of K <sup>+</sup> IDS	10
	Final comments of K <sup>+</sup> IDS	14
Chapter 5:	Chemical Ionization Theory 1	15
•	Chemical ionization mass spectrometry (CIMS) 1	
	Quantitative mixture analysis using CIMS	
	Results of quantitative metabolic profiling analysis using CIMS 1	
	Experimental1	
	Results and Discussion1	
Chapter 6:	Utilizing Ammonia-CI for Stable-Isotope Tracer Studies	65
Cp.o.	Introduction1	
	Isotope-ratio and isotope-dilution mass spectrometry 1	
	Investigation of Call Matcheliam Union Labelled Classes	7-
Chapter 7:	Investigation of Cell Metabolism Using Labelled Glucose	
	Introduction	
	Experimental	78

1	Results and Discussion	180
•	Conclusions	199
Chapter 8:	ECNI-MS with CCl <sub>4</sub> "pretreatment"	203
1	Introduction	203
	A novel ionization method for ECNI mass spectrometry	206
1	Experimental	207
1	Results and discussion on simple mixtures	209
Final Rer	marks	213
Appendix 1	<b>:</b>	216
	"Utility and Limitations of Electron Ionization and Chemical Ionization for the Determination of Position and Extent of	
	Labelling for <sup>18</sup> O-and <sup>13</sup> C- Containing Permethylated Alditols by Gas Chomatography Mass Spectrometry"	216
	"Urinary Metabolites of L-Threonine in Type 1 Diabetes Determined by Combined Gas Chromatography Chemical Ionization Mass Spectrometry"	222
	"Utility of Ion Source Pretreatment with Chlorine-Containing Compounds for Enhanced Performance in Gas Chromatography Negative Ionization Mass Spectrometry"	228
Appendix 2	: Table of molecular weights of unknowns determined from ammonia  CI and electron impact ionization	
Deference	•	260

# LIST OF TABLES

Table 1.	Twenty-five most abundant organic acids in MSUD urine identified from GC and GC-MS analyses55
Table 2.	Major organic acid metabolites identified from GC-MS data for (a) lactic acidemia, (b) isovaleric acidemia, (c) healthy; and (d) methylmalonic acidemia urines
Table 3.	Comparison of relative intensities from Na <sup>+</sup> IDS analysis and peak areas from GC analysis for the ten most abundant organic acids in methylmalonic urine
Table 4.	Fragments produce from protonated linear peptides (I) upon undergoing collisionally activated dissociation (CAD)-MS-MS95
Table 5.	List of structures, formulae, molecular weights and retention indeces for components of synthetic organic acid mixture
Table 6.	Comparison between actual concentrations of several two and three component organic acid mixtures with integrated peak areas obtained from GC-(NH <sub>3</sub> -CI)-MS and GC-EI-MS analyses
Table 7.	Comparison of integrated areas from EI and NH <sub>3</sub> -CI analyses on an eleven component organic acid mixture. Actual concentrations are shown in the lower half of this table
Table 8.	Identified metabolites of both cell fibroblasts and cell medium. Peak number 43-glutamic acid. Peak number 47-unknown (MW=437), believed to be a five-carbon aminoribose sugar
Table 9:	13C-Enrichment observed into various metabolite pools from fibroblast cells and cell medium for (a) Cytochrome oxidase, (b) Pyruvate Dehydrogenase, and (c) control lines
Table 10:	Fragment ions observed and number of trimethylsilyl groups associated with each fragment from the electron impact ionization mass spectrum of the d <sub>9</sub> -TMS and d <sub>0</sub> -TMS derivatives of Unknown (MW=437) 194 x.

# **LIST OF FIGURES**

Figure 1.	Two-dimensional graphical representation of the metabolic status of an individual from paper chromatographic analysis6
Figure 2.	Procedures for carrying out the isolation and derivatization of urinary organic acids for analysis by GC-MS10
Figure 3.	70 eV EI-MS mass spectrum of 2-hydroxyisovaleric acid (di-TMS) 12
Figure 4.	Thermodynamic considerations for alkali ion emission20
Figure 5.	Proposed mechanism for adduct ion formation of desorbing species, ABCD, from alkali aluminosilicate surface23
Figure 6.	Modified direct insertion probe (DIP) for use as a thermionic emitter for K <sup>+</sup> IDS analyses
Figure 7.	Schematic diagram of emission current power supply
Figure 8.	"Typical" K <sup>+</sup> IDS tuning file depicting K <sup>+</sup> ion abundance
Figure 9.	Na <sup>+</sup> IDS mass spectrum of five common organic acids (underivatized) 32
Figure 10.	K <sup>+</sup> IDS averaged mass spectrum of a 5:1:1:1 mixture of C-12, C-14, C-15, and C-16 free fatty acids; operating current, I, = 3.0 A
Figure 11.	$K^{+}IDS$ mass spectrum of same fatty acid mixture obtained at $I = 4.0 A 36$
Figure 12.	Analyte desorption and alkali ion emission profiles vs. time utilizing a single-filament K <sup>+</sup> IDS probe
Figure 13.	Selected ion monitoring (SIM) comparison of methyl stearate (400 ng) using (a) single-filament and (b) dual-filament K <sup>+</sup> IDS probe

Figure 14.	Detection limits for methyl stearate by K <sup>+</sup> IDS using dual-filament probe41
Figure 15.	Analyte desorption and alkali ion emission profiles vs. time utilizing a
	dual-filament K <sup>+</sup> IDS probe43
Figure 16.	Modified dual-filament K <sup>+</sup> IDS Probe (P). Filament 1 (F1) is electrically heated using resistive wire (W) and is the alkali ion emitter. Filament 2 (F2) is the analyte filament and solely experiences radiative heating
Figure 17.	Total ion current (TIC) profile (upper insert) and K <sup>+</sup> IDS mass spectrum of myristic acid (CH <sub>3</sub> (CH <sub>2</sub> ) <sub>12</sub> CO <sub>2</sub> H)51
Figure 18.	Na <sup>+</sup> IDS mass spectrum of an equimolar mixture of C-12, C-13, C-14, C-16, and C-17 free fatty acids
Figure 19.	Na <sup>+</sup> IDS averaged mass spectrum of a complex mixture of organic acids, fatty acids, and steroids analyzed simultaneously
Figure 20.	Simulated Na <sup>+</sup> IDS molecular weight profile of the 25 most abundant organic acids present in urine of a patient with Maple Syrup Urine Disease (MSUD)
Figure 21.	Experimentally obtained Na <sup>+</sup> IDS averaged mass spectra of organic acids from same patient with MSUD
Figure 22.	Averaged Na <sup>+</sup> IDS mass spectra of organic acids from (a) healthy, (b) lactic acidosis, and (c) isovaleric acidemia urines
Figure 23.	TIC profile of the trimethylsilyl derivatives of organic acids isolated from isovaleric acidemia urine
Figure 24.	Simulated Na <sup>+</sup> IDS molecular weight profile of the 25 most abundant organic acids present in urine of patient with isovaleric acidemia65
Figure 25.	Averaged Na <sup>+</sup> IDS mass spectra of urinary organic acids isolated from patient with methylmalonic acidemia67

Figure 26.	TIC profile of trimethylsilyl derivatives of organic acids isolated from a second methylmalonic urine70
Figure 27.	Averaged Na <sup>+</sup> IDS mass spectra of the underivatized organic acids from the same methylmalonic acidemia urine71
Figure 28.	K <sup>+</sup> IDS analyte TIC desorption profiles of C-12, -13, -14, -16, -17 fatty acids generated by K <sup>+</sup> IDS from a "contaminated" filament surface. Peak 1-free fatty acids; peak 2- fatty acid salts
Figure 29.	Averaged K <sup>+</sup> IDS mass spectra of the fatty acid mixture from (a) scan 19 of analyte desortption profile 1 and (b) scan 29 of analyte desortption profile 2
Figure 30.	$K^{+}IDS$ TIC analyte desorption profiles for stearic acid (10 $\mu$ g) obtained at (a) I= 3.1 A, (b) I = 3.55 A, and (c) I = 3.8 A
Figure 31.	Three-dimensional mass spectra of the two analyte desorption profiles for stearic acid. Mass axis from 280-380 u; scan axis = 35-8083
Figure 32.	Structure and assignment of major ions from thermal decomposition fragments of digitonin
Figure 33.	K <sup>+</sup> IDS mass spectrum of digitonin
Figure 34.	K <sup>+</sup> IDS mass spectrum of (a) digoxin and (b) assignment of ions formed from thermal decompostion fragments91
Figure 35.	Fast atom bombardment (FAB) mass spectrum of leucine-enkephalin in glycerol
Figure 36.	FAB MS-MS collisionally activated dissociation (CAD) mass spectrum of leucine-enkephalin
Figure 37.	Structure and possible thermal decomposition fragments for leucine- enkephalin arising from a Na <sup>+</sup> IDS analysis99
Figure 38.	Na <sup>+</sup> IDS mass spectrum of Leucine-Enkephalin

Figure 39.	Structure and possible thermal decomposition fragments for methionine-
	enkephalin arising from a Na <sup>+</sup> IDS analysis 103
Figure 40.	Na <sup>+</sup> IDS mass spectrum of methionine-enkephalin 104
Figure 41.	Structure and possible thermal decomposition fragments for the octa-peptide (Val-His-Leu-Thr-Pro-Val-Glu-Lys) arising from a Na <sup>+</sup> IDS analysis106
Figure 42.	Na <sup>+</sup> IDS mass spectrum of Val-His-Leu-Thr-Pro-Val-Glu-Lys107
Figure 43.	Cs <sup>+</sup> IDS mass spectrum of PPG 425 obtained on the JEOL HX-100 HRMS
Figure 44.	(a) FAB mass spectrum and (b) "Na <sup>+</sup> IDS by FAB" mass spectrum of arachidonic acid
Figure 45.	"K <sup>+</sup> IDS by FAB" mass spectrum of glycerol obtained using a split fab probe tip
Figure 46.	Methane-CI mass spectrum of 2-hydroxyisobutyric acid (di-TMS) 119
Figure 47.	Relationship of P(E) and k(E) for unimolecular decomposition120
Figure 48.	Distribution of internal energy in protonated analyte molecule following exothermic proton transfer
Figure 49.	Chemical ionization mass spectra of ammonia obtained at various ion source pressures
Figure 50.	Plot of ion source pressure vs. relative intensities of pseudo-molecular ions for 2-hydroxyisobutyric acid (di-TMS)
Figure 51.	SIM of p-hydroxybenzoic acid (di-TMS) comparing sensitivity obtained at optimum ion source pressure using (a) ammonia and (b) methane 137
Figure 52.	Comparison of true CI ion source pressure vs. source housing

Figure 53.	"Typical" chemical ionization tuning file using perfluorotributylamine
	(PFTBA) as the standard calibrant; m/z 69, (CF <sub>3</sub> <sup>+</sup> ); m/z 219 (C <sub>4</sub> F <sub>9</sub> <sup>+</sup> ); m/z
	414 (C <sub>8</sub> F <sub>16</sub> N <sup>+</sup> )142
Figure 54.	Effect CI ion source pressure has on overall sensitivity for (a) phydroxybenzoic acid (di-TMS), and (b) Maleic acid (di-TMS), m/z 261 (MH <sup>+</sup> ); m/z 278 (MNH <sub>4</sub> <sup>+</sup> )
Figure 55.	NH <sub>3</sub> -CI mass spectrum of (a) m-hydroxybenzoic acid (di-TMS) and (b) p-hydroxybenzoic acid (di-TMS)
Figure 56.	Dependence of fragment ions and abundances of 2-hydroxyisobutyric acid (di-TMS) on methane ion source pressure146
Figure 57.	Flow chart representing scheme for determining the quantitative strengths of NH <sub>3</sub> -CI relative to EI-MS149
Figure 58.	Comparison of quantitative strengths of EI and NH <sub>3</sub> -CI for the analysis of 2-hydroxyisobutyric and glycolic acids. (a) Reconstructed mass chromatograms showing isobaric ion interference for EI, and (b) comparison of NH <sub>3</sub> -CI and 70 eV EI mass spectra
Figure 59.	TIC profiles of the trimethylsilyl derivatives of an organic acid synthetic mixture obtained by (a) GC-EI-MS and (b) GC-(NH <sub>3</sub> -CI)-MS 156
Figure 60.	Comparison of TIC profiles of a mixture containing maleic acid (di- TMS) using NH <sub>3</sub> -CI at (a) P <sub>NH<sub>3</sub></sub> = 200, and (b) P <sub>NH<sub>3</sub></sub> = 320 mtorr 159
Figure 61.	Comparison of TIC profiles of derivatized urinary organic acids from a diabetic dog obtained using (a) NH <sub>3</sub> -CI, and (b) EI ionization 161
Figure 62.	Repeat analyses on urinary organic acids by NH <sub>3</sub> -CI demonstrating eproducibility from one run to another
Figure 63.	TIC profile for naturally occurring amino acids in a diabetic dog plasma obtained by (a) NH <sub>3</sub> -CI, (b) EI, and (c) electron-capture negative ion (ECNI) mass spectrometry

Figure 64.	Scheme for the clinical and biochemical investigation of patients with suspected congenital lactic acidoses
Figure 65.	GC-EI-MS TIC profiles of metabolites found in (a) control, (b) cytochrome oxidase deficient, and (c) pyruvate dehydrogenase deficient fibroblast cells
Figure 66.	GC-EI-MS TIC profiles of metabolites excreted into (a) control, (b) cytochrome oxidase (CytOx) deficient, and (c) pyruvate dehydrogenase (PDH) deficient cell medium
Figure 67.	NH <sub>3</sub> -CI mass spectrum of glucose (penta-TMS) obtained at the onset of pulse-labelling. Isotope enrichment observed at m/z 564 (MNH <sub>4</sub> <sup>+</sup> ) 186
Figure 68.	NH <sub>3</sub> -CI mass spectrum of lactic acid (di-TMS) from control fibroblasts collected during the pulse-labelling period189
Figure 69.	Plot of <sup>13</sup> C-enrichment vs. collection time for lactic acid in control, Cytochrome Oxidase, and PDH fibroblast cells190
Figure 70.	NH <sub>3</sub> -CI mass spectrum of glutamic acid from (a) cytochrome oxidase, and (b) pyruvate dehydrogenase fibroblasts192
Figure 71.	Plot of <sup>13</sup> C-enrichment vs. collection time for glutamic acid in control, CytOx, and PDH fibroblast cells
Figure 72.	Proposed structure and fragment ions for unknown (MW =437) presumed to be an aminoribose sugar metabolite
Figure 73.	Plot of <sup>13</sup> C-enrichment vs. collection time for Unknown (MW =437) in control, CytOx, and PDH fibroblast cells
Figure 74.	TIC profile of the trimethylsilyl derivatives of a synthetic mixture of organic acids obtained using (a) EI-MS, (b) conventional ECNI-MS, and (c) carbon tetrachloride "pretreatment" prior to ECNI analysis

Figure 75.	Comparison of TIC profiles of an equimolar mixture of three fatty	acid
	methyl esters, (C-14, C-16, and C-18) obtained using (a) convention	onal
	ECNI-MS, and (b) ECNI-MS following ion source pretreatment v	with
	CCl <sub>4</sub>	212
	4	

# **LIST OF SCHEMES**

Scheme	1	••••••	89
Scheme	2		96
Scheme	3		100
Scheme	4		121
Scheme	5		185

### Chapter 1: Complex Mixture Analysis

#### Introduction:

The ability to accurately characterize complex biological mixtures, both qualitatively and quantitatively, has been a problem which has plagued both chemists and biochemists for years. Numerous approaches to achieving these results have been attempted, perhaps the most widely used analytical approach being that of chromatography.

As early as 1951, analytical methods such as paper chromatography were used to separate complex mixtures of biological origin. With the advent of high performance liquid chromatography (HPLC) and gas-liquid chromatography (GLC), the scope of many biomedical and biochemical studies requiring mixture analysis expanded. The choice of the chromatographic technique was governed by the complexity and type(s) of compounds contained within the mixture. HPLC offered the advantage of the direct analysis of polar non-volatile samples. Analyses of relatively simple mixtures utilizing HPLC were shown to be readily achieved. However, for more complex mixtures, such as those of biological origin, HPLC analyses were often hindered by less than adequate chromatographic resolution than could be achieved. Furthermore, successful combinations of this technique with other analytical methods, such as mass spectrometry, are still being evaluated and in the developmental stage. Difficulties are still encountered in achieving the optimum interface for such a combination. Gas chromatography, on the otherhand, has made tremendous advances in the past two decades, specifically in the area of enhanced column chromatography performance as a result of the introduction of capillary

•

column technology. Even with the tremendous resolving capabilities of narrow bore capillary columns, shortcomings still were evident with these methods when used alone for accurate characterization of complex mixtures. Since identification of unknowns relied on the availability of chromatographic libraries (which contain accurate retention times, retention indices, etc.), identification of compounds not contained within these libraries was impossible. Introduction of a variety of gas chromatographic detectors (e.g., thermionic (TID), thermal conductivity (TCD), etc.) frequently simplified mixture analysis by demonstrating selective responses for specific compound classes, yet were limited in that data for identifying unknowns was not available.

However, not until 1956, when Morrel et al. <sup>2</sup> demonstrated the potential power of combining gas chromatography with mass spectrometry (GC-MS) did the ability to elucidate the identity of unknowns from complex mixtures appear to be possible. Later, in 1971 Horning and Horning<sup>3</sup> showed one of the earliest applications of GC-MS-DS, (DS = data system) for urinary metabolite identification. To date, this combination has proven to be perhaps the most powerful analytical method available for characterizing complex mixtures. Like all analytical methods, though, GC-MS suffers from some drawbacks in its utility as a "universal" method for mixture analysis. Even with "hyphenated" techniques such as these, some prior knowledge of the mixture to be analyzed is required. For thermally unstable and/or nonvolatile compounds, chemical derivatization of the mixture is required prior to analysis by GC and GC-MS. Knowledge of the origin, and/or the principal components of the mixture to be analyzed is thus required such that the most suitable derivatizing agent and appropriate stationary phases can be chosen. Derivatization and work-up procedures can often be tedious. Isolation and derivatization of steroids from urine, for example, require in excess of 24 hours for reactions to go to completion.

Furthermore, GC-MS analysis times can be exceedingly long and data handling and manipulation laborious.

These drawbacks are more than offset, though, by the absolute strengths of this combined technique for the analysis of very complex mixtures, especially those of biological origin which may contain more than 150 components. Even for mixtures as complex as these, GC-MS can accurately provide both quantitative and qualitative information. When the mass spectrometer is operated in the electron impact ionization (EI) mode, the detector simulates closely that of the FID detector, being responsive to all compounds that are introduced into the mass spectrometer in the gas phase. When the mass spectrometer is operated in one of several other modes (e.g., chemical ionization (CI), negative ion CI (NICI), etc.) the detector can now simulate the behaviors of more selective GC detectors, such as the TID, for example, demonstrating selective responses to individual components of the mixture. These added dimensions to the mass spectrometer make it ideal as a detector for the gas chromatograph.

### Metabolic profiling:

This thesis specifically deals with the analysis of complex mixtures of organic acids, and other metabolites isolated from physiological fluids such as urine. Mixtures of organic acids have been chosen for a number of reasons. Mixtures associated with metabolic profiling are truly complex. In physiological fluids such as urine, it is not uncommon to find more than 150 metabolites of varying concentration. Since any one of the metabolites found in the physiological fluids could be of considerable biological significance, it is critical that they be characterized sufficiently, and it is therefore important to have available an appropriate analytical method which will

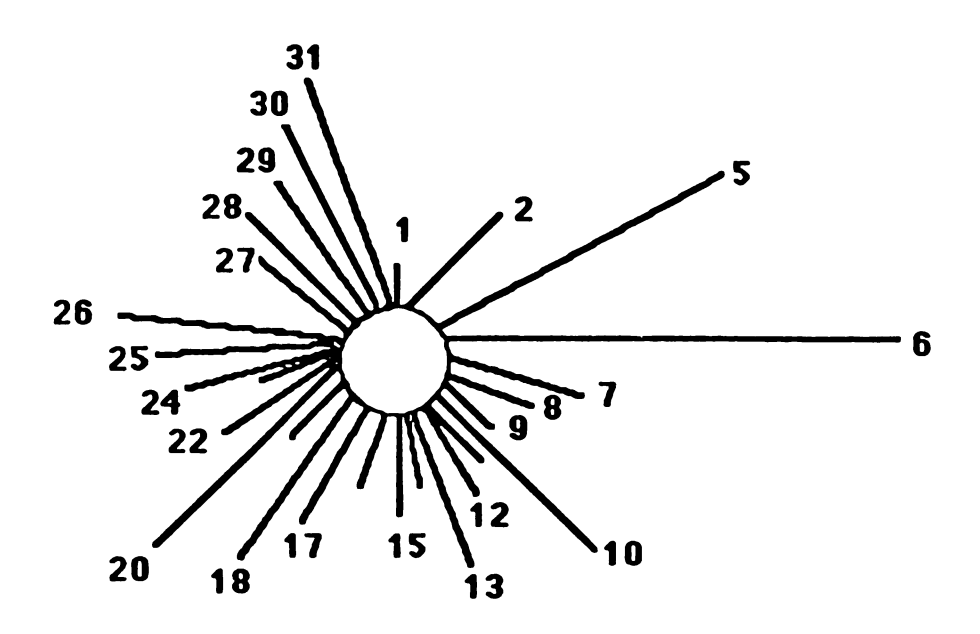
allow for the most extensive qualitative and quantitative analysis of each component contained within the mixture. Most work done in the area of organic acids analysis (in vivo) has been performed using GC-MS with electron impact ionization. A number of limitations are associated with EI yet only very sparse data can be found on alternative ionization approaches for characterizing these complex mixtures, limiting the capabilities of this hyphenated technique to date for metabolic profiling analyses. Attention will be given to this point later in this section. Information about the composition of urinary organic acids from healthy and disease-state patients may reveal insights into various metabolic pathways and possible inborn errors of metabolism. This thesis is in part devoted to the investigation of some known metabolic disorders for the purpose of obtaining a greater amount of information on the relationship of specifically excreted metabolites for healthy and disease-state conditions through the use of stable-isotope tracers and alternative ionization methods, such as GC-CIMS.

These types of analyses collectively fall under the name, or category of metabolic profiling. This term, first coined by Horning and Horning<sup>3</sup> has been given many definitions, but may loosely be defined as the analysis of components of physiological fluids (e.g., plasma, urine) for determining subtle and/or significant differences in the profiles of control (reference) and subject (disease-state) groups, as related to the composition of the particular fluid. This definition is quite general, and encompasses a large number of biochemical applications. As a screening technique, several components of the physiological fluid under study are measured and the concentrations of these measured metabolites are compared to some set of reference ranges of concentrations in which they are normally found. Screening, or multicomponent analysis can often be achieved for mixtures of various physiological metabolites, such as organic acids, steroids, and amino acids, simultaneously.

Metabolic profiling analysis, on the otherhand, involves the measurements of not only the absolute concentrations of individual components. but more importantly the relative relationship of these analytes to one another in a single analysis. In addition, the analytes measured in a profiling analysis are typically metabolically related and analyses are performed on one particular class of compounds such as isolated urinary organic acids. When the goal of analysis is to determine certain relationships between excreted metabolites and specific metabolic pathways, more elegant experiments, such as stable-isotope tracer experiments, are performed in order to determine whether some correlation exists between the administered precursor and some specifically excreted metabolite(s). An excellent review by Sweeley and coworkers describes the recent developments in the area of metabolic profiling.

The earliest graphical representation depicting the metabolic patterns of healthy individuals was developed by Williams<sup>1</sup> shown in Figure 1. The positions of the vectors (labelled 1-31) represented the types of compounds contained within the physiological fluid under investigation; the length of those vectors directly reflected the concentration of the individual components. Gas chromatograms soon became the accepted analytical tool for elucidating differences in the metabolic compositions of "normal" individuals. Horning and Horning<sup>5</sup> demonstrated the enormous power of gas chromatography for the analysis of very complex mixtures of organic acids from urine, and the derivatization procedures required to make this class of compounds amenable to the technique. GC found such wide-spread use in such studies for a number of reasons. The complexity of the number and amounts of several organic acids from a complex medium (such as urine) required a technique which (a) allowed for adequate separation of the compounds in order that identification could be made and (b) a large enough dynamic range such that components which were found in exceedingly low (or high) levels of concentration could be accurately quantified from

the remaining components of the mixture. Flame ionization detection (FID) for GC appeared to yield a sufficiently large dynamic range for the analysis of these types of compounds. In addition, rapid advances in capillary column chromatography made it



Adapted from Williams, R.J. with permission of the author (ref. 1).

Figure 1: Two-dimensional representation of the metabolic status of an individual derived from paper chromatographic analysis.

possible to completely separate greater than 100 organic acids from urine when megabore capillary colums have been employed. More recently, unique methods for characterizing differences between the metabolic patterns of healthy and disease-state individuals have been introduced. Sweeley, et al., have converted the qualitative and quantitative data contained within metabolic profiles into musical frequencies. 7

Intensities of the musical notes generated are correlated with the concentrations of the components of the urine specimen. Subtle differences in metabolic profiles which are difficult to differentiate visually (via gas chromatograms) may be shown to be more easily assessed.

However, it was not until the combination of gas chromatography-mass spectrometry was successfully achieved did the real potential for metabolic profiling analyses become evident. No one technique seems to parallel the enormous strength of this hyphenated technique for such studies. Perhaps this is why so few laboratories enjoy the ability to conduct research in this area, since the cost associated with obtaining GC-MS systems still precludes their wide-spread availability for most hospitals and clinical centers.

Following the breakthrough by Horning, et al.<sup>5</sup>, and one of the first published results utilizing GC-MS-DS for organic acid metabolic profiling analysis by Gates, et al.,<sup>8</sup> several research groups began exploring the possibility of differentiating between healthy and "disease-state" individuals based on either subtle or large differences in their metabolic patterns, as a consequence of some genetic disorder. This has made possible the identification of several inborn errors of metabolism.

Differences in urinary organic acid patterns from one individual to another were assumed to be attributed to differences in the genetic make-up of the various individuals. This was inferred from metabolic profiles obtained from identical twins which were essentially indistinguishable<sup>1</sup>. Advances in molecular biology through the ability to isolate specific enzymes from fibroblasts and determine their activity in "controls" and patients has now proven that a genetic basis exists for these classes of inherent errors of metabolism. Typically, inborn errors of metabolism are manifested in deficiencies in one or more enzymes that regulate carbohydrate, amino acid, lipid,

and/or other biosynthetic pathways. Deficiencies in these enzymes result in accumulation of a number of species, including amino acids in plasma and organic acids in plama and urine. Enzyme deficient individuals are frequently diagnosed based on monitoring for elevated levels of organic acids (relative to references ranges in which the metabolites are normally found) excreted in urine. The identification of these enzyme disorders has led to their classification as the organic acidurias. Organic acids, in addition, have been found to accumulate in amniotic fluid, 9,10 cerebral spinal fluid (CSF), 11 and other fluids. 12,13

Most metabolic profiling studies have involved the analysis of the <u>urinary</u> organic acids using GC-MS. The urinary organic acids are an attractive class of compounds since they are typically excreted in relatively high concentrations in urine, due to their relatively high water solubility and, because urine is a physiological fluid which is readily available and easily obtained. Furthermore, isolation and derivatization procedures required to make mixtures of organic acids amenable to gas phase analysis are relatively straight-forward, not nearly as time-consuming as those procedures required for the isolation and derivatization from other physiological media.

A drawback, however, to urinary organic acid analysis is that this physiological fluid is very much affected by dietary intake, and other factors (e.g., strenuous exercise), which can alter organic acid composition in urine. In some cases, false positives for various organic acidurias can be inferred from the urinary organic acid metabolic profiles assuming no other clinical observations are available. When special care is taken in obtaining urine specimens, however, these problems are sufficiently minimized.

GC-MS has been responsible for the diagnosis of more than 50 heritable disorders of metabolism (i.e., the organic acidurias). 15,16 Lactic acidemia, the most frequently diagnosed organic aciduria, is differentiated from "healthy" and other

"disease-state" conditions based on severely elevated levels of lactic acid in both plasma and urine. A number of enzyme deficiencies have been attributed to the excessive build-up of lactic acid in urine, including partial pyruvate dehydrogenase deficiency, pyruvate carboxylase deficiency, and many others. In fact, over 15 enzyme deficiencies have been correlated with the lactic acidemias alone! <sup>15</sup> Differential diagnosis of these specific enzyme defects has been difficult based on comparison of organic acid profiles.

The procedures required for carrying out urinary organic acid analysis are described in Figure 2. A complete set of isolation procedures and various derivatizing methods may be found in Organic Acids in Man. 17 Bis(trimethylsilyl)trifluoroacetamide (BSTFA)/Pyr (4:1) has been used most frequently for the analysis of organic acids and other components of urine due to the simplicity of the derivatization reaction. BSTFA/Pyr derivatizes carboxylic and hydroxyl moieties to their trimethylsilyl ester and ethers, respectively. Derivatization leads to better thermal stability of the organic acids which is a requirement for gas chromatographic analysiis. Trimethylsilylation also leads to an increase in the molecular weight of the compound, as 72u is added to the molecule for each carboxylic or hydroxyl group that experiences derivatization. This can be a problem when mass spectrometers with limited mass range capabilities are utilized. A number of other derivatizing agents has been employed, including diazomethane, which derivatizes carboxylic groups to the methyl esters, as to effectively offset the sometimes undesirable dramatic increase in the molecular weight that accompanies trimethylsilylation. Following various derivatizing procedures, GC-MS analyses of the urinary organic acids, as stated earlier, are most frequently performed in the EI ionization mode. Since identification of a particular organic aciduria is dependent on the elevated levels of one or more organic acids relative to the "normal range"

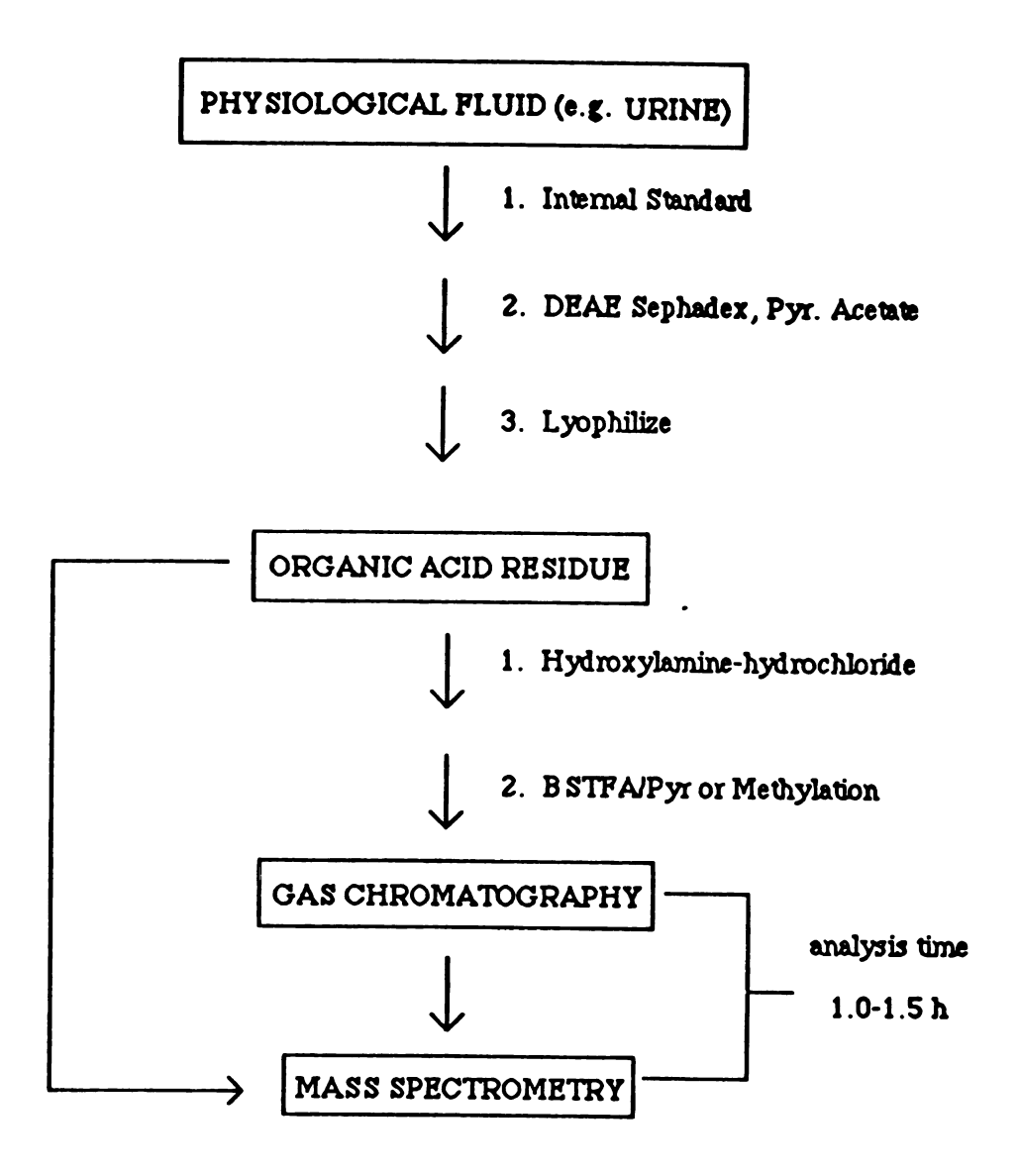


Figure 2. Procedures for carrying out the isolation and derivatization of urinary organic acids for analysis by GC-MS.

concentrations, it is obvious that a a technique which quantitatively represents the components of the mixture be employed. EI-MS has been found to be a quite reproducible and useful method based on its capacity to provide quantitative information from a mixture, due to the fact that ionization cross-sections for most molecules are nearly equivalent by conventional EI. 18 However, there are a number of inherent problems associated with EI-MS which makes this method of analysis often undesirable for specific organic acid profiling applications. The EI mass spectra of the trimethylsilyl (TMS) esters of organic acids are generally dominated by ions that are structurally insignificant. A typical EI mass spectrum of 2-hydroxyisovaleric acid (di-TMS) is shown in Figure 3. The major ions in the mass spectrum, m/z =73 [Si (CH<sub>2</sub>)<sub>3</sub><sup>+</sup>] and m/z = 147 [ (CH<sub>3</sub>)<sub>3</sub> Si - O = Si (CH<sub>3</sub>)<sub>2</sub><sup>+</sup>], are ions associated with the trimethylsilyl derivatizing agent, and are structurally insignificant. Only a very weak ion signal for the pseudo-molecular ion (m/z = 247;  $[M-CH_3^+]$ ) is obtained using electron impact ionization. This behavior is typical for all derivatized organic acids. A second drawback to EI-MS is that the resultant mass spectra are often unnecessarily complex. The capacity for accurately quantifying the components of a mixture becomes exceedingly difficult when the effluent from the gas chromatograph contains coeluting species that are presented to the mass spectrometer and analyzed by conventional EI. In addition, when the goal of the metabolic profiling analysis is to gain insight into specific metabolic pathways, it is generally necessary to perform stable isotope-, or radioisotope-labelled tracer experiments. A known, labelled precursor is administered to the subject under investigation and the flux of label (e.g., <sup>13</sup>C) from that precursor is measured for incorporation into various metabolites. The levels of enrichment observed in various metabolites is typically quite low. As a result, these kinds of experiments require relatively abundant ions that are unique to

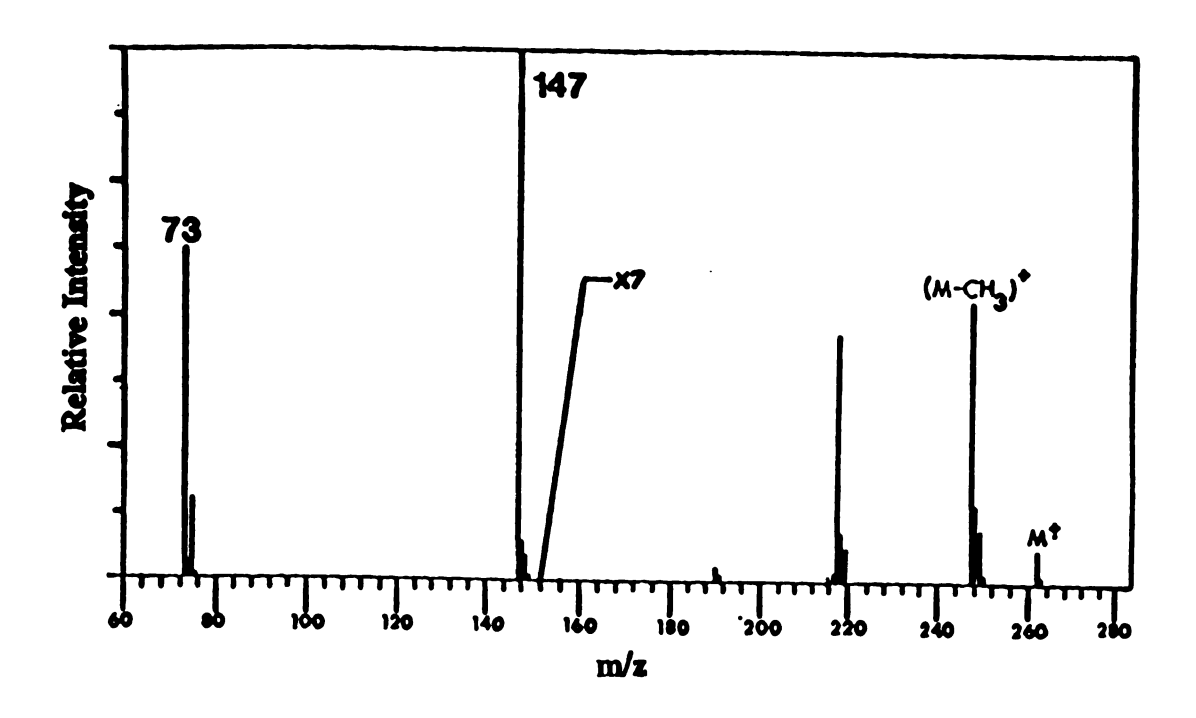


Figure 3. 70 eV EI-MS mass spectrum of 2-hydroxyisovaleric acid (di-TMS)

the metabolite such that accurate levels of enrichment may be measured. The mass spectra of organic acids under EI conditions are typically devoid of abundant high mass ions that are indicative of the analyte.

A more general concern regarding GC-MS analyses of these complex mixtures, arises from the desire to rapidly screen for enzyme disorders, since the organic acidurias can manifest themselves as very serious illnesses in the patients. As was shown in Figure 2, the work-up and derivatizing procedures for organic acids can be quite extensive. Derivatization procedures can also lead to an increase in the number of components of the mixture being analyzed. Furthermore, GC-MS analyses may take between 1.0-1.5 hours for complete characterization of a mixture. When the goal of the profiling study is to obtain a rapid screen or "fingerprint" for a particular organic aciduria, there is an obvious need to obviate the work-up procedures and time-consuming analyses.

This thesis invesitgates the utility of a novel desorption/ionization (DI) method, K<sup>+</sup>IDS, as a very rapid, and extremely attractive alternative to GC-MS analyses for the ability to distinguish between a number of organic acidurias. Chemical ionization methods, such as NH<sub>3</sub>-CI, are evaluated as to their capacity to provide as sastifactory quantitative alternative methods to EI for GC-MS analyses. In addition, this thesis will demonstrate that the quality and quantity of information which can be derived from a conventional metabolic profiling analysis can be enhanced significantly when chemical ionization methods are used in conjunction with EI mass spectral data for providing answers to specific metabolic profiling questions. The proper choice of ionization method will be shown to depend specifically on the type of profiling question which is to be addressed.

# Chapter 2: Desorption/Ionization (DI) and K+IDS theory

Prior to the mid 1970's, most mass spectrometric analyses required that the analyte be introduced in the gas phase prior to ionization and detection. This meant that the compound of interest either had to exhibit a relatively high degree of volatility or that some suitable chemical derivatization reaction be performed to enhance the volatility and thermal stability prior to mass spectrometric analysis. Sample heating techniques through the use of direct insertion probes (DIP) found success for both conventional EI and CI studies, but still required that the analyte be volatile, so that gas-phase ionization reactions could occur. Analyses utilizing chemical ionization mass spectrometry were becoming commonplace, thanks to the ground work of Field and Munson, 19 because intense peaks representing molecular weight information were shown to be obtained readily. In conjunction with the structural information available by EI, identifications of unknowns could now be made more accurately and with a greater degree of confidence. With these gas phase ionization methods it was found, though, that not all compounds gave rise to molecular ions in their mass spectra; some compounds were either considered too "non-volatile" for these gas-phase ionization reactions to occur or were found to readily undergo fragmentation to thermodynamically favored decomposition products. These concerns led to the investigation of ionization methods which could more effectively deal with the problems associated with non-volatile compound analysis. Field ionization (FI) 20 and field desorption (FD)21 techniques were shown to be quite useful methods for generating molecular ions having very low internal energies as a consequence of their respective ionization processes, and the mass spectra of non-volatile compounds utilizing these two techniques were generally

very simple to interpret. These two methods began to expand the range of compounds amenable to mass spectrometric analyses. In addition, rapid-heating methods, such as flash vaporization techniques, found success in that compounds previously considered to be non-volatile could, under the appropriate conditions, desorb intact into the gas phase. Beuhler showed through rapid heating techniques, that thermally labile compounds such as peptides could desorb from inert teflon surfaces. The rates of desorption and decomposition were found to be competitive, but conditions could be attained in which desorption of the intact analyte molecule was favored over a thermodynamically favorable decomposition pathway. <sup>22</sup>

Barber and coworkers developed the novel desorption/ionization method of fast atom bombardment (FAB)<sup>23</sup> in 1981 and demonstrated that mass spectrometry could be used to yield mass spectra of compounds which were previously considered thermally labile and unamenable to mass spectrometric analysis. The technique of FAB is now considered one of the most important desorption/ionization methods available to the mass spectrometrist. Fast atom bombardment ionization involves the deposition of a thermally labile compound (e.g., oligosaccharide; peptide) onto a probe tip containing a polar matrix (e.g., glycerol) which is used to solubilize the analyte species. A high energy beam of fast atoms (or ions), is focused onto the probe and the energy associated with the bombardment process is typically sufficient for desorption of the analyte to occur whereby it may participate in gas phase ion molecule reactions with the co-desorbing ions from the matrix. Other matrices have been introduced, such as dithiothreitol/dithioerythritol (DTT:DTE), thioglycerol, and others which have allowed for the analysis of a wide range of compound types by FAB-MS. 24-25 However, a number of inherent problems associated with FAB have warranted the investigation and implementation of other, new desorption/ionization methods in mass spectrometry. The implementation of some of

these methods has been a result of the need to overcome some of the inherent problems associated with FAB. The need for a matrix in FAB in the desorption process to produce long-lived ion signals (a) limits the number and type of thermally labile compounds that can be analyzed based on solubility constraints, and (b) unnecessarily complicates mass spectra due to severe matrix ion interferences. In addition, the technique has shown only little promise for quantitative analysis.

The analytical utility of all desorption/ionization methods lies in their ability to produce abundant molecular ions. Positive-ion FAB mass spectra are typically characterized by intense protonated molecules, which are presumed to arise through gas phase proton transfer from the more acidic glycerol molecules. Compounds can be induced to form molecular adduct ions with appropriate cationic species. In FAB, LDMS, FI and FD mass spectrometry, formation of [M+ alakali ion] has been observed for mixtures of alkali salts and organic compounds. For FAB-MS, cationization is made possible by pre-mixing glycerol (or other matrix) with an appropriate alkali salt (e.g., NaI, KI, etc.). The stability of these molecular adduct ions is an attractive feature, since mass spectra are relatively clean, and mixtures can often be characterized accurately due to the simplicity of the mass spectra that result. The stability of the alkali ion adducts lies predominantly in the fact that the charge associated with the molecular adduct species is localized on the alkali ion, due to its low recombination energy (identical in magnitude to its ionization potential which is low relative to most organic compounds).

The pioneering work in the area of cationization of organic compounds is a result of the elegant studies done by Rollgen and coworkers. <sup>26-28</sup> Early experiments in their laboratory utilized 10  $\mu$ M diameter tungsten field ionization emitters coated with a thin layer of alkali salt, most typically LiI. Low heating currents were applied to the emitter and Li<sup>+</sup> was found to be generated in copius amounts in the presence of

moderate electric fields. Organic compounds, such as carbohydrates, straight-chain alcohols and others, were desorbed through slower heating methods and introduced into the gas phase. Reactions between organic compounds and Li<sup>+</sup> on the surface of the emitter occurred, resulting in the formation of cationized molecular species in the presence of electric fields just below the threshhold level required for field ionization. Alkali ion attachment was shown to readily occur for numerous organic compounds, both volatile and thermally labile.

In addition, Rollgen et al.<sup>29</sup> described thermal desorption of ions such as [M+Na<sup>+</sup>] from heated mixtures of alkali salts and organic compounds on metal surfaces. One of their approaches incorporates a two-filament probe. A source of gas-phase alkali ions is generated through rapid heating of an alkali salt, such as KI, LiI, or NaI (contained within a silica gel matrix) from one emitter wire, and gas phase addition reactions are achieved with organic compounds which desorb from the second wire. The types of ions observed in the mass spectra primarily consist of alkali ion adducts.

A number of novel desorption/ionization methods have been proposed to increase the scope and capabilities of mass spectrometry in the area of thermally labile compound analysis. The technique of thermally-assisted (TA)-FAB has been found to effectively eliminate matrix interference through methods of background subtraction for certain classes of compounds <sup>30</sup>. The technique of continuous flow FAB, developed by Caprioli, et al., <sup>31</sup> in which the effluent from an HPLC column is deposited directly onto a FAB target containing a solution of glycerol and water has shown enormous potential as a reduction in chemical background is observed, possibly as a consequence of the fact that glycerol is diluted to a large extent in water. In addition, methods such as laser desorption and plasma desorption mass spectrometry (PDMS) are finding much greater use, especially for the analysis of high

mass compounds such as high molecular weight polymers and biopolymers, <sup>32-33</sup> due to the wealth of molecular weight information which is available from the mass spectra obtained using these ionization techniques. However, short-comings exist with all of these ionization methods which limit, to some extent, their utility for mass spectrometric analysis. Not of least concern is that implementation of many of these techniques requires sophisticated instrumentation resulting in relatively expensive methods for thermally labile compound analysis. The ideal desorption/ionization method would be amenable to all thermally-labile compounds, thus making it "universal" as an ionization method while being cost-effective.

This research has been focused on the continued development and characterization of a novel desorption/ionization method developed in this laboratory, called potassium ion ionization of desorbed species (K<sup>+</sup> IDS) which continues to show promise in being responsive to these two criteria mentioned above. K<sup>+</sup>IDS has shown tremedous potential in its universality as an ionization method for both volatile and thermally labile compounds. The technique of K<sup>+</sup> IDS has found applications, too, in areas as varied as industrial polymer and biopolymer analysis, and complex mixture analysis (including organic acids, and other marginally-volatile compounds). This ionization method is based on the production of gas phase metal ions (alkali ions are most frequently used) which are used to ionize thermally labile compounds which are desorbed into the gas phase by rapid heating.

#### K+IDS theory

K<sup>+</sup> IDS is based on the process of thermionic emission for the production of gas phase alkali ions. Bewlett and Jones demonstrated a simple method for producing metal ions in the gas phase<sup>34</sup> that could be used for mass spectrometric analysis. This method involved the use of thermionic emission materials, consisting of metal oxides contained within an aluminosilicate matrix. Metals ions have been found to be produced in copious amounts when glass materials and/or an alkali oxide-containing matrix is heated and biased appropriately. Temperatures greater than 700-800 °C have been proposed as the lower temperature limit for alkali ion emission to occur. For thermionic emission to occur, the energy available in the solid must be sufficient such that a positive ion can be formed and detected in the gas phase.

Shown pictorially in Figure 4 are the thermodynamic processes important in alkali ion emission from a aluminosilicate matrix. The overall process for alkali ion emission can be considered a combination of the heat of vaporization of the molecule  $(X_A)$ , the ionization energy (I.E.) of that molecule, and the work function  $(\Phi)$  of the surface. The thermodynamic values of the energy of diffusion  $(E_D)$ , the energy associated with the migration of an atom through the material, and  $X_A$ , the energy required to transfer an atom (or molecule) from the aluminosilicate surface to the gas phase, are considered negligibly small for metal oxides contained within this aluminosilicate framework. Ion scattering experiments have shown that potassium migrates readily to the surface of these aluminosilicate matrices. The observation of only small ion signals from other atoms indicates a high surface population of potassium ions  $^{36}$ . FAB analyses of these metal oxide containing aluminosilicate mixtures show that only the metal ion is formed to an appreciable extent in the gas phase, suggesting that potassium can migrate relatively freely to the surface of the

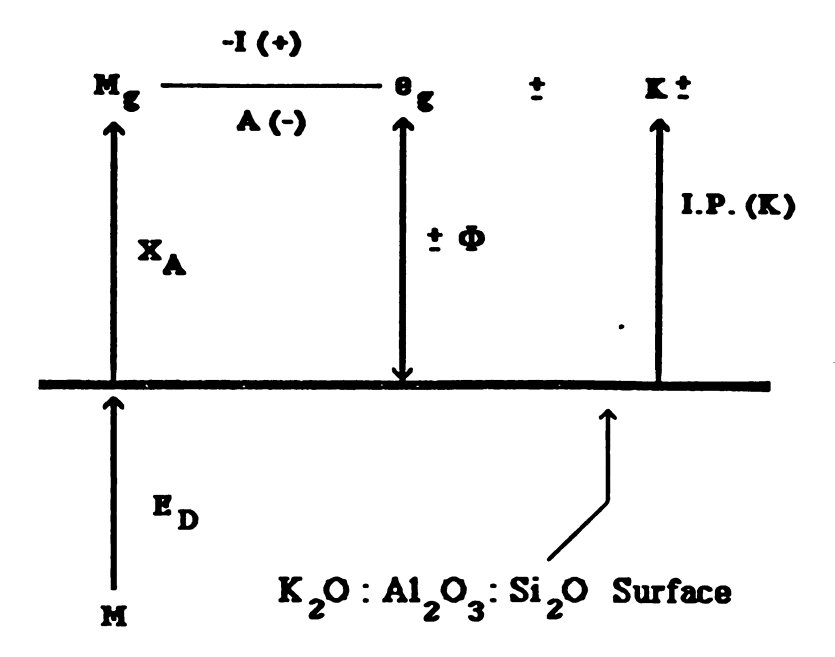


Figure 4: Thermodynamic considerations for K<sup>+</sup> ion emission.

matrix. The emission of alkali ions from the surface, therefore, may be approximated as only being dependent on its ionization energy and the work function of the material., as shown in equation 1,

$$E_{total} = I.E. - \Phi,$$
 (1)

where  $\Phi$ , in this example, represents the work function of the potassium aluminosilicate surface and I.E. (K) is 99.8 kcal mole<sup>-1</sup>. The work function of the material, in simple terms, represents the energy required to remove an electron from its surface. Typically, these work functions are on the order of a few eV energy. Low work function materials, such as aluminosilicate materials containing cesium can

more readily emit electrons under similar conditions than a high work function surface, such as an aluminosilicate material containing sodium. Bombick gives an exhaustive discussion of the types of work functions and their dependences on temperature. In addition, the properties of these materials are found to be affected dramatically by their chemical environment. 37

Based on the properties of these glass materials, it is possible to construct an alkali ion emitter that can be used to produce a high flux of alkali ions (or other metal ion) in the gas phase which can be used in ion molecule reactions. This is the basic premise of the K<sup>+</sup>IDS technique. Experimental considerations and theoretical aspects of the technique will be discussed in the following sections.

Early work in this laboratory used thermionic emitters for CIMS experiments in which alkali ions were employed as the reagent ions for these gas-phase reactions. A thermionic emitter containing this glass mixture was designed such that it could be introduced into the ion source of any mass spectrometer having a DIP inlet. The probe used in this laboratory is a modified DIP probe for an HP5985 quadrupole mass spectrometer. Potassium ions were found to be produced in copius amounts if the probe was heated to sufficiently high temperatures and biased positively with respect to the ion source housing. Introduction of sample gas, either through a "batch" inlet system or through the gas chromatograph at the same time that thermionic emission was occuring could lead to gas-phase alkali ion addition reactions. Bombick, Pinkston and Allison showed that addition reactions involving volatile analyte molecules (e.g., acetone) and these gas-phase alkali ions required that (1) the kinetic energy associated with the K<sup>+</sup> ions emitted from the surface fall into a narrow "bias" window and (2) a third body collision was required for the stabilization of the newly formed adduct ion. <sup>38</sup> This "bias" window, typically a 2-5 V positive bias on the thermionic probe tip relative to the ionization source housing, is necessary

for adduct ion formation to occur. It was determined that under conditions in which the bias voltage applied to the probe falls outside the range of this "bias window," surface ionization reactions can be overwhelmingly favored over gas-phase alkali ion attachment reactions for certain classes of compounds (e.g., amines).

These observations led Bombick and coworkers to investigate the types of ions that might be produced when a thermally labile compound was place directly onto the K<sup>+</sup> glass. The types of ions observed, when the alkali ion thermionic emitter containing thermally labile sample was heated, appeared to be a combination of K<sup>+</sup>-CI and thermal degradation products. The overwhelming majority of ions observed in the mass spectra of these compounds were K<sup>+</sup> adducts which are presumed to occur following desorption of analyte molecules into the gas phase; hence, the name, potassium ionization of desorbed species (K<sup>+</sup> IDS).

# Operative mechanism of K+IDS

As mentioned, K<sup>+</sup>IDS is a novel desorption/ionization developed in our laboratory that is based on thermionic emission materials for producing gas phase alkali ions which can be used as a source of reagent ions in reactions with most organic compounds (including thermally labile and volatile molecules) desorbed from a surface. As mentioned, the best proposed mechanism to date involves the desorption of analyte from a solid surface followed by gas phase alkali ion attachment. This mechanism has been further supported based on the implementation of a new probe design which was required for the analysis of mixtures of marginally-volatile compounds. This point will be discussed in detail. As the alkali aluminosilicate matrix containing analyte solution is rapidly heated, one of two

processes can occur. If the compound is sufficiently thermally stable, intact desorption of analyte can occur from that surface. However, if the compound is considered thermally labile, a number of thermal decomposition reactions can occur on the surface prior to desorption into the gas phase. The processes are summarized in Figure 5 below. A thermally labile species, denoted as ABCD, is coated onto the surface of the alkali aluminosilicate bead. When heated to temperatures above that required for alkali ion emission, K<sup>+</sup> (or other alkali ion) ionization and desorption of the alkali ion into the gas phase occurs. Concurrently, desorption of the thermally labile species, AB-CD occurs, in some form into the gas phase (i.e., as the intact molecule ABCD<sub>(g)</sub>, or as a thermal decomposition product, AB<sub>(g)</sub>, where (g) represents the gas phase) and alkali ion addition reactions with desorbed species are readily observed. It has been mentioned that adduct ion formation requires a third body for collisional stabilization of the initially formed adduct ion complex.

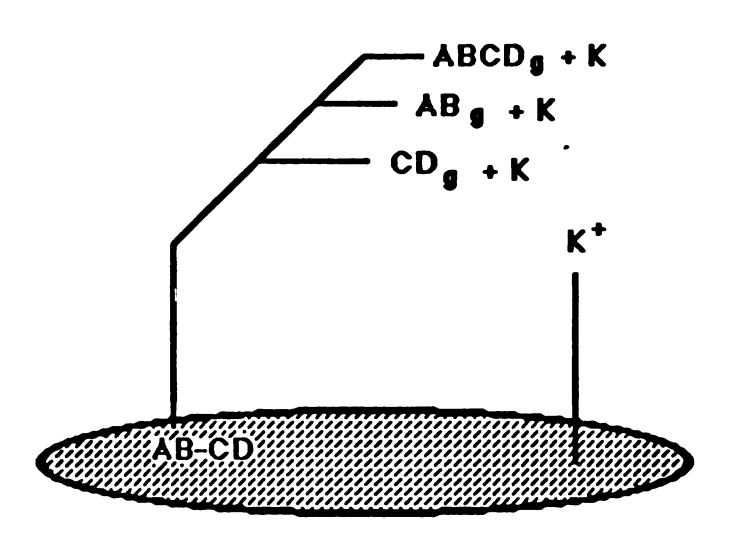


Figure 5: Proposed mechanism for adduct ion formation of desorbing species, ABCD, from alkali aluminosilicate surface.

The operative process envisioned is similar to the one proposed for both secondary ion mass spectrometry (SIMS) and FAB, in which a selvedge region is believed to exist directly above the surface. <sup>39</sup> This selvedge region in a K<sup>+</sup> IDS experiment is believed to be a high pressure region consisting of desorbed neutrals and K<sup>+</sup> ions. Bombick, et al. <sup>37</sup> demonstrated that by increasing the pressure in the ion source using a relatively inert gas, such as N<sub>2</sub>, an increase in the detectability of analyte ions could occur, lending further support to the requirements for third-body stabilization.

#### Experimental Considerations

A direct insertion probe for an HP5985 quadrupole mass spectrometer was modified by Bombick et al. to yield the "original" K<sup>+</sup> IDS probe shown in Figure 6. The tip of the probe consists of a two-holed ceramic rod through which a rhenium wire (0.007" diameter) is inserted and looped. An alkali aluminosilicate mixture containing potassium in the form of KNO<sub>3</sub> (converts to K<sub>2</sub>O when heated) is applied to the end of the "looped" rhenium wire filament as a slurried mixture suspended in MeOH. The bead is then conditioned under a bunsen burner for a few minutes to cause the alkali glass material to conform to a porous, ceramic-like glass. Electrical connections between the rhenium wire and extended K<sup>+</sup>IDS probe are made using low resistive copper wire.

Rapid and stable heating currents are achieved using a low current power supply designed by Martin Rabb, Electronics Shop, Department of Chemistry, Michigan Statee University. The probe tip may be biased relative to ion source housing (or ion focusing lenses) through an internal variable low voltage source contained within the

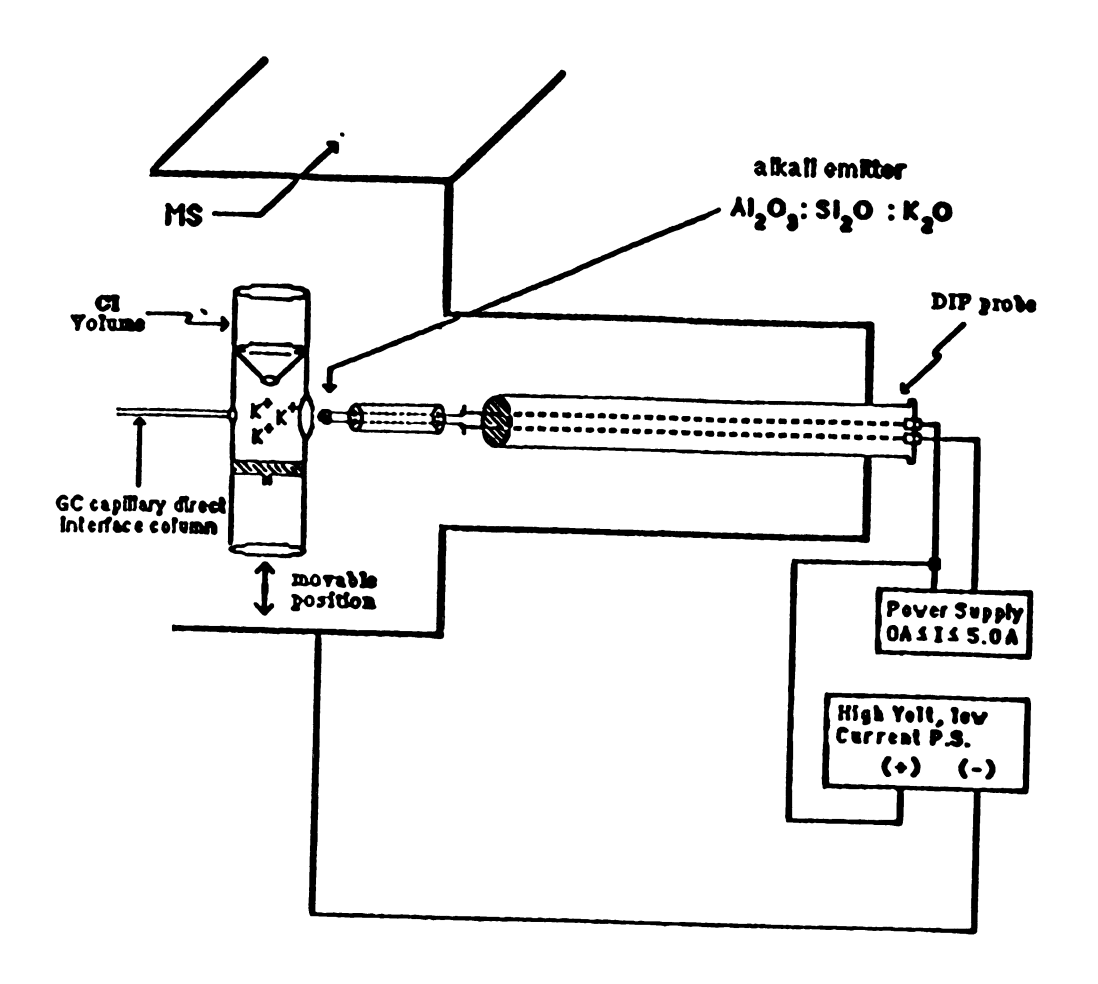


Figure 6. Modified direct insertion probe (DIP) for use as a thermionic emitter for K<sup>+</sup>IDS analyses

current source. The schematics of this current power supply are shown in Figure 7 as reference. The emission current source is a current power supply which is capable of delivering up to 5 amps DC. The current output is floating on a bias supply which is referenced to the reference voltage input. The current amplifier compares the voltage generated by the load current flowing through a 0.1 ohm resistor with the voltage set on the current control and via a power transistor, drives the current to the desired value. A current limit transistor senses part of the voltage across the two 0.1 ohm resistors which are in series with the load current and limits the output to a controlled value. Current may be preset to a desired value prior to being turned on by a front panel toggle switch. The bias voltage may be adjusted to a maximum of  $\pm$  15V DC or  $\pm$  200 V DC, with lo-hi and polarity toggle switches and front panel potentiometer.

The probe is inserted into the source of the mass spectrometer via the direct insertion inlet as shown in Figure 6 and again conditioned by slowly heating the probe tip in approximately 0.5A increments up to c.a. 0.25 A above maximum operating current for analysis. Alkali ion emission is optimized by: (a) varying the bias potential to the K<sup>+</sup>IDS probe; (b) probe positioning; and perhaps most importantly (c) tuning the ion focusing lenses and repeller.

A typical tuning file achieved after conditioning of the bead is shown in Figure 8. Peaks corresponding to m/z = 39 and 41 (K<sup>+</sup> and its natural isotope) are optimized for best peak shape and abundance. Mass axis calibration is generally achieved under EI conditions using a high mass calibrant which readily forms low mass fragment ions, so that calibration can be achieved over a wide mass range. The mass of the potassium ion in this tuning file was calibrated to m/z = 39.05 u. Also implied from the tuning file is that at low electron multiplier (EM) settings (0V  $\leq$  EM  $\leq$  3000) it is possible to generate substantial potassium ion current. It does not necessarily follow

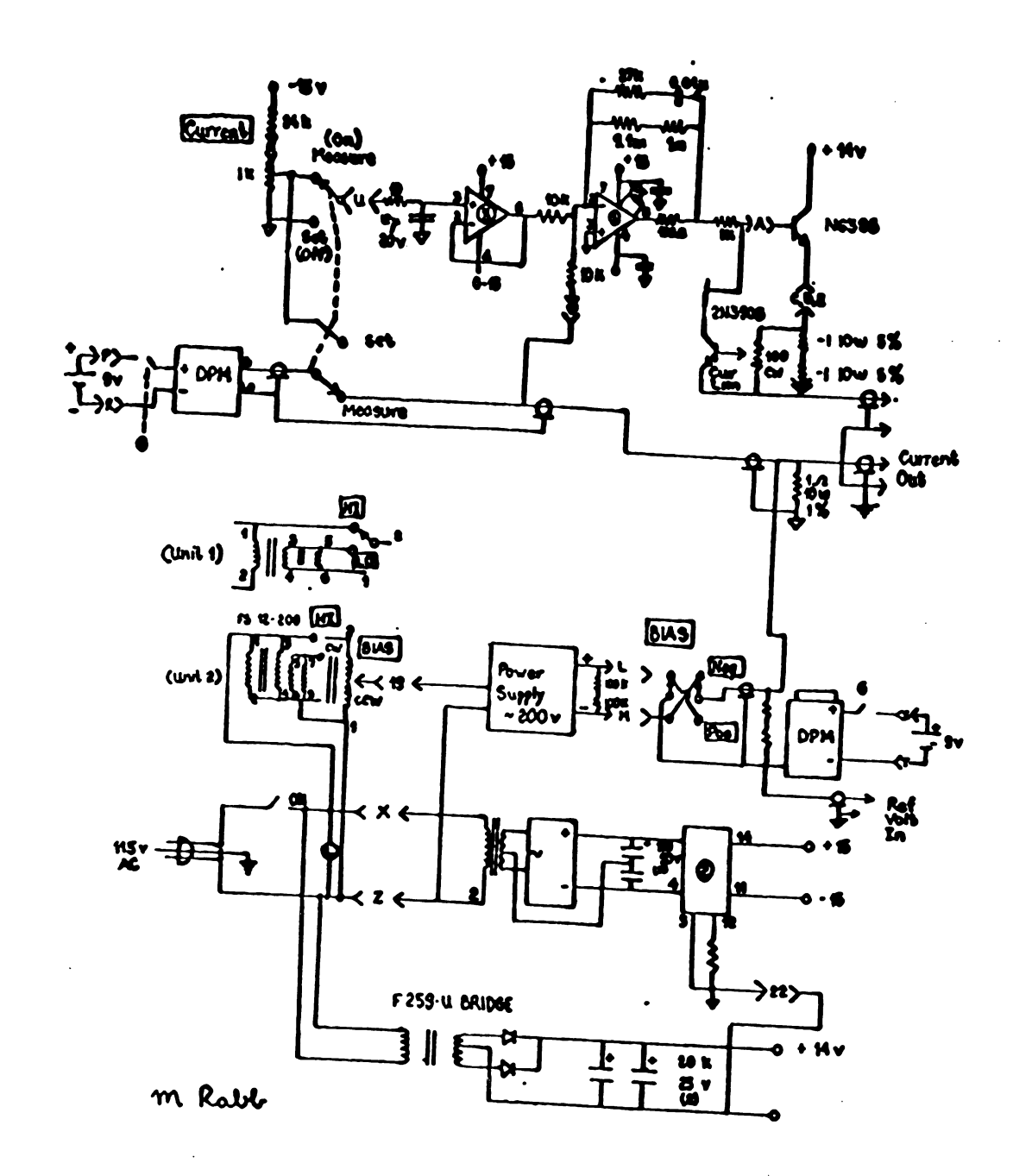


Figure 7. Schematic diagram of emission current power supply.

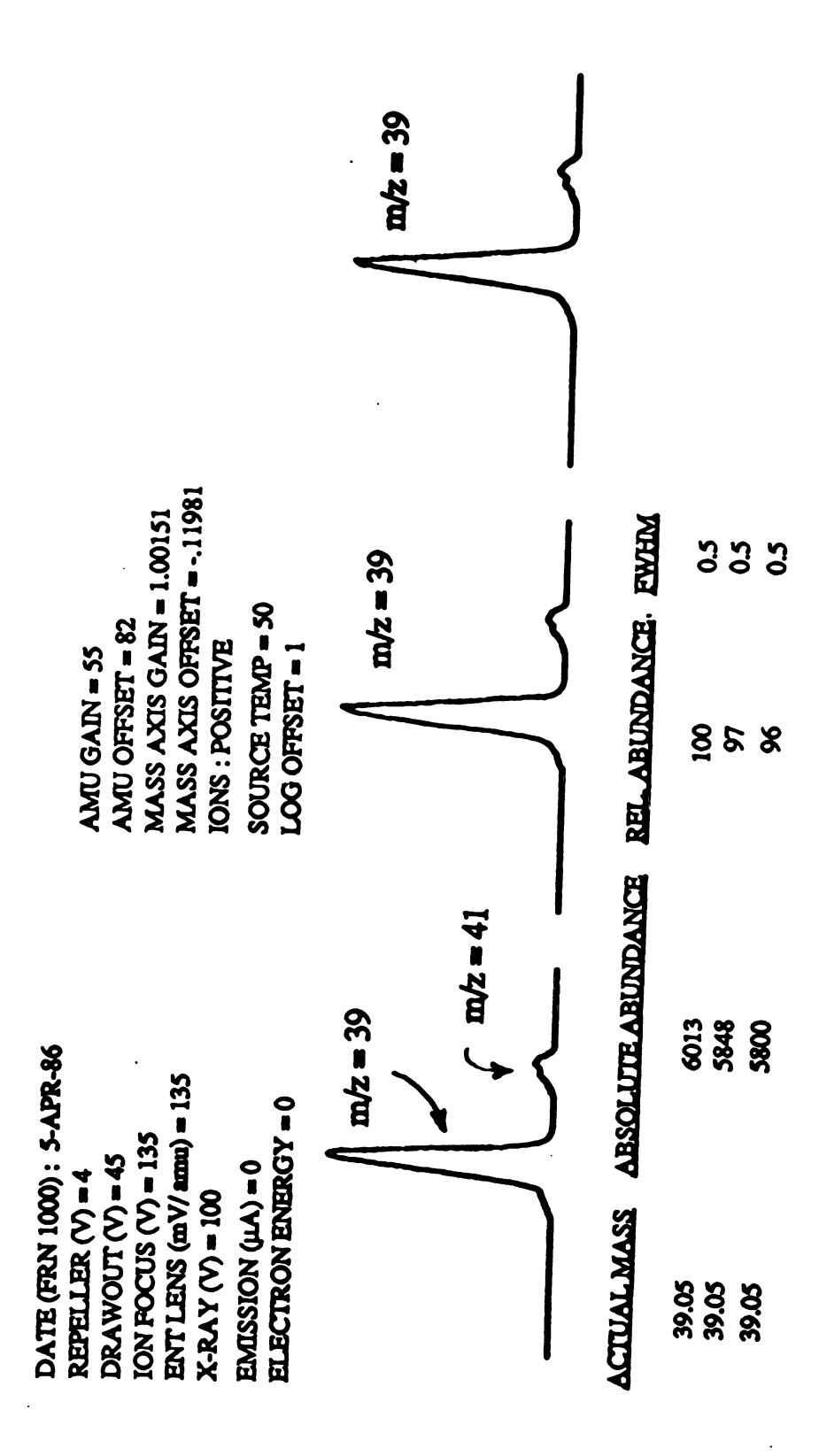


Figure 8: "Typical" K<sup>†</sup>IDS tuning file depicting K<sup>†</sup> ion abundance.

that alkali ion emission current increases with increased probe current. Typically, as power supply current is increased, a change in bias voltage is required to optimize potassium ion signals. Currents used above 4.0A have been found to significantly decrease the life time of existing glass beads, yet as will show later, these higher currents can result in benefits in the analysis of certain classes of organic compounds.

Following optimization of K<sup>+</sup> emission, the probe is removed from the source and the compound to be analyzed is deposited onto the emitter as a solution in methanol, hexane, or acetone. These transport solvents are generally chosen due to their ease of evaporation. Evaporation of aqueous solutions are difficult and time-consuming, and frequently poorer sensitivity has been observed when water is used as the transport medium.

Bombick gives examples of many types of compound classes that are amenable to the K<sup>+</sup> IDS ionization method, <sup>37</sup> including analysis of pharmaceuticals, oligosaccharides, and polymers, to name only a few. Discussed in this thesis are the results of experiments which have utilized this nearly "universal" ionization method for (a) determining the quantitative and qualitative strengths of the technique for complex mixture analysis, (b) improving upon existing detection limits to make the technique competitive with other ionization methods for similar compound analyses, and (c) further defining the boundaries of this ionization method (as to the types and numbers of compounds amenable to analysis using the technique).

# Initial results utilizing K<sup>+</sup>IDS for mixture analysis

The potential of the K<sup>+</sup>IDS technique for yielding an accurate and quantitative representation of the components of a mixture has previously been suggested.<sup>40</sup>

Bombick and Allison demonstrated that the K<sup>+</sup>IDS technique yields mass spectra that accurately reflect the molecular weight distribution of low molecular weight oligomeric components of a polymeric mixture. For example, the analysis of the K<sup>+</sup>IDS mass spectrum of poly(propylene glycol) 725 (average MW = 725), yielded an average molecular weight of 710, based on the intensities of the (M+K)<sup>+</sup> ions of the individual components in the complex mixture. Typically, several mg of polymeric material were coated onto the probe tip and resultant TIC profiles of these polymers showed gaussian type behavior, with extensive tailing, due to desorption of analyte from both "hot" and "cold" spots on the ceramic rod. Typically a mixture of thermal degradation products and desorption products were observed in the K<sup>+</sup>IDS mass spectra. Thermal degradation products were observed generally at late times during analysis and are believed to have resulted from desorption from these "cold" spots on the thermionic emitter. Averaging of mass spectra over the entire elution profile could not be used for determining the relative concentrations of the components of the mixture. Typically, one region within the entire polymer desorption profile was found to most accurately reflect the components, and their relative concentrations of the mixture.

These initial results on the analysis of polymers suggested that the K<sup>+</sup>IDS technique might be useful for mixture analysis. Part of the goals outlined in this thesis are to further investigate the capabilities of K<sup>+</sup>IDS for providing "batch" analyses of mixtures. Of specific interest are the organic acids, and other metabolites of physiological fluids. The following chapter will concentrate on results utilizing the K<sup>+</sup>IDS approach for rapid characterization of several of the organic acidurias. The problem of sensitivity constraints, which to date limited the analytical utility of the technique for biochemical analysis had to be addressed, since the concentration of organic acids in urine are not likely to exceed several tens of µg/ml urine at best and

generally fall in the range of low  $ng - \mu g/ml$  urine concentration.

Polymers, as mentioned, were found to undergo both thermal degradation and intact desorption and this has been found to depend on the amount of material and heating currents used in their analysis. Situations in which both intact analyte ions and thermal degradation products are observed in K<sup>+</sup>IDS mass spectra are non-ideal for mixture analysis since spectra can become exceedingly complicated and quantitation of the components difficult. Thus, for mixture analysis, the K<sup>+</sup>IDS mass spectra ideally would be nearly as simple as possible, yielding only one peak for each component of the mixture.

The K<sup>+</sup>IDS technique was evaluated as to whether it would be capable of yielding [M+K]<sup>+</sup> information on compounds typically excreted in urine, such as organic acids, fatty acids and amino acids. Experiments using the single-filament probe required the deposition of several µg of organic acid onto the K<sup>+</sup>IDS probe tip. Experiments utilizing operating currents below 2.75 A (c.a. 1000 °C) resulted in no analyte ion signals. Only when the probe was heated to currents above this temperature were analyte ions of the form [M+K]<sup>+</sup> produced and detected. This was a unique requirement since all K<sup>+</sup>IDS mass spectra obtained by Bombick used heating currents between 2.0A and 2.5A. Subsequent studies revealed that these higher power supply currents were required to generate a high flux of potassium ions more rapidly. This situation allowed for better spatial overlap to occur between the desorbing analyte and K<sup>+</sup> ions available in the gas phase.

Fortunately, K<sup>+</sup>IDS mass spectra of volatile compound classes such as short-chain carboxylic acids, amino acids, fatty acids, and others are indeed quite "clean". Shown in Figure 9 is the K<sup>+</sup>IDS mass spectrum of a mixture containing five commonly occurring organic compounds, of varying concentrations. The mass spectra are very clean, exhibiting only [M+K]<sup>+</sup> adduct ions for each species.

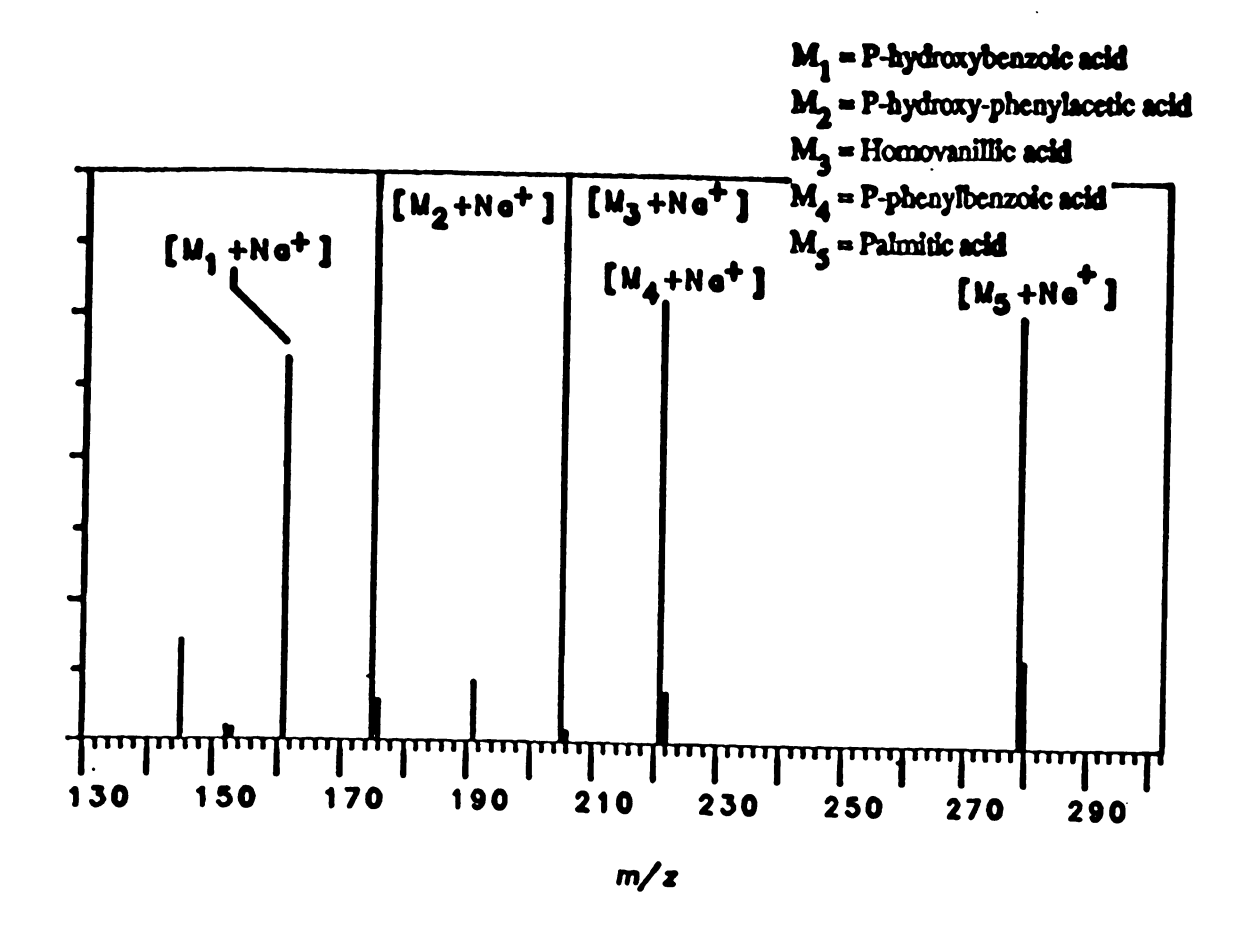


Figure 9. Na<sup>+</sup>IDS mass spectrum of five common organic acids (underivatized)

However, the ion currents associated with these compounds are quite short-lived. TIC profiles are considerably shorter in duration than those obtained for thermally labile compounds, due to smaller sample loads (relative to polymers) and low temperatures required for volatilization of the compounds. Nevertheless, these types of compounds exhibit the <u>ideal</u> behavior that was needed for the analysis of complex mixtures by K<sup>+</sup>IDS.

Several simple mixtures of organic acids, fatty acids, and steroids were prepared in order to be analyzed by the  $K^+IDS$  technique. Shown in Figure 10 are averaged mass spectra of a 5:1:1:1 mixture of C-12, 14, 15, and 16 free fatty acids obtained in one  $K^+IDS$  analysis. Four important observations regarding the types and quantities of ions observed in the mass spectra are: (1) only  $[M+K^+]$  ions are generated for each component of the mixture, (2) the  $K^+IDS$  mass spectra do not accurately reflect the relative concentrations of the components of the mixture, (3) higher mass ions increase in intensity at later times during the  $K^+IDS$  analysis, and (4) when higher heating rates are used  $(I \ge 3.5A)$ , the relative intensities of the species are slightly improved to more closely represent the true mixture composition. This type of behavior has been observed not only for fatty acid mixtures but for mixtures of other marginally-volatile compound classes, such as short-chain organic acids and amino acids.

These results were discouraging since analysis of polymeric materials suggested that relative ion intensities could be used to accurately reflect the composition of complex mixtures, whereas simple mixtures of organic acids and fatty acids now appeared to show preferential response towards the higher mass species, since higher mass ions were observed to contain the larger fraction of total ion intensity. The concept of preferential ionization needed to be considered since there are a number of

reports in literature which suggest that adduct ion formation does not necessarily occur with equal probability for similar compounds, even isomers.<sup>41</sup>

However, this preferential ionization towards higher mass molecules (for the homologous series of straight-chain fatty acids) might be a result of differing degrees of volatility of the organic components. This proposed explanation for the results stemmed from a number of experimental observations. As briefly mentioned, when higher heating rates are used (i.e., I=3.5-4.0A) the relative ion intensities appear to more closely resemble the true composition of the mixture. This behavior is shown pictorially in Figure 11. The preferential ionization of higher mass ions is proposed to be a result of the lower molecular weight species desorbing from the glass surface at such rapid rates that the majority of these analyte molecules are evacuated from the ion source prior to production of a sufficient [K<sup>+</sup>] ion concentration needed in the gas phase to participate in alkali ion addition and stabilization reactions. A steady-state K<sup>+</sup> ion concentration may be attained more rapidly when utilizing higher heating rates. Theoretical plots of alkali ion emission and analyte desorption profiles vs. time for thermally labile compounds such as polymers were described by Bombick and are shown in Figure 12. The importance of these plots is that desorption of analyte occurs prior to alkali ion emission, and only where the two curves overlap may addition reactions occur. Verification of this type of behavior for the analysis of fatty acids, and other volatile compounds was made. Desorption profiles of fatty acids were generated by placing a solution of fatty acids onto the K+IDS probe tip. rapidly heating without a bias potential and forming ions by electron ionization. It was found that at low source temperatures (T<sub>source</sub> ≤ 40 °C), ions were formed almost instantaneously (slightly less than 1 sec) upon application of probe current. Potassium ion emission profiles, on the other hand, were obtained by inserting the

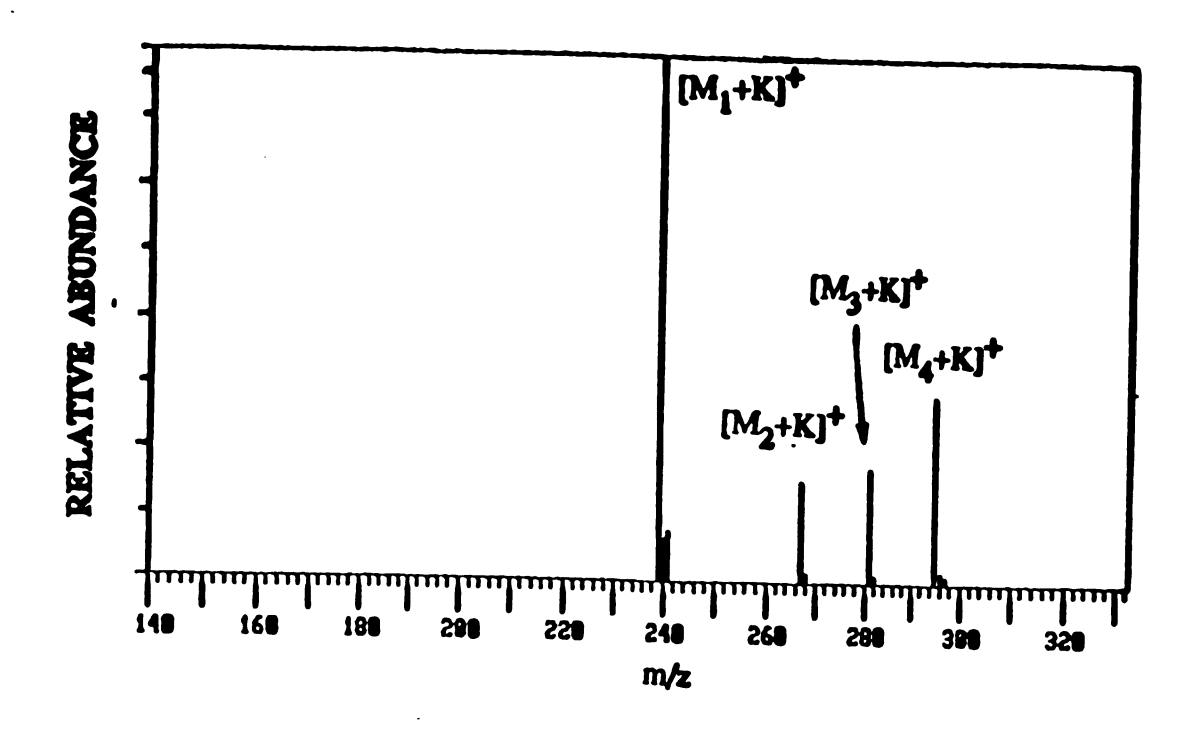


Figure 11. K<sup>+</sup>IDS mass spectrum of same fatty acid mixture obtained at I = 4.0 A

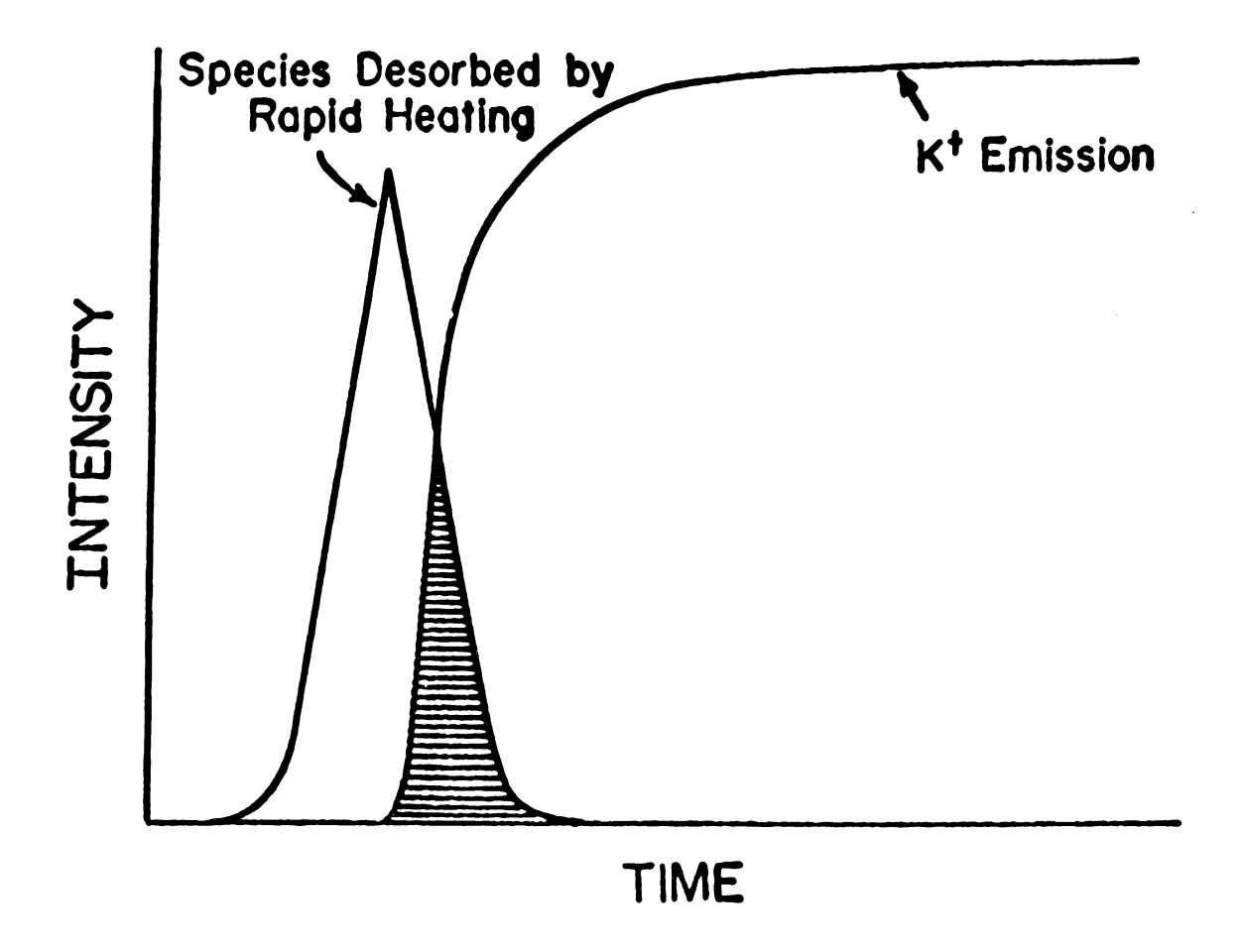
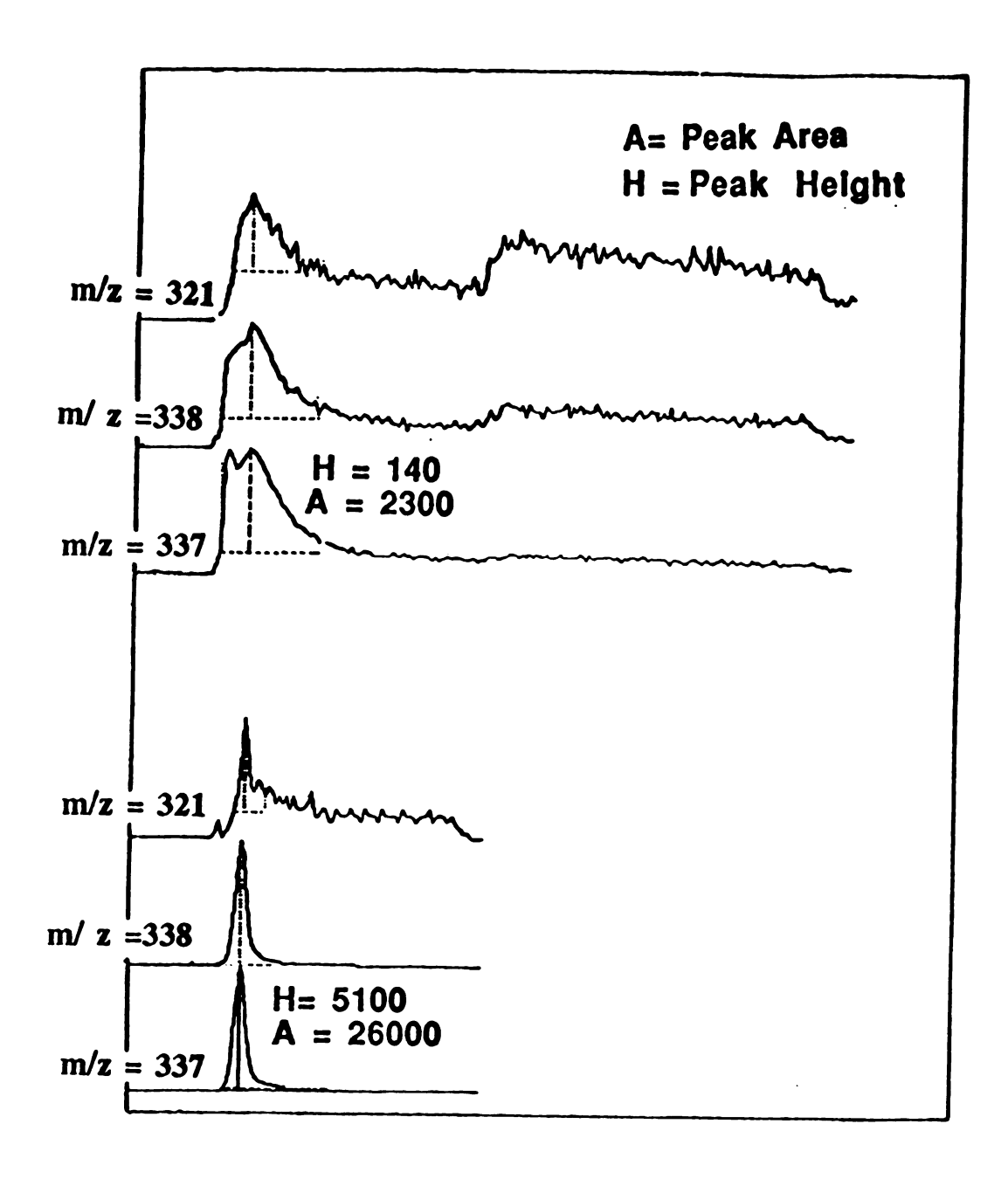


Figure 12. Analyte desorption and alkali ion emission profiles w. time utilizing a single-filament K<sup>+</sup>IDS probe

probe without analyte into the mass spectrometer, applying the same current and now adding the appropriate bias voltage to "push" potassium ions from the surface. K<sup>+</sup> emission was found to reach a steady-state approximately 6 sec following the application of current. These results suggest that addition reactions are preceded by desorption of a majority of analyte prior to sufficient alkali ion emission. For the higher molecular weight species, desorption occurred at a slightly slower rate than for the lower molecular weight species, resulting in better overlap between the analyte and K<sup>+</sup> emission profiles. These observations were also of utility in explaining why such large sample loads were required using the "original" probe design.

These observations led to the consideration of a modification of the existing probe so that the analyte desorption and alkali ion emission profiles would better overlap for all species contained within the mixture, with the intent of improving both the sensitivity and quantitative nature of the technique in the analysis of these marginally volatile compounds. A dual-filament K<sup>+</sup> IDS probe was utilized to try to effectively eliminate the inherent problem of poor overlap between analyte desorption and alkali ion emission profiles associated with the original design. Of note is that a similar design modification was presented by Rollgen and coworkers 42 who demonstrated the use of a two-filament design mounted on a common "push-rod." The question of sensitivity was addressed first since the amount of organic compound required to produce appreciable ion signals using the original probe design were such that it precluded the analytical capacity for mixture analysis of components of biological interest. Bombick demonstrated that the lower limit of detection for polyphenyl ether was approximately 500 ng at a signal-to-noise ratio (S/N) of five. When a modifying gas such as N<sub>2</sub> was introduced into the ion source at high pressures (c.a. 1 torr) the detection limits were lowered to approximately 250 ng (S/N =5). The presence of this modifier gas further supported the proposed gas-phase mechanism in which a thirdbody was required for stabilization, since lower detection limits resulted. Implementation of the dual-filament probe modification has resulted in an approximate 30- to 40-fold enhancement in detection limits for the technique. Methylstearate is typically used for determining the relative sensitivities of ionization techniques such as CI and EI, where specifications for full scan detection limits in the EI mode are typically 1ng for methyl stearate. Results of selected ion monitoring (SIM) analyses on methyl stearate shown in Figure 13 are compared using the original and modified probe designs. Comparison of peaks heights (H) and peak areas (A) of the  $[M+K]^+$  ions (m/z = 337) illustrate the enhancement in detectability. Selected ion monitoring on the natural isotope peak of methyl stearate, m/z = 338, further demonstrated this tremendous improvement in sensitivity. The amount of methyl stearate required to achieve a S/N = 5 using the dual-filament probe has been determined to be 3ng (SIM) and 10ng (full scan, 50-450u / 0.5 sec). A calibration curve monitoring SIM ion counts vs. ng methyl stearate onto the bare rhenium wire is shown in Figure 14. The detection limits for this class of compounds is certainly comparable to other desorption/ioniation methods. In FAB, for example, 1-5 µg material are "typically" required for analysis. However, it must be pointed out that the ion signals achieved by FAB are much longer-lived than those obtained using the K<sup>+</sup> IDS technique.

Reasons for the dramatic increase in sensitivity can be attributed to better overlap in analyte and alkali ion desorption profiles. By placing the analyte solution onto a second filament which now only experiences radiative heating from its close proximity to the potassium emitter, the onset of desorption of volatile analyte from this filament is slightly slower than in the original design. K<sup>+</sup> emission has also been



## Scan time

Figure 13. Selected ion monitoring (SIM) comparison of methyl stearate (400 ng) using (a) single-filament and (b) dual-filament K<sup>+</sup>IDS probe

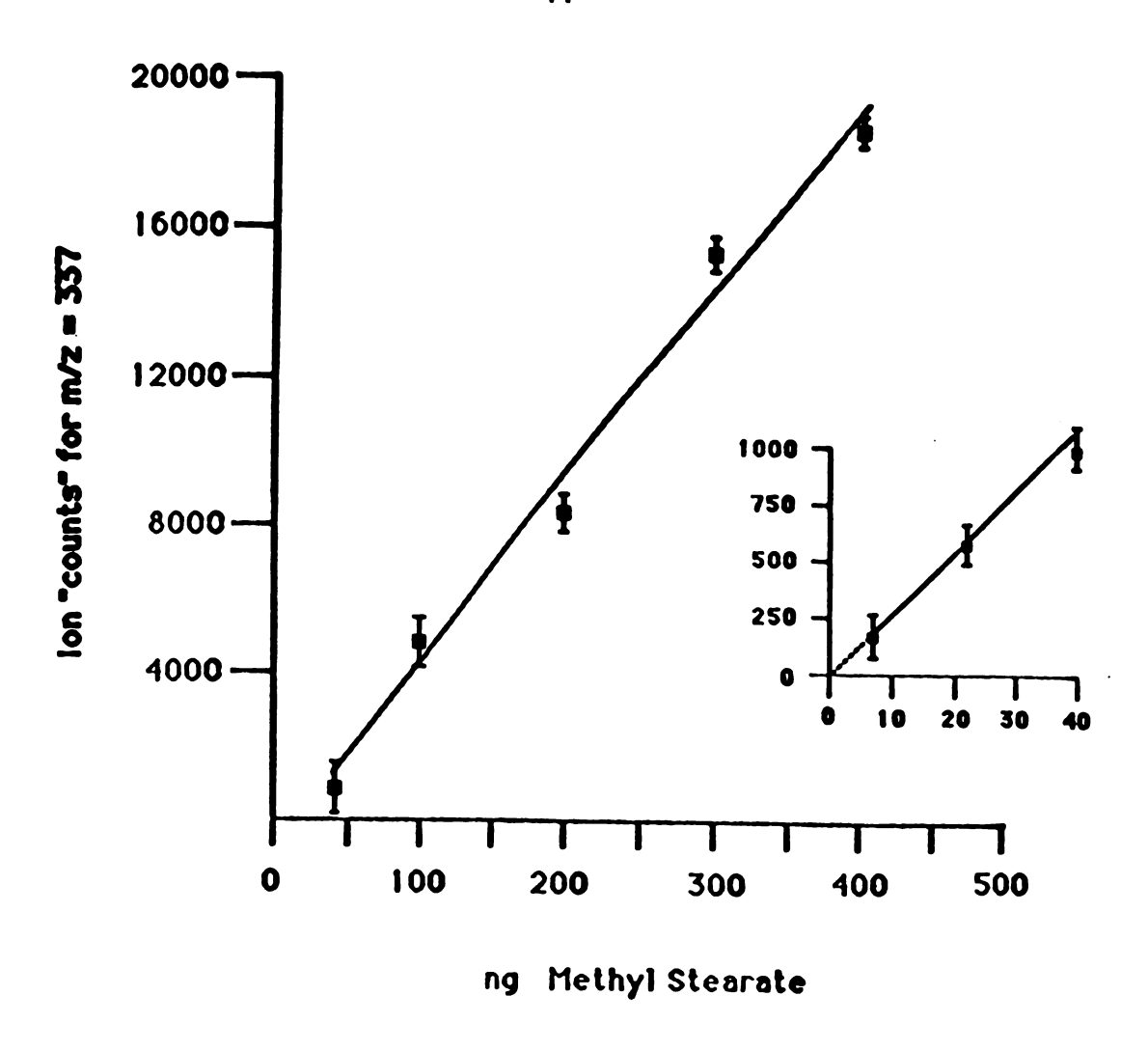


Figure 14. Detection limits for methyl stearate by K<sup>+</sup>IDS using dual-filament probe

found to occur more rapidly from the free emitter surface. In the original probe design, K<sup>+</sup> ions were required to migrate not only through the aluminosilicate framework, but in addition, through the bulk of analyte sample that was deposited onto the aluminosilicate material. By removing this second migration constraint for the K<sup>+</sup> ions, emission into the gas-phase is achieved more rapidly. The result has been a reduction in the amount of time required for K<sup>+</sup> emission to reach a steady-state value (c.a. 4 sec). Comparison of desorption profiles using the one and two-filament designs is shown in Figure 15. As can be seen, better overlap is achieved when the two-filament design is implemented resulting in a greater fraction of desorbing analyte molecules undergoing collisions with gas-phase alkali ions.

The improvements in detection limits obtained using the modified probe design has now allowed this  $K^+$  IDS technique to be utilized in the analysis of complex mixtures of organic acids isolated from urine specimens of both healthy and disease-state individuals. The following chapter gives a description of the currently used probe design and demonstrates the capabilities of the  $K^+$ IDS technique for providing both qualitative and quantitative information for complex mixtures. The strengths of the  $K^+$ IDS technique are demonstrated using appropriate "real-life" examples in the area of metabolic profiling. A brief discussion is presented first on the need for evaluating alternative ionization methods in the area of metabolic profiling. The results summarized in the following chapter are as they appear in a manuscript that has recently been accepted for publication in *Biomedical and Environmental Mass Spectrometry*.

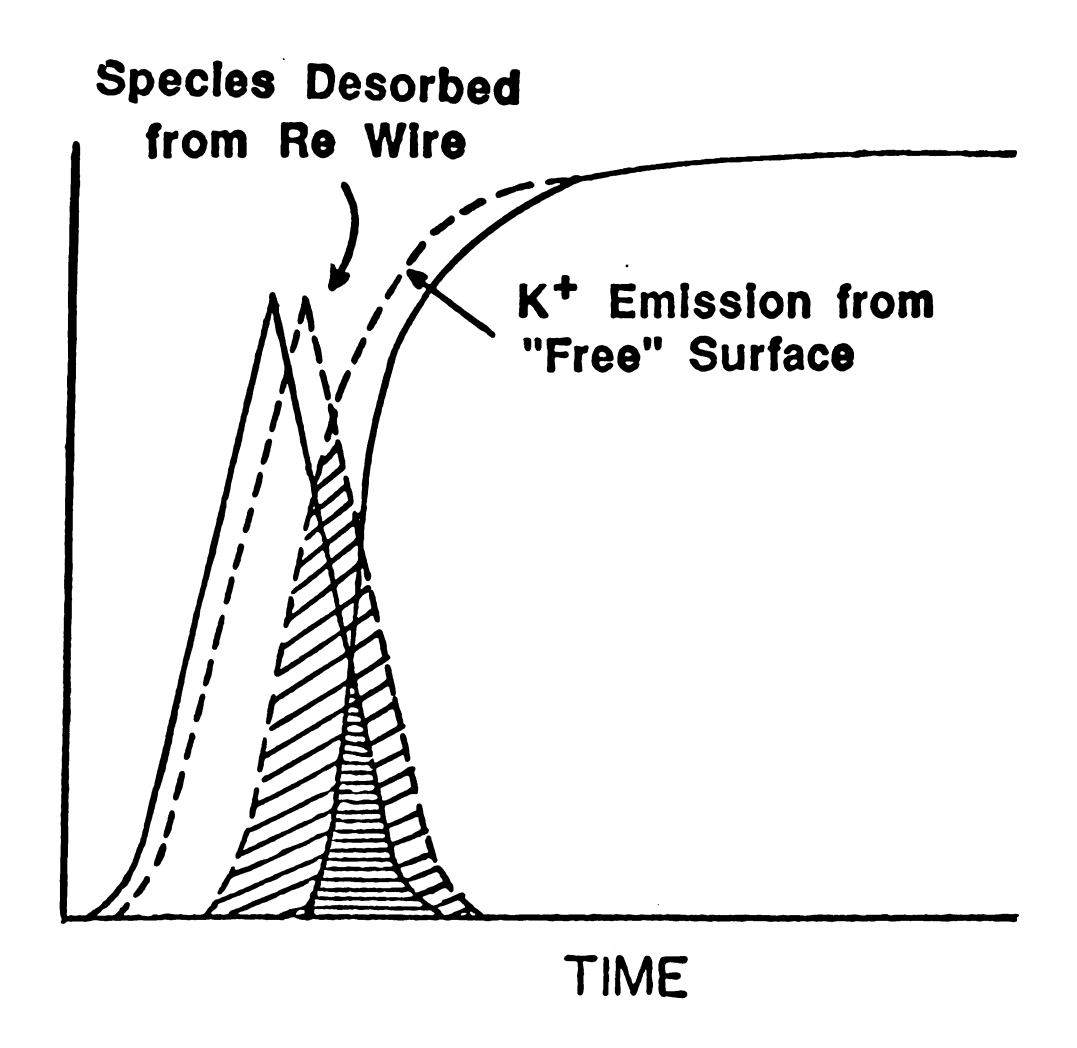


Figure 15. Analyte desorption and alkali ion emission profiles w. time utilizing a dual-filament K<sup>+</sup>IDS probe

Chapter 3: A Novel DI Method, K<sup>+</sup>IDS, for the Rapid Screening of Urine for Organic Acidemias

#### Introduction

The gas chromatograph-mass spectrometer (GC-MS) combination has been a powerful tool for the screening of physiological fluids for disease-state identification and characterization. Inborn errors of metabolism in which amino acid, lipid, and/or carbohydrate pathways may be altered, frequently lead to physiological states known as the organic acidurias (or acidemias) -characterized by elevated concentrations of one or more organic acid in plasma or urine. More than 50 organic acidemias have been identified, and a number of reviews have recently appeared on the diagnostic utility of GC-MS in this field. 4,15,43 In general, identification of the organic acidemias requires the ability to determine that one or more organic acids are excreted at levels above those that exist in "healthy" individuals. One of the most widely reported disorders of this type is lactic acidemia. A number of enzyme defects have been associated with the lactic acidemias, and result in the accumulation of lactic acid in both plasma and urine. 14,15 Diagnosis of this condition is frequently made by monitoring for excessive levels of this metabolite by GC-MS, as well as by monitoring the excretion of 2-hydroxybutyric acid. 44

Of considerable interest are those organic acidemias resulting from disorders in branched-chain amino acid (BCAA) metabolism. <sup>45</sup> Isovaleric acidemia, for example, is the result of isovaleryl-CoA dehydrogenase deficiency, <sup>46</sup> which affects the oxidation of leucine. This enzyme deficiency leads to the accumulation of isovaleric acid, which itself is neurotoxic to experimental animals. "Stores" of glycine are normally available to conjugate with  $\alpha$ -hydroxyisovaleric acid to form the

more water soluble metabolite, isovalerylglycine. In fact, orally administered doses of glycine are frequently part of the dietary regime for treating this condition. It is this metabolite that is frequently observed to be excreted in 2000-fold excess relative to "healthy" conditions and disease-state identification is generally made on the basis of the elevation of this metabolite in urine. In Maple Syrup Urine Disease (MSUD), 47 which results from branched-chain ketoacid dehydrogenase deficiency, elevated levels of 2-hydroxyisovaleric, 2-hydroxybutyric, and 2-hydroxy-3-methylvaleric acids have been observed, in addition to increased valine, leucine, and isoleucine plasma concentrations.

A number of alternative approaches to GC-MS has been suggested for situations in which the goal of analysis is to identify the specific metabolic disorders involving the organic acidemias. Analyses that utilize GC-MS are time-consuming since: (a) derivatization of the isolated organic acids from urine is required to make the mixture amenable to analyses using gas chromatography, and (b) long GC analysis times are required to achieve suitable separation of the organic acid components. The protocol for isolation and derivatization of organic acids for gas chromatographic analysis was shown to be quite extensive (see Figure 2). Numerous attempts have been made to simplify the work-up procedures of organic acids by bypassing the gas chromatograph. Alternatives to GC-MS for screening for organic acidurias have included LC-MS, MS-only, MR, MR, and TLC-MS 52.

Recent attempts to distinguish between the metabolic profiles of various disease-state and healthy individuals on a more rapid time-scale include direct exposure probe-chemical ionization-MS. In these studies, the mixtures of organic acids are introduced directly into the mass spectrometer. Heating, rather than derivatization, is used to volatilize the analyte mixture. Issachar and Yinon<sup>50</sup> demonstrated that this MS-only method using isobutane chemical ionization could qualitatively differentiate

between disease-state and healthy urinary organic acid profiles. Although this approach yielded a very rapid alternative to GC-MS analysis, it could not be used to accurately quantify the components of the mixture. Organic acids had to be seaparated into "volatile" and "non-volatile" classes. Volatile compounds were considered those for which isobutane-CI mass spectra could be obtained at ion source temperatures of 70 °C. Non-volatiles required source temperatures of 190 °C for their vaporization to occur. As a result, two individual analyses were required for each isolated organic acid fraction. This situation posed problems since operating conditions (i.e., reagent gas pressure) could not be maintained rigorously constant. As a result, chemical ionization mass spectra were subject to fluctuations in ion source pressure and these variations have been found to have a pronounced influence on relative intensities of ions in the chemical ionization mass spectra.

Tandem mass spectrometry (MS-MS) has also been suggested as a viable alternative to GC-MS for complex mixture analysis. Hunt and Giordani<sup>53</sup> investigated the potential of this technique for disease-state identification of the organic acidurias. Although this method certainly provides a much more rapid approach, and often yields data as informative as that obtained by GC-MS, the cost associated with such an experiment may preclude its widespread use for routine clinical diagnoses.

K<sup>+</sup>IDS is evaluated as an extremely rapid and effective "batch" mass spectrometric approach for differentiating various organic aicdurias. For the analysis of organic acids from urine, no derivatization is required. The potential of this method as an alternative to GC-MS for characterizing and differentiating complex mixtures of organic acids in urine is described.

#### Experimental

Procedures for a typical K<sup>+</sup>IDS experiment have been described elsewhere. In previous K<sup>+</sup>IDS experiments, nonvolatile compounds or mixtures were deposited directly onto a thermionic emitter glass bead. When rapidly heated, analyte desorption and K<sup>+</sup> emission occurred from the same surface, with K<sup>+</sup> attachment to the desorbed neutrals occurring (in the gas phase) to yield the species observed in the resulting mass spectrum. The probe design initially employed has been modified as mentioned in the last chapter; the new design is schematically shown in Figure 16. The probe consists of two filaments; one supports the alkali-aluminosilicate mixture, and the other supports the sample. Filament 1 is resistively heated and appropriately biased to generate K<sup>+</sup> ions in the gas phase. Filament 2 is positioned a few millimeters from Filament 1 and is not electrically heated. Samples experience radiative heating from Filament 1 and desorb from the surface. The benefits of incorporating such a configuration for K<sup>+</sup> IDS analyses have recently been discussed. Separation of the analyte from the K<sup>+</sup> emitter has resulted in substantial improvements in sensitivity and much improved quantitative capabilities.

No matrix (e.g., glycerol) is required for K<sup>+</sup>IDS, unlike other desorption/ionization (DI) methods such as fast atom bombardment (FAB). Appropriate volatile solvents, such as MeOH, CH<sub>3</sub>CN, and others are used solely to assist in the transport of analyte to Filament 2. Once transport has been achieved, the solvent is evaporated and the probe is inserted into the mass spectrometer, rapidly heated, and the resulting mass spectra collected.

No source modifications were required to the quadrupole mass spectrometer.

K<sup>+</sup>IDS analyses were performed in the EI source configuration, with introduction of the K<sup>+</sup>IDS probe through the direct insertion probe inlet. Ion source temperature was

# New Dual-Filament K+IDS Probe Design

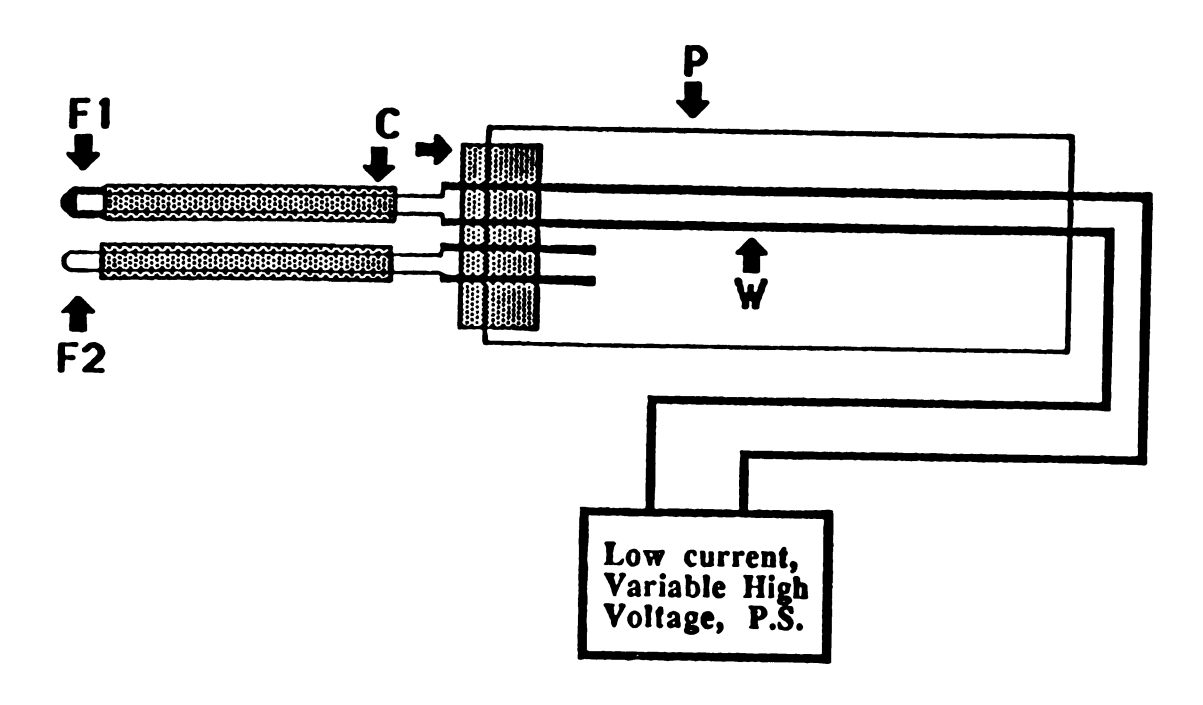


Figure 16. Modified dual-filament K<sup>+</sup>IDS Probe (P). Filament 1 (F1) is electrically heated using resistive wire (W) and is the alkali ion emitter. Filament 2 (F2) is the analyte filament and solely experiences radiative heating

maintained at 40 °C for analysis of the underivatized organic acids. No electron filament was employed. A high flux of alkali ions (Na<sup>+</sup> or K<sup>+</sup>) was generated by rapidly heating the alkali-aluminosilicate mixture to temperatures of 800-1000 °C. The mass spectrometer was scanned from 50-350 u at a rate of 0.4 sec/scan. The mass spectra shown here were obtained by averaging over the entire elution profile (usually 20 scans or less).

Urine samples from organic acidemic patients and from age-matched controls were obtained from Meridian Instruments, Inc., Okemos, MI. The urinary organic acids were quantitatively extracted onto a column of DEAE Sephadex. The preparation of the ion exchange column has been described elsewhere. A 1.0 ml aliquot of urine at pH = 7 was passed through the ion exchange column at a flow rate of approximately 0.1 drop/sec. The column was washed thoroughly with doubly-distilled water and acidic components were eluted off with pyridinium acetate (1.5M). The collected organic acid fraction was concentrated by lyophilization. The residue was then dissolved in approximately 2 ml of acetonitrile and approximately 5-10 ul of the resultant solution was deposited onto the K<sup>+</sup>IDS probe.

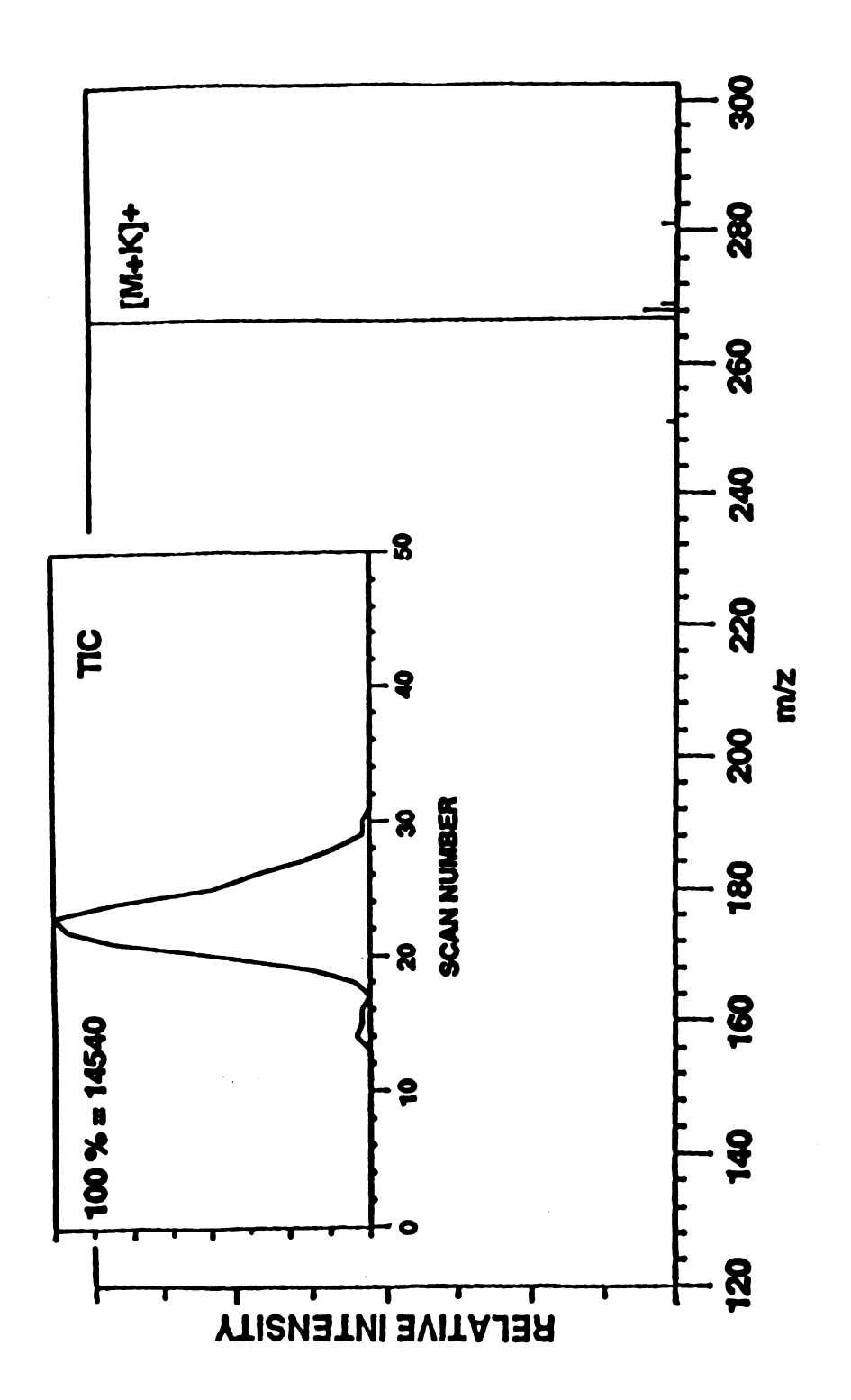
#### Results of mixture analysis utilizing "dual-filament" probe

In K<sup>+</sup>IDS, the analyte or analyte mixture is rapidly heated. The mass spectra that result show that analyte molecules fall into one of three categories with respect to their behavior upon rapid heating. Type I compounds exhibit desorption rates that are much higher than degradation rates (at the temperature required for K<sup>+</sup> emission by the K+IDS probe). Upon heating, type I molecules desorb intact, and the (M+K)<sup>+</sup> adduct ion is observed in the resulting mass spectrum. Only molecular weight

information is provided in the mass spectrum. Type II compounds have competitive desorption and decomposition rates at the temperatures used in  $K^+IDS$ . Intact analyte molecules, M, and thermal degradation products,  $D_i$ , appear in the gas phase above the heated surface leading to  $(M+K)^+$  and  $(D_i+K)^+$  ions in the mass spectrum, yielding molecular weight and structural information. Type III molecules are those for which degradation and desorption rates are strongly temperature dependent within the temperature range accessible in the  $K^+IDS$  experiment. For this class of compounds, the temperature variable can be controlled to favor desorption or degradation.

K<sup>+</sup>IDS analyses of mixtures of type II compounds yield exceedingly complex mass spectra that would be difficult to interpret for quantitative information. If mixtures of type I and/or type III compounds are analyzed by K<sup>+</sup>IDS, experimental conditions can be selected such that each component (M<sub>i</sub>) will lead to ion current at only one m/z value (as well as its natural isotope peaks) corresponding to the (M<sub>i</sub>+K)<sup>+</sup> species. If rates of (M<sub>i</sub>+K)<sup>+</sup> formation are approximately independent of the chemical nature of M<sub>i</sub>, the resulting mass spectrum will be a "molecular weight profile" of the mixture. The following sections show that: a) organic acids behave as type I compounds; b) K<sup>+</sup>IDS spectra of synthetic mixtures represent the relative concentrations of the species present; and c) K<sup>+</sup>IDS spectra can be obtained for complex mixtures of organic acids isolated from urine. From these first studies, we suggest that these spectra can be used, in many cases, for the rapid screening of urine samples for the identification of organic acidurias.

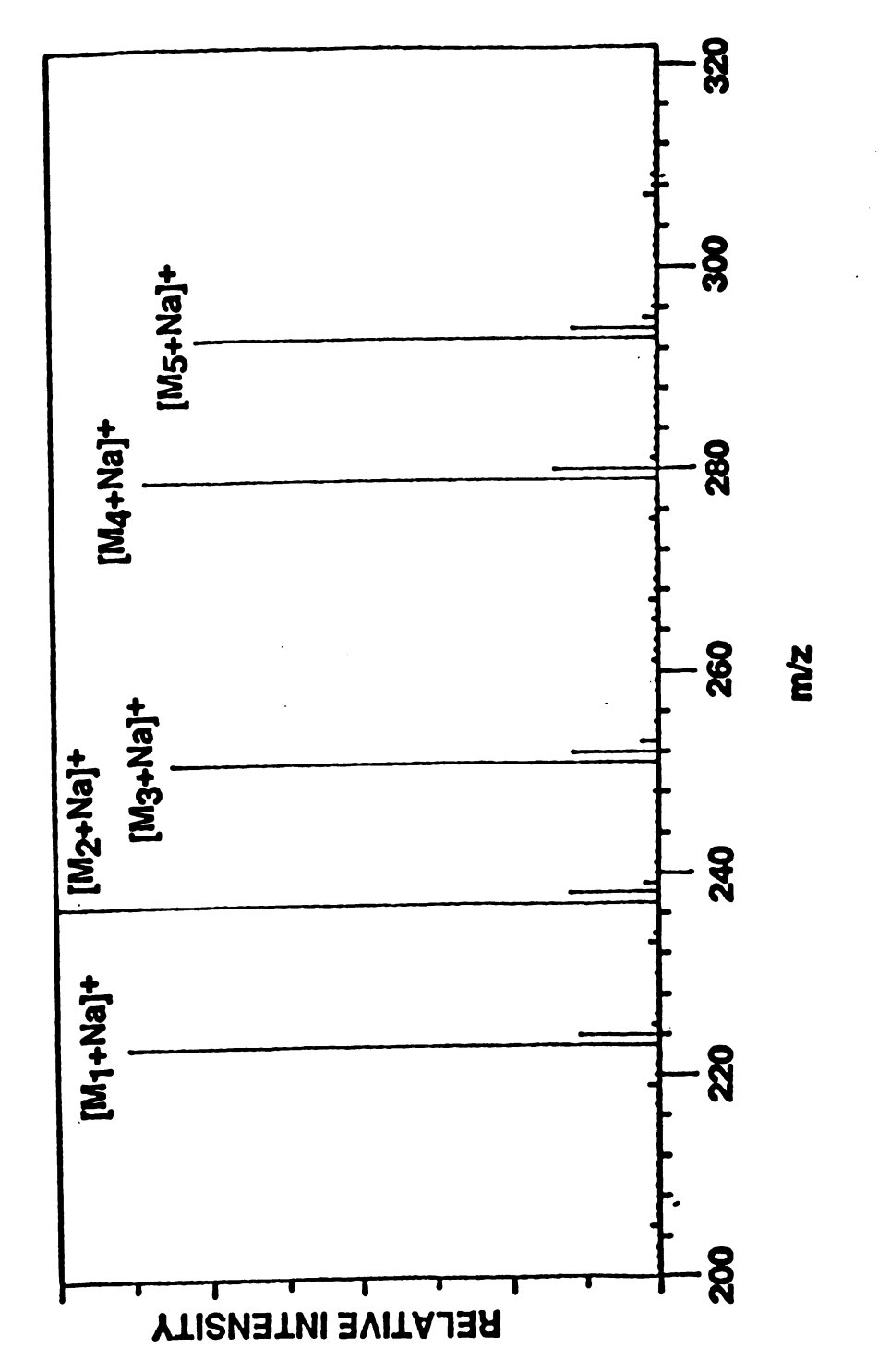
The results of a K<sup>+</sup>IDS analysis of myristic acid, CH<sub>3</sub>(CH<sub>2</sub>)<sub>12</sub>COOH, are shown in Figure 17, in order to demonstrate behavior typical of the organic acids incorporating the new probe design. Upon rapid heating, the desorption profile is fairly short-lived, as shown in the upper insert. Desorption of analyte generally occurs



Total ion current (TIC) profile (upper insert) and K<sup>1</sup>IDS mass spectrum of Myristic acid (CH<sub>2</sub> (CH<sub>2</sub>)  $^{1}_{2}$  CO<sub>2</sub>H). Figure 17:

over 15 scans. Rapid heating of the alkali emitter to approximately 1000 °C results in the desorption of the intact acid. Alkali ion attachment yields an (M+K)<sup>+</sup> ion at m/z 267 as the only ion observed at m/z values greater than those for the K<sup>+</sup> ions at m/z 39 and 41.

There are, of course, many chemical events that can occur when a mixture is heated, even if thermal degradation does not occur. One possibility is reaction involving two or more components, yielding species not originally present in the mixture. To test this for organic acids, a synthetic mixture of five fatty acids was studied. In the analysis of fatty acids, organic acids, and other analytes, it was found that better sensitivity is observed when Na<sup>+</sup> is used in place of K<sup>+</sup>. The experiments that follow will all utilize Na<sup>+</sup> (i.e., Na<sup>+</sup>IDS). The only difference is that the thermionic emission material is an aluminosilicate material made with sodium oxide. Figure 18 shows the Na<sup>+</sup>IDS mass spectrum for a nearly equimolar mixture (c.a. 4 nmoles each) of five fatty acids. The (M+Na) + ions are observed for each component of the mixture. The five ions are of approximately equal abundance, reflecting the equimolar nature of the mixture. A more accurate representation of the mixture is obtained from the data that results from integrating over the entire elution profile. The integrated areas for each of the five (M<sub>i</sub>+Na<sup>+</sup>) ions over the entire reconstructed mass chromatograms reveal deviations from the mean relative concentrations that are no greater than 10 per cent. No ions suggesting reaction between these components are observed. Thus, it is believed that the Na<sup>+</sup>IDS analysis of this simple mixture shows that the Na<sup>+</sup>IDS spectra of more complex mixtures will reflect the distribution of the components of the mixture separated on the basis of their molecular weights, thereby providing a molecular weight profile. In fact, this behavior is observed even for a complex synthetic mixture of steroids, organic acids,



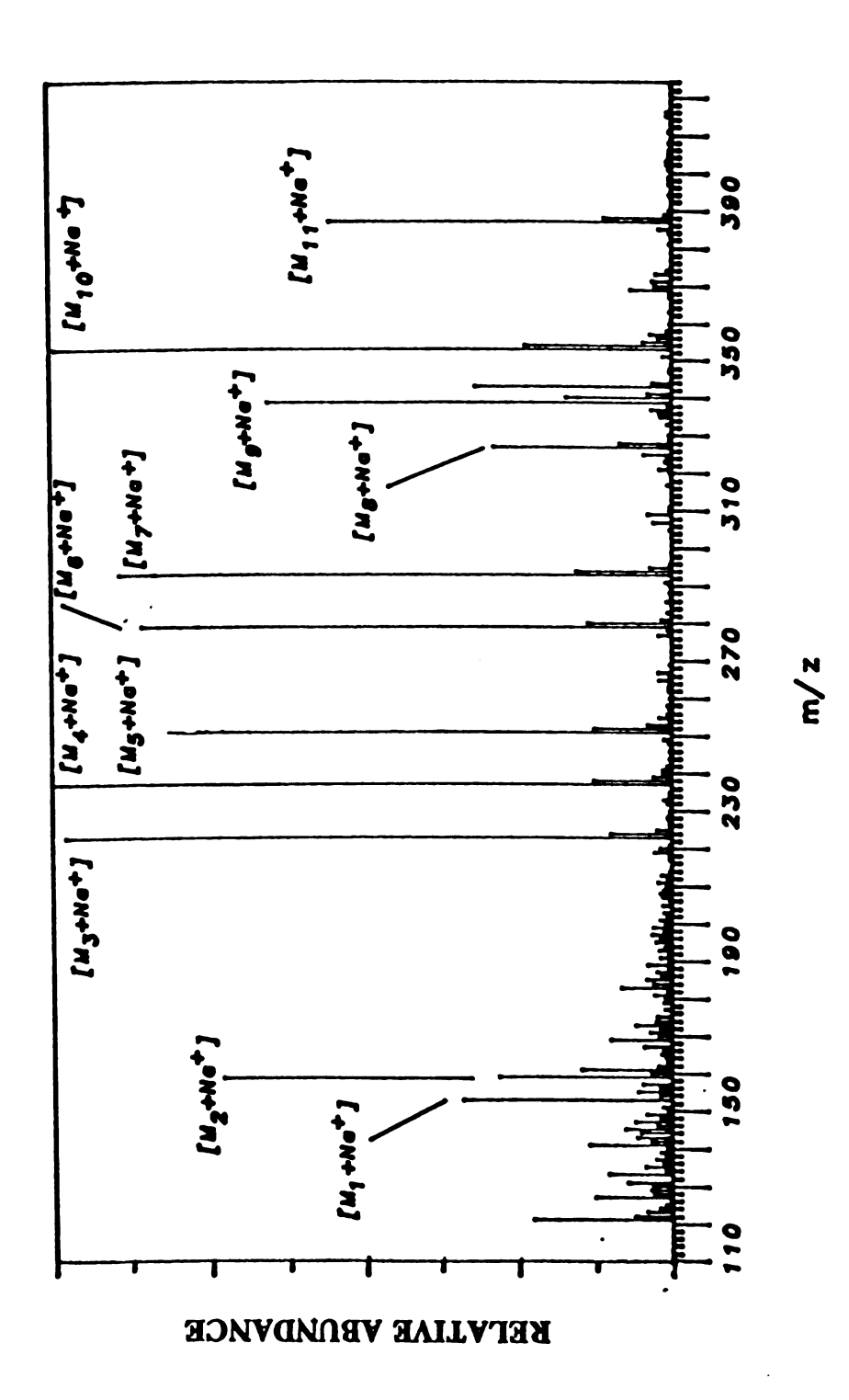
Na<sup>+</sup>IDS mass spectrum of an equimolar mixture of C-12, C-13, C-14, C-16, and C-17 free farry acids. Figure 18:

and fatty acids. The same five fatty acids discussed earlier were added to a mixture of low molecular weight organic acids and steroids. The combined mixture was placed onto the sample filament holder and a K<sup>+</sup>IDS analysis performed. The results of such an experiment are summarized in Figure 19. The relative intensities of the fatty acid mixture are maintained, even in the presence of other simultaneously desorbing species. There is no evidence in the mass spectra of mixtures of this type for chemical reaction between species. Molecular weight information is generated solely for individual components of the synthetic mixture.

### K+IDS for urinary organic acid profiling:

For simple mixtures, K<sup>+</sup>IDS (or Na<sup>+</sup>IDS) mass spectra not only represent the individual components of the mixture, but also reflect the relative concentrations of these species. This information is available on a very rapid time-scale. The results presented above suggest that this technique may be extended to the analysis of organic acids in urine, for the rapid differential diagnosis of various metabolic disorders.

Patients exhibiting the condition of MSUD are found to excrete abnormally high levels of 2-hydroxyisovaleric, 2-hydroxy-3-methylvaleric, and 2- and 3-hydroxybutyric acids in urine. Data from GC and GC-MS analysis of the derivatized organic acids of MUSD urine were obtained in collaboration with Chamberlin, et al. 55 and are summarized in Table 1. The most abundant organic acids in the mixture are identified and their concentrations relative to the internal standard, tropic acid, are given. Based on the information presented in Table 1, it is possible to



Na DS averaged mass spectrum of a complex mixture of organic acids, fatty acids, and steroids analyzed simultaneously. Figure 19:

Table 1. Twenty-five most abundant organic acids in MSUD urine identified from GC and GC-MS analyses.

Ref. Int. (RD) 9.58 9.55 9.55 9.55 9.55 9.55 9.55 9.55	. 6. 9. 8. 9. 8. 9. 8. 9. 8. 9. 8. 9. 8. 9. 8. 9. 8. 9. 8. 9. 8. 9. 8. 9. 8. 9. 8. 9. 9. 9. 9. 9. 9. 9. 9. 9.
Int. Area(IA)*  2 4 4 4 4 4 4 4 4 4 4 4 4 4 4 4 4 4 4	48 41 <b>4</b>
113 113 113 113 113 127 127 127 131 141 141 143 143 153 155 155 155 155	202 203 215
74 74 76 76 76 76 76 76 76 76 76 76 76 76 76	180 192
Organic Acid Glycolic Lactic Oxalic 2-ketobutyric 2-bydroxybutyric 3-bydroxybutyric 3-bydroxybutyric 2-ketovaleric 2-ketovaleric 3-bydroxyisovaleric Succinic Met bylmalonic 4-deoxythreonic 4-deoxythreonic 2-deoxythreonic 2-deoxythreonic 2-deoxythreonic 2-deoxythreonic 2-bydroxybenylactic Glutaric 2-OH-3-Me-valeric Glutaric 2-OH-3-Me-valeric Glutaric 2-bydroxybenylactic	. Hippuric Dextrose Citric
#176465432110 2210	22.5

(a) Values are obtained relative to the internal standard, tropic acid (10µg/ml urine) and are in arbitrary units.

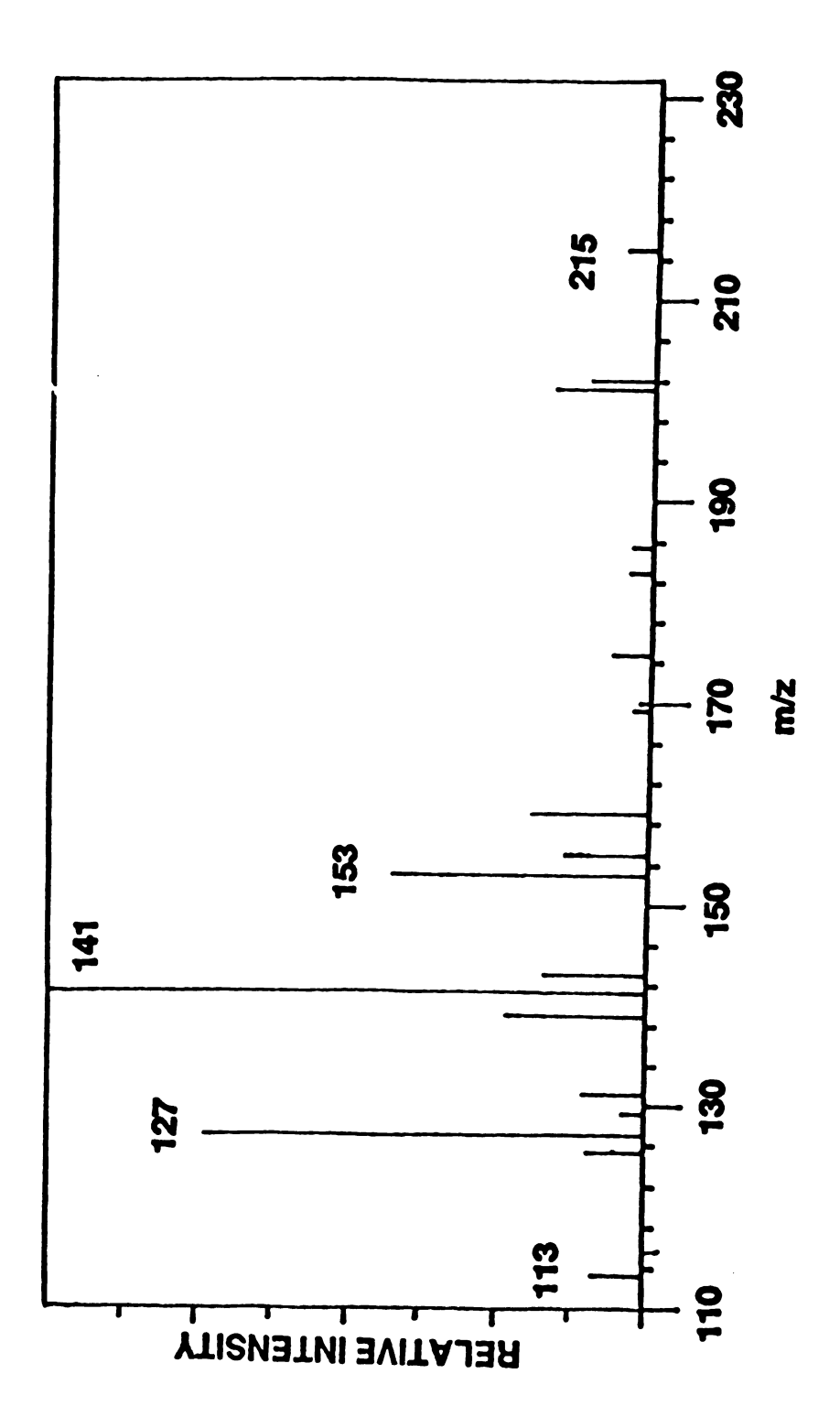
(b) Relative intensities (R.I.) are generated from integrated areas (I.A.). e.g.,

Lactic = [ LA. (lactic) /  $\Sigma$  LA. (m/z 141) ] x 100.

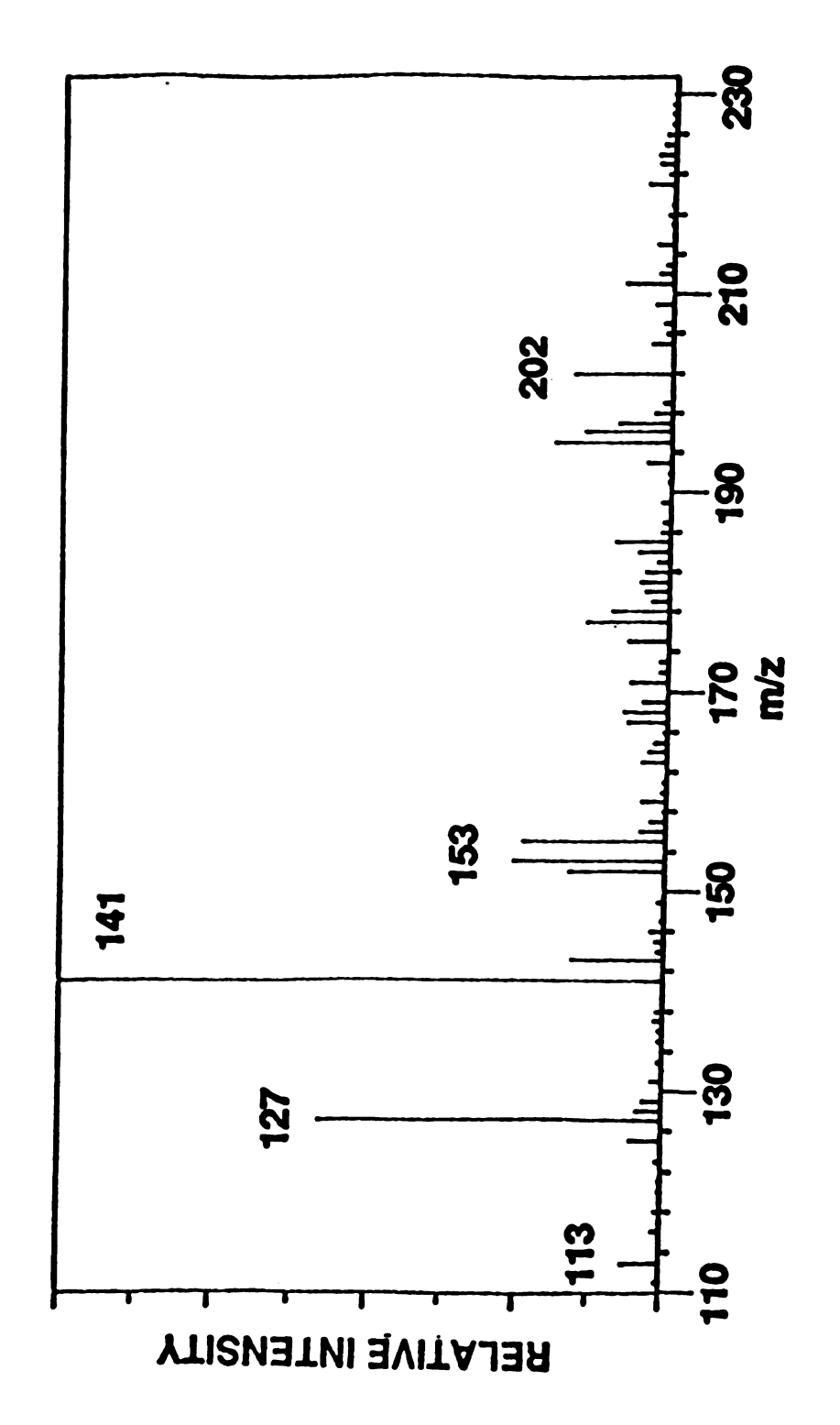
(c,d) Coeluting species, concentrations estimated from ion intensities from GC-MS analyses.

construct a simulated molecular weight profile of the major components in the MSUD urine, as would be expected in the Na<sup>+</sup>IDS mass spectrum. For each compound whose concentration and molecular weight is known, 23u is added to simulate Na<sup>+</sup> attachment to the neutral molecule. All species of the same molecular weight will be indistinguishable in such a representation. The relative intensities of all components of the same molecular weight are added, giving a summed intensity for that particular This simulated Na<sup>+</sup>IDS spectrum can then be compared to the experimentally obtained one. Shown in Figure 20 is this reconstructed composite mass spectrum reflecting the identified compounds from GC and GC-MS analysis. Although isobaric compounds may not be differentiated in such a representation, information may still be gleaned from perusal of the molecular weight distribution of the organic acids from this urine. The designate ion for this metabolic condition is found at m/z 141, corresponding principally to [2-hydroxyisovaleric acid + Na<sup>+</sup>]. Confirming ions for this disease state are at m/z 127 and 153, corresponding to Na<sup>+</sup> adducts of 2-, and 3-hydroxybutyric acids, and 2-keto-3-methylvaleric acid, respectively, based on their intensities relative to the Na<sup>+</sup> adduct of 2hydroxyisovaleric acid.

The Na<sup>+</sup>IDS molecular weight profile for the organic acids isolated from the urine of a patient suffering from MSUD is shown in Figure 21. As expected, the major organic acid metabolite is 2-hydroxyisovaleric acid, leading to the signal at m/z 141 (the [M+Na<sup>+</sup>] adduct). The confirming ions for the disease-state are also evident in the mass spectrum. The similarities between the simulated Na<sup>+</sup>IDS mass spectrum of the mixture of organic acids from this urine based on the available GC and GC-MS data and the experimentally obtained Na+IDS mass spectrum are quite striking. Slight differences in the two profiles might be attributed to the fact that not all of the



organic acids present in urine of a patient with Maple Syrup Urine Discase (MSUD). Simulated Na DS molecular weight profile of the 25 most abundant Figure 20:



Experimentally obtained Na IDS averaged mass spectra of organic acids from same patient with MSUD. Figure 21:

components from GC and GC-MS analysis have been identified. Unknowns cannot be included in the simulated molecular weight profile since no molecular weight information is available for these species to date.

Obviously a molecular weight profile of a complex mixture of organic acids will not allow isobaric species to be individually identified. Thus, quantifying species, on an absolute scale, is not always possible. For the diagnosis of the organic acidurias, however, there is typically one component present at a concentration that is extremely elevated in urine, which may be used to identify the disease state. The relative concentration differences between a "healthy"-state and disease-state is often the information of interest when screening for organic acidurias. Targeting for a specific urinary organic aciduria based on the elevation of a particular organic acid allows this direct method to be useful for differential diagnosis.

The average Na<sup>+</sup>IDS mass spectrum of the urinary organic acid from healthy, lactic acidotic, and isovaleric acidemic individuals are shown in Figure 22 (a-c), respectively. Inspection of these molecular weight profiles certainly suggests that disease-state and healthy urinary organic acid profiles can be differentiated easily.

The lactic acidosis condition is characterized by excessive levels of lactic acid in both plasma and urine. Pyruvate dehydrogenase deficiency, an enzyme defect frequently associated with lactic acidemia, causes accumulation of this organic acid in urine. The Na<sup>+</sup>IDS mass spectrum of acids isolated from this urine indeed suggests, that lactic acid which appears as the Na<sup>+</sup> adduct at m/z 113 is the major excreted metabolite. Summarized in Table 2 are the prominent organic acids from the Na<sup>+</sup>IDS mass spectrum and their relative concentrations (obtained from available GC and GC-MS data). The relative concentrations of the organic acids are in good agreement, in general, with the ion abundances observed in the Na<sup>+</sup>IDS-mass spectrum.

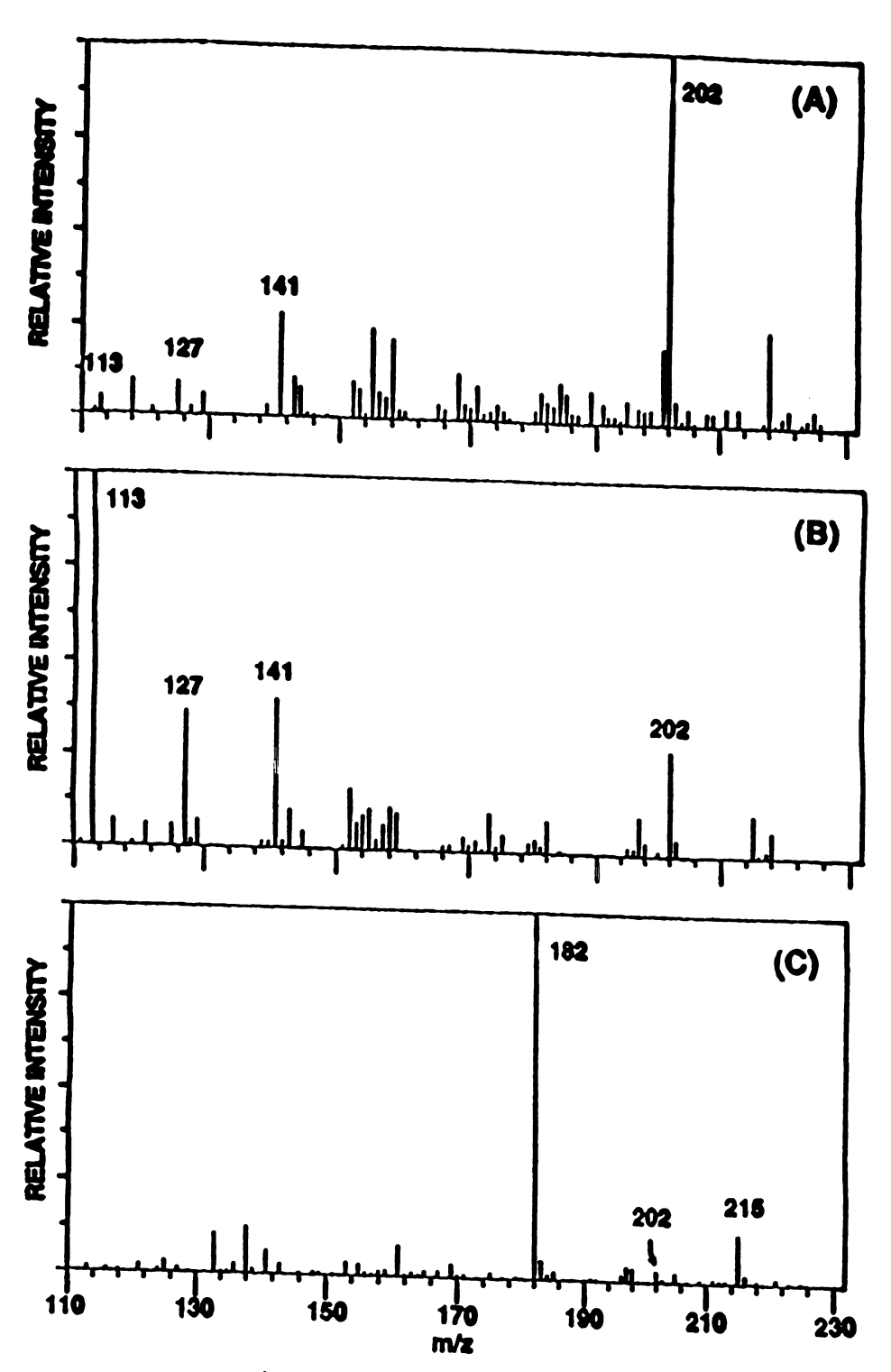


Figure 22. Averaged Na<sup>+</sup>IDS mass spectra of organic acids from (a) healthy, (b) lactic acidosis, and (c) isovaleric acidemia wrines

Table 2. Major organic acid metabolites identified from GC-MS data for the ten most abundant organic acids in methylmalonic urine.

	Organic Acid	Concentration (a.u.) <sup>‡</sup>	m/z (M+Na+)
•	(a) Lactic, Oxalic, 3-hydroxypropionic 2-hydroxybutyric, 3-hydroxybutyric 3-hydroxyisovaleric, 3-hydroxyvaleric, succinic Hippuric Citric, Isocitric	600 130 63 · 120 60	113 127 202 215
<b>a</b>	(b) Erythronic, Threonic Isovalerylglycine Hippuric Citric, Isocitric	240 3100 60 300	159 182 202 215
<b>9</b>	(c) Lactic, Oxalic 2-hydroxybutyric, 3-hydroxybutyric, 2-hydroxyisobutyric, 3-hydroxyisobutyric 3-hydroxyisovaleric, 3-hydroxyvaleric, Succinic Hippuric	61 68 11c 74 350	113 127 14 202
€	(d) Lactic, Oxalic Methylmalonic, Succinic 3-hydroxy-3-methylglutaric Hippuric	83 1300 63 330	113 141 185 202

‡ Concentration values for organic acids are determined from GC and GC-MS data of the derivatized species and have concentration values relative to the internal standard.

Similarly, the isovaleric acidemia condition may be identified easily from extremely elevelated levels of isovalerylglycine excreted in urine. The reconstructed total ion current (TIC) profile (Figure 23) from the GC-MS analysis of the derivatized organic acids of the isovaleric acidemia urine shows the massive accumulation of this metabolite. The Na<sup>+</sup>IDS mass spectrum of the underivatized organic acids from the same urine reveals an identical situation. The base peak in the Na<sup>+</sup>IDS mass spectrum is due to isovalerylglycine, (m/z of [M+Na<sup>+</sup>] = 182). The major organic acids identified, and their relative concentrations are also summarized in Table 2.

The results are not surprising, since numerous reports on this condition suggest that isovalerylglycine may be excreted at levels more than 2000-fold over those in healthy individuals. To confirm that the Na<sup>+</sup>IDS mass spectra provide reasonable quantitative representations of the actual organic acid compositions, a simulated molecular weight profile was constructed for the isovaleric acidemia urine, in a manner identical to that described for the MSUD urine. The "simulated" molecular weight profile in Figure 24 is compared with the experimentally obtained Na<sup>+</sup>IDS mass spectrum (see Figure 20). In general, the profiles are in good agreement.

The results from a Na<sup>+</sup>IDS analysis of the control urine reveals the major metabolite of this urine to be hippuric acid (m/z of [M+Na<sup>+</sup>] = 202). Again, the results from the Na<sup>+</sup>IDS analysis parallel closely those obtained from GC and GC-MS.

The feasibility experiments presented here suggest that the K<sup>+</sup>IDS (or Na<sup>+</sup>IDS) method is capable of differentiating between some of the more commonly occurring organic acidurias such as lactic acidemia, isovaleric acidemia, MSUD, and controls. However, one might expect that this method would fall short in its utility for distinguishing between those disease conditions in which the principal metabolites are

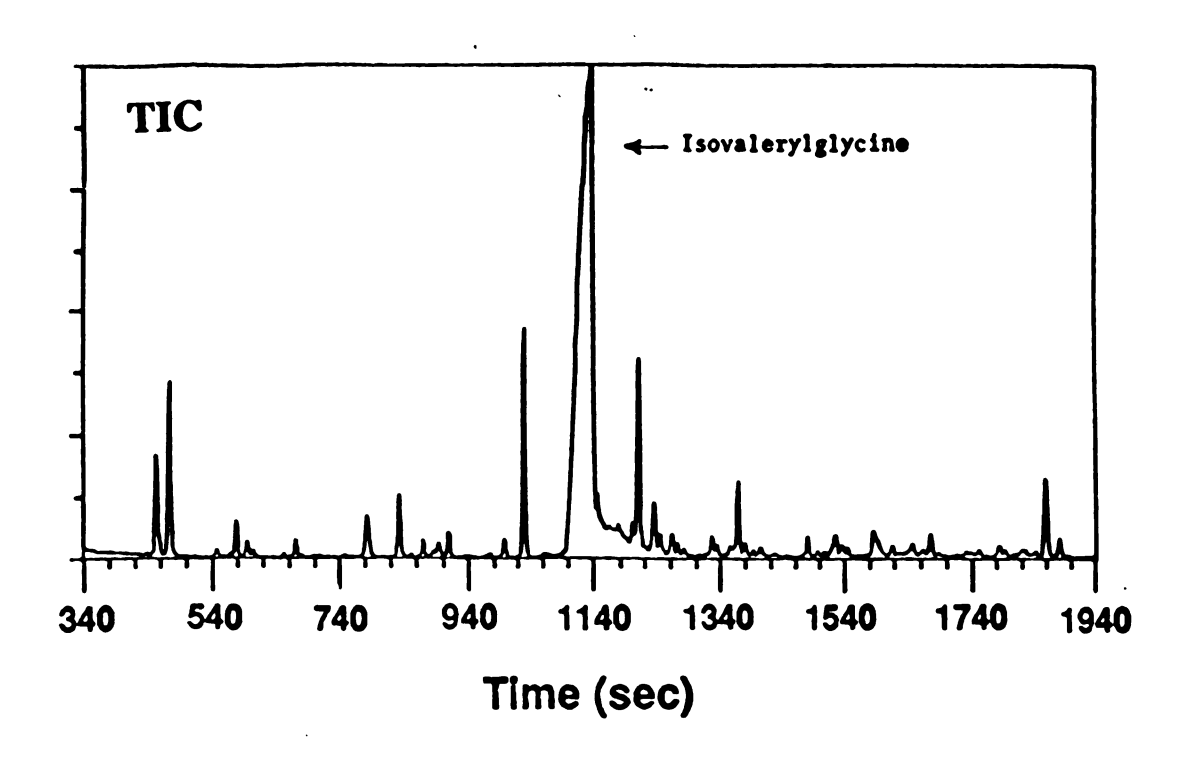
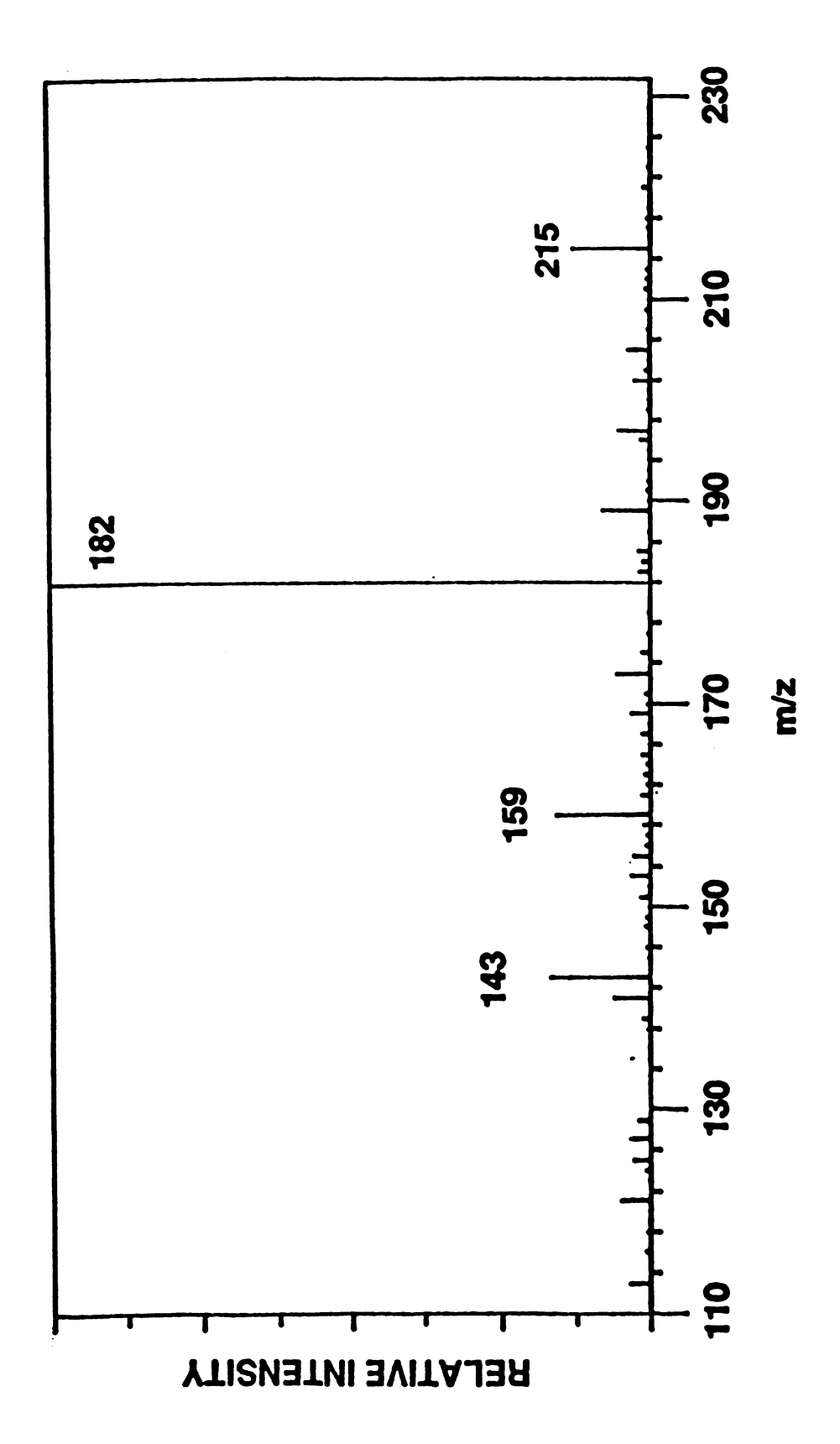


Figure 23. TIC profile of the trimethylsilyl derivatives of organic acids isolated from isovaleric acidemia urine

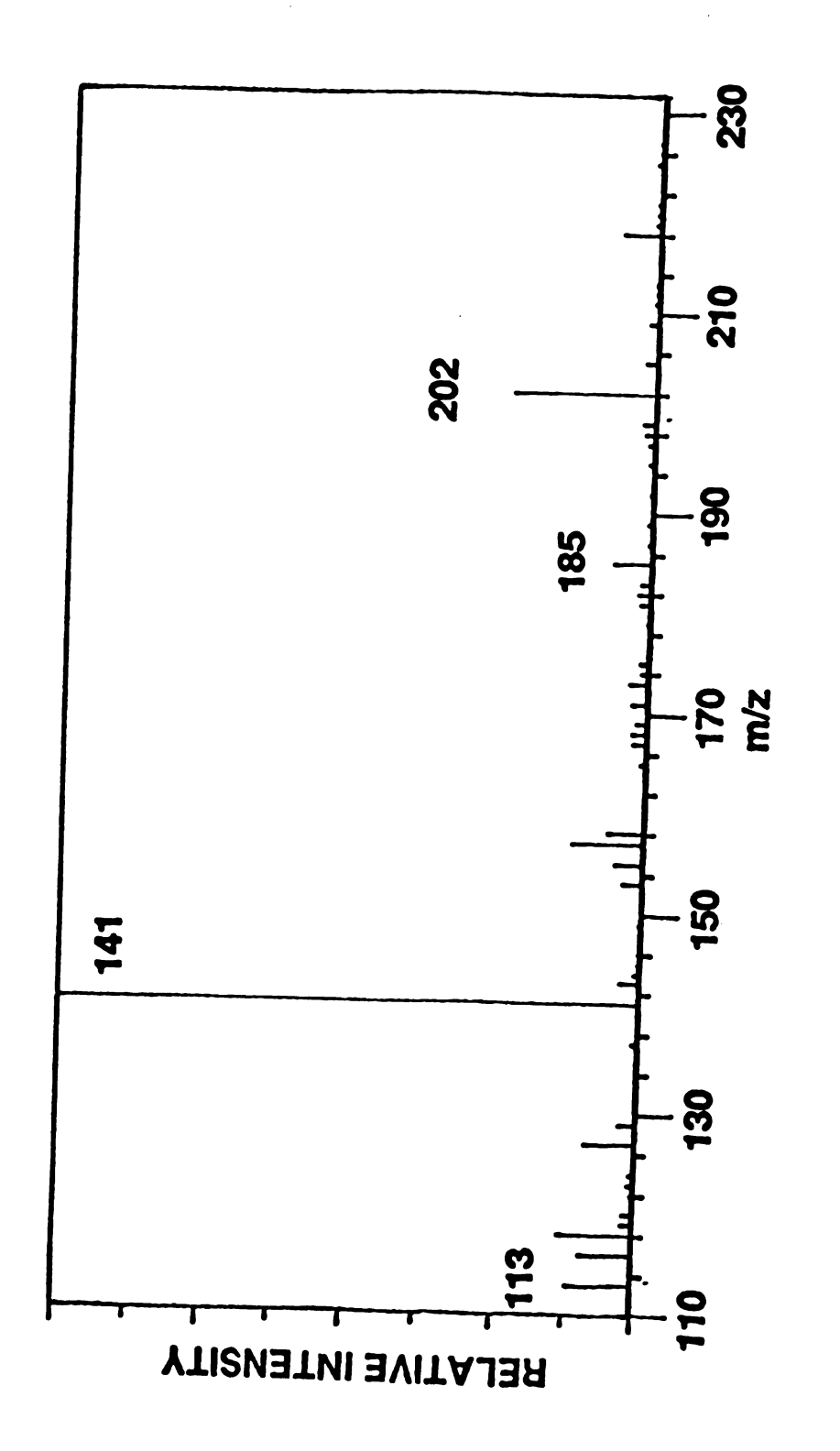


Simulated Na DS molecular weight profile of the 25 most abundant organic acids present in urine of patient with isovaleric acidemia. Figure 24:

of the same nominal molecular weight (but each arising from different metabolic pathways). A suitable example describes the capacity of the Na<sup>+</sup>IDS technique to differentially diagnose methylmalonic acidemia and MSUD. In the two cases, the major metabolites, methylmalonic acid and 2-hydroxyisovaleric acid, respectively, have molecular weights of 118 Daltons, leading to the (M+Na<sup>+</sup>) adduct at m/z 141 in a Na<sup>+</sup>IDS analysis.

Can these two disease-states be differentiated, even though the major metabolites associated with the conditions are of the same nominal mass? The answer is found by examining not only the designate ion for the diseases but also the confirming ions expected for each disorder. In the case of MSUD, these species have been identified, and their intensities relative to the peak at m/z 141 have been discussed. For methylmalonic acidemia, on the other hand, these compounds are of only relatively low concentration and do not lead to prominent ions for this disease-state. The Na<sup>+</sup>IDS mass spectrum of the organic acids isolated from the methylmalonic acidemia urine are shown in Figure 25. Other ions in addition to methylmalonic acid that have been identified in the Na<sup>+</sup>IDS mass spectrum are summarized in Table 2.

In cases where the differences may not be entirely obvious, K<sup>+</sup>IDS may be utilized in mass spectrometers that provide additional features. For example, if information is required on isobaric ions, a high resolution mass spectrum may be of utility. If true isomers must be differentiated, K<sup>+</sup>IDS as an ionization method with subsequent MS/MS analysis may be a viable approach. The feasibility of the K<sup>+</sup>IDS experiment on simple mixtures using a high resolution JEOL HX110 double-focusing mass spectrometer is currently being evaluated.



Averaged Na IDS mass spectra of urinary organic acids isolated from patient with methylmalonic acidemia. Figure 25:

#### Conclusions

Over 50 organic acidurias have been identified and only a few of the more commonly occurring organic acidurias have been shown to be quickly and easily identified using the desorption/ionization method of K<sup>+</sup>IDS. As a screening procedure, this method appears to be a viable, low-cost and extremely rapid alternative to GC-MS. Although not as useful for studying metabolic pathways, when combined with more advanced systems such as high resolution mass spectrometers, these questions may be addressed. Future work will deal with extending the dynamic range of this method for such analyses of complex mixtures.

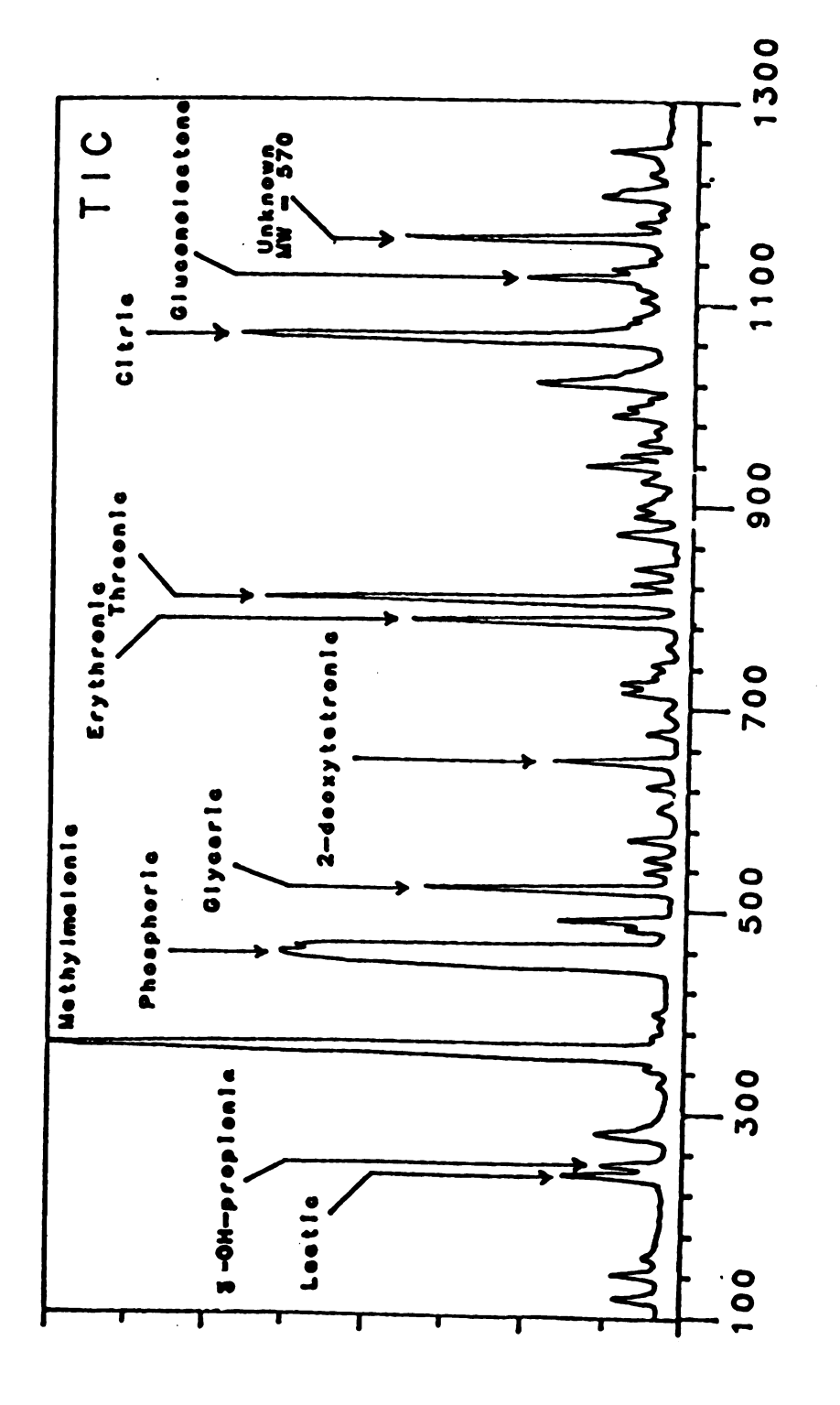
The final question that must be answered is whether or not these K<sup>+</sup> IDS molecular weight profiles are <u>truly</u> representative of the components of a complex mixture. Comparisons between simulated molecular weight profiles and those obtained experimentally suggested that K<sup>+</sup> IDS mass spectra do indeed represent fairly accurately the components of a mixture. Simulated molecular weight profiles were constructed based on results of the known, 25 most abundant species from available GC data and compared to the experimentally obtained K<sup>+</sup> IDS spectra. However, a number of unknowns exist in the gas chromatographic libraries of the organic acids. These unknowns can often be fairly concentrated components of urine, and when their concentrations are great, these unknowns must be taken into account.

The best way to go about elucidating the identity of the unknowns from GC analyses is to combine GC with mass spectrometric detection. In the production of simulated molecular weight profiles the molecular weight of the unknowns is what is desired. As will be shown in the next few chapters, EI mass spectra of derivatized organic acids frequently are devoid of molecular ions. The technique of NH<sub>3</sub>-CI

mass spectrometry is capable of providing abundant molecular weight information on organic acids.

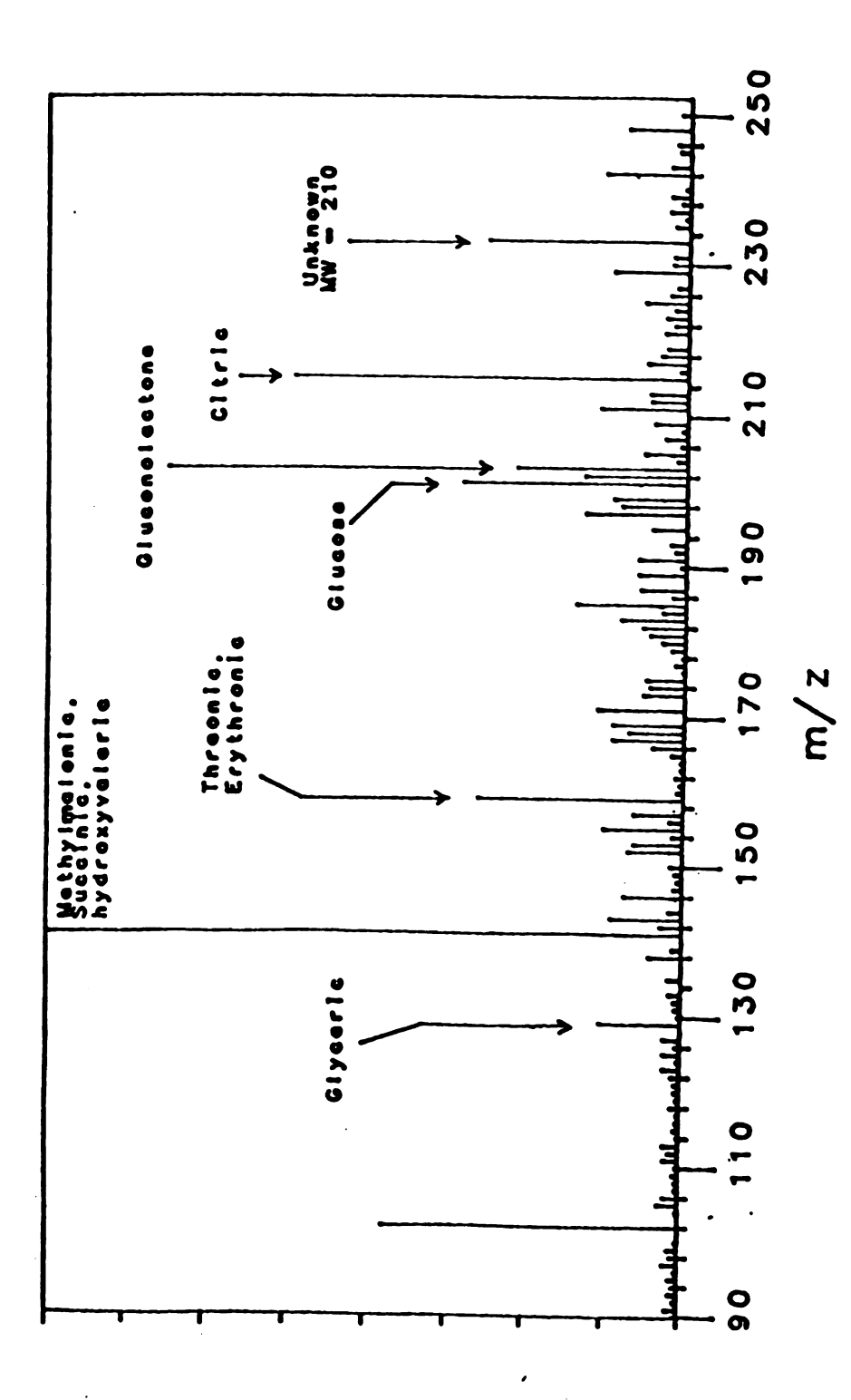
To better evaluate the quantitative capabilities of K<sup>+</sup>IDS (Na<sup>+</sup>IDS) for metabolic profiling, the urinary organic acids from another patient suffering from methylmalonic acidemia were isolated and lyophilized. The organic acid residue was dissolved in approximately 2ml of acetonitrile. One half of the solution was evaporated to dryness and derivatized with BSTFA/Pyr to form the trimethylsilyl derivatives. The other half was stored for "batch" analysis by Na<sup>+</sup>IDS.

The derivatized organic acids were analyzed by both EI and NH<sub>3</sub>-CI in order to obtain molecular weight information on the major organic acid constituents. Shown in Figure 26 is the reconstructed TIC chromatogram of the derivatized organic acids. The major component, as expected was methylmalonic acid (di-TMS). A major component which eluted late during the GC-MS analyses was found to have a (derivatized) molecular weight of 570 from NH<sub>3</sub>-CI results. This compound was found to have a total of five TMS groups, as determined from analyses using the deuterated analog of BSTFA. From these data, the underivatized molecular weight of species was determined to be 210 u. In addition, a number of molecular weight determinations were made on other unknowns contained in the mixture. This information was useful for comparing the molecular weights of all species contained within the mixture with the molecular adduct ions observed as a result of the susbsequent Na<sup>+</sup>IDS analysis. The GC-MS analysis was followed by the "batch" Na<sup>+</sup>IDS analysis on the other isolated organic acid fraction. The averaged Na<sup>+</sup>IDS mass spectra of the underivatized organic acids is shown in Figure 27. The base peak in the mass spectrum was the [M+Na<sup>+</sup>] adduct ion of methylmalonic acid and other isobaric species were found to contribute, to a small extent, to the overall abundance of this ion at m/z 141. The unknown having a MW = 210 was also observed as the



TIC profile of trimethylsilyl derivatives of organic acids isolated from a second methylmalonic urine. Figure 26:

Scan



Averaged Na IDS mass spectra of the underivatized organic acids from the same methylmalonic acidemia urine. Hgure 27:

sodium adduct ion at m/z 233. The Na IDS mass spectra in general accurately reflected the true composition of organic acids in this disease-state condition. Integrated areas are compared to relative ion intensities for the most abundant organic acids in this mixture and are summarized in Table 3.

The one major differences in these two profiles is that a large peak corresponding to phosphoric acid was observed in the reconstructed TIC chromatogram but no ion corresponding to the sodium adduct (i.e., m/z =125) was found in the Na<sup>+</sup>IDS mass spectrum. A possible explanation for this difference is as follows. Results from negative ion surface ionization mass spectrometry have suggested that compounds such as these can readily decompose on "hot" surfaces, resulting in the formation of the PO<sub>3</sub><sup>-</sup> and P<sub>2</sub>O<sub>5</sub><sup>-</sup> anions. <sup>37,56</sup> These species arise from decomposition on the surface followed by electron attachment from a surface of relatively low work function (i.e., Cs<sub>2</sub>O:Al<sub>2</sub>O<sub>3</sub>:SiO<sub>2</sub>). Na<sup>+</sup> adducts of these neutral decomposition products were not observed and would not be expected to undergo addition reactions with alkali ions.

The capabilities of K<sup>+</sup>IDS for mixture analysis has been demonstrated for compound classes as varied as polymers, synthetic mixtures of fatty acids and complex mixtures of urinary organic acids. In addition, the relative concentrations of fatty acid components have been found to be unaffected by the presence of other compound types in a K<sup>+</sup>IDS analysis. The ability to derive quantitative information from mixtures containing several different classes of compounds appears to be possible using this technique. Future studies utilizing K<sup>+</sup>IDS for the diagnosis of organic acidurias might include a "true" batch mixture analysis of the components of urine. Work-up procedures might only involve the precipitation and acidification of inorganic salts without isolation of any particular class of compounds prior to their

Table 3. Comparison of relative intensities from Na<sup>+</sup>IDS analysis and peak areas from GC analysis for the ten most abundant organic acids in methylmalonic urine

Peak #	Compound	Area TIC_	Rel. Area	m/z [M+Na <sup>+</sup> ]	Rel. Int.
1	Lactic	48500	•	113	3
2	2-hydroxybutyric	41000	7	127	4
3	methylmalonic	5010 <b>00</b>	100	141	
4	succini <b>c</b>	530 <b>00</b>		141	100
5	glyceric	111000	20	129	13
6	2-deoxytetronic	47000		143	11
7	threonic	118000	21	159	•
8	erythronic	221000	39	159	31
9	citr <b>ic</b>	275000	49	215	65
10	UNK MW = 210	116000	21	233	28

lyophilization. Differentiation of organic acidurias by K<sup>+</sup>IDS might be achieved because these conditions are typically characterized by extremely elevated concentrations of one or more components in urine. The main problem with such an analysis is that urine has a high water content. As was alluded to earlier, water appears to be an undesirable transport medium for K<sup>+</sup>IDS studies, independent of the alkali oxide material utilized.

The real strength of this technique lies in its capabilities for producing a rapid "fingerprint" profile for various physiological conditions. It has not been developed to the extent to which it could be used exclusively for diagnosing these organic acidurias. Therefore, at present time, other methods, such as gas chromatographic analysis would be required in order that unequivocable diagnoses be made. In general, the K<sup>+</sup>IDS technique shows great promise for mixture analysis. As a desorption/ionization method that is free from matrix interferences and requires no modifications to existing mass spectrometers, this method will no doubt find greater acceptance in the area of analytical chemistry. The present design has improved dramatically the detection limits of the technique but work still remains in improving the dynamic range of the technique.

# Chapter 4: Extension of the Utility and Applications of K+IDS

Research efforts have also been concentrated on better characterizing the K<sup>+</sup>IDS technique as to its "universality" and/or limitations for organic compound analysis. These types of studies have all been performed in the context of how the K<sup>+</sup>IDS ionization technique compares to other commercially available DI methods. A major emphasis of the research in this laboratory has been to demonstrate that K<sup>+</sup>IDS may, in many cases, produce comparable mass spectra, and be a very cost-effective alternative to other more complicated and DI methods. Recall, K<sup>+</sup>IDS can be implemented on instruments as simple as table-top quadrupole mass spectrometers. The only requirement is that the instrument be equipped with a direct insertion probe inlet system. Typically, other D/I techniques require sophisticated instrumentation. In addition, techniques such as FD and FI, for example, require a great deal of expertise in the production of the ionization emitters required for non-volatile analyses.

# Organic synthesis on the K+IDS emitter surface

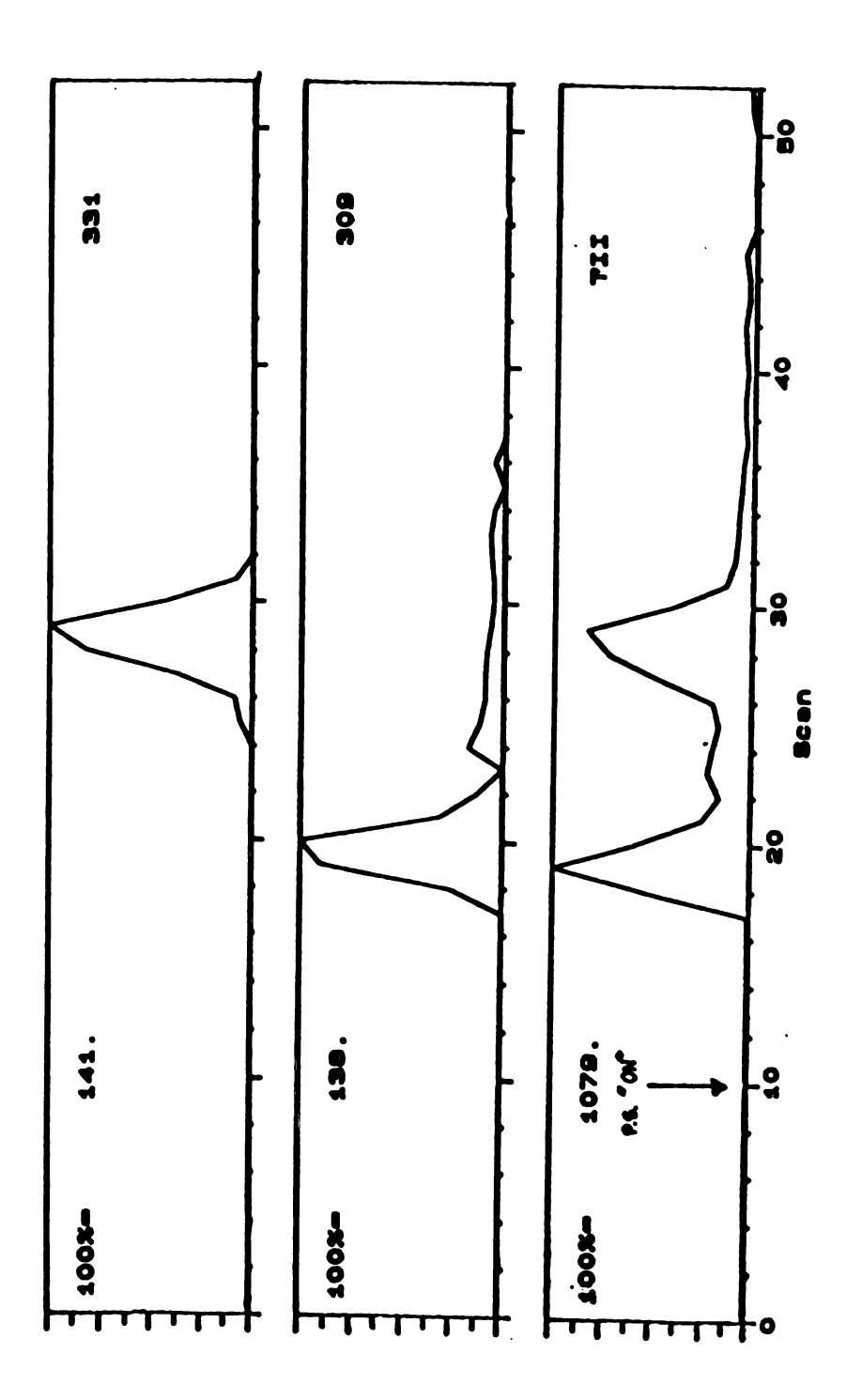
Desorption/ionization methods such as LDMS and FAB frequently utilize a salt (e.g., NaI) as part of the target containing analyte for the purpose of producing molecular adduct ion species that are frequently required in order to confirm the molecular weight of unknowns. Cationization of analyte species occurs in the gas phase. <sup>57</sup> Frequently, reactions between the two species can occur in which labile (or acidic) hydrogen atoms are replaced with alkali atoms, r leading to ions of the type [M+2A-H]<sup>+</sup>, where A = Li, Na, or K. This phenomenom has been discussed for reactions involving glycerol and various alkali salts by fast atom bombardment. <sup>57</sup> Under certain conditions, the K<sup>+</sup>IDS technique has been found to produce similar species and is capable of desorbing salts into the gas phase whereby they undergo K<sup>+</sup> ionization.

When a salt solution that is deposited onto the K<sup>+</sup>IDS probe is rapidly heated, cationization of the desorbed salt may occur. Salts of the type R-CO<sub>2</sub>Na have been found to desorb intact upon rapid heating and readily undergo adduct ion attachment to form the [R-CO<sub>2</sub>Na + Alkali ion]. This process is generally not observed using other desorption/ionization methods. The desorption of these salts, though, is not always complete and memory effects can carry over into subsequent analyses. These memory effects are easily eliminated by taking care in the cleaning of the analyte filament before another analyte solution is applied. Unique chemistry can occur on the surface of a emitter that has not been totally free from salt contamination.

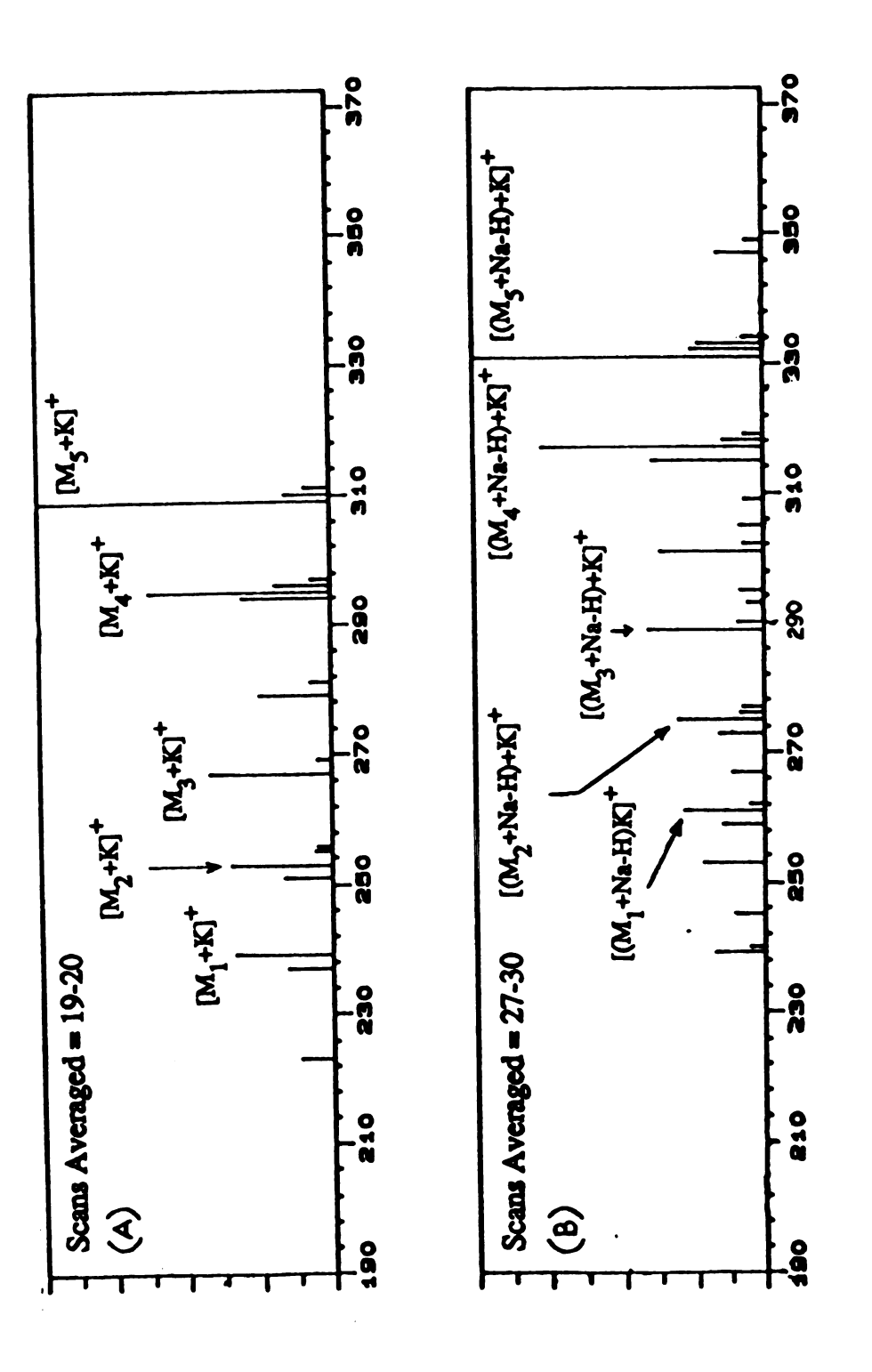
A disulfonated, biphenyl sodium salt was submitted for analysis using the technique of K<sup>+</sup>IDS since no molecular weight information was attained using other ionization methods, such as FAB. The results of analysis by K<sup>+</sup>IDS yielded

molecular weight information on the molecule through K<sup>+</sup> attachment to the desorbed species. Following the analysis of this organic salt by the K<sup>+</sup>IDS technique using the two-filament design, a mixture of five free fatty acids (C-12,13,14,16, and 17) was placed onto the analyte filament and analysis by K<sup>+</sup>IDS was performed. The results of analysis by K<sup>+</sup>IDS showed two distinct analyte desorption profiles, the second desorption profile occurring approximately 6 scans (c.a. 3 sec) following the desorption of the first species. Heating rates employed in this experiment were approximately 250°C/sec as the final current chosen was I = 3.0 A (final emitter temperature approximately 1100-1200 °C). The power supply was turned on before the tenth scan; the analyte filament was presumed to continue heating long past the time of the second analyte desorption. The TIC profile and reconstructed mass chromatograms of m/z 309 and 331 (from heptadecanoic acid) are shown in Figure 28 below. The reconstructed mass chromatogram of m/z 309 represented the [M+K<sup>+</sup>] ion for heptadecanoic acid; m/z 331 represented the [ (M+ Na - H) + K<sup>+</sup>] ion. A comparison of mass spectra obtained from the individual analyte desorption profiles revealed that all the components of the free fatty acid mixture experienced competitive salt formation prior to gas-phase K<sup>+</sup> ionization. The averaged mass spectra are compared in Figure 29 a-b. The mass spectrum of the five fatty acids obtained from the first desorption profile ) is represented predominantly by the [M+K<sup>+</sup>] ions, as labelled M<sub>1</sub>, M<sub>2</sub>, ..., M<sub>5</sub>. The averaged mass spectra from the second desorption profile showed that each of the ions were offset by 22 u, suggesting a hydrogen-sodium exchange. This process is described in more detail for palmitic acid as shown in equation 2.

$$CH_3(CH_2)_{14}CO_2H + "Na" -----> CH_3(CH_2)_{14}CO_2Na + "H"$$
 (2)



generated by K<sup>†</sup>IDS from a "contaminated" filament surface. Peak 1-free K<sup>+</sup>IDS analyte TIC desorption profiles of C-12, -13, -14, -16, -17 fatty acids; peak 2- fatty acid salts. Hguro 28:



Averaged K<sup>+</sup>IDS mass spectra of the fatty acid mixture from (a) scan 19 of analyte desortption profile 1. **Figure 29:** 

Sodium, present in some form on the emitter surface readily undergoes an exchange reaction to form the fatty acid salt. The formation of the salt species is not believed to occur through a gas phase exchange reaction since two distinct desorption profiles were observed for the clean mixture originally deposited onto the K<sup>+</sup>IDS probe.

These results were quite surprising. TIC chromatograms revealed that salt formation followed by K<sup>+</sup> addition was competitive with [M+K<sup>+</sup>] formation for the free fatty acids. In addition, the mass spectra of the fatty acid salts revealed no preferential surface chemistry between any one of the 5 fatty acids since relative ion intensity ratios comparing the free fatty acids and the fatty acid salts were maintained. Fatty acid salt formation was believed to be a result of a reaction on the surface of the analyte filament that was contaminated by the previously analyzed disulfonated, biphenyl salt. Presumably this salt did not completely desorb and coating of this salt to the rhenium filament surface was sufficient for the facile exchange reaction to occur.

Similar results for salt formation have been obtained when alkali glass materials other than the aluminosilicate alkali material are used.  $K_2CO_3$  has been used and investigated as an alternative glass material for  $K^+IDS$  analyses. In general, these materials are not nearly as long-lived as the aluminosilicate glass materials, though  $K^+$  formation from  $K_2CO_3$  occurs quite readily and  $K^+$  ion currents are quite large.  $K_2CO_3$  and other materials (e.g.  $CH_2=O$ ) are being investigated for the purpose of enhancing the local  $K^+$  ion "plasma" and local ion source pressure (just directly above the potassium emitter material). Recall, higher local ion source pressures were found to improve detection limits of the  $K^+IDS$  technique. Several mg of  $K_2CO_3$  were deposited onto the filament containing a thin coating of  $Na_2O:Si_2O:Al_2O_3$  to determine what effect, if any, the addition of this salt had on ion formation by

Na<sup>+</sup>IDS.

Stearic acid (C<sub>17</sub>H<sub>35</sub>CO<sub>2</sub>H, c.a. 10 µg) was deposited onto the second filament and the Na<sup>+</sup>IDS analysis was performed. At low m/z values, only K<sup>+</sup> was formed in high yield, apparently overshadowing Na<sup>+</sup> ion production from the aluminosilicate matrix. Similar to the results described for the fatty acid mixture in Figure 29 above. two analyte desorption profiles were observed when this compound was applied to the "clean" rhenium filament. Again, these two analyte desorption profiles were found to include both the free and the salt forms of the C-18 fatty acid. Furthermore, the extent to which stearic acid had undergone alkali exchange to form the fatty acid salt was dependent on the operating current chosen for analysis. Salt formation was found to be inversely proportional to applied heating rates to the K<sub>2</sub>CO<sub>3</sub> emitter, as shown in Figure 30 a-c. When an operating current of I=3.8A was employed in the analysis of stearic acid, only a small fraction of the free fatty acid was converted to the fatty acid salt. Intermediate free fatty acid and fatty acid salt desorption was found when operating currents of I=3.35-3.55A were employed. Salt formation was found to be favored for slower heating rates, but typically occurred at the expense of total ion abundance for the analysis, as a dramatic reduction in signal intensity was observed for identical sample loads when comparing TIC "counts" for the three analyses.

The mass spectra of the two analyte peaks observed for the K<sup>+</sup>IDS analysis performed at I=3.1A were compared. Only the  $[M+K]^+$  adduct ion, m/z = 323, was observed for the free acid form, corresponding to the first analyte signal. The second analyte signal was composed of the fatty acid salt, m/z  $[M+2K-H]^+ = 361$  as well as a number of other ions, including the  $[(M+Na-H)+K^+]$ , m/z = 345, and the free acid potassium adduct, at m/z 323. The individual mass spectra obtained for both analyte profiles are best represented by the three-dimensional mass spectral map of Figure 31 delineated in the following manner: the X-axis being defined by a 280-380 u mass

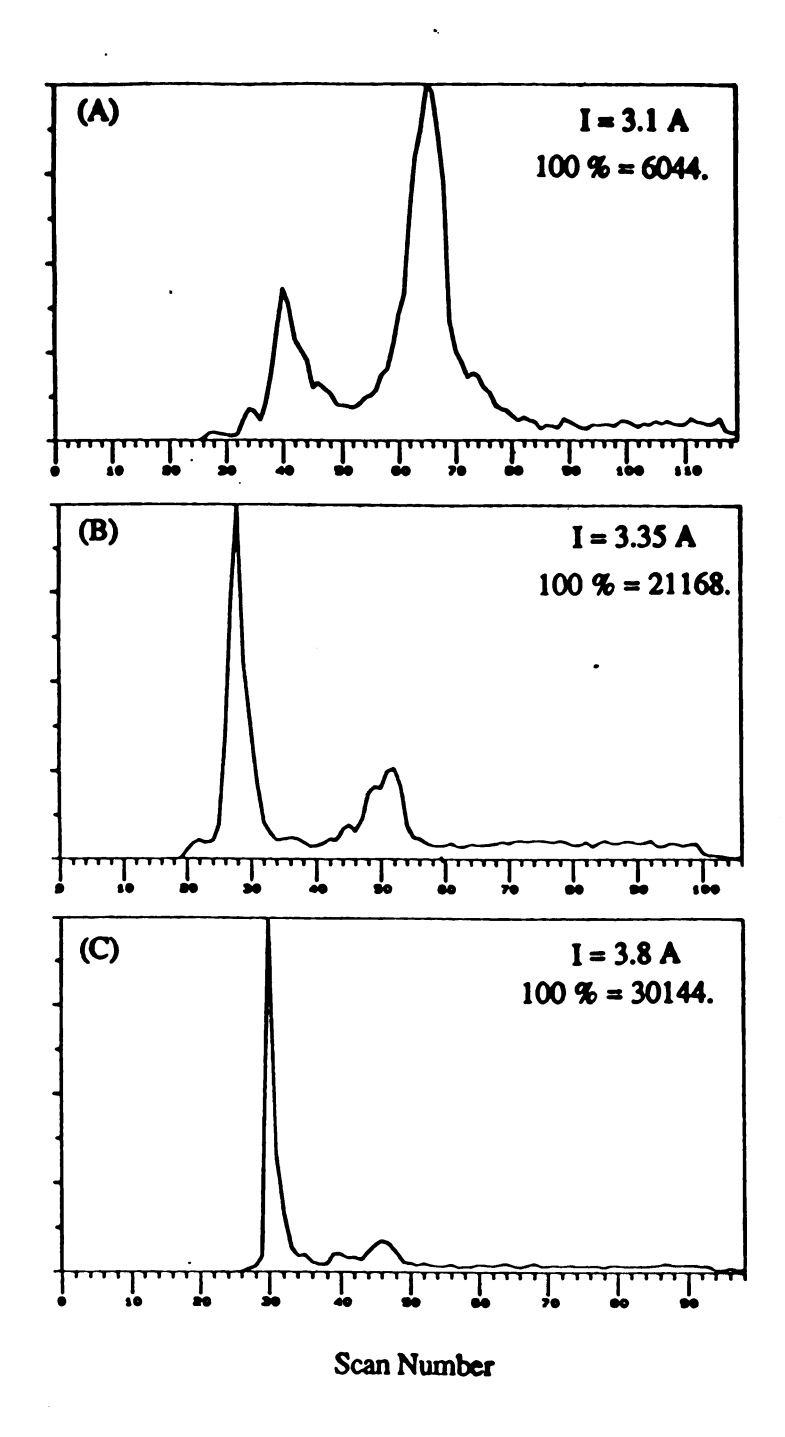
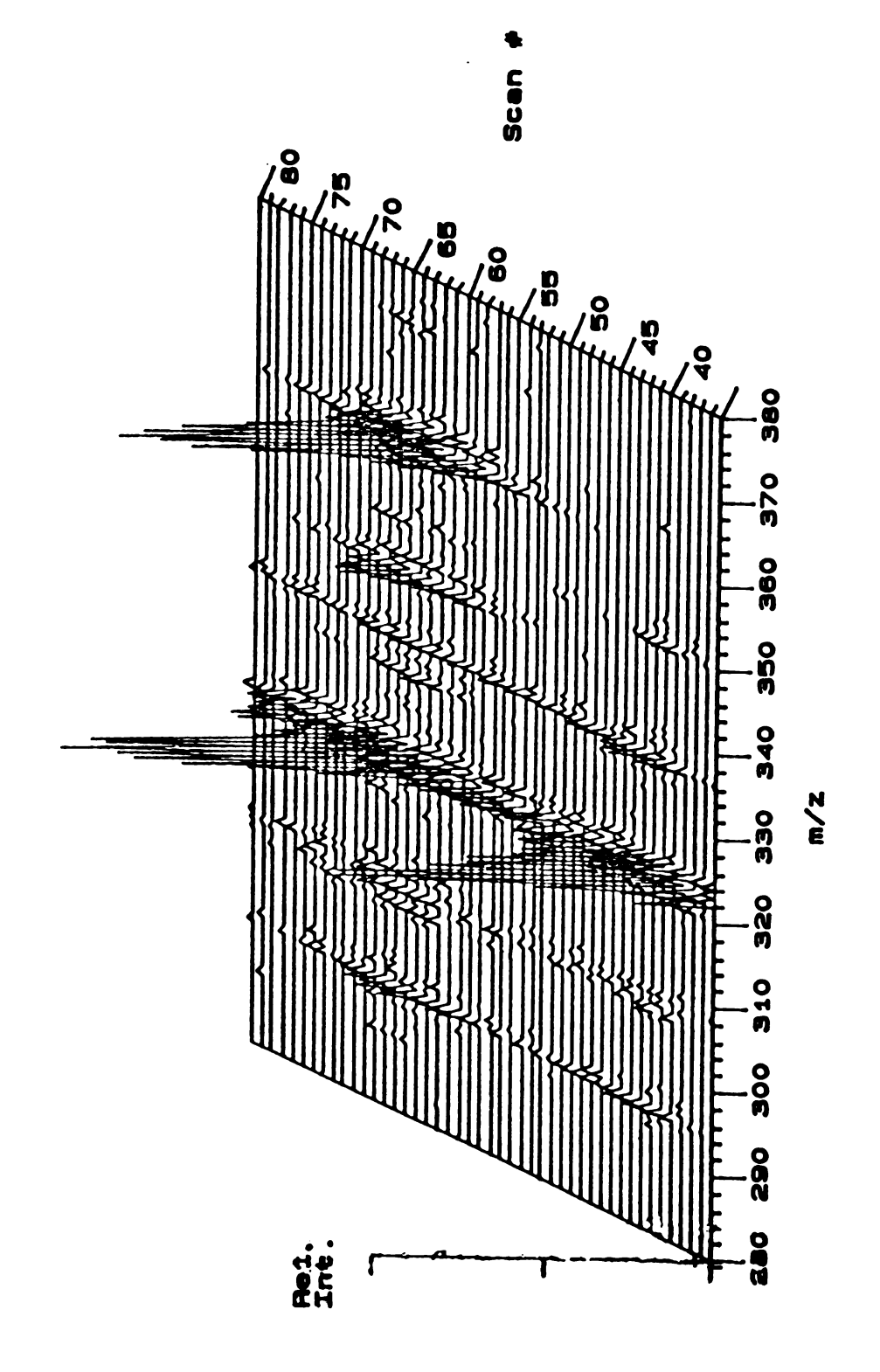


Figure 30. K<sup>+</sup>IDS TIC analyte desorption profiles for stearic acid (10  $\mu$ g) obtained at (a) I= 3.1 A, (b) I = 3.55 A, and (c) I = 3.8 A



Three-dimensional mass spectra of the two analyte desorption profiles for stearic acid. Mass axis from 280-380 u; scan axis = 35-80. Figure 31:

window; the Y-axis, represented by the normalized ion intensities; and the Z-axis represented by the scan number (correlated with time and temperature). Early in the analysis (c.a. scans 35-50) only the [M+K<sup>+</sup>] ion of m/z 321 was observed for stearic acid. Between scans 60-70, a mixture of [M+K<sup>+</sup>] and [M+2K-H]<sup>+</sup> ions were observed. Clearly, rates for salt formation and desorption were now found to be competitive with those for free acid desorption. Unlike the situation described earlier for the five component fatty acid mix, in which the second peak was solely represented by the adduct ions of the salt species, the second analyte peak was not only represented by the salt species, but by the free form of the acid, as well. These two species found in the second scan region were separated in time as well, thus lending support to a surface reaction rather than a gas-phase process. Possible explanations for this behavior are proposed which support a surface mechanism. In both the examples, salt desorption was found to occur at late times during analysis. A possible explanation for this behavior is that salt formation on the surface requires time. Conversion of the free acid form to the salt form may be nearly exothermic. Secondly, salt formation and desorption require high temperatures. Temperature studies have been performed in this laboratory 58 to determine how rapidly the second filament heats based solely on the radiative heating that is experienced from the electrically heated alkali ion emitter. These studies have revealed that the second filament continues increasing in temperature for several minutes after the alkali ion emitter reaches its maximum temperature. Salts of carboxylic acids are known to have higher heats of sublimation than the corresponding free acids. The TIC chromatograms suggest that higher temperatures must be required for desorption of the salt species.

For stearic acid, a  $K_2CO_3$  solution was applied to the alkali emitter surface in the

form of slurried suspension. It is likely that upon rapid heating of alkali emitter that sputtering of  $K_2CO_3$  to the analyte filament occurred which allowed this salt to participate in hydrogen-potassium exchange reactions with the fatty acid. Regardless of the final temperature chosen for the alkali emitter, sputtering no doubt occurred to some extent. When lower heating rates were employed, the analyte molecules (i.e., stearic acid) resided on the filament surface for a slightly greater amount of time than when higher heating currents were employed (I=3.8A). The increased residence time on the filament surface using low heating currents (I=3.1A) might be sufficient for reactions between  $K_2CO_3$  and stearic acid to occur. It is proposed that using high heating rates, the residence time of stearic acid molecules on the surface was sufficiently short-lived such that salt formation from the free acid could not occur.

Another explanation for salt formation may be that desorption of analyte is occurring from the bulk of the sample first and only when the surface monolayers are reached does the desorption of salt occur. This must be considered as a possible operative mechanism for the situation involving the deposition of the free fatty acid mixture onto the contaminated sodium sulfonate surface. Reactions between analyte and alkali atom (in some form) would presumably have a greater time to interact due to desorption from the bulk prior to desorption from the surface monolayers.

The scope of compounds amenable to the K<sup>+</sup>IDS method has been extended to the analysis of salts, as they are found to be capable of desorbing intact into the gas phase. The utility of K<sup>+</sup>IDS in the analysis of these salts might be unparalleled Frequently, compounds must either be converted to a free form, or extracted from buffer solution prior to analysis by other desorption ionization methods For GC-MS analyses, these salts must be converted to their free form prior to derivatization and subsequent analysis by GC-MS. The reactions observed on the surfaces of these K<sup>+</sup>IDS emitters might offer a method for performing in situ derivatizations, or

determining what functional groups are present. Here, salt formation gives the indication that the compound under analysis contains a carboxylic moiety. This type of behavior would not be observed for olefins, for example.

## K+IDS analyses of cardiac glycosides

Cardiac glycoside are of interest to the biomedical community due to their accepted use in treating conditions of arrythmia and congestive heart failure. So Numerous mass spectrometric techniques have been shown to provide both structural and molecular weight information on these molecules. These include FAB-MS, 60 FD-MS, 61 FI-MS, 62 and LD-MS. 63 K+IDS is demonstrated here as a low-cost alternative DI method for obtaining both molecular weight and structural information on these thermally labile compounds.

The potential of K<sup>+</sup>IDS for cardiac glycoside analysis was realized when digitonin (a widely used drug for treating arrythmias) was deposited onto the bare rhenium wire of the dual-filament K<sup>+</sup>IDS probe and the mass spectrum obtained was rich in structural information. Although the molecular weight of this compound was beyond the mass range of the HP quadrupole mass spectrometer, structural information was still available from the numerous fragment ions produced that were indicative of both the steroid (aglycone) and sugar moieties of the molecule. The structure and mass assignments for the major ions formed from thermal decomposition fragments of digitonin in the K<sup>+</sup>IDS analysis are shown in Figure 32. The molecular weight of this compound is 1228, beyond the mass capabilities of the instrument. An averaged K<sup>+</sup>IDS mass spectrum of digitonin is shown in Figure 33. A number of fragment ions are observed in the mass spectrum which assist in elucidating the structure of this compound based on mass spectrometric analysis. The

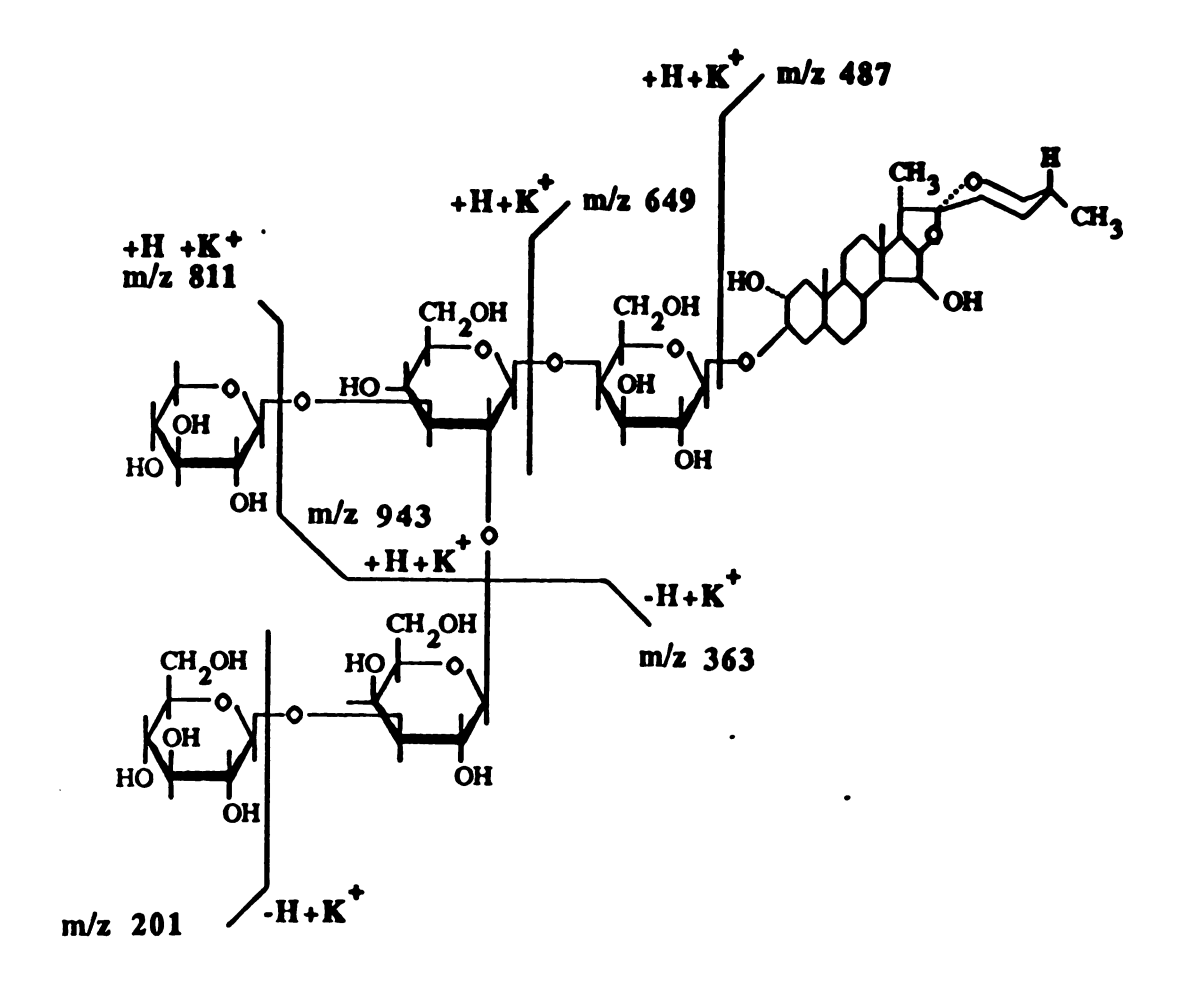


Figure 32. Structure and assignment of major ions from thermal decomposition fragments of digitonin

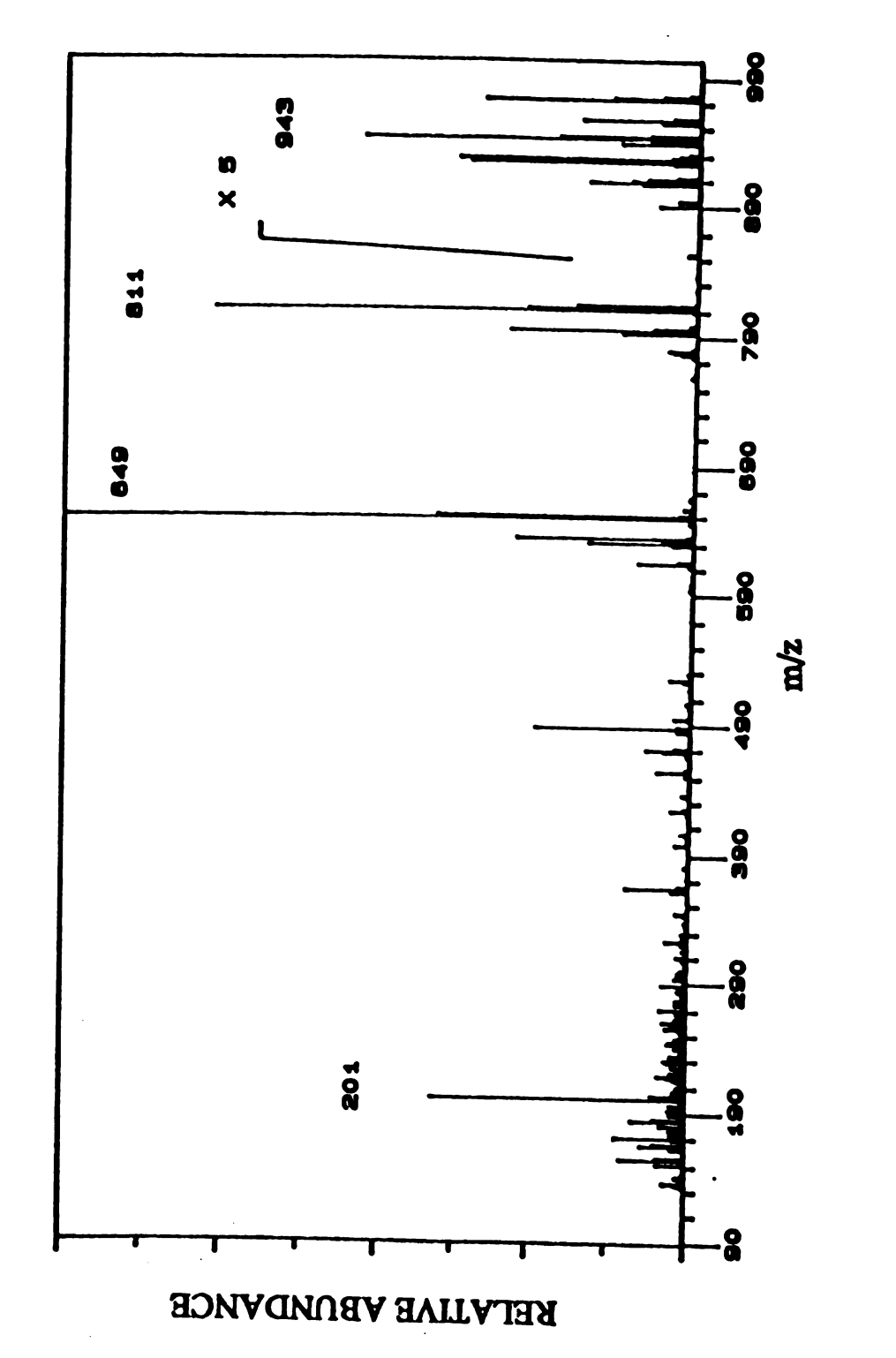


Figure 33: K<sup>+</sup>IDS mass spectrum of Digitonin.

most abundant peaks in the mass spectrum arise from cleavage along the sugar backbone of the molecule with corresponding  $\beta$ -hydrogen shifts (i.e., a 1,2 elimination) to yield the ions shown in Figure 32. 1,2-Eliminations at the ether linkage of the sugar backbone results in the formation of two neutral fragments, both of which are available for K<sup>+</sup> attachment. These 1,2 eliminations requiring the breaking and reforming of two bonds, as shown in Scheme 1 below.

#### Scheme 1

Cleavage between the aglycone (steroid) moiety and sugar backbone also involves a 1,2-elimination and subsequent alkali ion attachment gives rise to the peak corresponding to m/z 487. This kind of fragmentation mechanism has been observed for several classes of compounds when analyzed by the K<sup>+</sup>IDS technique. The production of stable neutral species as a result of 1,2-eliminations is a thermodynamically favored process. The reaction in which two neutral products are formed upon cleavage of the intact molecule through this two step mechanism is frequently found to be exothermic. The activation energy required for this reaction pathway is relatively low since the thermal energy supplied is sufficient to produce these stable decomposition products.

A similar cardiac glycoside, digoxin, has a molecular weight within the mass range of the HP5985 quadrupole mass spectrometer. The structure and K<sup>+</sup>IDS mass spectrum of digoxin are shown in Figure 34. For this lower molecular weight compound a molecular adduct ion is observed in addition to the numerous decomposition products. Cleavages along the sugar backbone occur readily, giving rise to intense peaks separated by 130u, that correspond to neutral losses of the polyhydroxy deoxyhexose moieties, of the form, C<sub>6</sub>H<sub>10</sub>O<sub>3</sub>. Again, cleavages occur as a result of 1,2-eliminations to form neutrals which readily undergo alkali ion attachment. The respective neutral fragments generated are not found to form potassium adducts to the same extent. This is best shown for the cleavage between the S<sub>2</sub> and S<sub>3</sub> sugar moieties of digoxin, which produce peaks at m/z 559 and 299 in the K<sup>+</sup>IDS mass spectrum. The intensity relationship between the two ions is not equivalent, even though both neutrals are formed. This type of behavior might be useful for trying to determine certain branch point linkages in cardiac glycosides. Costello and coworkers have investigated unique fragmentation pathways and the fragment ion intensities associated with these reactions for branched-chain cardiac glycosides that are used extensively in Chinese medicine with the technique of FAB MS-MS. 64 We are currently evaluating whether K<sup>+</sup>IDS might be useful for determining exact branched-sites directly for these cardiac glycosides without the need for MS-MS analyses.

The presence of both molecular weight information and abundant structural information available from a single K<sup>+</sup>IDS mass spectrum makes this technique an attractive alternative to FAB, in which MS-MS is required in order to generate similar fragment ions. Interestingly, the the types of ions observed in the K<sup>+</sup>IDS analyses of this class of compounds parallel closely those ions observed by Marshall and coworkers <sup>63</sup> using laser desorption FT-ICR-MS. The amounts of sample required to

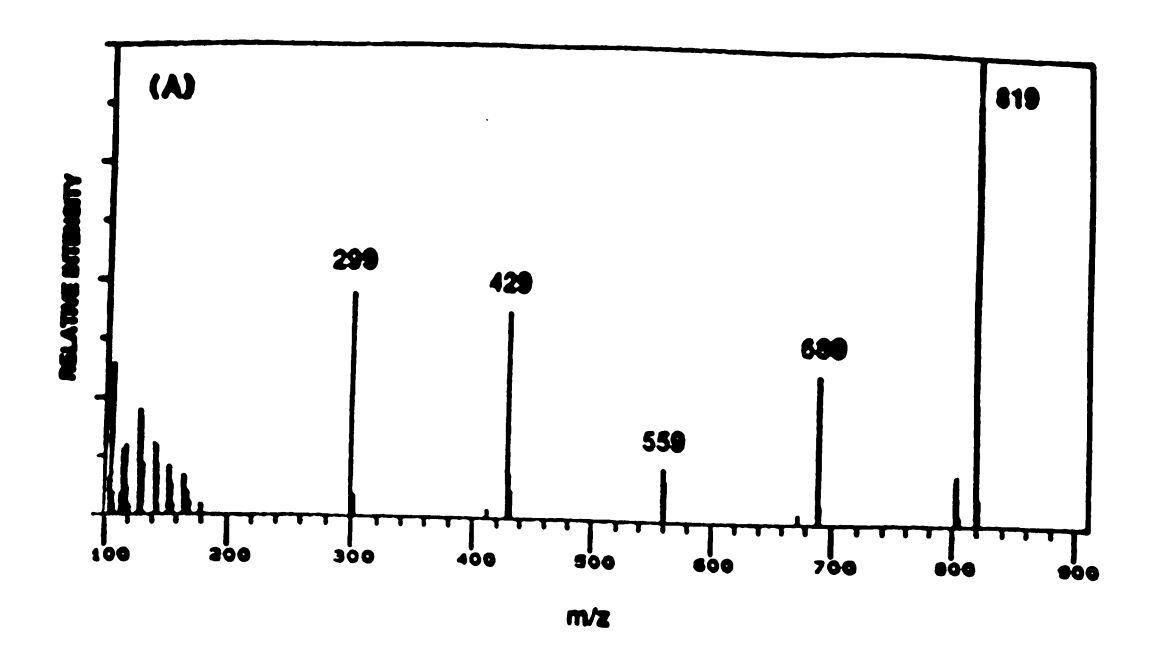
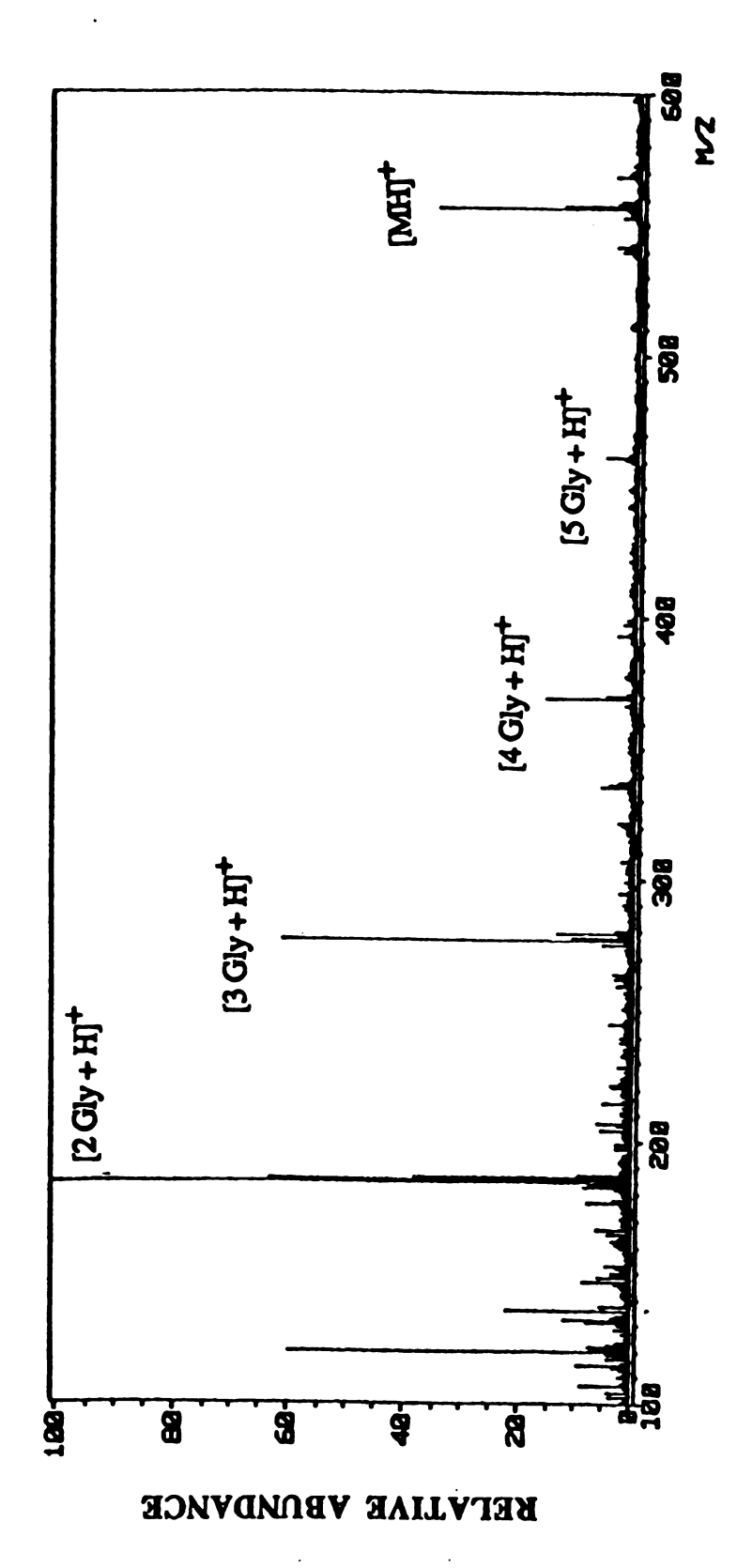


Figure 34. K<sup>+</sup>IDS mass spectrum of (a) digoxin and (b) assignment of ions formed from thermal decompostion fragments

achieve acceptable signal to backgroud has been demonstrated to be nearly equivalent for the two techniques. A much more detailed study on the applications of K<sup>+</sup>IDS to cardiac glycoside analysis has been completed in collaboration with a fellow graduate student. The manuscript is in preparation for publication in *Organic Mass Spectrometry*. 65

### The utility of K+IDS for peptide mapping

Martin and Biemann<sup>66</sup> offer an excellent review on the present state of peptide sequencing by mass spectrometry. A number of approaches have been used for obtaining either sequence information or molecular weight information on high molecular weight peptides. PDMS using time-of-flight mass (TOF) spectrometry is a technique capable of yielding molecular weight information on peptides consisting of more than 200 amino acid residues. FAB, on the other hand, has been used almost exclusively for providing sequencing information on smaller peptide fragments (c.a., 5-20 amino acids in length). The real strength of mass spectrometry in the area of protein chemistry lies in its ability to rapidly and accurately sequence small peptide molecules that are not amenable to other sequencing techniques such as Edman degradation. 67 FAB-MS of these small peptide fragments gives rise to abundant protonated molecules with very little fragment ion information. The mass spectrum of Leucine-Enkephalin (Tyr-Gly-Gly-Phe-Leu) obtained by FAB-MS using a JEOL HX-110 double focusing mass spectrometer is shown in Figure 35. The only ions for the peptide molecule above background noise are the protonated parent and molecular adduct ion species, [M+Na<sup>+</sup>] and [M+K<sup>+</sup>], the latter two ions a result of a mix of NaI/KI being added to the glycerol matrix. The lower molecular weight ions



Fast atom bombardment (FAB) mass spectrum of Leucine-Enkephalin in glycerol. Figure 35:

observed in this mass spectrum are primarily the solvated protonated glycerol molecules of the form [Gly+H]<sup>+</sup>, [2Gly+H]<sup>+</sup>, [3Gly+H]<sup>+</sup>, and [4Gly+H]<sup>+</sup>. Sequence information is obtained by collisionally activated dissociation (CAD) of the protonated molecule. In FAB MS-MS analyses the protonated molecule undergoes decomposition upon reaction with some collision gas (e.g., He) to form a number of fragments that are detected by linked-scanning techniques. The fragment ions in the FAB MS-MS mass spectrum are indicative of cleavages of peptide bonds from both the C- and N-teminus ends of the molecule. Roepstorff developed a nomenclature scheme for the fragment ions produced from protonated linear-chain peptides following CAD. <sup>69</sup> The types of fragment ions most commonly observed are summarized in Table 4. (not shown are immonium ions and W-ions, which can also arise from CAD of the protonated molecule). <sup>70</sup> A pictorial representation of these fragment ions will be presented shortly.

A-, B-, and C-ions all originate from the N-terminus of the peptide chain. X-, Y-, and Z-ions, on the other hand, all originate from the C-terminus. The most commonly observed peptide fragment ions are of the B- and Y-types. The intensity of these ions relative to the other fragment ions, though, is dependent on the amino acid composition of the peptide molecule. Y-type ions result from cleavage of the peptide bond and the fragment ions formed contain the C-terminus of the molecule. These ions generally result from proton transfer and corresponding hydrogen shift to the nitrogen functionality from the  $\alpha$ -carbon adjacent to the carbonyl group of the amino acid residue as shown in scheme 2 for the general case of a tripeptide above. The ions originating from the carboxy terminus are commonly designated as Y ions, since the

Table 4. Fragments produce from protonated linear peptides (I) upon undergoing collisionally activated dissociation (CAD)-MS-MS

$$\begin{bmatrix} H_{2}N - \overset{R}{C}H - CO - (NH - \overset{R}{C}H - CO)_{1} - NH - \overset{R}{C}H - COOH + H \end{bmatrix}^{+}$$

$$I$$

$$H - (HN - \overset{R}{C}H - CO)_{m1} - \overset{R}{N}H = \overset{R}{C}H$$

$$+ CO - NH - \overset{R}{C}H - CO - (NH - \overset{R}{C}H - CO)_{m1}OH$$

$$a_{n}$$

$$x_{n}$$

$$H - (HN - \overset{R}{C}H - CO)_{m1} - NH - \overset{R}{C}H - CEO + H$$

$$b_{n}$$

$$Y_{n}$$

$$H - (HN - \overset{R}{C}H - CO)_{m1} - NH - \overset{R}{C}H - CO - \overset{R}{N}H$$

$$+ \overset{R}{C}H - CO - (NH - \overset{R}{C}H - CO)_{m1}OH$$

$$+ \overset{R}{C}H - CO - (NH - \overset{R}{C}H - CO)_{m1}OH$$

$$C_{n}$$

$$C_{n}$$

$$C_{n}$$

$$C_{n}$$

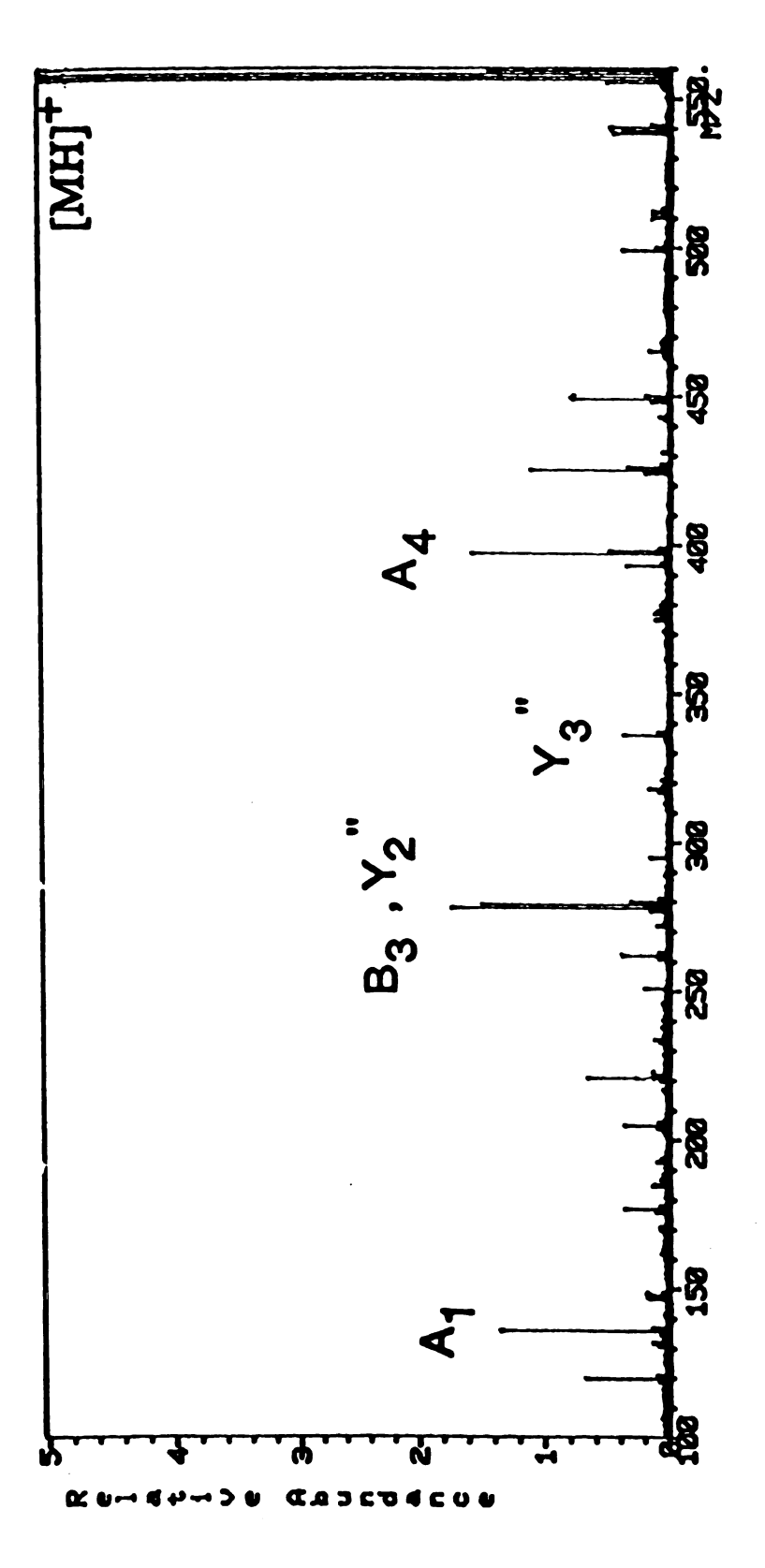
$$C_{n}$$

(Reproduced from Mass Spectrom. Rev. 66 with permission of Martin, et al.)

Scheme 2

fragment resulting from cleavage between the peptide bond is found to contain two additional hydrogen atoms. B-type ions, on the other hand result from cleavage between peptide bond and the fragment ion formed contains the N-terminus of the molecule. Sequential cleavages along the backbone of the molecule originating from both the C- and N-termini allow for one to accurately deduce the correct amino acid sequence for the molecule.

The FAB MS-MS mass spectrum of Leucine-Enkephalin is shown in Figure 36. A number of fragment ions are observed which are used for determining the amino acid sequence of this molecule. The abundance of these ions is quite low, though, relative to the protonated molecule. The most intense fragment peak (m/z 278, corresponding to the B<sub>3</sub> ion) is only two per cent the intensity of the protonated molecule. A number of A, B, and Y-type ions are also observed in the FAB MS-MS mass spectrum of Leu-Enkephalin which assist in the determination of the true amino acid sequence. The major drawback to doing an MS-MS analysis on the protonated parent is that a significant portion of total ion current is dispersed amongst a number of decomposition products upon collisionally activated dissociation of the parent ion and the ion signals associated with these fragment ions are weak. However, matrix interferences due to glycerol are eliminated when MS-MS analyses are performed,



FAB MS-MS collisionally activated dissociation (CAD) mass spectrum of Leucine-Enkephalin. **Figure 36:** 

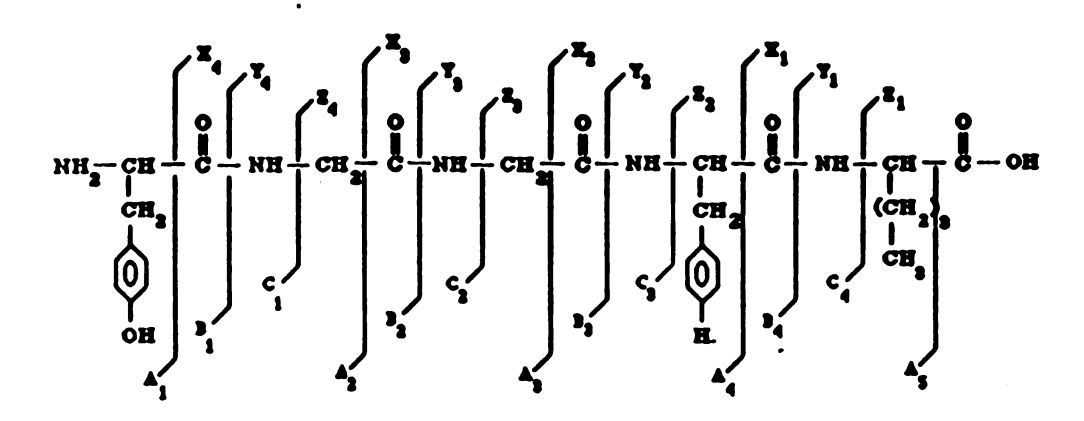
and as a result the S/N for these fragment ions is more than sufficient for identifications to be made.

The applications of K<sup>+</sup>IDS for peptide sequencing has been implied from earlier studies using this technique on hexaglycine and the tri-peptide, Alanyl-Leucyl-Glycine.<sup>37</sup> The results of such studies were encouraging from the standpoint of the ability of the technique to provide both molecular weight and structural information in one analysis. These studies have now been extended to more complex peptides, including Leucine-Enkephalin and others.

Small molecular weight peptides have been studied by K<sup>+</sup>IDS to determine this techniques' ability to directly produce both molecular weight and structural information simultaneously. Peptide molecules fall into the category of Type II molecules, as discussed in chapter 3. The lability of peptide bonds is such that little energy is required for bond-breaking to occur. By controlling the heating rates, however, it is possible to increase or decrease the relative amount of decomposition products generated in a K<sup>+</sup>IDS analysis. K<sup>+</sup>IDS analyses result in the desorption of both the intact molecule and structurally significant decomposition products. Leucine-Enkephalin (Tyr-Gly-Gly-Phe-Leu, MW = 555) is discussed for the purpose of demonstrating the capabilities of the K<sup>+</sup>IDS technique in the analysis of low molecular weight peptides. The structure of Leu-Enkephalin and the masses of the structurally significant ions that may be formed following alkali ion attachment are summarized in Figure 37.

The Roepstorff nomenclature scheme has been maintained for identifying the cleavages along the backbone of the peptide molecule. As an example, cleavage of the first peptide bond originating from the C-terminus of the molecule results in the formation of two radical species, designated as B<sub>2</sub> and Y<sub>3</sub>. These radical species have

## Possible Fragment Ions in the Na IDS Mass Spectrum of Leucine Enkephalin (Tyr-Gly-Gly-Phe-Leu, MW =555)



Designate Fragment	Nominal mass	m/z [frag + Na*]	Designate Fragment	Nominal mass	m/s (frag + Na <sup>+</sup> )
A,	136	159	x,	158	171
В,	164	187	٧,	130	153
c,	179	202	21	115	138
A <sub>2</sub>	193	216	X <sub>2</sub>	305	328
8,	221	244	٧2	277	300
c,	236	259	z,	262	285
۸,	250	273	X <sub>a</sub>	362	385
•,	278	301	Ya	334	357
<u> </u>	293	316	Z,	319	342
A4	397	420	X4	419	442
84	425	448	Y4	391	414
C4	440	463	24	376	399
As	510	533	2 6	539	582
Bç	538	561		l	

Figure 37. Structure and possible thermal decomposition fragments for leucineenkephalin arising from a Na<sup>+</sup>IDS analysis

nominal molecular weights of 221 and 334u, respectively. If no hydrogen shift was observed for these species prior to their desorption into the gas phase, these [M+Na<sup>+</sup>] adducts would be observed at m/z 244 and 357, respectively. However, the formation of these two radical species is unfavored, from a thermodynamic standpoint. A method for making this reaction exothermic has been proposed. As was described earlier for the cardiac glycosides, cleavages at these labile bonds frequently involve 1,2-eliminations to produce very stable neutral molecules, and this mechanism would be expected for the peptides as well. The general case for the 1,2-elimination reactions is shown in Scheme 3. The two neutral species formed are very similar in nature to the B- and Y-type fragment ions observed for the tri-peptide described earlier. Hence, the two neutral species above represent the B-type and Y-type fragments. Upon desorption of these neutrals and susbsequent gas-phase alkali ion attachment, B- and Y-type alkali ions are formed.

$$R^{III} - NH - C = C = O + NH - CH - CO_2H$$

$$R^{III} - NH - C = C = O + NH - CH - CO_2H$$

$$H R^{III} - H - CH - CO_2H$$

Scheme 3

The Na +IDS mass spectrum obtained following deposition of 3 µg of Leucine-Enkephalin onto the bare rhenium wire of the dual-filament K<sup>+</sup>IDS probe is shown in Figure 38. The [M+Na<sup>+</sup>] ion is observed at m/z=578 and is of relatively low abundance. The alkali adduct of the Y<sub>3</sub> ion is found at m/z 358, 1u above that reported in Figure 37 (designated as [Y<sub>3</sub>'+ Na<sup>+</sup>]). Alternatively, the alkali adduct of the B<sub>2</sub> ion is observed at m/z 243, 1 u less than the the value reported in Figure 37 (designated as  $[B_2-H+Na^+]$ ). This is consistent with the  $\beta-H$  shift (i.e., a 1,2elimination reaction) from the B<sub>2</sub> containing fragment, as shown in Scheme 3. A number of other decomposition products are formed from both the C- and N-termini of the molecule. As can be seen clearly, the amount of information that is available on this pentapeptide by K<sup>+</sup>IDS is more than sufficient for determining the amino acid sequence. All of the Y-type ions are observed in the mass spectrum, the most intense being the [Y<sub>3</sub>'+Na<sup>+</sup>]. The majority of ions observed in the K<sup>+</sup>IDS mass spectrum of Leu-Enkephalin are the cationized species. However, low mass surface ionization products are also observed. The peak observed at m/z 91 is believed to be the C<sub>7</sub>H<sub>7</sub><sup>+</sup> ion from the R-chain of phenylalanine. Other prominent ions in the K<sup>+</sup>IDS mass spectrum of this molecule are a result of neutral losses of H<sub>2</sub>O and NH<sub>3</sub> which are also observed as decomposition products.

Methionine-Enkephalin (Tyr-Gly-Gly-Phe-Met) provides as another example of the strengths of  $K^+IDS$  in the analysis of these compounds. The structure and masses of possible fragment ions that are commonly observed are summarized in Figure 39 (and are analagous to those described for Leu-Enkephalin). The Na<sup>+</sup>IDS mass spectrum of Met-Enkephalin is shown in Figure 40. A peak for the molecular adduct ion,  $[M+Na]^+$ , observed at m/z = 596 is relatively abundant. In fact, the intensity of this peak is dependent on the heating rate used for the analysis. The base peak in the

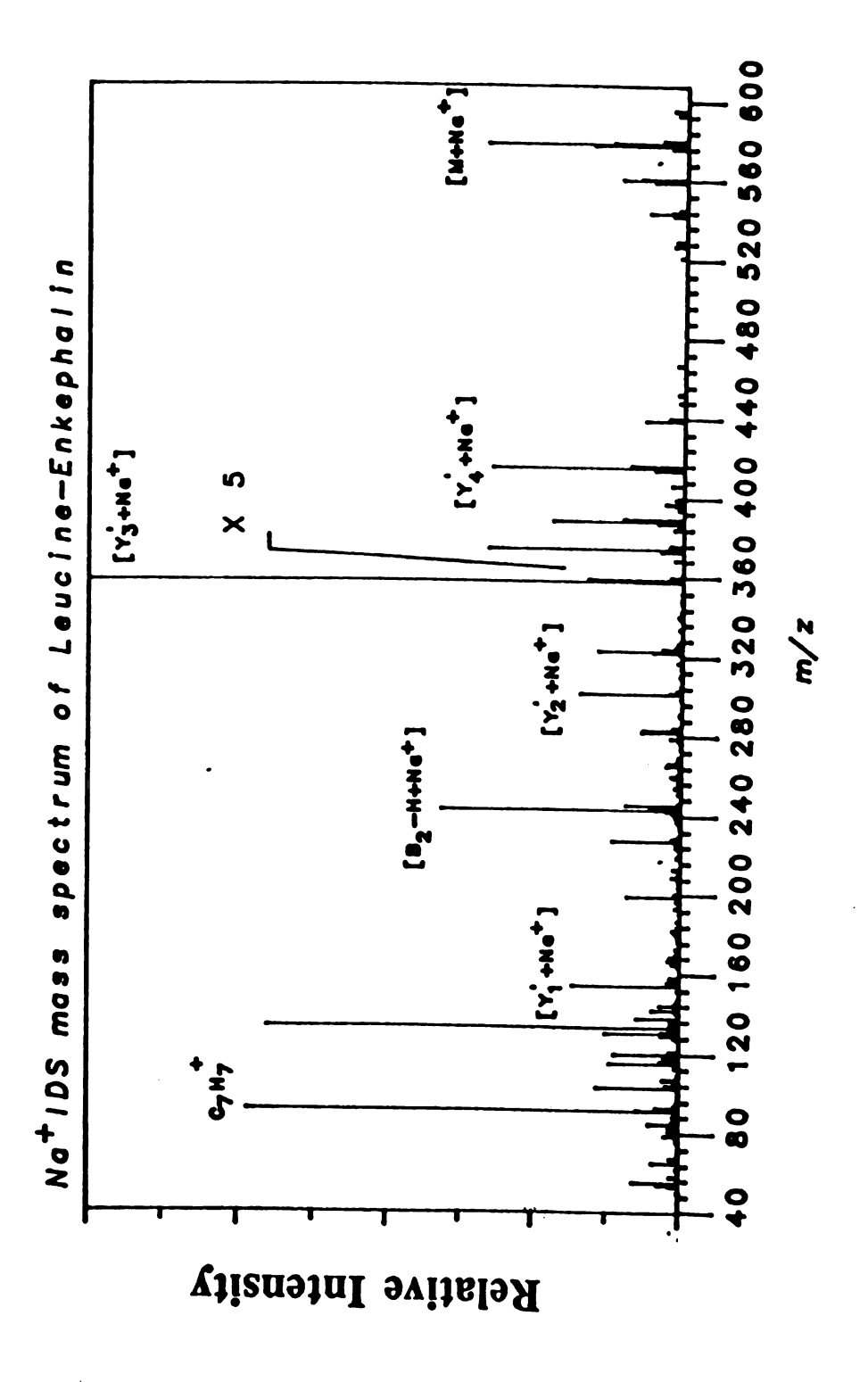


Figure 38: Na TDS mass spectrum of Leucine-Enkephalin.

# Possible Fragment Ions in the Na IDS Mass Spectrum of Methionine-Enkephalin (Tyr-Gly-Gly-Phe-Met, MW = 573)

Designate Fragment	Nominal mass	m/z (frag + Na )	Designate Fragment	Nominal mass	m/z (frag + Na <sup>†</sup> )
A <sub>1</sub>	136	159	x,	176	199
8,	164	187	Ϋ́	148	171
c,	179	202	Z <sub>1</sub>	133	156
A <sub>2</sub>	193	216	X <sub>2</sub>	323	346
8,	221	244	Y 2	295	318
c,	236	259	z	280	303
A,	250	273	X <sub>a</sub>	380	403
В,	278	301	٧,	352	375
с,	293	316	Z,	337	360
A4	397	420	X <sub>4</sub>	437	460
B.4	425	448	Y4	409	432
C4	440	463	<b>Z</b> 4	394	417
Ag	528	551	Yg	572	595
Bç	556	579	Zg	557	580

Figure 39. Structure and possible thermal decomposition fragments for methionine-enkephalin arising from a Na<sup>+</sup>IDS analysis.

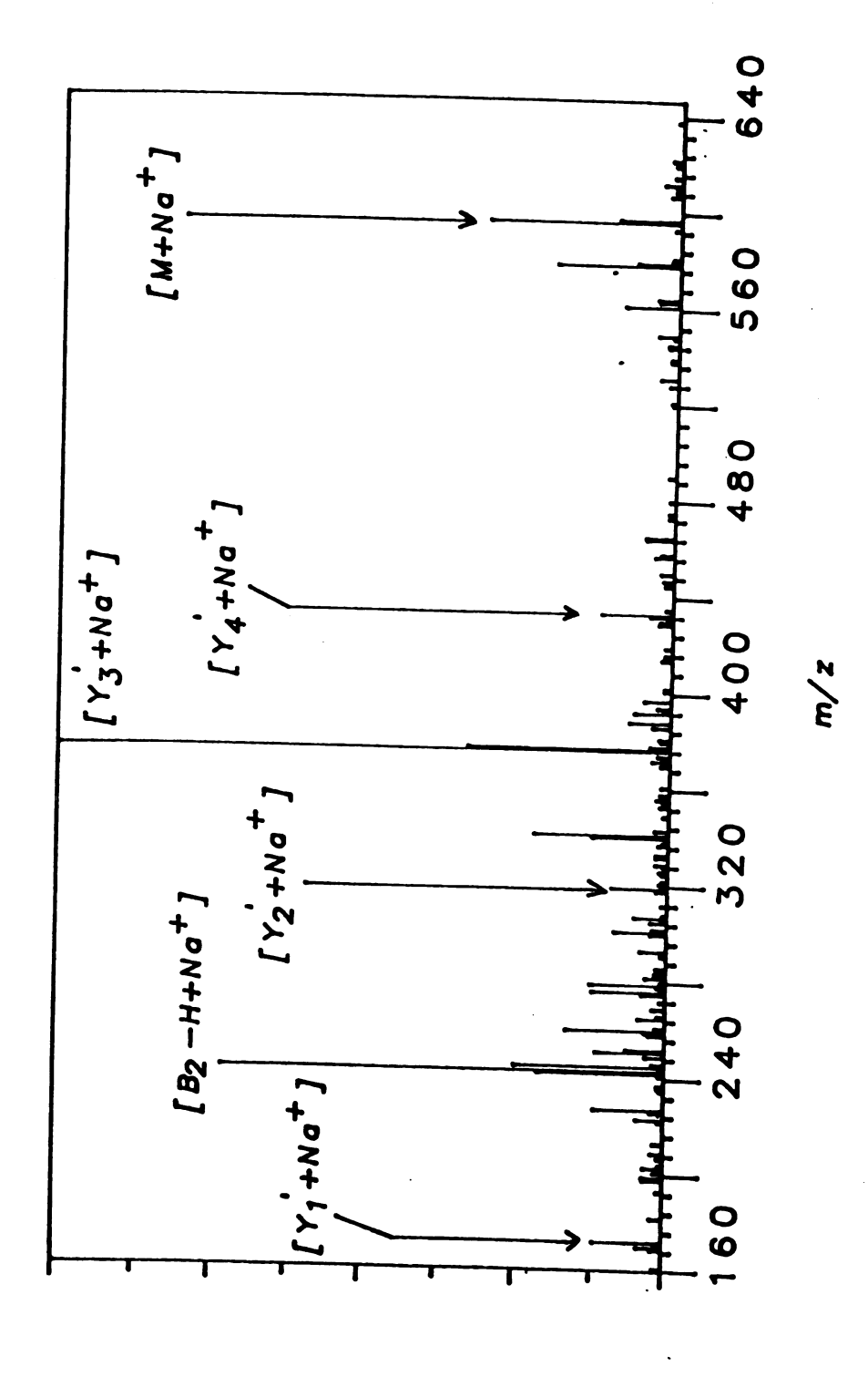


Figure 40: Na 1DS mass spectrum of Methionine-Enkephalin.

mass spectrum of Methionine-Enkephalin is also the [Y<sub>3</sub>'+Na<sup>+</sup>] species. Again, major decomposition products correspond to cleavage of the peptide bond, resulting in the production of predominantly B-type and Y-type ions. A number of low intensity peaks have been observed in the K<sup>+</sup>IDS mass spectra and are not fully characterized at this time.

Analyses by K<sup>+</sup>IDS on longer chain peptide fragments, such as bradykinin (Arg-Pro-Pro-Gly-Phe-Ser-Pro-Phe-Arg) and another commonly studied peptide, Val-His-Leu-Thr-Pro-Val-Glu-Lys (VHLTPVEK), have not been as informative. The structure and possible sodium adduct ions that may be found in a typical Na<sup>+</sup>IDS mass spectrum of VHLTPVEK are summarized in Figure 41. For some reason, K<sup>+</sup>IDS analyses have been unsuccessful in generating discernible molecular adduct ions for these compounds. The Na<sup>+</sup>IDS mass spectrum of the peptide VHLTPVEK is shown in Figure 42. A few ions that were expected to be observed are indeed present in the Na<sup>+</sup>IDS mass spectrum of this compound. The base peak in the mass spectrum corresponds to the  $[B_2^- - H + Na^+]$  ion observed at m/z 259. In addition, a number of C-type ions are also identified in the lower mass region of the mass spectrum. The  $[C_3^- + Na^+]$  ion is observed at m/z 389. Two intense peaks in the mass spectrum, labelled at m/z 301 and 359 have not been assigned to a typical Roepstorff designation.

It is clear that the types of ions observed for this peptide are not at all what one would expect from a K<sup>+</sup>IDS analysis based on the results for both Leu-Enkepahlin and Met-Enkephalin. No molecular adduct ion is observed. The unique feature of this peptide and bradykinin is the presence of proline residues. Perhaps the rigidity of this ring system is such that peptide bond cleavage does not occur readily. Initial results indicate that sequence information can be obtained up to the proline residue,

-cHcH -cHcH NH-	
Ė	153 153 262 361 476 478 579 692 829
C-NH-CH-C-NH-CH-C-1  CH(CH), CH, CH, CH, CH, CH, CH, CH, CH, CH, CH	6 7 7 7 7 7 7 7 7 7 7 7 7 7 7 7 7 7 7 7
сн (сн <sup>2</sup> )	168 168 297 297 297 707 944 943
	4 4 4 4 4 4 4 4 4 4 4 4 4 4 4 4 4 4 4
CHOHOCH-CH-CH-CH-CHOH) CHOY) CHOY) CHOY) CHOY	138 275 388 489 586 685 685
CH-C-NH-CH-CH-CH-CH-CH-CH-CH-CH-CH-CH-CH-CH-CH	9
- NA	123 123 260 373 474 571 670
CH—C—NH—CH—C—NH—CH—C—C—C—C—C—C—C————————	
CH (CH)	

Structure and possible thermal decomposition fragments for the octa-peptide (Val-His-Leu-Thr-Pro-Val-Glu-Lys) arising from a Na DS analysis. Figure 41:

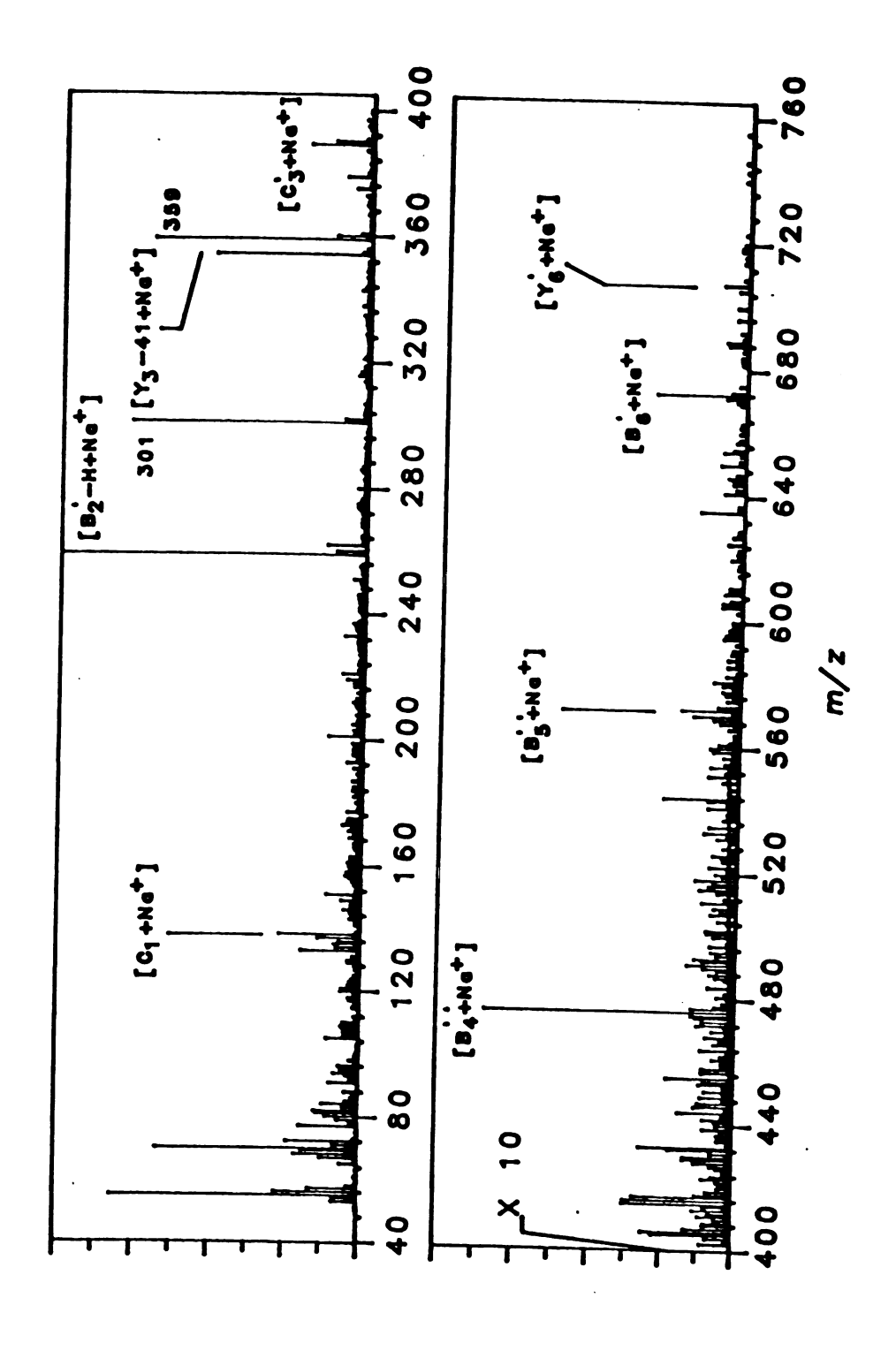
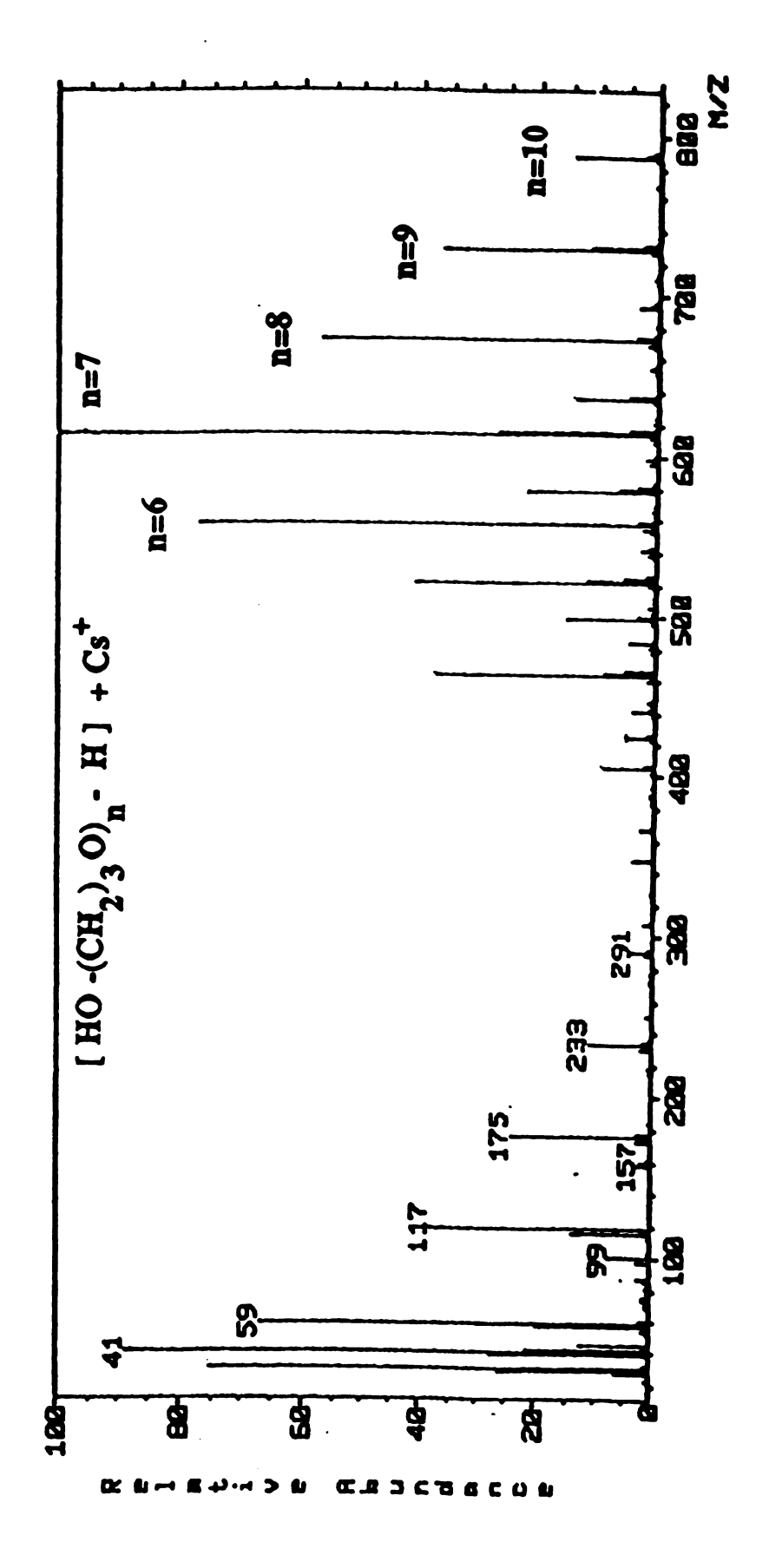


Figure 42: Na TDS mass spectrum of Val-His-Leu-Thr-Pro-Val-Glu-Lya.

but little information is available beyond this peptide linkage. FAB MS-MS on VHLTPVEK also has been found to be less informative than it is for other small-chain peptides. Little fragmentation has been observed in the CAD-MS mass spectra of this compound. The K<sup>+</sup>IDS technique does show promise, though, in the analysis of some peptide molecules. It is difficult, though, to assess the capabilities of the technique for amino acid sequencing since we have been limited to using a quadrupole mass spectrometer for all studies. The upper mass limit of the quadrupole instrument available in our laboratory is 1000 u.

Under investigation is the possibility of implementing the K<sup>+</sup>IDS technique on the high resolution JEOL HX110 mass spectrometer. Currently, studies involving K<sup>+</sup>IDS on the JEOL HX-110 are limited in that a direct chemical ionization (DCI) probe must be used. The specifications for the upper current limit of the probe is 1.5 A, which is just sufficient for K<sup>+</sup>emission to occur. In addition, the current probe design employs only one filament. For K<sup>+</sup>IDS to be implemented effectively on the high resolution, high mass instrument, a dual-probe design similar to the one currently employed for use on the HP 5985 quadrupole is needed. Initial results of a K<sup>+</sup>IDS analysis of poly(propylene)glycol (PPG) (average molecular weight, 425) in which the maximum current of I=1.5A was used to desorb the polymer from a K<sup>+</sup>IDS emitter in the presence of a high flux of cesium ions from the single filament DCI probe are encouraging. Cs<sup>+</sup> was found to be generated in copius amounts under very unusual operating conditions. Desorption of the polymer in the presence of this high flux of Cs<sup>+</sup> resulted in the formation of a number of [M+Cs<sup>+</sup>] adducts ion of relatively high abundance. Shown in Figure 43 is the Cs<sup>+</sup>IDS TIC profile and mass spectrum of PPG 425. All ions observed in this mass spectrum are Cs<sup>+</sup> adducts of the



Cs<sup>+</sup>IDS mass spectrum of PPG 425 obtained on the JEOL HX-100 HRMS. Figure 43:

oligomeric species of this PEG mixture, and have the formula [H(OCH<sub>2</sub>CH<sub>2</sub>CH<sub>2</sub>-)nOH + Cs<sup>+</sup>], where n=1-10. The results parallel quite closely those obtain using K<sup>+</sup>IDS for the analysis of PPG 425 on the quadrupole mass spectrometer. An analysis of Leu-Enkephalin was made in an identical manner, by rapidly heating the peptide from the direct chemical ionization (DCI) wire in the presence of a high flux of Cs<sup>+</sup>. [M+Cs<sup>+</sup>] adduct of B- and Y-type ions were observed, and the amino acid sequence could indeed be deduced from interpretation of the complex mass spectrum.

## Future studies utilizing the strengths of K<sup>+</sup>IDS

These results are encouraging since it induce the possibility of using the K<sup>+</sup>IDS technique for the analysis of much higher molecular weight species. Compounds such as digitonin and other high molecular weight thermally labile compounds may be shown to give rise to abundant molecular-type ions in the K<sup>+</sup>IDS analysis.

In addition, a novel approach to using alkali aluminosilicate materials for mass spectrometry is under investigation. This technique has been named "K<sup>+</sup>IDS by FAB". K<sup>+</sup> (or Na<sup>+</sup>) ions can be generated in the gas phase from bombardment of high energy (c.a. 10 kV) atoms on to a surface containing an appropriate alkali aluminosilicate material. If a sample is placed directly onto a surface coated with the alkali glass material, and is subjected to high energy fast Xe atoms, molecular adduct ions of the form [M+A<sup>+</sup>], and [M+2A-H]<sup>+</sup>, where A=alkali ion, can be formed. This may be an attractive method for obtaining molecular weight information on compounds that are not found to give rise to protonated molecules in conventional FAB analyses. A comparison of the conventional FAB mass spectrum of arachidonic acid and that obtained by the "K<sup>+</sup>IDS by FAB" approach, shown in Figure 44 a-b.

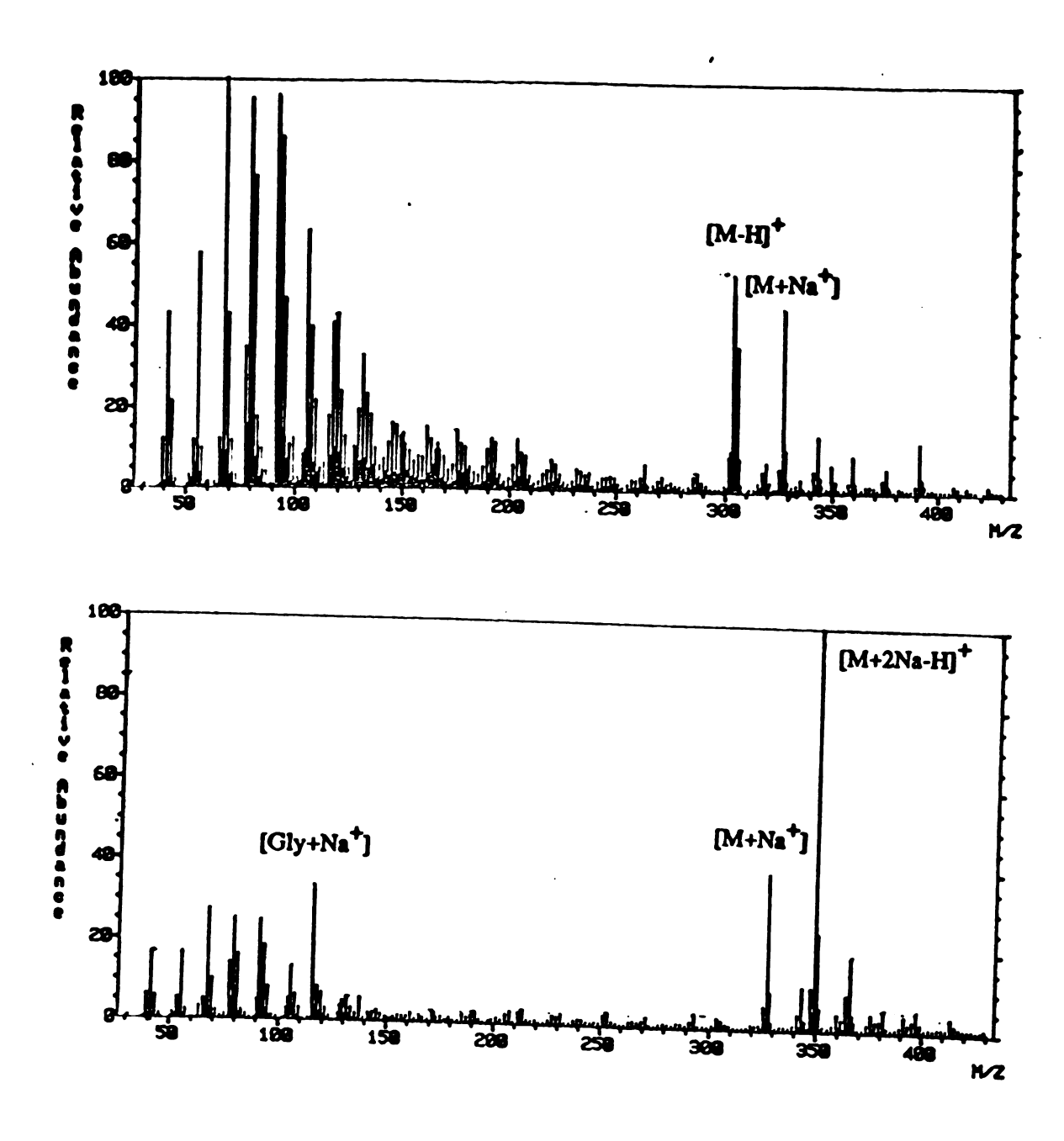
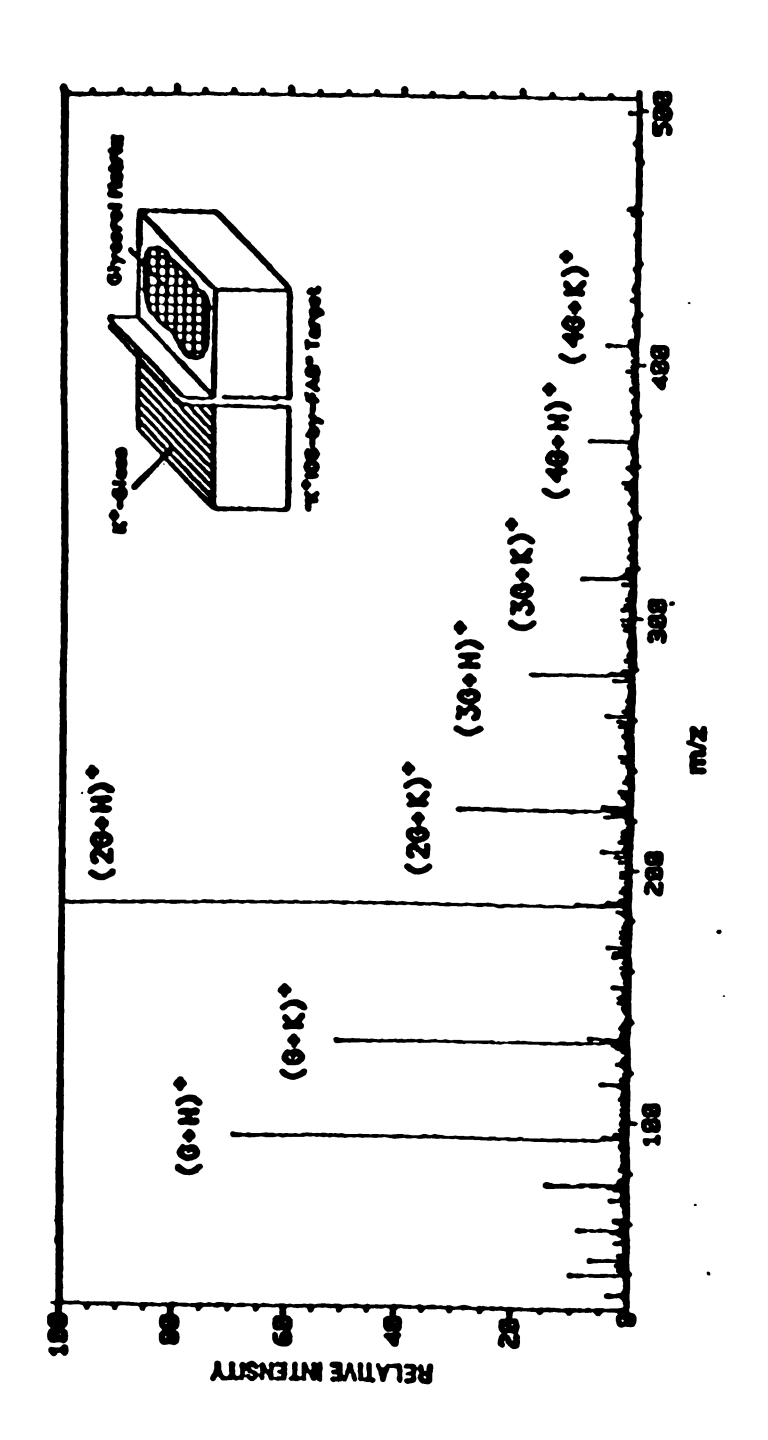


Figure 44. (a) FAB mass spectrum and (b) "Na +IDS by FAB" mass spectrum of arachidonic acid

This type of approach is also being investigated to help clarify and support the proposed gas-phase mechanism for ion formation in FAB-MS. <sup>71</sup> A normal FAB probe-tip has been modified to accomodate an alkali aluminosilicate mixture on one side of the probe-tip while the other is coated with appropriate analyte solution, in this case, glycerol. The two surfaces are physically separated by a finite distance, in order to ensure that mixing does not occur between the two surfaces, even if subjected to a high energy fast atom beam. The probe tip and mass spectrum obtained for glycerol using this split-probe design is illustrated in Figure 45. Molecular weight information in the form of the protonated glycerol molecules and K<sup>+</sup> adduct ions is observed.

This type of approach would be attractive for those compounds for which no protonated molecule is observed in the conventional FAB mass spectrum. Musselman and coworkers 72 showed that cholic acid, when analyzed by conventional FAB, produced no MH<sup>+</sup> ion, but the highest mass ion in the mass spectrum was the [M+Gly]<sup>+</sup> adduct ion. If this were an unknown, the ion might be presumed to be the protonated molecule and thus inaccurate molecular weight determinations would be made. Addition of AgNO<sub>3</sub> to the glycerol matrix resulted in attachment of a Ag<sup>+</sup> ion to the analyte which was useful for determining the exact molecular weight of the species due to the distinct isotope pattern associated with the silver ion. The question remained as to whether adduct ion formation was occurring in solution or in the gas-phase for attachment. An elegant way for determining whether or not species such as cholic acid actually desorb into the gas phase prior to adduct ion formation is to incorporate the "K<sup>+</sup>IDS by FAB" design. By placing cholic acid on one portion of the K<sup>+</sup>IDS probe tip and the alkali aluminosilicate material on the other, formation of [cholic acid + alkali ion] adducts would suggest



"K\*IDS by FAB" mass spectrum of glycerol obtained using a split fab probe tip. Figure 45.

a gas phase mechanism is operative in FAB analyses. This experiment is currently being pursued.

### Final comments on K<sup>+</sup>IDS

This DI technique continues to show promise in its applicability to a wide range of organic compounds. Sensitivity problems initially associated with the technique have been curtailed, yet work still remains in optimizing the performance of the current probe design. A better understanding of the temperature relationship between the two filaments currently employed, is needed and is currently under investigation. Results of such studies may induce a design alteration that will lower even further the detection limits associated with the technique. A method for generating lower detection limits might be achieved on a mass spectrometer equipped with dual insertion probes. In this experiment, the potassium emitter could be inserted into the ion source and heated to a point at which the highest flux of K<sup>+</sup> ions could be generated. A second direct insertion probe containing the analyte could be inserted and the thermally labile compound flash vaporized using rapid heating techniques. Assuming a localized high pressure region could be achieved very near the two DIP probes, best overlap could be achieved for analyte desorption and alkali emission, leading to the most optimum sensitivity of the technique.

### **Chapter 5: Chemical Ionization Theory**

#### Chemical ionization mass spectrometry (CIMS)

Chemical ionization (CI) mass spectrometry is based on ion/molecule reactions for gas phase chemical analysis. As early as 1916, reactions involving proton transfer between H<sub>2</sub> and H<sub>2</sub><sup>+</sup> were observed by Dempster. <sup>73</sup> The analytical utility of CI-MS was not really exploited until the early 1960's, when Field and Munson discovered that gas phase ion molecule reactions involving methane at high pressures (c.a. 1 torr) could be used to produce unique chemistry. <sup>74</sup> Shown in equations 3-4a, 4b are the major reactant ions that occur following electron impact ionization of CH<sub>4</sub> in a high pressure source:

CH<sub>4</sub> -----> 
$$CH_4^+$$
,  $CH_3^+$ , etc.(+2e-) (3)

$$CH_4^+ + CH_4^- ---- > CH_5^+ + CH_3^-$$
 (4a)

$$CH_3^+ + CH_4^- - C_2H_5^+$$
 (4b)

Electron impact on neutral methane molecules results in the production of a number of ions, mainly  $CH_3^+$  and  $CH_4^{+}$ . These ions then undergo reactions with neutral reagent gas to produce  $CH_5^+$  and  $C_2H_5^+$  in varying degrees and the relative abundance of these two ions becomes approximately equivalent as source pressure is increased above 0.2 torr. These reagent ions are then utilized as chemical ionization

reagents for gas-phase proton transfer reactions. In addition, a small fraction of  $CH_4$  is converted to the  $C_3H_5^+$  ion via a reaction between  $C_2H_3^+$  and  $H_2$ , and this species is solely observed to participate in adduct ion formation (i.e.,  $[M+C_3H_5^+]$  formation) reactions with analyte, M.

The strengths of methane-CI for numerous analytical applications lie in the fact that the two product ions,  $CH_5^+$  and  $C_2H_5^+$ , are relatively strong acids, from a Brønsted-Lowry definition. Since most organic compounds of biological interest, including organic acids, steroids, and amino acids act as weak Brønsted acids, 75 proton transfer from the more acidic  $CH_5^+$  molecule is expected to occur fairly readily. Shown in equations 5-6 are the general cases for reactions involving the methane reagent ions with organic compounds. Equations 5a-5c show some reactions that occur for analyte molecule, M, with  $CH_5^+$ :

$$CH_5^+ + M$$
 ----->  $MH^{+*} + neutral, \Delta H_{ren}$  (5a)

$$MH^{+*}$$
 .....  $MH^{+}$  (5b)

$$C_2H_5^+ + M - (6a)$$

$$C_2H_5^+ + M$$
 ----->  $MH^{+*}$  (6b)

$$MH^{+*}$$
 .....  $MH^{+}$  (6c)

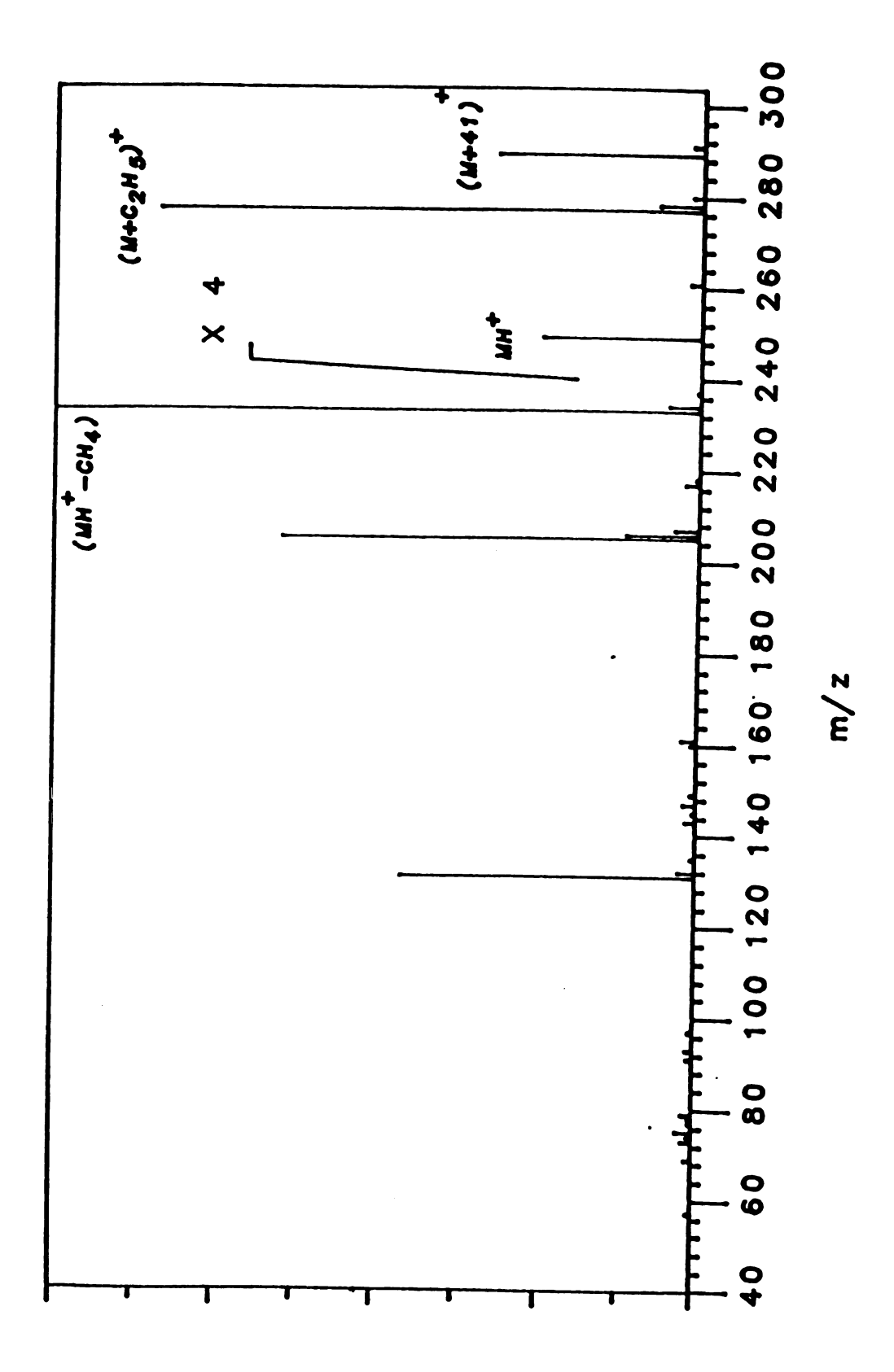
Ion formation is governed by direct proton transfer from the Brønsted acid species to the more basic species. The energy associated with such a proton-transfer reaction, shown in eq. 5a, is the  $\Delta H_{TXIL}$  and is directly related to the difference in proton affinities of the conjugate bases of the reacting species. In general, these proton transfer reactions are exothermic (i.e.,  $\Delta H_{TXIL} \leq 0$ ), though under certain conditions,

endothermic proton transfer reactions have been observed. Typical proton affinity (PA) values for methane have been reported as 130.5 kcal mole<sup>-1</sup>. <sup>76</sup> For the reacting analyte, proton affinities can vary significantly. For example, amino-containing compounds, such as triethylamine are reported to have PA = 230 kcal mole<sup>-1</sup>. 75 In contrast, ethers, such as diethylether, exhibit proton affinities that are substantially lower (c.a. 199.4 kcal mole<sup>-1</sup>). 77 For most organic compounds, nevertheless, their proton affinities exceed that of CH<sub>4</sub> by several kcal mole<sup>-1</sup> of energy. Therefore, the product ion formed in the initial reaction, eq. 5a, will have a maximum amount of excess internal energy equal to the difference in proton affinity between the reagent gas and the neutral analyte (M). Generally, the energy difference in the proton affinities of the two reacting species is distributed between the two reacting species. so that the internal energy (Eint) associated with the newly formed protonated molecule may be expressed as  $E_{int}$  (MH<sup>+</sup>)  $\leq$  PA (M) - PA (CH<sub>4</sub>). The product ion may be stabilized by a collision with neutral reagent gas, if the difference in proton affinity between M and CH<sub>4</sub> is sufficiently small, giving rise to the protonated molecule observed in eq. 5b. On the other hand, if this energy difference is large, then the excited product ion may be more likely to undergo decomposition to a set of fragment ions, typically through some low-energy pathway (e.g., elimination of stable neutral molecules). Therefore, the exothermicity of reaction (which is determined by relative differences in proton affinities) governs to a large extent the amount of fragmentation resulting from the chemical ionization experiment. Examples of CI mass spectra of various compound classes (e.g., amines, alcohols, hydrocarbons) may be found in a detailed review by Harrison. <sup>78</sup>

Equations 6a-6b suggest that other methane reagent ions may participate in proton transfer or adduct ion-formation reactions. In an analogous manner to that described for the CH<sub>5</sub><sup>+</sup> ion interaction with neutral molecule, M, C<sub>2</sub>H<sub>5</sub><sup>+</sup> can react by proton

transfer to the more basic species, M. Again, depending on the exothermicity associated with this hydrogen transfer reaction, either stabilization to the protonated molecule, or decomposition to lower energy fragment ions can occur. A frequently observed reaction for  $C_2H_5^+$ , and even  $C_3H_5^+$ , with many organic molecules is the formation of the stable adduct ion. Adduct ion formation typically occurs for those analyte molecules that exhibit proton affinities very near that of the reagent ion. The PA (C<sub>2</sub>H<sub>4</sub>) has been shown to be approximately 165-170 kcal/mole. The higher PA (C<sub>2</sub>H<sub>4</sub>) more closely parallels the PA values for most organic molecules, and as a result, adduct ion formation involving C<sub>2</sub>H<sub>5</sub><sup>+</sup> is favored over proton transfer. Shown in Figure 46 is the methane-CI mass spectrum of the trimethylsilyl (TMS) derivative of 2-hydroxyisobutyric acid. In addition to the weak ion signal for the protonated molecule observed at m/z 249, two peaks of relatively high abundance are observed at m/z 277 and m/z 289, corresponding to [M+C<sub>2</sub>H<sub>4</sub>]<sup>+</sup> and [M+C<sub>3</sub>H<sub>4</sub>]<sup>+</sup>, respectively. The exothermicity associated with the proton transfer and adduct ion formation reactions, as suggested, determines to a large extent the amount of fragmentation that will be observed in a chemical ionization mass spectrum.

The amount of fragmentation, however, is also governed by the kinetics of these reactions. A brief kinetic description of the important processes in electron ionization mass spectrometry is required first, and is summarized here. In EI-MS, molecular ions, M<sup>+</sup>, are formed as a result of electron impact with a 70 eV particle beam on gaseous analyte molecules. A distribution of internal energies ranging from the lowest energy required to form the molecular ion (i.e., the ionization potential of the molecule) to an internal energy several eV above that required for ion formation will be observed, since several eV of energy can be transferred to the analyte molecule following the ionization event. <sup>79</sup> This distribution of internal energy in the molecular ion is generally represented by a unique probability function, P(E), for the



Methane-CI mass spectrum of 2-hydroxyisobutyric acid (di-TIMS). Figure 46.

molecule, called the Wahraftig diagram, <sup>80</sup> as shown in Figure 47.

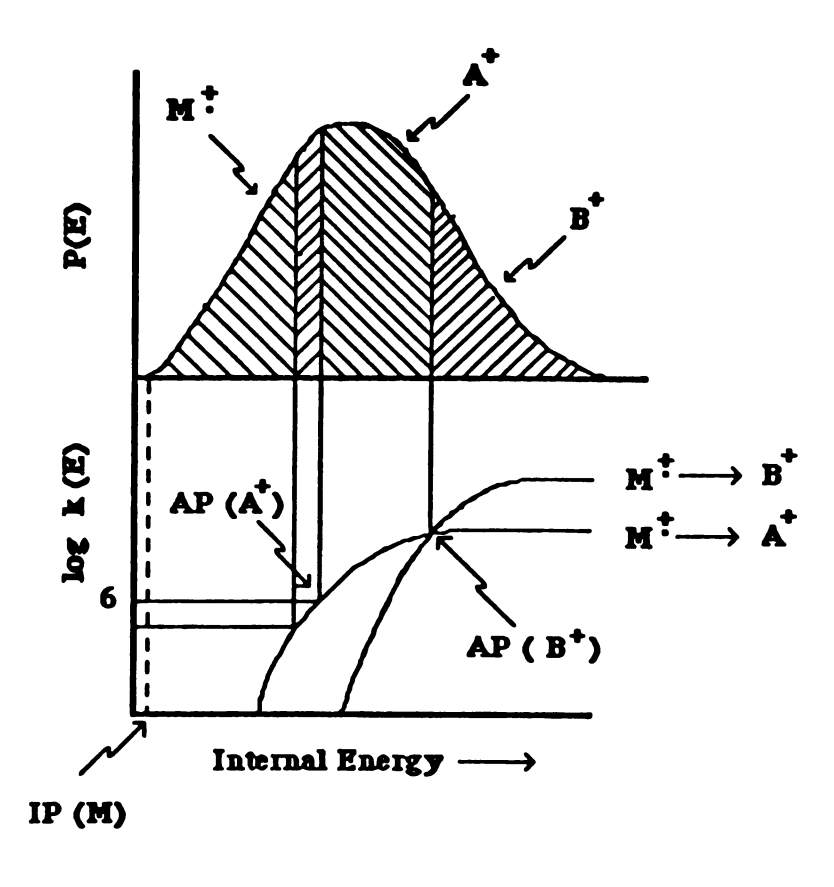


Figure 47. Relationship of P(E) and k(E) for unimolecular decomposition.

Decomposition of M<sup>+</sup>. to a fragment ion, A<sup>+</sup> requires an amount of energy equal to the sum of the IP (M<sup>+</sup>) and the bond dissociation energy, D (M-A), required to form A from M. The fragment ion, A<sup>+</sup>, is generally observed at an energy slightly above this lower limit, and this is called the appearance potential. The appearance potential (AP) of A<sup>+</sup> from M<sup>+</sup>. is the amount of absorbed energy at which the rate constant for reaction is 10<sup>6</sup> sec<sup>-1</sup> (i.e., lifetimes are 10<sup>-6</sup> sec or less). This value has been determined to be the time required for an ion to leave an ion source in which it was

formed, in order that it may be detected. In EI, the extent to which fragmentation occurs is dependent on the amount of internal energy associated with the molecular ion and the rates of unimolecular decomposition to a set of fragment ions. The rate constants for decomposition to a set of fragment ions are affected by the precursor ion's internal energy. Molecules which readily stabilize both a radical and positive charge, such as unsaturated ring-containing compounds, will be more likely able to stabilize this excess internal energy, leading to less fragmentation. Fragmentation is also determined by the rate constants of reaction for the decomposition of the excited state of the molecular ion as shown in Scheme 4 below:

Scheme 4

These rates,  $k_1$  and  $k_2$  are unique to the fragment ions,  $A^+$  and  $B^+$ , respectively, and will depend on the amount of internal energy associated with the molecular ion. The lifetime of the excited molecular ion, which determines its stability, as stated earlier, is the limiting factor in determining the amount of fragmentation observed. For higher internal energies, as shown in Figure 48, the fragment ion  $B^+$  may be more favored than decomposition to  $A^+$ , and the point at which the rate curves intersect is the appearance potential, AP ( $B^+$ , M).

An analogous situation may be operative for the chemical ionization experiment. Equation 5a showed that the formation of the protonated molecule upon reaction of neutral analyte with an acidic reagent ion, such as  $CH_5^+$ , will have a distribution of

internal energies. As discussed earlier the maximum energy,  $E_{max}$ , is the difference in [PA(M) - PA(CH<sub>4</sub>)]. This behavior is described pictorially in the upper curve of Figure 48.

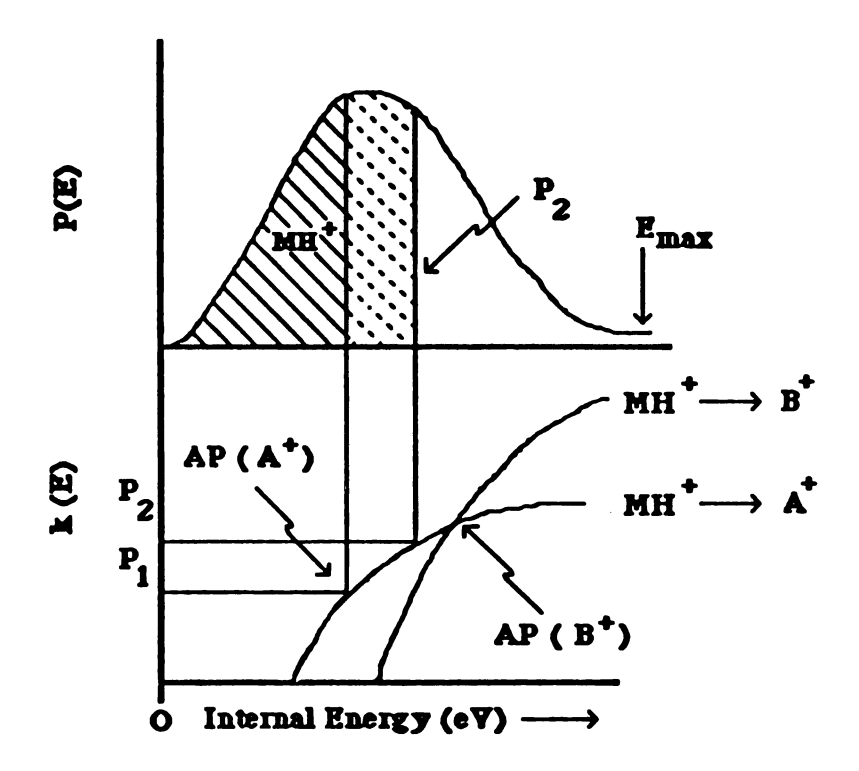


Figure 48. Distribution of internal energy in protonated analyte molecule following exothermic proton transfer.

Decomposition to a set of fragment ions has been shown to be dependent on the amount of excess energy associated with the MH<sup>+\*</sup> complex. The more facile the fragmentation process, the lower the energy requirement, and as a result, the faster the rate of dissociation to fragment ions. The rate of dissociation will be affected, though, by how rapidly the protonated molecule can dissipate its excess energy, specifically through collisional stabilization. Shown in a Wahraftig-type diagram,

Figure 48, are the effects of low ion source pressure k<sub>collision</sub> (P<sub>1</sub>) and high ion source pressure k<sub>collision</sub> (P<sub>2</sub>) on the stabilization of the protonated molecule. For MH<sup>+\*</sup> to undergo decomposition to an observed A<sup>+</sup> ion, an amount of energy equal to the AP (A<sup>+</sup>, M) is required. If collisional stabilization can occur in a sufficiently short time, insufficient internal energy will be available to A<sup>+</sup> for fragmentation to occur. Thus, upon increasing the ion source pressure from P, to P2, a smaller fraction of MH<sup>+\*</sup> will be converted to the fragment ion species, A<sup>+</sup>, and a greater fraction of MH<sup>+\*</sup> will be stabilized to the MH<sup>+</sup> ion. The dependence of rate of reaction on ion source pressure is thus an important variable in determining the amounts of fragmentation observed in a chemical ionization experiment. Alcohols, for example, are found to readily undergo decomposition to the [M-H<sub>2</sub>O]<sup>+</sup> ion from the excited, protonated molecule. These rates of reaction are so fast that even at high ion source pressures, in which the collision frequency is high, stabilization of the MH<sup>+\*</sup> does not occur before elimination of H<sub>2</sub>O occurs. For many CI experiments, though, decomposition reactions do not proceed at such a facile rate, and therefore will be dependent on the how rapidly the MH<sup>+\*</sup> complex can be collisionally stabilized. If the protonated molecule is capable of undergoing several stabilizing collisions in a very short time (less than that required for fragmentation) with other neutral reagent molecules, the amount of excess energy associated with the excited protonated molecule will be dissipated, and as a result, an insufficient amount of energy will be available for bond-breaking to occur.

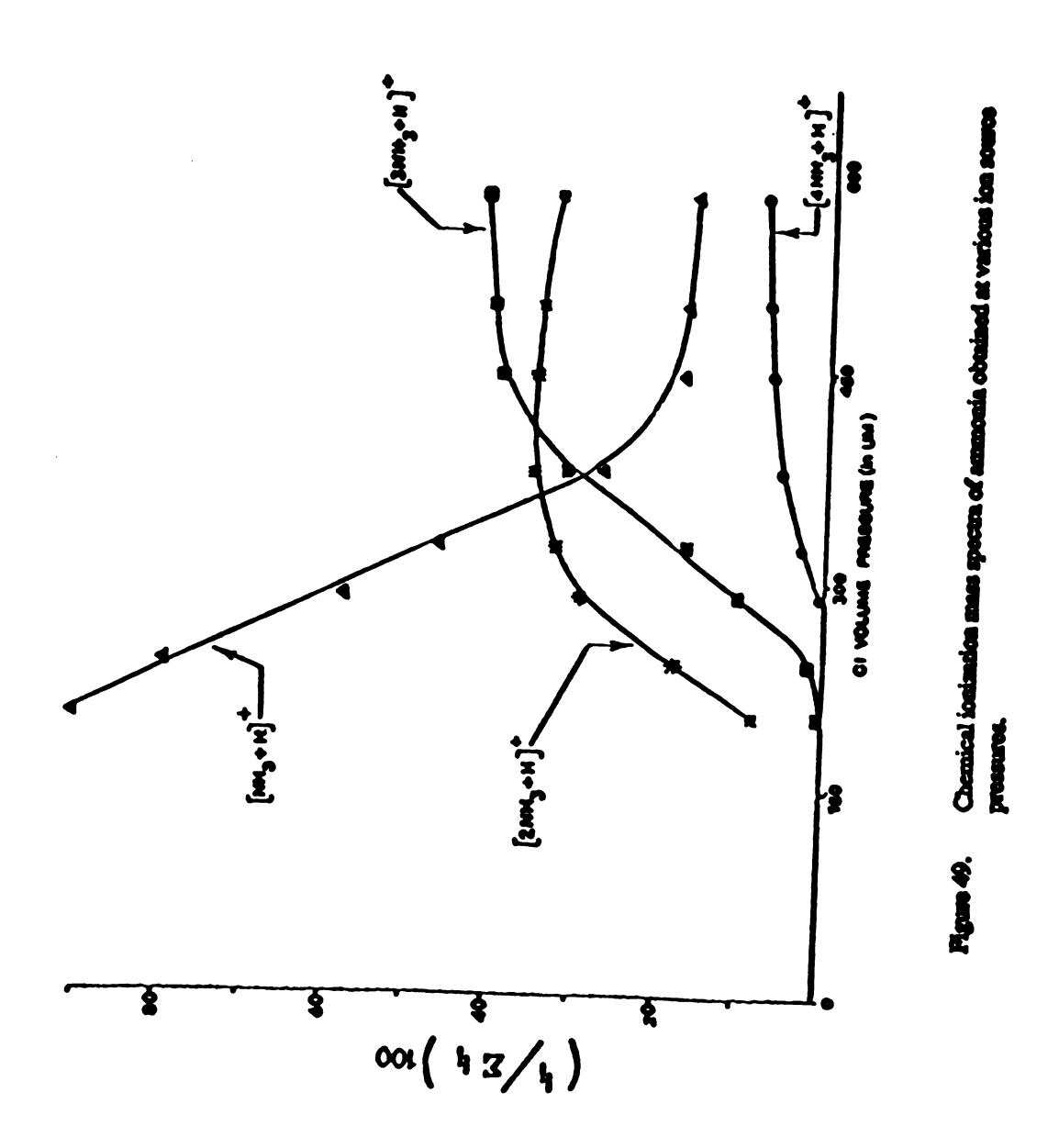
Methane has perhaps been chosen most frequently for most CI applications due to the relatively low PA of the CH<sub>4</sub> molecule and the general reactivity that is observed, including reactions with alkanes, <sup>81</sup> aromatics, <sup>82</sup> and alcohols. <sup>83</sup> However, a plethora of reagent gases are found in literature which are described for particular CI experiments. For positive ions, these reagents include hydrogen, <sup>84</sup>

tetramethylsilane, 85 diethylamine, 86 and isobutane. 87 Research investigations in this laboratory have used ammonia CI-MS for enhanced qualitative and quantitative information in the analysis of organic acids. The proton affinity of NH<sub>2</sub> is quite high relative to methane; values are reported between 202-205 kcal mole<sup>-1</sup>, <sup>88,89</sup> implying that this chemical ionization reagent is a very weak Brønsted acid, and will protonate only the most basic compounds, such as amines. The reagent ions formed upon electron impact of NH<sub>3</sub> are summarized in eq. 7. At pressures above c.a. 300 mtorr of NH<sub>3</sub>, solvation of the ammonium ion about neutral NH<sub>3</sub> molecules readily occurs, even though rates for clustering reaction are quite slow relative to the bimolecular proton transfer reactions, 90 due to the fact that a third body collision is

$$NH_3 + e^-$$
 .....  $NH_3^+, NH_4^+$  (7a)

$$NH_3 + e^-$$
 .....  $NH_3^+$ ,  $NH_4^+$  (7a)  
 $NH_4^+ + NH_3$  .....  $H(NH_3)_n^+$ ,  $n = 2-4$ . (7b)

required for stabilization of the solvated molecule. The extent to which ammonia will solvate about itself to produce the ammonium cluster ions is pressure dependent, and as will be shown later, the proper choice of operating pressure is important for the quantitative studies undertaken. A typical chemical ionization mass spectrum of ammonia is shown in Figure 49 below. At relatively low ion source pressures, as measured by a thermocouple probe positioned near the CI source and pressure measured with a Hastings gauge, the NH<sub>4</sub><sup>+</sup> ion predominates. As ion source pressure is increased to greater than 0.2 torr, solvated ions of the form [2NH<sub>2</sub>+H]<sup>+</sup> are the most abundant reagent ions. Keough and DeStefano<sup>91</sup> reviewed recently the reactivity of analyte molecules with NH<sub>3</sub> reagent ions. A number of equations



representing the possible reactions between analyte molecule, M, and NH<sub>4</sub><sup>+</sup> are summarized below. If the PA of M is greater than the PA (NH<sub>3</sub>), then ions characteristic of the molecular weight of the analyte may be formed, as shown in eqs. 8a and 8b. If however, PA (M) is less than PA (NH<sub>3</sub>), then electrophilic attachment

$$M + NH_4^+$$
 ----->  $[M+H]^+ + NH_3$  (8a)

$$[M+H]^{+} + NH_{3} - - - [M\cdot NH_{4}]^{+}$$
 (8b)

$$M + NH_4^+$$
 .....  $[M \cdots H \cdots NH_3]^{+*}$  (9a)

 $NH_3$ 

$$[M \cdots H \cdots NH_3]^{+*}$$
  $[M \cdot NH_4]^+$  Fragments (9b)

$$[M \cdots H \cdots NH_3]^{+*} - \cdots > M + NH_4^{+}$$
 (10)

of NH<sub>4</sub><sup>+</sup> to the analyte may occur, as shown in eq. 9a and 9b. As for cases observed with methane-CI, the process most likely to be observed will depend on the relative difference in PA between analyte, M, and NH<sub>2</sub>.

Analogous to the situation described for methane, the stability of the initially formed [M·NH<sub>4</sub>]<sup>+\*</sup> complex is dependent on the excess internal energy associated with the complex and it is this which is important in determining whether or not the complex will be sufficiently stabilized by mild collision with neutral NH<sub>3</sub> molecules, or whether or not the excess internal energy is sufficient to cause bond dissociation to either the protonated molecule, fragment ions, or the initial reactant ions. When PA

(M) is significantly lower than that of NH<sub>3</sub> it is likely that the complex will dissociate back to the initial reactants, resulting in no net reaction (eq. 10). A lower limit value of PA = 188 kcal/mole has been reported for autodissociation to occur.  $^{92}$ 

The ammonium adduct ion has been ascribed to electrophilic attachment of NH<sub>4</sub><sup>+</sup> to the neutral analyte with stabilization occurring by collision with other neutral reagent gas molecules. This product typically arises when the PA (M) is intermediate to that required for eq. 8, and that for eq. 10 to occur. Often, when there is slight exothermicity associated with this adduct ion formation, it is possible for the newly formed adduct ion to dissipate some of this excess energy through elimination of neutral species. Several fragmentation pathways describing this behavior are found in literature, <sup>93</sup> and mechanisms for the formation of these ions are discussed in detail elsewhere. <sup>94</sup>

Little attention, however, has been given to reactions of analyte, M, with the reagent ions of the form  $H(NH_3)_n^+$ , where n=2-4. For organic acids analyzed by  $NH_3$ -CI, increasing the source pressure leads to an increase in the abundance of the  $[M \cdot NH_4]^+$  ion relative to  $[MH]^+$  ion. This behavior is shown for 2-hydroxyisobutyric acid (di-TMS) in the Figure 50. At relatively low ion source pressures (0.2-0.3 torr), the intensity of the protonated molecule is nearly equivalent to the adduct ion,  $[M+NH_4]^+$ . The abundance of the protonated molecule decreases rapidly with higher reagent gas pressure. This behavior is typical for almost all the organic acids that have been analyzed to date. Literature values of the proton affinities of chemically similar compounds (e.g.,  $CH_3COCH_2CH_3$ ) are very near that of ammonia; PA ( $CH_3COCH_2CH_3$ ) = 201.3 kcal mole -1. The small difference in these two values suggests that proton transfer and adduct ion formation reactions may be somewhat competitive. Two possibile explanations for the observed increase in adduct ion formation may be considered: (a) increased ion source pressure leads

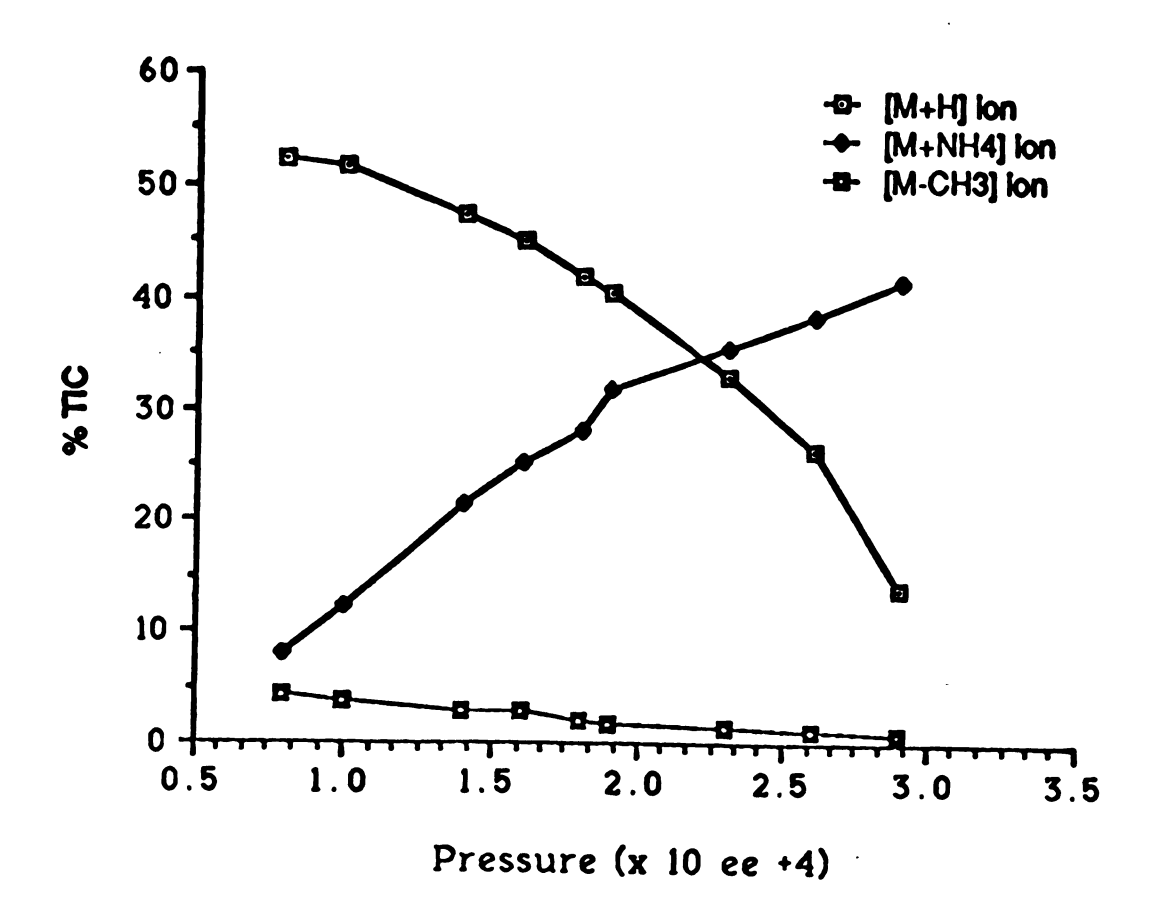


Figure 50. Plot of ion source pressure vs. relative intensities of pseudo-molecular ions for 2-hydroxyisobutyric acid (di-TMS)

more effectively the [M··H··NH<sub>3</sub>]<sup>+\*</sup> intermediate and/or (b) the ions of the form  $H(NH_3)_n^+$  may actually participate to some extent in the direct formation of the molecular adduct ion species. Little attention has been placed on these solvated ions and their immediate effect on analyte ion formation. Kebarle<sup>95</sup> suggests that the solvated ammonium ions do not participate, to an appreciable extent, in proton transfer reactions since the thermochemical stability of solvated ions increases with increased clustering, and as a result, proton abstraction from the solvated ion becomes more difficult. The question as to the extent to which adduct ion formation is affected by increased abundance of solvated ammonium ions has not been fully addressed.

One method for determining the role these solvated ions play in the formation of the [M·NH<sub>4</sub>]<sup>+</sup> adduct is to actually monitor a decrease in abundance of H(NH<sub>3</sub>)<sub>n</sub><sup>+</sup> ions as a function of eluting analyte from a gas chromatograph. This technique has come to be known as reactant ion monitoring (RIM). This technique has found widespread use for determining relative response factors in chemical ionization experiments. 96,97 This point will be taken up later in the section on quantitation using chemical ionization mass spectrometry. A RIM experiment was performed on malic acid (tri-TMS) and adipic acid (di-TMS) in order to determine the effect of these solvated ions on [M+NH<sub>3</sub><sup>+</sup>] ion formation. The results of this reactant ion monitoring analysis suggested that the ammonium adduct ions of the form H(NH<sub>2</sub>)<sub>2</sub><sup>+</sup> and H(NH<sub>3</sub>)<sub>3</sub><sup>+</sup> do not have a direct impact on the equilibrium concentration of the Two possible explanations for this behavior are molecular adduct ion species. considered. (1) Steric effects do not allow the "bulky" clustered ammonium reagent ions to come in sufficiently close proximity to the analyte molecule for ammonium attachment to occur since attachment to an analyte requires an available electron lone

pair. For most esters, both proton transfer and ammonium ion attachment have been found to be thermodynamically favored at the carbonyl oxygen. The same site of reaction is presumed for trimethylsilyl derivatives of organic acids. 98-100 (2) The bond strength of the hydrogen atom to the solvated ammonia molecules is too strong for the analyte to overcome. As Kebarle suggests, the hydrogen atom is bound tightly through solvation of ammonia molecules that the bond strength is much greater than the proton affinity of the analyte for adduct ion transfer to occur.

## Quantitative mixture analysis using CIMS

Chemical ionization mass spectrometry has been used routinely in analytical chemistry for providing quantitative information on known compounds. Accurate measurements of the amount of a particular substance present in an often complex medium may be made. A number of approaches to attaining quantitative results on unknowns have been described (using not only CI, but also EI, and others). Perhaps the most widely used method has been to add a stable-isotopically labelled analog of known concentration to a mixture containing the species to be measured. This is the basis of isotope-dilution mass spectrometry. The amount of unknown present may be deduced from a comparison of the mass spectrometric response of the unknown and the known labelled analog. Care must be taken in using stable isotopically labelled substrates, though, for quantitative determinations. The prevalence of isotope-effects is a well documented phenomenom. 101-102 Deuterium, for example, can cause severe isotope effects. Rate constants for reactions comparing the protium and deuterium analogs (measured mass spectrometrically) can differ by a several orders of magnitude. In addition, protonation and fragmentation reactions can also be different for the unlabelled and labelled analogs. This point will be addressed more

fully in a later section.

Problems associated with chemical ionization, especially when combined with gas chromatography have been described in detail by Millard. The capacity of chemical ionization mass spectrometry as a successful quantitative analytical method for mixture analysis has been the subject of much debate. Munson addresses the question of quantitation by chemical ionization in a recent review. Much of the discussion has been summarized here.

In order to determine the quantitative capabilities of this technique it is first important to determine the sensitivity of the method and how it may differ with structural changes in molecules (e.g., polarity). Methane-CI will be used for the following discussions since it is the most common chemical ionization reagent gas, although the discussion is valid for any other reagent gas which is involved in proton-transfer reactions.

As was discussed earlier, reactions of the analyte with either  $CH_5^+$  and/or  $C_2H_5^+$  can result in both the formation of the protonated molecule and a variety of fragment ions, depending on the exothermicity of the reaction. The following equations represent the reactions of these two reagent ions with the analyte, M, where  $\sum P_i$  represents the total number of ions produced (i.e., both fragment ions and molecular ions) by the ion molecule reactions described earlier. The rates of

$$^{k}_{17}$$
 $CH_{5}^{+} + M \longrightarrow \Sigma P_{i}$  (11)

$$c_{2}H_{5}^{+} + M - \Sigma P_{i}$$
 (12)

reaction for equations (11) and (12) are determined by the rate constants for proton

transfer. The rate equation governing these two processes may be given in the form of a differential equation, which may be approximated as a difference, since conversion of reactant ions to product ions is small (i.e., [reagent ions] >> [product ions], c.a. 1000:1) as shown in Equation 13 below. Since no product ions are present initially, the difference

$$d[\Sigma P_{i}]/dt = \{k_{17}[CH_{5}^{+}] + k_{29}[C_{2}H_{5}^{+}]\}[M]$$
 (13)

is equivalent to the final concentration of the added sample. In addition, the ion currents measured in the mass spectrometer are representative of the relative concentrations of the samples being analyzed, that is,  $\sum P_i$  may be approximated by  $\sum I_i$ , where  $I_i$  is the intensity of ion with molecular weight of i. This equation assumes that transmission of all ions through the ion source, and detection of the ions is equivalent for all ions, which is generally valid. Upon integration the reaction can be rewritten (eq. 14), where t refers to the residence time of the reactant ions:

$$\sum I_{i} = t \left\{ k_{17} (I_{i})_{17} + k_{29} (I_{i})_{29} \right\} [M]$$
 (14)

This parameter is typically the most difficult to measure accurately for determining rates of reaction (which accurately define sensitivities in CI). Two approaches have been most frequently employed for determining this parameter accurately. The residence time of the reagent ions in the ion source can be determined by studying reactions of known rate. Secondly, these values have been found to be estimated very accurately from drift velocity measurements.

Theoretical rate constants (k) for reactions involving methane have been

determined from Langevin ion induced-dipole theory, 105-106 average Dipole Theory (ADO), 107 which more accurately estimates rate constants for polar molecule-ion interactions, and other more recent theories. 108 Experimentally obtained results, in general, compare favorably with theoretically obtained rate constants. In addition, experimentally obtained values have been found to differ by no more than two orders of magnitude for compounds as different as acetone and steroid molecules. For a homologous series of aliphatic hydrocarbons, experimentally obtained rate constants have been determined to be nearly identical (c.a.  $1.0 \times 10^{-9}$ cm<sup>3</sup>mol<sup>-1</sup>sec<sup>-1</sup>). Determinations of rate constants from experimental data require knowledge of the ion intensity relationship between reagent ion and product ion and residence time of the reagent ion. Field et al. demonstrated that the rate constants for ion molecule reactions of methane could be determined from this precursor-product ion relationship. <sup>107</sup> Small variations in the rate constants are attributed to changes in structures of the neutral compounds. These variations can be related to the mass of the ions (and molecules), dipole moments and their polarizabilities.

For determination of rate constants from experimentally obtained data, it is critical that the ion source pressure being maintained constant throughout analysis. This becomes an especially important consideration when analysis of mixtures is made by GC-MS and relative concentrations of unknowns are to be determined accurately. Munson demonstrated that rate constants for a variety of ion molecule reactions could be estimated fairly accurately through RIM, as mentioned earlier. RIM is analogous to selected ion monitoring (SIM). Instead of monitoring ions which are indicative of the analyte under investigation, RIM monitors a depletion in reagent ion concentration as ion molecule reactions take place in the ion source. Rate constants for eluting species from a gas chromatograph may determined based on the knowledge that as a component elutes from the gas chromatograph, a decrease in

reagent ion concentration will be observed (presuming ion molecule reactions occur). As an example, Munson and coworkers showed that the rate constant for the reaction  $C_2H_5^+$  with an eluting species, E, may be obtained from manipulation of eq. 14, as shown in eq. 15, below. Assuming the peak shape of a eluting species is nearly triangular, the rate constant for reaction may be modified to the form shown in eq. 16, where  $t_2$ - $t_1$  is defined as the width at base of the chromatographic peak, F is the

$$k = \ln \left\{ 1 - \Delta I_{C_2 H_5}^+ / I_{(C_2 H_5^+)_0} \right\} / 2E t$$
 (15)

$$k = -F(t_2 - t_1) \ln \{1 - \Delta I_{C_2 H_5}^+ / I_{C_2 H_5}^+ \}_{max} / 2Et$$
 (16)

helium gas flow rate, and  $\Delta I_{C_2H_5}^+$  is the peak minimum observed for the reactant ion  $C_2H_5^+$  as the species elutes from the gas chromatograph. Since t is known with the least amount of accuracy, it is customary to determine <u>relative</u> rates of reaction, by comparing the rates for two components eluting from the gas chromatograph. In this way, the residence time of the reagent ion may be eliminated from the reaction. It is evident from this equation that small fluctuations in reagent gas pressure will affect the measured rate constants. Recall that slight differences in ion source pressure can result in dramatic variations in the abundances of reagent ions. As a result, inaccurate measures of relative rate constants and relative concentrations will be made. A method for achieving such a regulated ion source pressure has been to incorporate a pressure regulator.

The importance of calculating these relative rate constants lies in the fact that these values are an accurate measure of the relative molar sensitivities of the gas chromatographic effluents. The dearth of data on experimentally obtained rate constants for reaction and those obtained by theoretical calculations are generally in

good agreement. In addition, when comparing homologous series of compounds by the RIM method, results suggest that CI can indeed be used accurately to quantitate the components of a mixture.

There has been a great deal of concern about the utility of chemical ionization mass spectrometry for the analysis of complex mixtures of organic acids (and others) isolated from physiological fluids. It is suggested that due to the diverse chemical nature and complexity of the isolated organic acids, rate constants for reaction may differ substantially from one component to the next. For complex mixtures such as organic acids in urine it is <u>not</u> uncommon to have coeluting species in both GC and GC-MS analyses. Obviously, by GC alone, no quantitative information can be derived for the analytes. However, by GC-MS, especially when using a relatively "reliable" method such as EI, the concentrations of the coeluting species can often be determined based on the intensity relationship of analyte ions. If coeluting species give rise to an identical fragment ion in the EI mass spectrum, the capacity to accurately quantitate the two species will be markedly decreased.

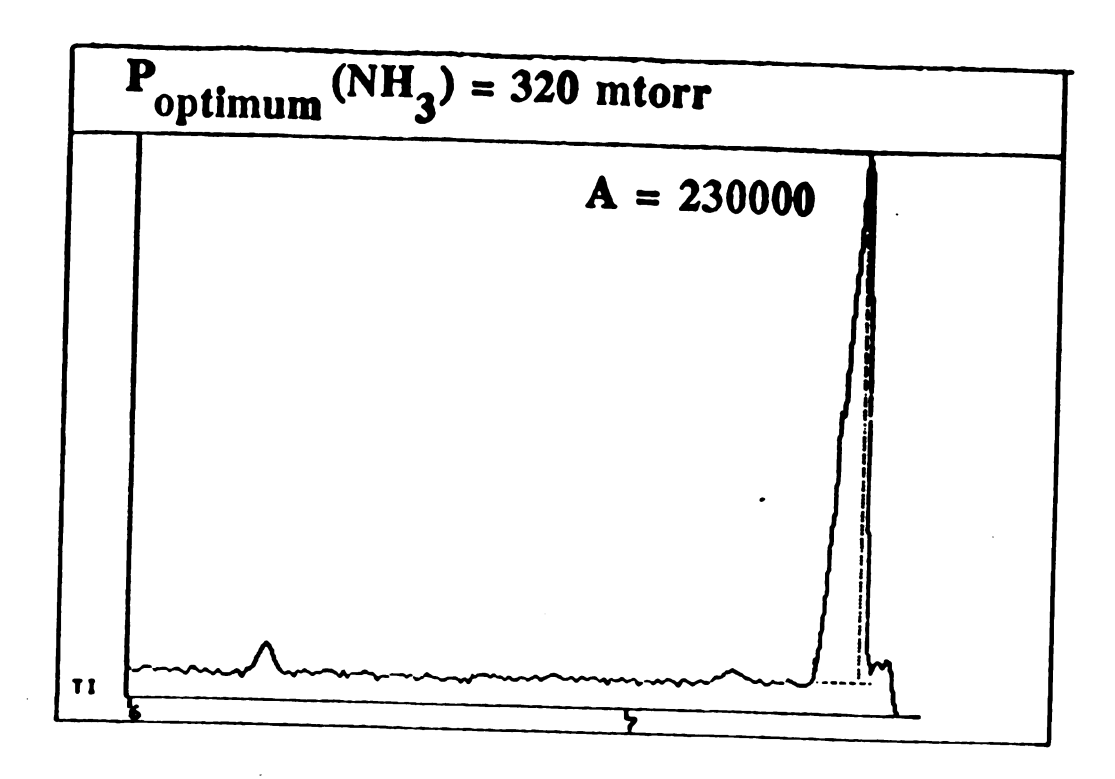
Chemical ionization is evaluated as to whether the quantitative relationship of coeluting species can be accurately reflected. The ability of the technique is further tested when one of the two (or more) coeluting species is in large excess relative to the other eluting species (a situation not at all uncommonly observed in metabolic profiling analyses). It has been suggested that preferential ionization of the major eluting species will occur, leading to an inaccurate quantitative representation of the co-eluting species. In addition, a rapid depletion of CI reagent ions available in the ion source is assumed as a concentrated analyte elutes from a GC column, thus causing fluctuations in reagent ion source concentration. As was shown in eqs. 15 and 16, this can lead to variations in calculated rate constants, and result in poorly represented relative molar sensitivites.

### Results of quantitative metabolic profiling analysis using CIMS

Experiments have been performed to identify whether CI-MS accurately reflects the composition of mixtures exhibiting the type of behavior just mentioned. A portion of this thesis investigates chemical ionization mass spectrometry and its capacity for providing quantitative information on complex mixtures of organic acids in complex media (e.g., urine). The following sections do not give a rigorously detailed treatment of CI as a quantitative method (i.e., by yielding calculations of rate constants for reactions) but the results presented suggest clearly that, when conditions are held rigorously constant in a CI experiment, the ionization method is capable of producing results that parallel those obtained from GC-EI-MS.

The results to be presented are obtained using ammonia as the reagent gas. There are a number of reasons for this choice of reagent gas. Comparison of results using methane, isobutane, and ammonia (at optimized ion source pressure for best sensitivity) on simple mixtures of derivatized organic acids revealed that NH<sub>3</sub>-CI is nearly three-fold more sensitive than CH<sub>4</sub>-CI for the analysis of these types of compounds. SIM results on p-hydroxybenzoic acid (di-TMS) are shown in Figure 51 a-b. Isobutane-CI also has been investigated. Typically, ion yields are found to be 5-10 times lower than those obtained using NH<sub>3</sub>-CI for these compounds. In addition, results on simple mixtures suggest that the most accurate reflection of the composition of the mixture is obtained when NH<sub>3</sub>-CI is used. This point will be taken up in greater detail shortly.

The TMS derivatives of organic acids are an interesting class of compounds to investigate for quantitative studies involving ammonia since these ester moieties typically exhibit proton affinities (experimentally determined and are based on



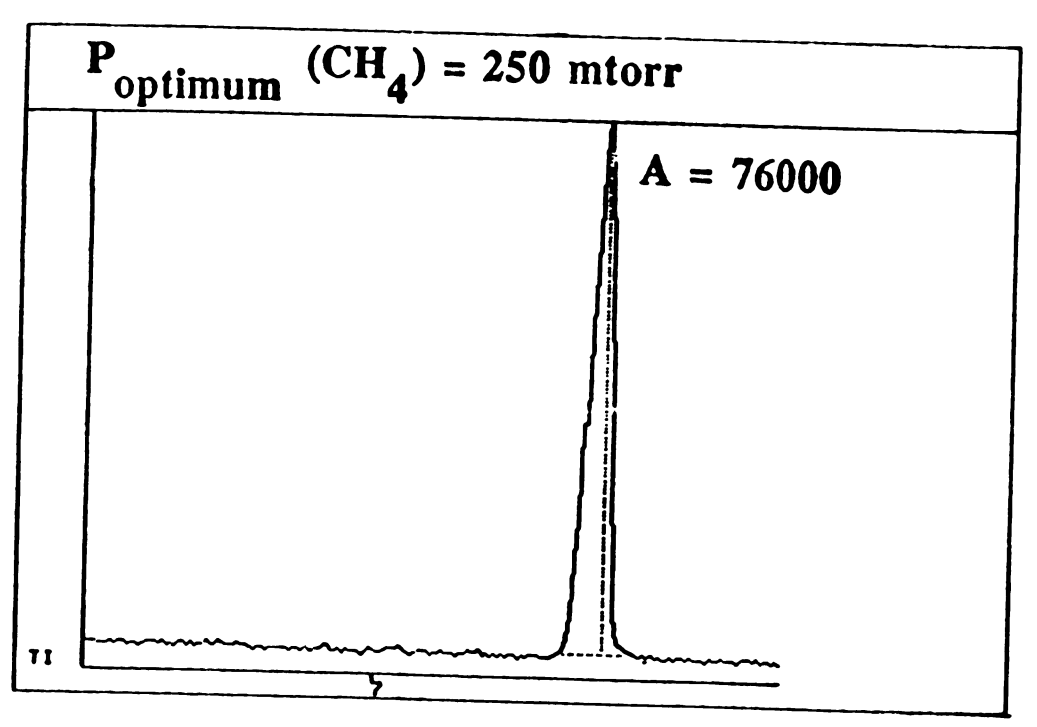


Figure 51. SIM of p-hydroxybenzoic acid (di-TMS) comparing sensitivity obtained at optimum ion source pressure using (a) ammonia and (b) methane

responses relative to other CI reagent gases, such as *i*-butane, methane, etc.) that are very near, but usually slightly lower than that of ammonia, itself. For many of these organic acids relatively intense [M+H]<sup>+</sup> ions may be observed in the CI mass spectrum even though the proton affinities of these analytes are presumed to be less than that of NH<sub>3</sub>. Explanations for this result may be based on the fact that in a molecule, some sites may be more basic than others, affecting to some degree the site at which proton attachment may occur. Form a thermodynamic standpoint, the carbonyl oxygen may be sufficiently basic for either proton transfer or NH<sub>4</sub><sup>+</sup> attachment to occur. In any case, the differences in overall proton affinities between reagent gas and derivatized organic acids is sufficiently small such that only [M+NH<sub>4</sub>]<sup>+</sup> and [M+H]<sup>+</sup> ions are observed in the CI mass spectrum of these compounds.

## Experimental

All experiments were performed using a Hewlett Packard 5985 GC/MS/DS equipped for capillary column chromatography. In most cases a 25m HP-5 megabore capillary column (i.d. 0.52mm) was used. A non-vitreous deactivated capillary column (0.11 mm i.d.) was interfaced to the gas chromatograph and mass spectrometer, providing a split ratio of approximately 5:1. The helium flow rate using the megabore column was adjusted to approximately 5ml/min. When wide-bore capillary columns were employed (0.32mm i.d.) the helium pressure was maintained at approximately 1-2 ml/min flow rates. Reagent gas pressure was regulated by use of a Granville-Phillips Pressure Regulator (model # AC-7096).

Source temperature for EI and CI analyses was maintained at 150 °C for the

analysis of derivatized organic acids. In the chemical ionization mode, the operating ion source pressures were maintained between 100-500 mtorr, though best sensitivity was typically obtained near 300 mtorr. The electron energy was maintained at 120-150 eV and emission current was 325  $\mu$ A. For electron ionization, the electron energy was 70 eV and emission current was 300  $\mu$ A.

Ultra high purity methane (> 99.9 %) and ultra high purity ammonia (> 99 %) were obtained from Matheson Chemical Co., Joliet, II. Organic acid standards were obtained from Sigma Chemical Co. TMS-derivatives were made using bis(trimethylsilyl)trifluoracetamide (BSTFA) purchased from Regis Chemical Co. Urine samples were supplied from Meridian Instruments, Okemos, MI.

#### Results and Discussion

The proper choice of operating pressure is important in any chemical ionization experiment. Ion source pressures are typically measured (quite inaccurately) based on ion guage measurements, which are typically located far from the ionization region for CI analyses. Figure 52 shows plots of ion guage pressure readings w. pressures obtained from the postioning of a thermocouple at the entrance of the CI volume with measurements of pressure made using a Hastings guage for ammonia and methane. These values are more accurate measures of the CI ion source pressure.

Furthermore, tuning of the instrument at one particular pressure for optimum calibrant signal does not always ensure that this <u>same</u> pressure is the optimum pressure for gas chromatographic analysis. The best approach to achieving the most reliable chemical ionization results is obtained following a standard experimental design. For proper calibration of the instrument for CI analyses, perfluorotributylamine (PFTBA) is used. Tuning is achieved using methane as a

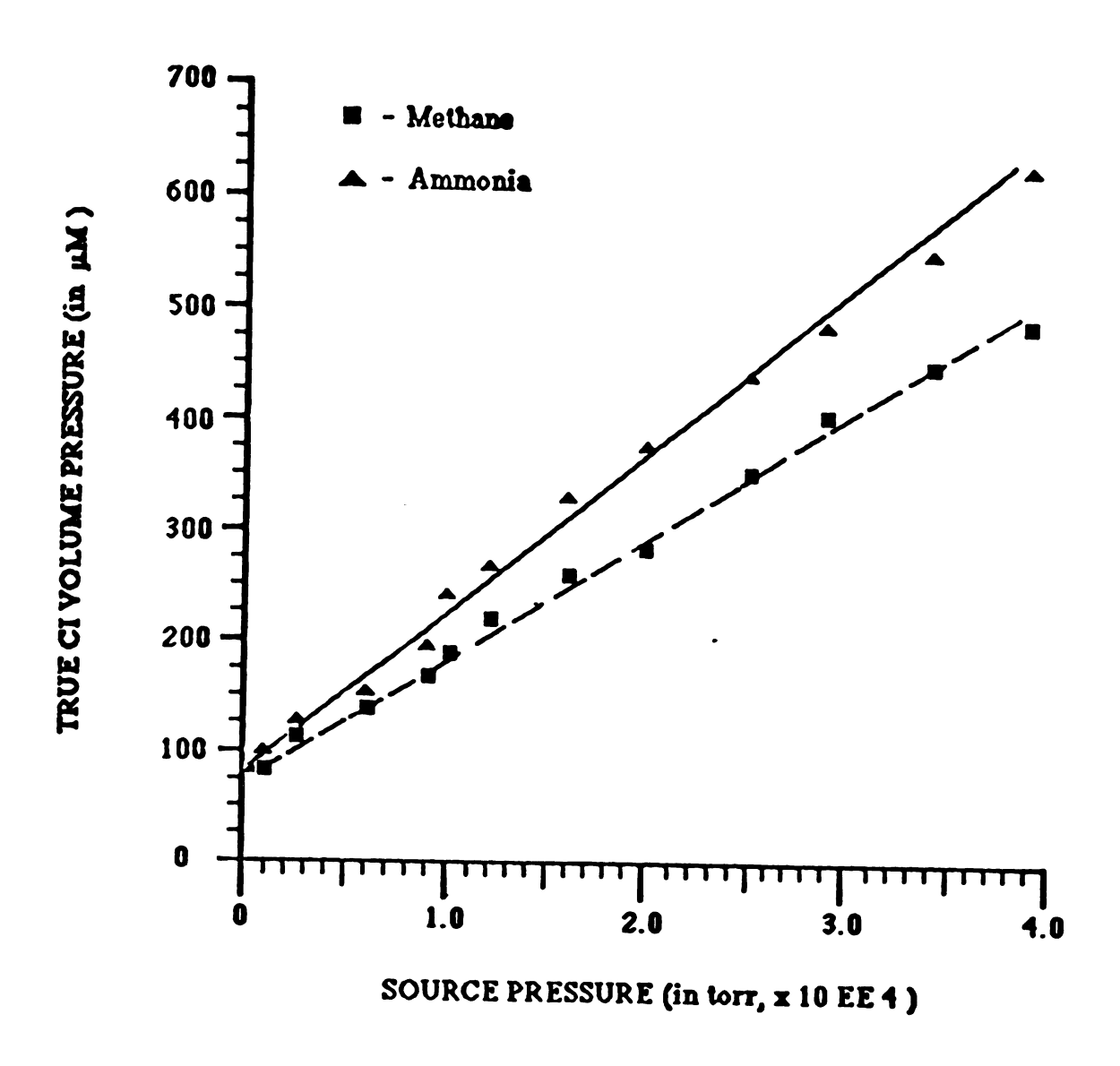
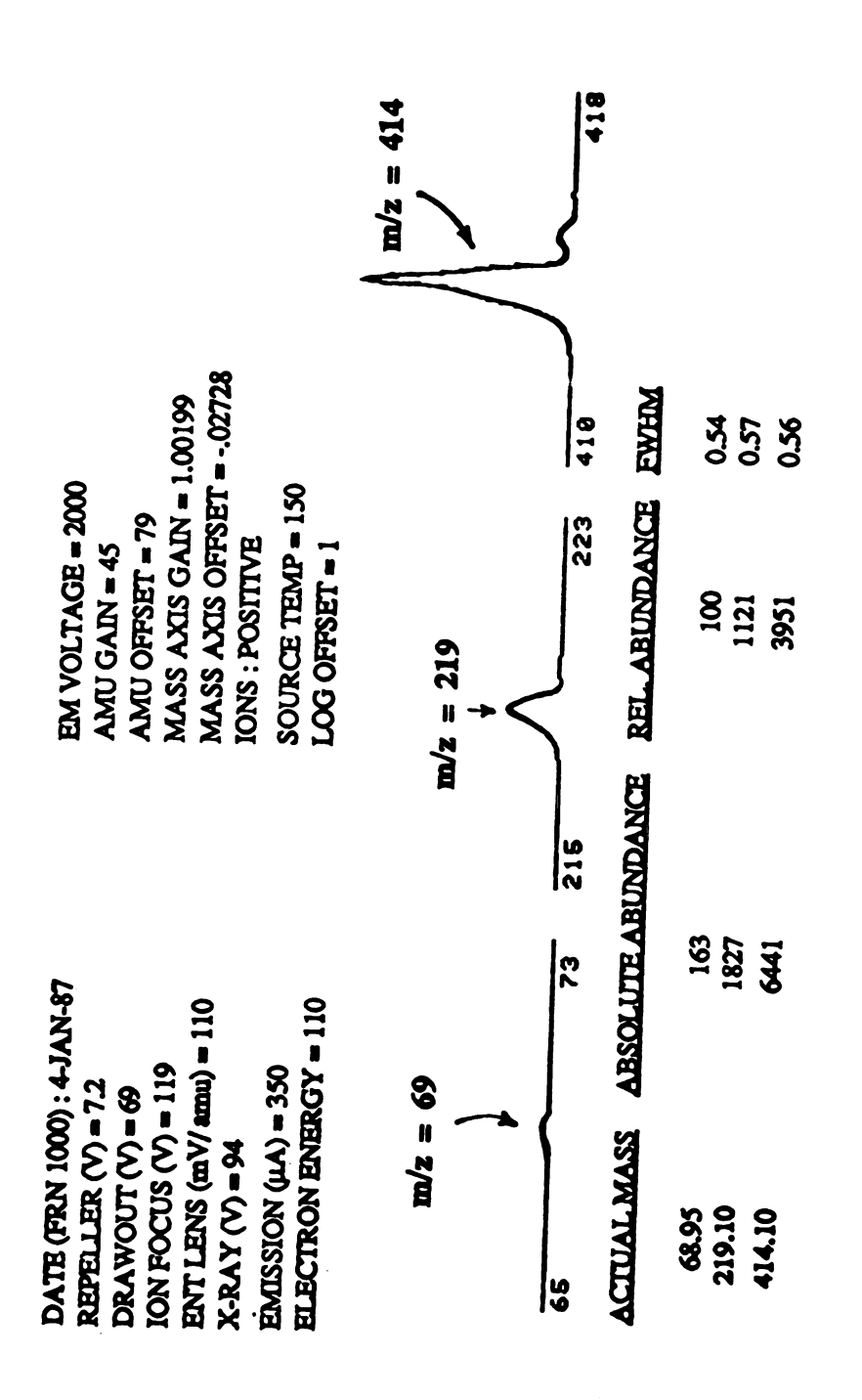


Figure 52. Comparison of true CI ion source pressure vs. source housing pressure

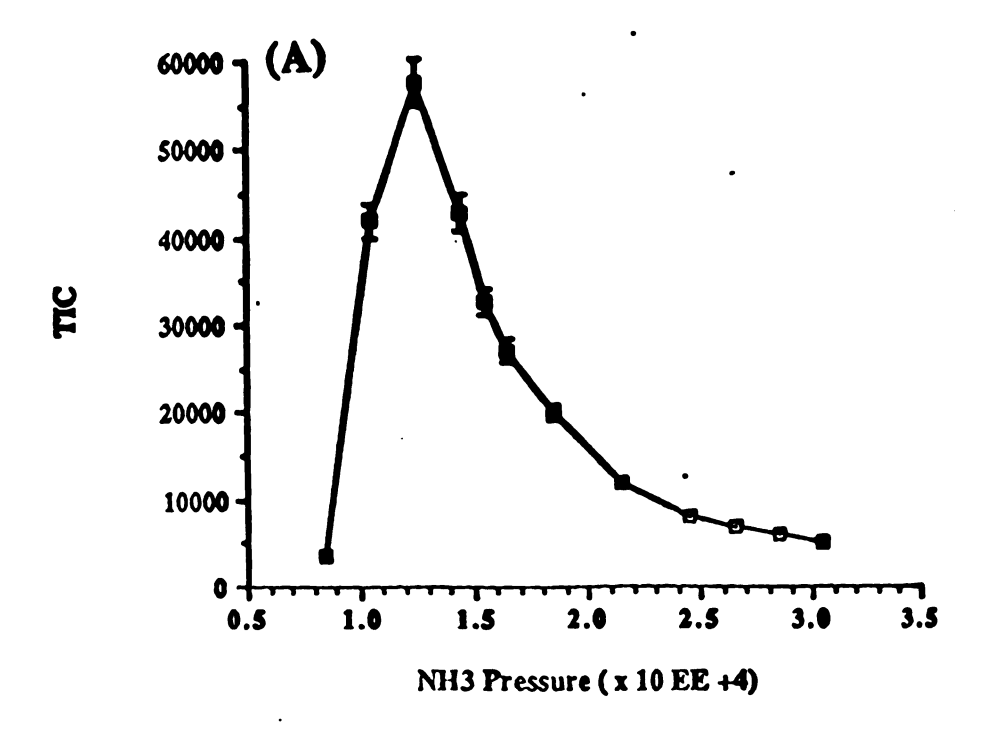
reagent gas, regardless of whether or not the analyses to follow will use ammonia, isobutane, methane, or some other reagent gas. A typical tuning file is shown in Figure 53 below. The relative peak heights of m/z 69 ( $CF_3^+$ ), 219 ( $C_4F_9^+$ ), and 414 ( $C_8F_{16}N^+$ ) are manipulated by optimally tuning the ion lenses and repeller. It is important that; (a) the instrument be tuned daily when operating in the CI mode (since performance degradation occurs more rapidly in this ionization mode than in the EI mode) and (b) tuning files do not change dramatically from one day to another. That is, the relative ion intensity ratios for the calibrant should remain nearly identical if CI results are to be used for quantitation.

Once these tuning procedures have been accomplished, a series of standards should be run to determine by GC-MS to determine the optimum operating pressure for analysis. Shown in Figure 54a and 54b below is the relationship between ion source pressure and ion counts for maleic acid (di-TMS) and p-hydroxybenzoic acid (di-TMS). Typically, optimum sensitivity is achieved at an ion source pressure of 300 mtorr. However, as ion source degradation occurs over time, experience has shown that higher source pressures are needed to obtain optimum ion signals.

More importantly, for quantitation, is to investigate the relationship between analyte ion signals and ion source pressures. Molecular weight information, in the form of the protonated molecule and molecular adduct ion species, are observed in the NH<sub>3</sub>-CI mass spectra of most derivatized organic acids. Figure 54 also shows how ion source pressure affects the intensity relationship of these two ions. In most cases, the ammonium adduct ion, [M+NH<sub>4</sub>]<sup>+</sup>, reaches a maximum abundance at about a pressure of 300 mtorr. This information is important for the reason that the intesity relationship between the protonated molecule and molecular adduct ion species can often be used to differentiate isomers. As an example, the mass spectra of p-hydroxy



"Typical" chemical ionization tuning file using perfluorocributylamine (PFIBA) as the standard calibrant; m/z 69, (CF<sub>3</sub><sup>+</sup>); m/z 219 (C<sub>4</sub>F<sub>9</sub><sup>+</sup>); m/z 414 (CgF16N+). Figure 53:



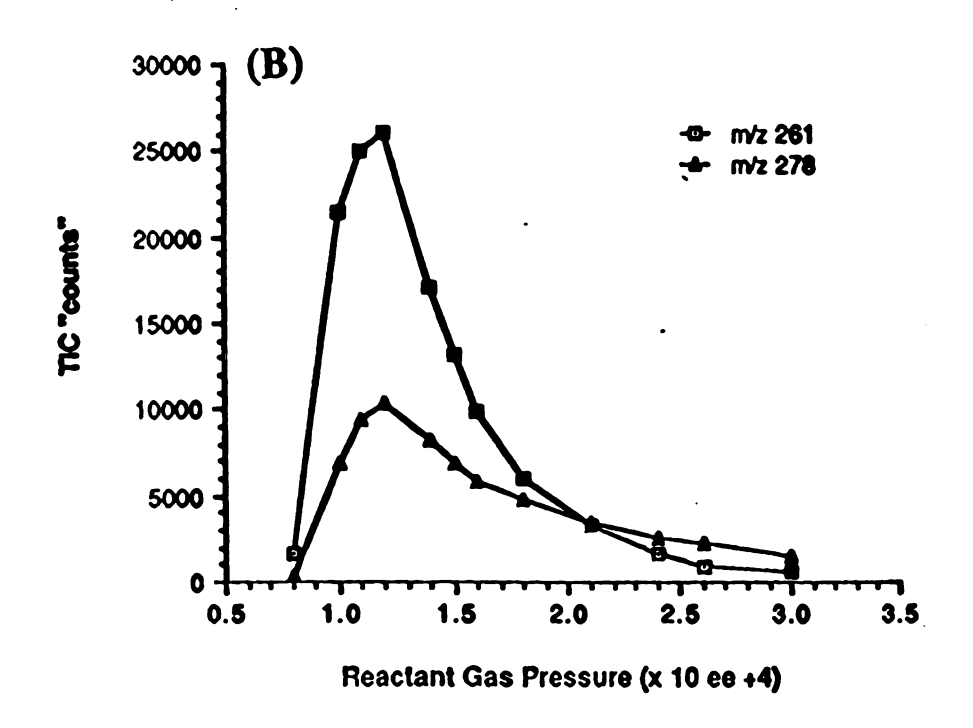


Figure 54. Effect CI ion source pressure has on overall sensitivity for (a) phydroxybenzoic acid (di-TMS), and (b) Maleic acid (di-TMS), m/z 261 (MH<sup>+</sup>); m/z 278 (MNH<sub>4</sub><sup>+</sup>)

,

benzoic (di-TMS) and m-hydroxybenzoic (di-TMS) acids, are shown in Figure 55 ab. The differences in peak heights of the MH<sup>+</sup> and MNH<sub>4</sub><sup>+</sup> ions allow the two isomers to be differentiated fairly readily, and the fidelity of the ion intensity ratios seems to hold over a wide range of ammonia pressures.

When methane CI has been employed for the analysis of the same class of compounds, the spectra appear be much more pressure dependent. As an example, shown in Figure 56 is the affect methane reagent gas pressure has on the ions formed in the analysis of 2-hydroxybutyric acid (di-TMS). At higher source pressures the protonated molecular adduct ion, [M+ C<sub>2</sub>H<sub>5</sub>]<sup>+</sup>, begin to increase in abundance relative to the lower mass fragment ions. The lifetimes of these pseudomolecular ions are affected by the increased ion source pressure, as was discussed earlier. Increased rates of collisions between neutral reagent molecules and analyte ions causes more rapid stabilization of the ion. As a result, decomposition will not occur sufficiently fast compared to the collisonal stabilization reactions. A second factor for observing an increased abundance of molecular adduct ions is that the concentration of [C<sub>2</sub>H<sub>5</sub><sup>+</sup>] is increased in the ion source and more of this reagent ion is available for both proton transfer and attachment reactions. Difference in proton affinities between analytes and methane is sufficiently large that even  $C_2H_5^+$  can play a <u>large</u> role in governing proton transfer reactions. As a result, spectra are influenced to a larger degree by high ion source pressures, where the [C<sub>2</sub>H<sub>5</sub><sup>+</sup>] concentration is enhanced.

As mentioned, an overall enhancement in sensitivity has been observed when ammonia is used rather than methane. The reason for this enhancement in sensitivity may be a result of the dramatic affect ion source pressure has on governing the rates of reactions in the ion source. The initial reaction observed in the methane-CI

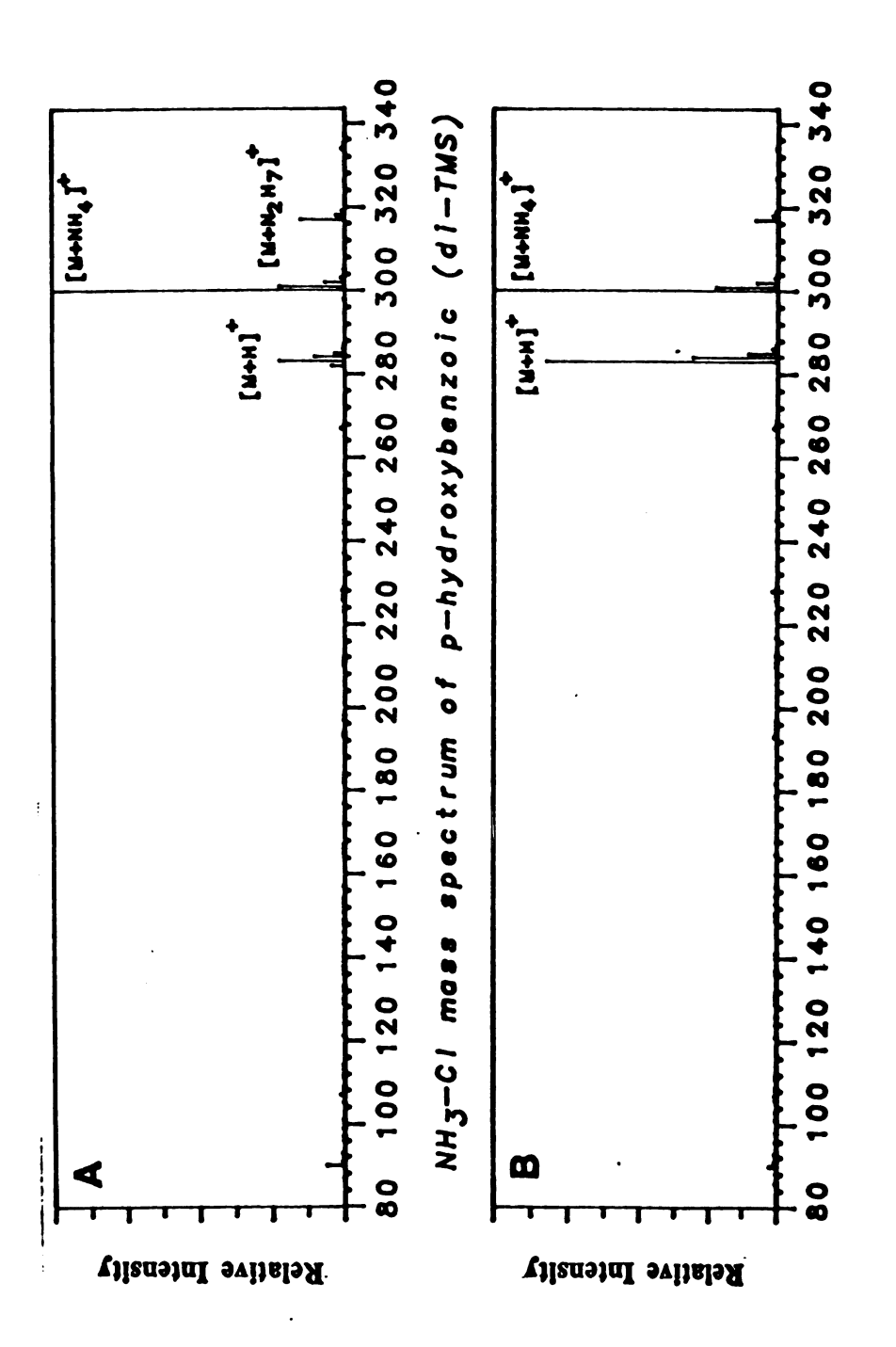


Figure 55: NH<sub>3</sub>-CI mass spectrum of (a) m-hydroxybenzoic acid (di-TMS) and (b) p-hydroxybenzoic acid (di-TMS).

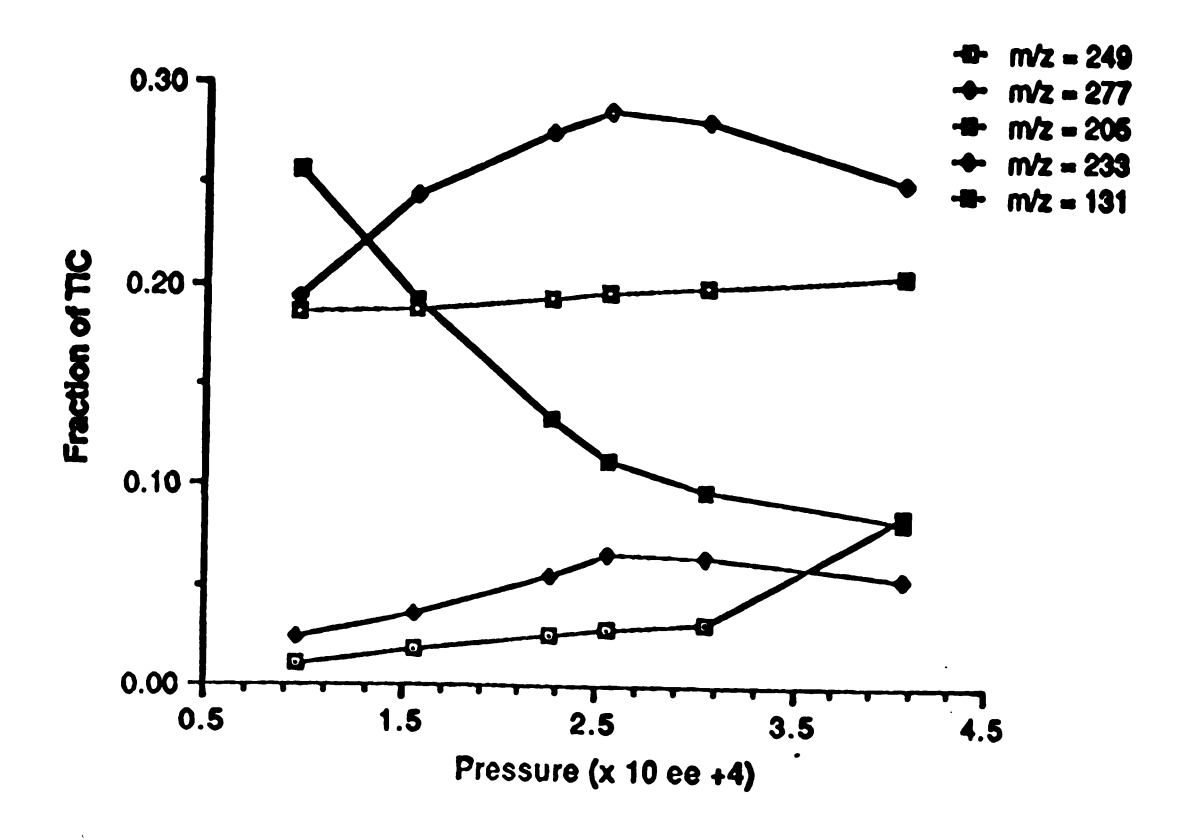


Figure 56. Dependence of fragment ions and abundances of 2-hydroxyisobutyric acid (di-TMS) on methane ion source pressure

experiment is proton transfer from the acidic CH<sub>5</sub><sup>+</sup> ion to the less acidic organic compound. Under ammonia-CI conditions, the most likely initial reaction is the formation of the [M+NH<sub>4</sub>]<sup>+\*</sup> ion, as was described in eq. 9a. These initial reactions occur at appriximately the same rate. Under high ion source pressures, stabilization of the analyte ion occurs readily, leading to the formation of the [M+NH<sub>4</sub>]<sup>+</sup> ion in the CI mass spectrum.

It was mentioned earlier that NH<sub>3</sub>-CIMS analyses more accurately reflect the quantitative composition of synthetic mixtures of organic acids than does CH<sub>A</sub>-CI, and for this reason ammonia has been chosen for the quantitative studies. These experimental observations are based on a presumed spread in the proton affinities for the complex mixtures of organic acids; the effect that methane reagent ions have on relative molar sensitivities and spectral variations is large relative to ammonia. Recall that the PA (NH<sub>3</sub>) = 205 kcal mole<sup>-1</sup>, PA (CH<sub>4</sub>) = 130.5 and PA (C<sub>2</sub>H<sub>4</sub>) = 160.5. For most organic acids, proton affinities are believed to be much greater than those of the methane and ethylene. Therefore, they will act as Brønsted bases in gas phase reactions with methane reagent ions. Differences in proton affinities of the organic acid molecules, due to differences in their polar character, for example, will result in slightly different reactivities with methane. Though literature values of rate constants for proton transfer reaction appear not to differ by more than a factor of two to three for most organic compounds, slight variations in reactivity will be observed, causing an inaccurate representation of the relative concentrations of the components of the mixture by GC-CIMS.

For reactions involving ammonia, on the otherhand, results suggest that a electrophilic attachment reactions play a major role in governing the types and quantities of ions produced in the NH<sub>3</sub>-CI mass spectrum. For organic acids, the site

of electrophilic attachment has been shown to be at the carbonyl oxygen of the carboxylic acid moiety, <sup>99,100</sup> which is a common feature to all organic acids. Only for cases in which the carbonyl oxygen is sterically hindered will ammonium ion attachment be potentially less favorable. This situation might occur for the ketoacids (i.e., organic acids containing a keto group at the α-carbon to the carboxylic group) that have been derivatized with hydroxylamine-HCl followed by trimethylsilylation to form the (Me<sub>3</sub>)<sub>3</sub>SiO<sub>2</sub>C-C=N-O-Si(Me<sub>3</sub>)<sub>3</sub> moiety. The bulky trimethylsilyl group might create some steric interference for ammonium ion attachment to occur. However, results on complex mixtures of organic acids isolated and derivatized from urine extracts do not reveal significant variations in relative response factors for these species using ammonia-CI.

Studies involving ammonia-CI for determining the quantitative strengths of this technique relative to electron impact ionization (the preferred method for organic acid metabolic profiling analyses) are the focus of the following section. In order to determine the relative capabilities of NH<sub>3</sub>-CI as a suitable chemical ionization reagent gas, an experimental procedure had to be devised which would take into account conditions for which CI methods have been previously considered incapable of yielding quantitative information (e.g., situations in which component A is found in large excess relative to a coeluting species, B). A flow chart representing the types of mixtures analyzed and compared by both EI and NH<sub>3</sub>-CI are shown in Figure 57. This flow chart represents a number of synthetic organic acid mixtures that have been prepared and analyzed by both EI and NH<sub>3</sub>-CI mass spectrometry. Small mixtures containing coeluting organic acids and components added in large excess have been studied. More complex mixtures varying in concentration from low ng to µg quantities have also been compared using both EI and NH<sub>3</sub>-CI with the long-term goal of determining the quantitative strengths of this CI method in the analysis of the

# Synthetic Mixtures Used for Determining Quantitative Strenths of Ammonia-CI Relative to 70 eV EI-MS

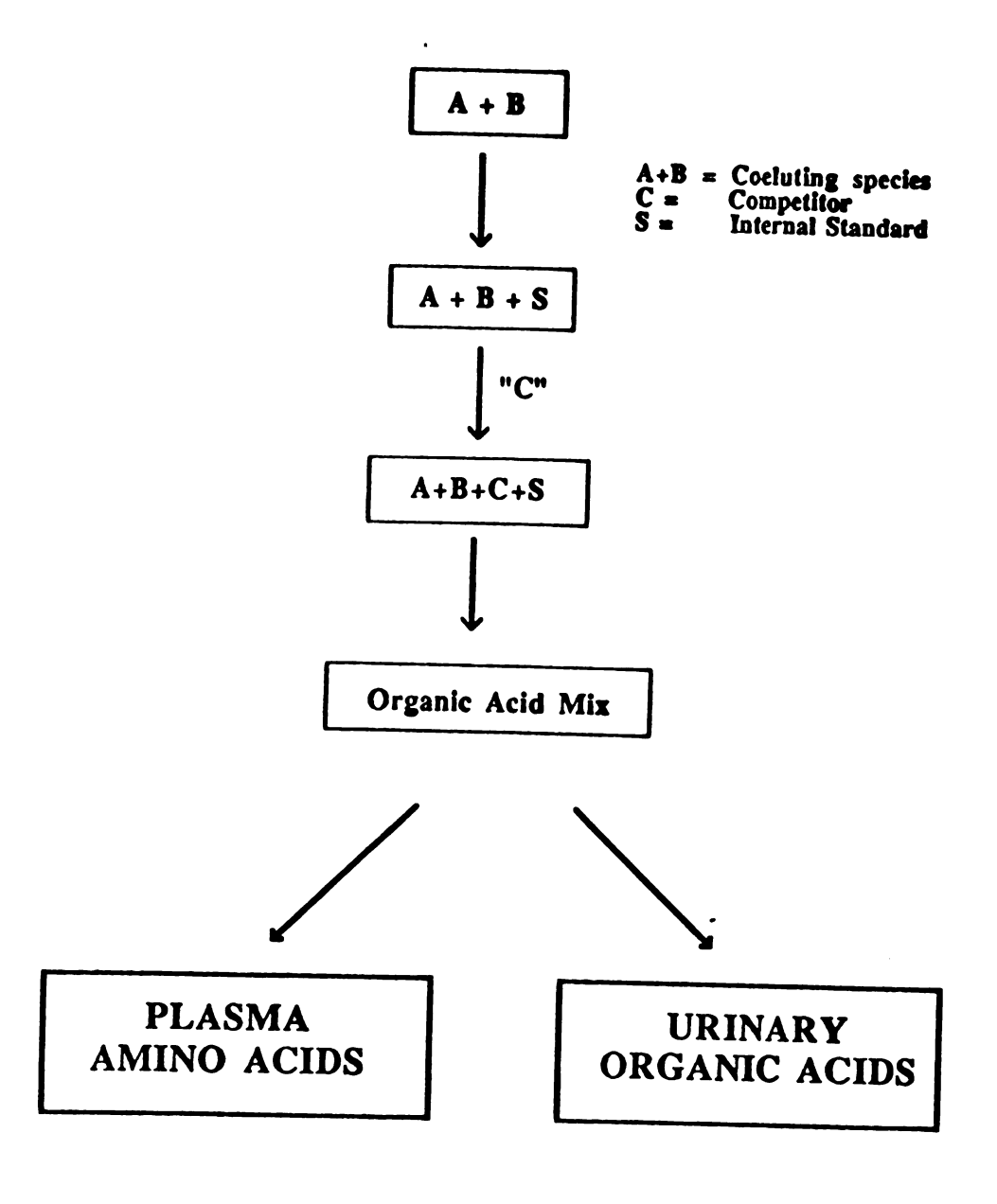


Figure 57. Flow chart representing scheme for determining the quantitative strengths of NH<sub>3</sub>-CI relative to EI-MS

urinary organic acids. A number of goals have been outlined for the use of ammonia-CI as a routine ionization method in metabolic profiling studies. They are as follows:

- 1. Determine the effect interferent or analyte species have on the ability to obtain qualitative and quantitative information on the analyte of interest.
- 2. Show the quantitative strengths of the technique and also those situations in which they exceed the capabilities of conventional EI.
- 3. Show reproducibility of technique from one experiment to the next.
- 4. Show that an enhancement in sensitivity may be achieved over EI. when comparing only those ions that are indicative of the analyte.

Synthetic mixtures of organic acids commonly found in urine were prepared. Table 5 shows the organic acids used in preparing both simple and more complex synthetic mixtures. Mixtures of some of these organic acids were prepared to contained at the least, (a) coeluting species, (b) intentionally added competing organic acids (that is, an organic acid added in varying concentration to the coeluting species with a retention time very near that of the principal analytes), and (c) interferents (e.g., byproducts of derivatization procedures) in order to simulate as closely as possible conditions typically observed in the analysis of real urine samples.

A two-component mixture of the coeluting species 2-hydroxybutyric (140ng/µl) and glycolic acids (100ng/µl) was prepared and analyzed by both conventional EI and NH<sub>3</sub>-CI. Earlier it was mentioned that there are cases in which coeluting species can give rise to identical ions in conventional EI mass spectra. This experiment was designed to demonstrate that in some cases ammonia-CI can provide more accurate determinations of the relative concentrations of the components of a mixture than EI-

Table 5. List of structures, formulae, molecular weights and retention indeces for components of synthetic organic acid mixture

- ·	,
Acid: Adipic Chemical Formula: C <sub>6</sub> H <sub>16</sub> O <sub>3</sub> Molecular Weight: 146 Retention Index: 1501	(TMS) HO -C- (CH <sub>2</sub> ) <sub>4</sub> - C-OH (TMS)
Acid: Glycolic Chemical Formula: C <sub>2</sub> H <sub>4</sub> O <sub>3</sub> Molecular Weight: 76 Refention Index: 1072	(IW2) HO - C- CH3 OH (INS)
Acid: α-hydroxyisobutyric Chemical Formula: C <sub>4</sub> H <sub>8</sub> O <sub>3</sub> Molecular Weight: 104 Retention Index: 1068	(CH <sub>3</sub> ) <sub>2</sub> - C - C- OH (TMS)
Acid: α-hydroxyisovaleric Chemical Formula: CH <sub>10</sub> 03 Molecular Weight: 118 <sup>5</sup> H <sub>10</sub> 03 Refention Index: 1171	(TMS) BO O  CH <sub>2</sub> CH <sub>2</sub> - C - C- OH (TMS)
Acid: Maleic Chemical Formula: C <sub>4</sub> H <sub>4</sub> O <sub>4</sub> Molecular Weight: 116 Retention Index: 1278	O O (TMS) HO — C— CH=CH — C— OH (TMS)
Acid: Malic Chemical Formula: C <sub>4</sub> H <sub>6</sub> O <sub>5</sub> Molecular Weight: 134 Retention Index: 1501	O OH (TMS) O (TMS) HO -C-CH-CH <sub>2</sub> -C-OH (TMS)
Acid: methylmalonic Chemical Formula: C <sub>4</sub> H <sub>6</sub> O <sub>4</sub> Molecular Weight: 118 <sup>4</sup> Retention Index: 1212	(TMS) HO - C- CH - C- OH (TMS)
Acid: Oxalic Chemical Formula: C <sub>2</sub> H <sub>2</sub> O <sub>4</sub> Molecular Weight: 90 Retention Index: 1119	СН <sub>3</sub> О О (TMS) НО—С—С— ОН (TMS)
Acid: Phenylacetic Chemical Formula: C <sub>8</sub> H <sub>8</sub> O <sub>2</sub> Molecular Weight: 136 Refention Index: 1280	$ \begin{array}{c}                                     $
Acid: m-hydroxybenzoic Chemical Formula: C <sub>7</sub> H <sub>6</sub> O <sub>3</sub> Molecular Weight: 138 Retention Index: 1570	C - OH (TMS)
Acid: p-hydroxybenzoic Chemical Formula: C <sub>7</sub> H <sub>6</sub> O <sub>3</sub> Molecular Weight: 138 Retention Index: 1622	O OH (TMS)  (TMS) HO—C OH (TMS)

MS. The mass spectra obtained of glycolic and 2-hydroxyisobutyric acids by ammonia-CI and EI are compared in Figure 58a and 58b, respectively. Designate ions in the EI mass spectra of 2-hydroxybutyric acid are m/z = 233, 205, and 131 and for glycolic acid, m/z = 205, 177, and 161, as shown in their individual mass spectra. The isobaric ion for these two species is m/z = 205, corresponding to [M-CO]<sup>+</sup> and [M-CH<sub>3</sub>]<sup>+</sup> for 2-hydroxybutyric and glycolic acids, respectively. When determining the relative concentrations of analytes in a mixture the integrated areas under the peaks are typically measured and compared with the integrated area under the peak for the internal standard.

However, when two or more species are contained within one chromatographic (i.e., reconstructed TIC) peak, then relative concentrations are determined based on the integrated areas of the designate ions for each species. In the case of the two components shown, the isobaric ion of m/z =205 makes determination of the relative concentrations difficult. If fact, calculations of the relative concentrations based on these designate ions yield very poor quantitative results. When the same species are analyzed by ammonia-CI, the problem of isobaric ions is removed. Only molecular ions are observed in the NH<sub>3</sub>-CI mass spectra of these compounds. No interfents in the mass spectra are present to make calculations of the relative concentrations complicated. The results comparing the quantitative strengtts of these two techniques for this simple mixture are summarized in Table 6 (see mix 1). In addition, several other simple mixtures were prepared and the results of calculated concentrations based on EI and NH<sub>2</sub>-CI mass spectral data are also summarized in Table 6 and compared with the known starting concentrations. The comparison between actual concentrations of the organic acids and the "counts" obtained upon integration of the TIC chromatograms is made on a relative scale. For Mix 6, as an example, the

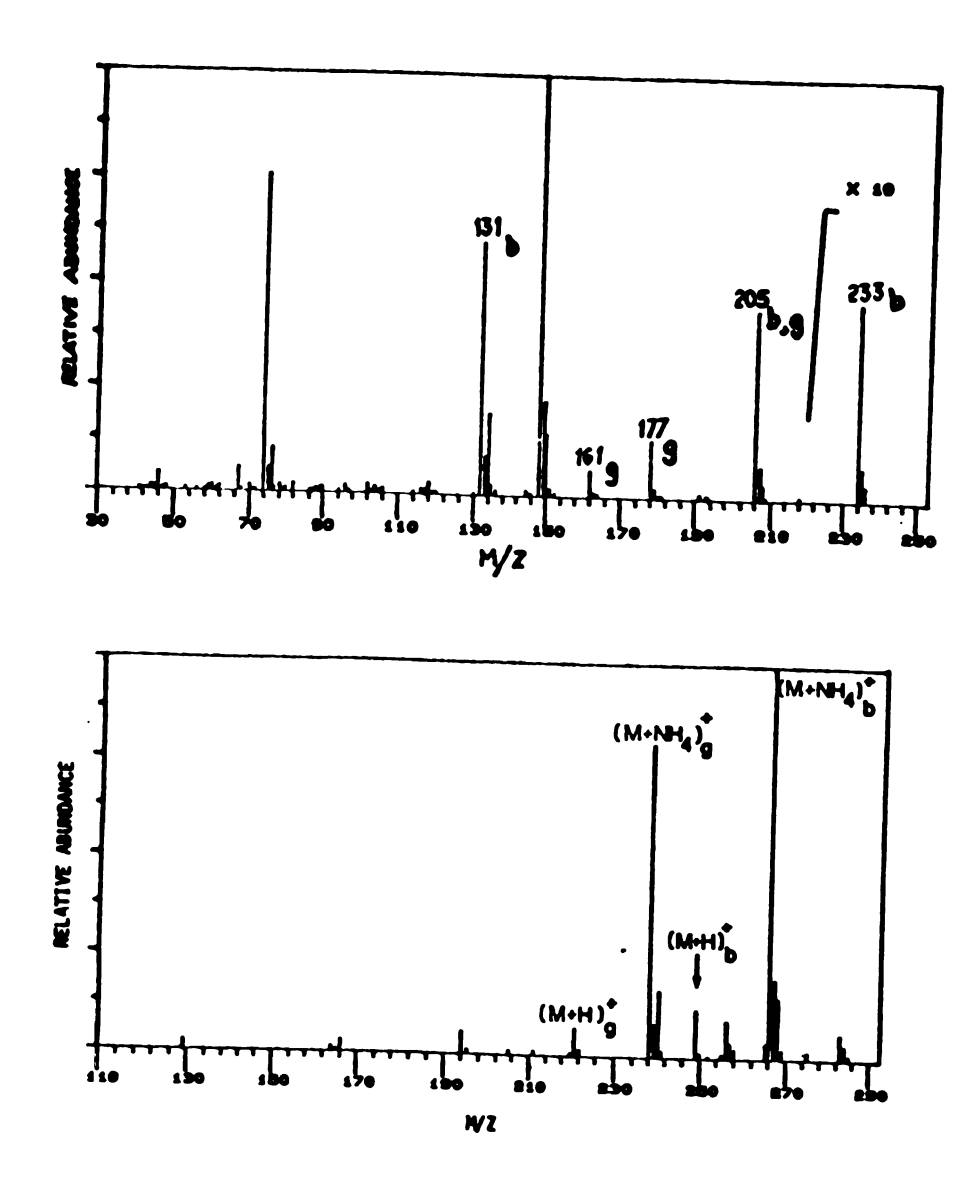


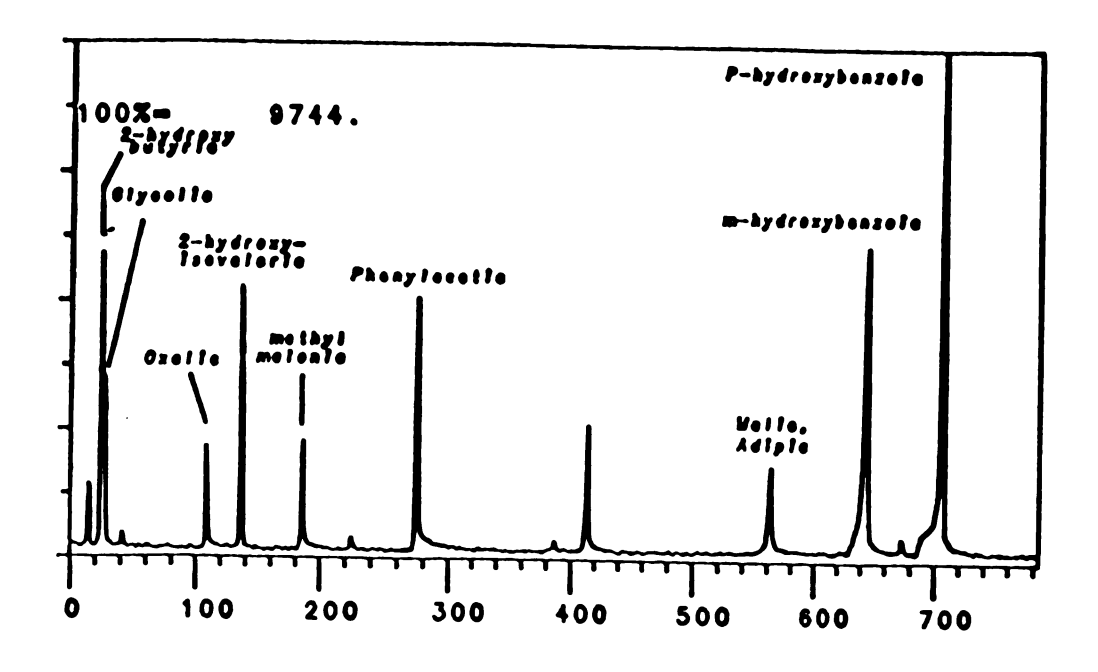
Figure 58. Comparison of quantitative strengths of EI and NH<sub>3</sub>-CI for the analysis of 2-hydroxyisobutyric and glycolic acids. (a) Reconstructed mass chromatograms showing isobaric ion interference for EI, and (b) comparison of NH<sub>3</sub>-CI and 70 eV EI mass spectra

COURT DY EL	1700 + m/s 205 "counts"	500 + m/z 205 "comis"	3500 +1 (205) } 3678	2100 + 1 (205)	30000	1	ı	100200	i	1	175000	00006	15000	34600	3400	18700	15600
SOUND DYNH, -CI	1000	1300	13500	<b>88</b>	21000	14000	909	114000	13000	900	186000	232000	61000	21000	49000	33000	34000
ACTUAL CONG (SK)	. 80	8	%	28	8	992		27.	<b>3</b> 8	128	989	828	82	\$	\$	218	921
COMPONENTS	Olycotte	2-lydraxysolveryds	Olyeotic	2-hydroxysobacydo	Orașie	Olyeotte	2-hydroxystoburyd	Oxalle	Obcole	2-hydroxyteobatyd	Orașie	P-kydroxybenaoic	m-hydroxybensoic	P-lydroxybeanole	se-kydroxy&easode	pheryheete	malete
MA	•	-		~			•			•		v	•	•	•	•	•

Comparison between actual concentrations of several two and three component organic acid mixtures with integrated peak areas obtained from GC-(NH<sub>3</sub>-CI)-MS and GC-EI-MS analyses. Table 6:

known, relative concentration ratio of p-hydroxybenzoic: m-hydroxybenzoic acid is approximately 4:1. A comparison of the A<sub>TIC</sub> by NH<sub>3</sub>-CI confirms the 4:1 relationship, whereas the results from EI suggest that the relative concentration relationship is approximately 6:1. In many cases, the results from EI and NH<sub>3</sub> parallel each other quite closely. The results on the analysis of these simple mixtures suggest the potential of ammonia-CI as providing very accurate quantitative information on simple mixtures. Even in those cases for which one component is found in large excess relative to the other components of a mixture, such as in mixtures 3 and 4, an accurate determination of the relative concentrations can be made.

The capabilities of ammonia-CI relative to EI are further tested by comparing the results on a larger synthetic organic acid mix (the structures of the components contained within this mixture are found in Table 5). The TIC plots obtained using NH<sub>3</sub>-CI and EI are shown in Figure 59 below. The relative responses of the components of the mixture are quite similar for the two techniques. Summarized in Table 7 are the calculated integrated peak areas from the experimental results which are compared with the "true" values of those compounds. In general, the two techniques accurately reflect the concentrations of the components of the mixture. In addition, an increase in the TIC is observed for the ammonia-CI analysis. In general, the TIC "counts" for EI and NH<sub>3</sub>-CI analyses are very comparable for the analysis of the trimethylsilyl derivatives of organic acids. It must be mentioned, though, that much of the TIC generated in an EI analysis is in the form of structurally useless ion current, where as the majority of ion current afforded in a NH<sub>3</sub>-CI analysis is associated with the protonated molecule and molecular adduct ion species (usually ≥ 90 per cent).



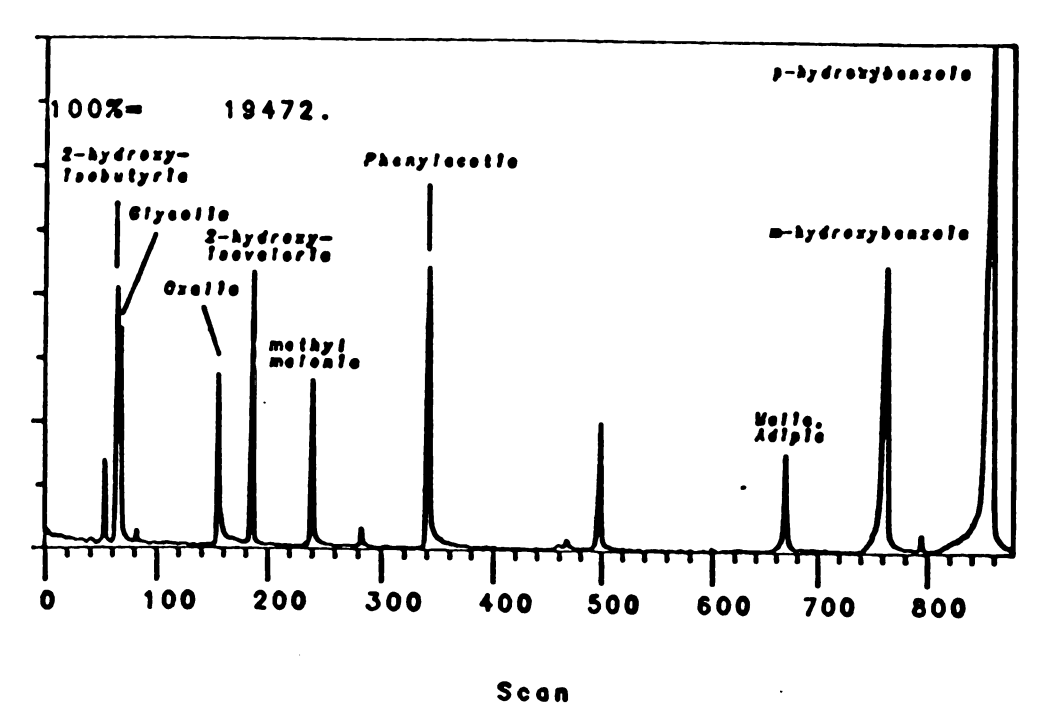


Figure 59. TIC profiles of the trimethylsilyl derivatives of an organic acid synthetic mixture obtained by (a) GC-EI-MS and (b) GC-(NH<sub>3</sub>-CI)-MS

Table 7. Comparison of integrated areas from EI and NH<sub>3</sub>-CI analyses on an eleven component organic acid mixture. Actual concentrations are shown in the lower half of this table

COMPOUND	A_(EI)	REL. CONC.	A '(NH <sub>3</sub> -CD)	REL. CONC.	
Oxalic	3000	0.07	16000	0.12	
α-hydroxylsobutyric	16000	0.3	29700	0.22	
glycolic	14000	0.3	22200	0.17	
a-hydroxyisovaleric	11000	0.2	23200	0.17	
methylmalonic	370	0.08	13900	0.11	
phenylac <b>etic</b>	10300	0.2	35100	0.26	
Unknown (MW=292)	5800	0.1	13900	0.10	
Malic					
Adipic	1600	0.1	11500	0.08	
m-hydroxybenzoic	22000	0.5	63100	0.47	
p-hydroxybenzoic	46000	1.0	134600	1.0	

## ACTUAL CONCENTRATIONS AND REL. ABUNDANCES

	ng/µl inj.	Rel. Conc.
Oxalic	80	0.1
a-hydroxylsobutyric—	310	0.3
glycolic ———	280	0.5
α-hydroxyisovaleric	200	0.2
methylmalonic ———	95	0.1
phenylacetic ———	220	Q2
Unknown (MW=292)		-
Malic	75 ·	0.5
Adipic	45	0.8
m-hydroxybenzoic —	460	0.5
p-hydroxybenzoic	920	1.0

The capacity for obtaining quantitative information on these mixtures depends on the NH<sub>3</sub> ion source pressure utilized in the CI experiment. Maleic acid is unique to the list of organic acids summarized in Table 6 due to its unusually high proton affinity. Maleic acid (di-TMS) readily abstracts a proton from NH<sub>4</sub><sup>+</sup> under conditions of low ion source pressure ( $\leq$  300 mtorr). When operating pressures are such that proton transfer is favored for this organic acid, poor quantitative representations of the components of a mixture containing maleic acid will result. However, if the operating ion source pressure is such that stabilizion of electrophilic NH<sub>4</sub><sup>+</sup> attachment to the organic acids is favored, accurate measures of the relative concentrations of the components of mixtures containing maleic acid can be obtained.

Figure 60 compares the response of maleic acid (di-TMS) relative to phenylacetic acid (di-TMS) by  $NH_3$ -CI at (a) low, and (b) high ion source pressure. The analysis performed at  $P_{NH_3} = 200$  mtorr showed a marked deviation in relative response of maleic acid when compared with results available from EI-MS (which were taken as the "true" relative concentrations of the two species). However, when the ion source pressure was increased to  $P_{NH_3} = 330$  mtorr, the relative response of maleic acid more closely paralleled the results from the EI analysis. These results further support the idea that the initial reaction between  $NH_4^+$  and organic acids is in the formation of the  $[M\cdots H\cdots NH_3]^{++}$  complex. When operating pressures are low (and hence the time between collisions with neutral reagent molecules is greater) proton transfer can occur to species such as maleic acid. At higher operating source pressures, the frequency of collisions is such that the  $[M\cdots H\cdots NH_3]^{++}$  complex is sufficiently stabilized to yield the adduct ion,  $[M+NH_4]^+$ .

The results on these synthetic mixtures of organic acids suggest that the types of responses obtained for EI and NH<sub>3</sub>-CI are quite similar for these compound classes.

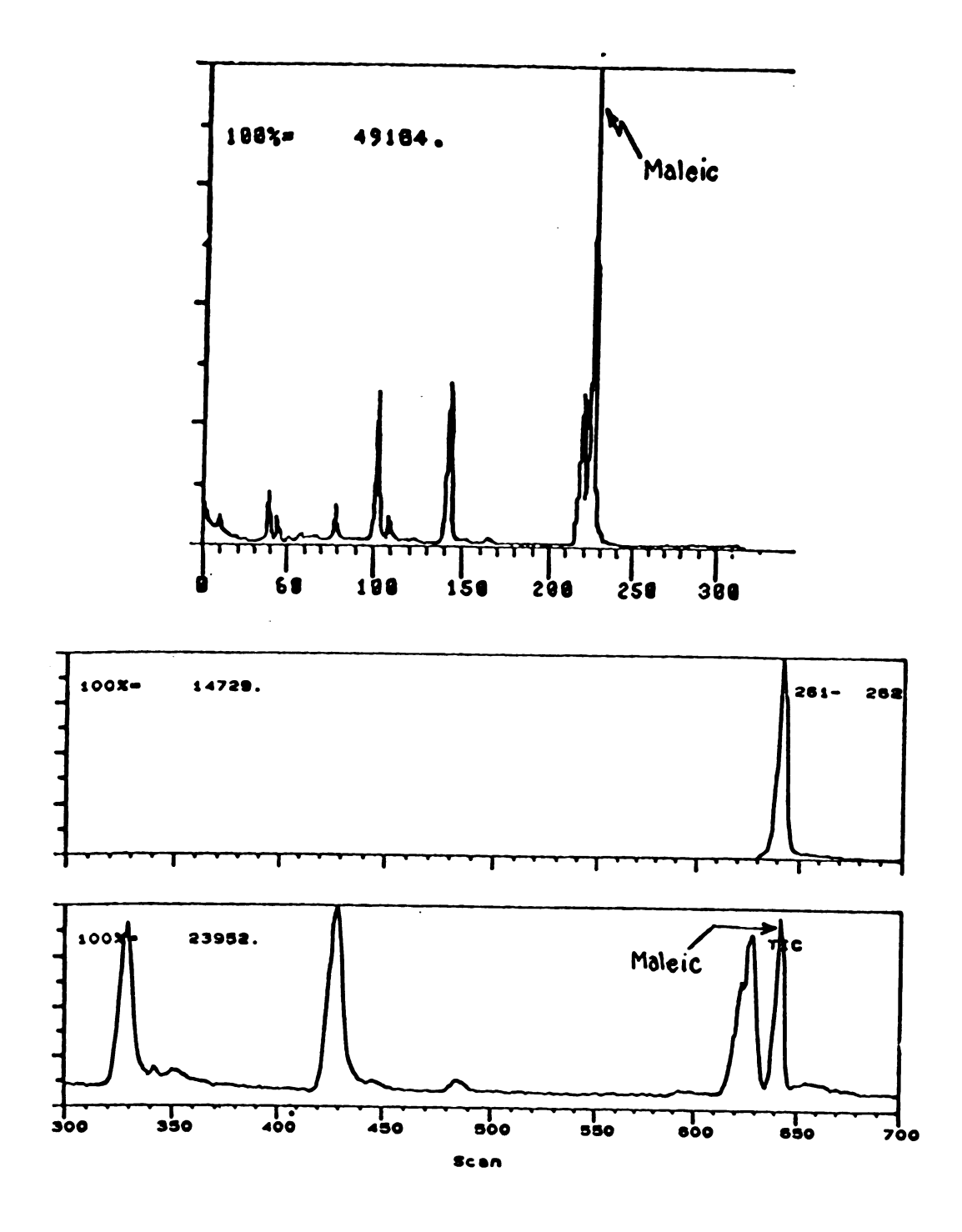


Figure 60. Comparison of TIC profiles of a mixture containing maleic acid (di-TMS) using NH<sub>3</sub>-CI at (a)  $P_{NH_3} = 200$ , and (b)  $P_{NH_3} = 320$  mtorr

The next step was to determine whether the profiles obtained by ammonia-CI would parallel those obtained by conventional EI for mixtures of organic acids isolated from urine. Shown in Figure 61a-b below are the reconstructed TIC profiles of urinary organic acids isolated from a diabetic patient obtained by EI and NH<sub>3</sub>-CI. Inspection of the two profiles does reveal variations in the relative peak intensities, but these differences are slight. This situation was of some concern. When repeat analyses of this urine mixture were made in the EI mode, the profiles also showed slight differences, just as was observed when comparing the EI and NH<sub>3</sub>-CI profiles. Repeat ammonia-CI analyses on the same mixture were quite reproducible, as illustrated in Figure 62. The reasons for the slight variations in reproducibility in the TIC profiles from one run to the next might be attributed to poor equilibration of the gas chromatograph prior to analysis, resulting in slightly different rates of heating, and poor reproducibility in injection technique.

Quantitation by NH<sub>3</sub>-CI is not limited to the analysis of urinary organic acids. NH<sub>3</sub>-CI has been found to very accurately represent the concentrations of synthetic mixtures of TMS derivatives of steroids. The relative responses obtained by NH<sub>3</sub>-CI and EI are further compared for the analysis of plasma amino acids, as shown in Figure 63. The trifluoroacetate derivatives of the amino acids were formed and the resultant derivatized mixture was analyzed by EI, NH<sub>3</sub>-CI, and negative ion chemical ionization (NICI), and compared. In the cases of NICI, relative responses differ significantly for the components of the mixture. However, the TIC profiles obtained by EI and NH<sub>3</sub>-CI are more closely related.

As stated earlier, the treatment of ammonia-CI here as a quantitative tool has not been as rigorous as the ones summarized earlier in the work of Munson and coworkers in which relative rate constants for reaction of homologous series of

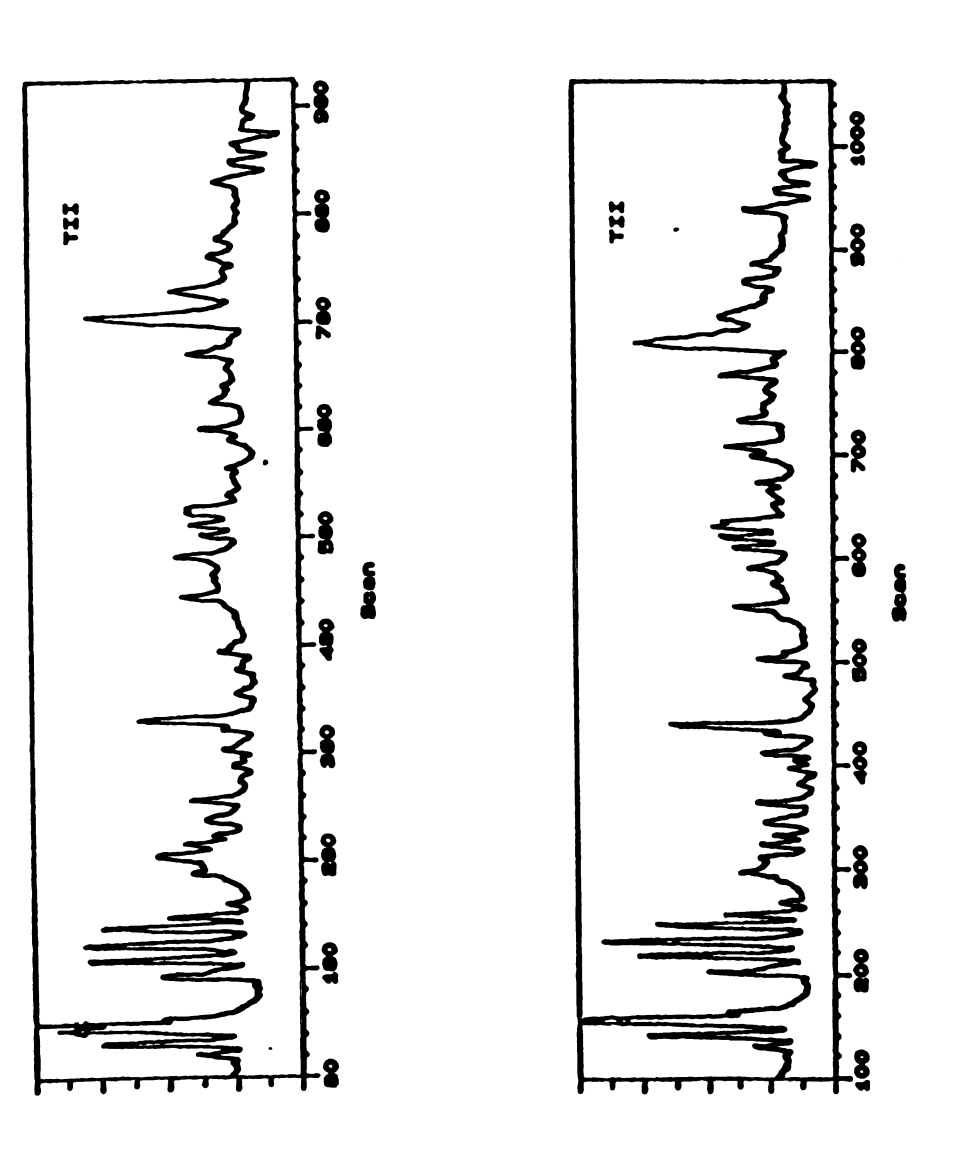


Figure 62: Repeat analyses on urinary organic acids by NH<sub>3</sub>-CI demonstrating reproducibility from one run to another.

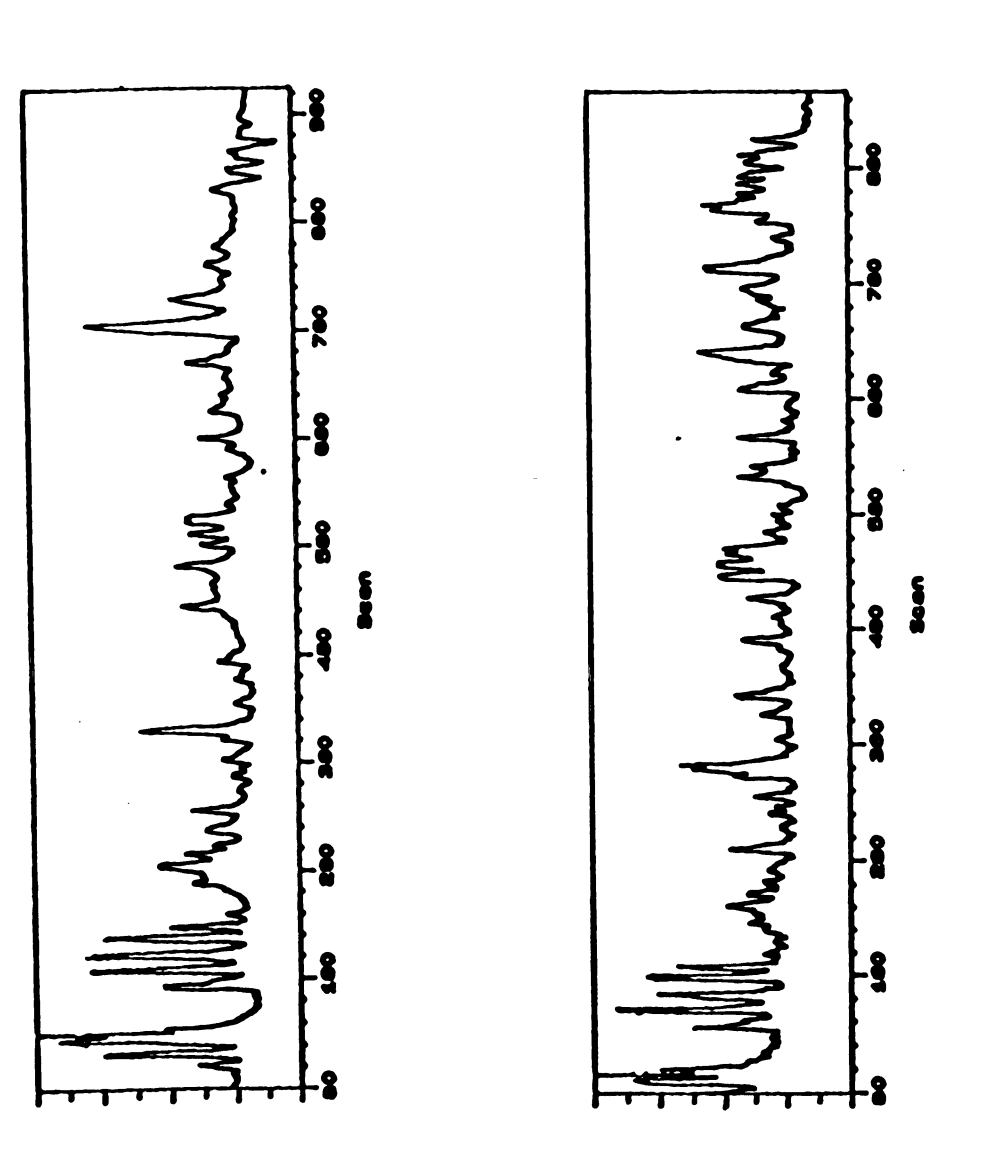


Figure 61: Comparison of TIC profiles of derivatized urinary organic acids from a diabetic dog obtained using (a) NH<sub>3</sub>-Cl, and (b) El ionization.

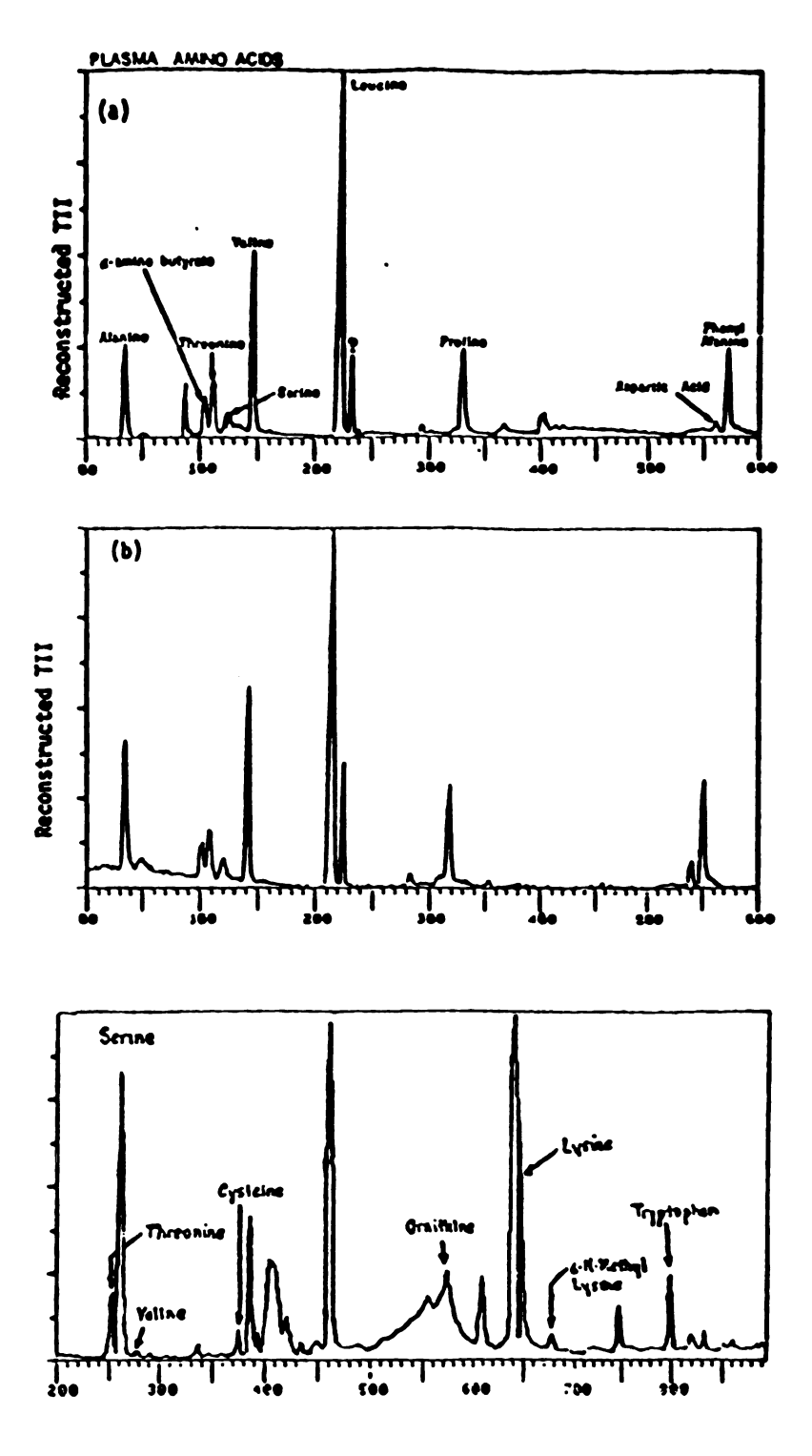


Figure 63: TIC profile for naturally occurring amino acids in a diabetic dog plasma obtained by (a) NH<sub>3</sub>-CI, (b) EI, and (c) electron-capture negative ion. (ECNI) mass spectrometry.

compounds have been determined. What the results presented here do show is that ammonia-CI can, under rigorously controlled conditions, yield data which compare quite favorably to the data generated from the accepted, conventional EI ionization approach. Reconstructed TIC chromatograms are found to be quite accurately represented, whether EI or NH<sub>3</sub>-CI is employed. Furthermore, integration of individual peaks in the generated reconstructed TIC chromatograms represent accurately the actual concentrations of the components of the synthetic mixtures. In some cases, the strengths of NH<sub>3</sub>-CI surpass those of EI for quantitating on coeluting species.

To this point ammonia-CI has been shown provide an accurate representation of the components of complex mixtures. However, the real strengths of the technique lie in the fact that the ions generated in an NH<sub>3</sub>-CI analysis almost exclusively represent the analyte (i.e., very little or no ion current is associated with the derivatizing agent). This is an attractive feature of the CI method since much lower limits of detection can be attained when monitoring for a known compound in a complex mixture. The presence of only molecular-type ions in the ammonia-CI mass spectra can be exploited. For metabolic profiling analyses stable-isotopes are frequently used to investigate metabolic pathways of either previously known disease-conditions or to investigate unknown conditions. The use of chemical ionization methods for these types of experiments is the focus of the following chapter.

# Chapter 6: Utilizing Ammonia-CI for Stable-Isotope Tracer Studies

### Introduction

Modern methods for research in biochemistry, physiology, and nutrition typically have involved the use of either radiolabelled or stable-isotopically labelled substrates to determine metabolic pathways of significance. Early studies exclusively used radiolabelled species due to the fact that these species were relatively easy to obtain and methods for detecting the presence of radioactive materials were relatively sensitive as well as inexpensive. For analyses involving radioactive labels, techniques such as radioimmunoassay have found a great deal of success. The use of these radiolabelled species is prevalent in the area of in vitro metabolism. 111 The inherent dangers associated with the use of these substrates, however, make them often undesirable for use in chemical analyses, especially when those analyses involve investigation of human metabolism. 112

With the advent of mass spectrometry, it has now been possible to incorporate stable-isotopically labelled substrates to determine an enormous range of information about analyte(s) under investigation. Stable-isotopically labelled substrates (or tracers) are an attractive class of compounds due to the fact that they are readily detected using mass spectrometry, and are safe to use. The major drawbacks associated with the use of stable isotope species is that their cost and preparation is quite high, often precluding their attainability for routine chemical analyses. A second drawback, as mentioned earlier, is that these stable-isotope species can often cause severe isotope effects. Perhaps the most sever isotope effects have been observed with deuterium labelled substrates. Chromatographic retention times, for example, can be quite different comparing the non-labelled and isotopically labelled

substrates. In addition, ionization efficiencies can differ for the labelled and unlabelled analogs. These different ionization efficiencies affect rate constants for reactions, and these effects must be evaluated before they can be used properly for obtaining both qualitative and quantitative information from mass spectral analysis. Stable-isotopes have found applications, nevertheless, especially for kinetic studies, 113-114 use as internal standards for quantitative analysis by MS. 115 as well as several for other purposes. 116 Perhaps the greatest number of applications of stable-isotope experiments to mass spectrometry today is in the investigation of biochemical pathways. Insights into various metabolic processes may be determined through the use of these labelled precursors and the results are often useful for assisting in the identification of specific metabolic errors, from which a proper regiment for treatment of disease may be made. A number of stable isotopes have been used to study various aspects of carbohydrate metabolism. 116-118 amino acid metabolism, 118-121 and the Krebs (TCA) cycle. 122 The applications of stableisotopically labelled analogs in evaluating various aspects of drug metabolism 123 is unsurpassed.

The types of stable-isotopes incorporated have been nearly as varied as the numbers of stable-isotope labelled tracer experiments performed. Much attention has been placed on the use of <sup>2</sup>H, <sup>13</sup>C, <sup>18</sup>O, and <sup>15</sup>N labelled substrates for these tracer-type experiments. Studies involving deuterium have been found to be hindered by the fact that the deuterium labelled species can, in many cases, readily undergo exchange reactions. This can present severe problems in determining accurate levels of label enrichment. However, due to the relatively low cost associated with obtaining deuterium-labelled substrates, this labelled species continues to be the most widely employed. <sup>13</sup>C-labelled substrates are playing an increasingly important role in metabolism studies. The preparation of uniformly labelled <sup>13</sup>C-precursors however,

is still not trivial, thus making the cost associated with these types of labelled species quite high.

A number of questions are addressed, in general, when incorporating labelled substrates for these types of studies. They are: (a) what metabolic products result from the metabolism of the labelled precursor molecule?, (b) how much of the label is incorporated into the metabolite product(s)?, and (c) at what position in the metabolite product(s) is the label incorporated? The proper choice of mass spectrometric method will depend on the type of information sought in the analysis. Typically, the greatest source of information to the analyst is the determination of the metabolite products of the ingested labelled precursor. Determinations of the metabolites arising from the labelled precursor by mass spectrometry requires that an appreciable enrichment in isotope labelled ions be observed. The flux of <sup>13</sup>C from a labelled precursor, such as [U-<sup>13</sup>C]-glucose, into various metabolite pools requires that the extent of isotope enrichment be discernible from natural isotopic contributions.

Most metabolism studies utilize only very low concentrations of fully labelled precursors introduced to the system. As a result, the flux of labelled substrate into various metabolite pools will, in general, be quite low. This especially becomes a concern when there are already large natural isotopic contributions to contend with. In the analysis of the trimethylsilyl derivatives of organic acids, for example, at minimum, a 5.1 % natural isotope is observed at the  $(A+1)^+$  ion and 3.4 % enrichment at the  $(A+2)^+$  ion (corresponding to the natural isotopes of silicon). In addition, contributions from naturally occurring  $^{13}C$  and  $^{18}O$  isotopes further add to often very large natural isotopic levels. Only when the natural isotopic contribution is known accurately can the measurement of label incorporation from a stable-isotope precursor be deduced. This requires that measurements of isotopic enrichment be measured with a high degree of precision and accuracy.

# Isotope-ratio and isotope-dilution mass spectrometry

A technique which has found the greatest success in determining very trace levels of isotope enrichment (less than 0.1 % enrichment) is that of isotope-ratio mass spectrometry. 124-127 This technique is based on the simultaneous detection measurements of natural isotopic levels (of a reference species) with the analyte under investigation using null point methods. Isotope-ratio mass spectrometry may involve the analysis of permanent gases, such as CO2, N2, and H2O for determining very precisely and accurately low levels of isotope enrichment, or inorganic transition metals for determining accurately the relative amounts of their natural isotopes. One of the most commonly measured isotopes in isotope-ratio mass spectrometry is <sup>13</sup>C, which is determined from carbon dioxide in respired air. The air is collected in an evacuated chamber and the CO<sub>2</sub> is purified and isolated by distillation. <sup>128</sup> Analysis is typically carried out along with reference CO<sub>2</sub> and mass spectral analyses are carried out simultaneously, yielding very precise and accurate measurement of isotopic enrichment of the test sample. Hachey, et al. reviews this technique for stable-isotope studies in the nutritional sciences. 129 The limitations of isotope-ratio mass spectrometric analyses are obvious. The sample being analyzed must be presented to the mass spectrometer in its most elemental form. The technique is not capable of the analysis of intact organic molecules, since combustion of the organic compound is required by the isotope-ratio method.

Isotope-dilution mass spectrometry (IDMS) on the otherhand, is a technique which has found a place in analytical chemistry for problems requiring the very precise and accurate quantitation of analytes from complex media, such as plasma, serum, and/or urine. As early as 1970, stable-isotope dilution methods were being incorporated to make quantitative determinations of biologically important metabolic

species, such as prostaglandins, <sup>115</sup> possible. A number of papers are reported yearly using IDMS for determining the amounts of organic constituents of serum (and other physiological fluids). <sup>130-132</sup> Typically, GC or HPLC methods <sup>133</sup> are used in conjunction with mass spectrometric analyses by this isotope-dilution method.

In such experiments, a labelled analog of the analyte to be measured is incorporated at some point prior to extensive work-up of the physiological fluid. This allows for factors such as loss due to derivatization and isolation to be effectively eliminated. Prior to introduction, however, solutions containing labelled analyte and unlabelled species are prepared in varying concentration. Typically, these standard calibrant solutions can range from 1:1 mixtures of unlabelled to labelled species to ratios as low as 1:1000, depending on the species being sought and the medium from which the analyte is measured. Once a linear calibration curve has been obtained based on measurements of the integrated areas of unlabelled and labelled species, analyses on the physiological mixture can then be conducted in order to determine the amount of analyte in that medium. The accuracy associated with this technique for determining concentrations of unknowns contained within complex physiological solutions is great. In addition, isotope-dilution methods have been used in the study of kinetics of bile acid metabolism, and others. 134-136

The majority of stable-isotope experiments performed today involve the study of metabolic pathways, such as differences in the metabolism of healthy and disease-state conditions. Stable isotope tracers have been used predominantly for measuring the flux of an ingested stable-isotopically labelled precursor into various metabolic pools for metabolic profiling analyses. The labelled substrate is typically administered (either orally or parenterally) into both a "control" and "disease-state" subject, in order to determine subtle and/or significant differences in the metabolism of the precursor molecule. These experiments require the ingestion of a known

labelled precursor for a pre-determined period (frequently referred to as pulselabelling period) followed by periodic collections of physiological fluids, (such as urine, plasma, etc.) during a "chase" period from which the compounds of interest can be isolated and analyzed for label enrichment as well as the position to which the precursor molecule may transfer label.

The number of papers in which labelled precursors are utilized for determining various metabolic pathways involving intermediary organic acids and amino acids is growing rapidly. 137-138 The technique best-suited for these analyses is gas chromatography combined with mass spectrometry. As mentioned earlier, the ionization mode employed will be determined by the type of questions to be addressed. The chromatographic step is obviously needed so that the components of the complex medium can be sufficiently separated and mass analyzed. Determinations of the presence of precursor label into various metabolite pools requires the presence of high mass ions in the mass spectra of organic compounds so that accurate isotope enrichment measurements may be made. Similar to procedures incorporated for isotope-ratio mass spectrometry, the measurement of label enrichment in these experiments is determined by comparison to reference values of the natural isotopic abundance. Typically, then, a control experiment (free from labelled substrate) is performed coincident to the metabolic profiling analysis and the control values for natural isotopic abundance of specific metabolites are determined. As a result, accurate measurements of the extent of label enrichment into these metabolite pools can be made.

Electron ionization often falls short from meeting this criterion, especially in the analysis of organic acids from urine, as was shown earlier. The appropriate choice of ionization method can also lead to an increased sensitivity for analysis. Methods such as ammonia-CI concentrate the majority of ion current (>95 %) in useful ions for

organic acid analyses. Recall that the majority of the ion current from EI analyses of derivatized organic acids resides in fragment ions indicative of the derivatizing agent. Accurate isotope measurements require selected ion monitoring (SIM) analyses on the enriched metabolites for the the best ion statistics to be achieved. Total ion current measurements obtained in the full-scanning mode of the mass spectrometer comparing EI and NH<sub>3</sub>-CI have been shown to be nearly equivalent in the analysis of synthetic mixtures of organic acids. As a result, analyses by SIM should lead to much lower limits of detection by NH<sub>3</sub>-CI since the total ion current resides in one or two m/z values, which are utilized in SIM analyses.

There are cases, however, when not only are the levels of isotope enrichment desired but, also the position of the label in the metabolite under study. Answers to these questions require ionization methods which generate a sufficient number of fragment ions. Ionization methods such as NH<sub>3</sub>-CI would be unsuited towards answering these types of questions. On the otherhand, structural information is readily attained using EI-MS and these structurally useful ions provide insight as to location of the stable-isotope in the molecule. A suitable example describing these behaviors are found in an early application paper written, and published in Anal. Chem , entitled, "Utility and Limitations of Electron Ionization and Chemical Ionization Mass Spectrometry for Determining the Postion and Extent of Labelling in Permethylated Sugars." This paper may be found in Appendix I. In this paper, ammonia-CI is found to be the preferred chemical ionization method for determining the extent of label enrichment where as methane-CI and EI can be used to determine the position of label enrichment. For the class of compounds studied in this paper, electron ionization would be a very poor choice if used exclusively for making accurate determinations of label enrichment. The types of ions observed in the EI mass spectra of these permethylated alditols are subject to exchange and

rearrangement reactions, and EI results are found to yield artificially low values of enrichment due to the prevalence of these processes. These initial experiments demonstrated the capabilities of ammonia-CI for providing abundant molecular ions in the mass spectra of derivatized sugars, amino acids, organic acids, and steroids. The potential utility of this ionization method in investigating metabolic pathways associated with the class of disease conditions termed the organic acidurias was evident.

Initial experiments using ammonia-CI for measuring the flux of labelled precursors into various organic acid metabolic pools stemmed from a collaborative project with Sweeley and Martin (Department of Biochemistry, Michigan State University), and Schall (Veterinary School of Medicine, Michigan State University) investigating various aspects of Juvenile Onset (Type 1) diabetes. In conditions of diabetes it is not uncommon to observe elevated levels of ketone bodies (e.g., β-hydroxybutyrate, acetoacetate) in urine of the uncontrolled condition, since their release from adipose tissue is a result of the need for mobilization of free fatty acids to supply necessary energy (ATP) to the system. A major area of research in this laboratory has been to evaluate organic acid metabolism of diabetic patients under insulin-control therapy. A study by Shigematsu et al. 139 revealed significant differences in the amounts, and types of organic acids excreted by diabetics under insulin-control therapy and those of age-matched controls. It was found that diabetics consistently excrete elevated levels of 2-hydroxybutyric acid, 4-deoxythreonic acid, and others.

An investigation as to the origin of 2-hydroxybutyric and 4-deoxythreonic acid was made, since the levels of these metabolites in several diabetic patients were found to be abnormally high. It had been postulated that these two organic acid metabolites

might arise from metabolism of L-threonine. An elegant method for determining whether these species do indeed arise from threonine metabolism is to perform stable-isotope tracer experiments incorporating uniformly labelled threonine, and monitoring for label enrichment into these metabolite pools. The results of this study, which were published in Biomed. Environ. Mass Spectrometry, entitled, "Urinary Metabolites of L-Threonine in Type 1 Diabetes Determined by Combined Gas Chromatography/Chemical Ionization Mass Spectrometry" may be found in Appendix II. This study revealed that threonine is the precursor to both of these two metabolites. In addition, it was determined that 4-deoxyerythronic acid also was a metabolite of threonine. Evaluation of the isotopic enrichment using EI-MS was extremely difficult in this experiment since only very low levels of <sup>13</sup>C-enrichment were observed (c.a. 1-3 per cent, corrected for natural isotopic contribution). Only when NH<sub>3</sub>-CI was employed were these levels of <sup>13</sup>C-label enrichment observed and accurately measured.

One of the most significant studies presently being pursued involves determining the feasibility of such stable-isotope tracer experiments for differentiating between enzyme deficiencies associated with the lactic acidemias. These conditions are often difficult to differentiate based on (a) clinical observations, and (b) urinary organic acid metabolic profiles, due to the similarities in the types and quantities of metabolites excreted in urine. Recall, lactic acidemia is a condition that can result from a number of partial enzyme deficiencies and lactic acid is the principal metabolite excreted in urine for all of these conditions. For those situations in which the patient is suffering from partial pyruvate dehydrogenase deficiency, for example, a partial enzyme block has been found to occur in the conversion of pyruvic acid to acetyl-CoA, which is the first intermediate in the Krebs pathway. Deficiency in this enzyme typically causes a large build up of pyruvic acid (pyr) in serum. In addition, a

concomitant increase in lactate serum levels is observed. For some disease conditions, it is possible to measure Pyr/Lactate ratios from plasma samples to determine the metabolic state of the individual. For this class of lactic acidemias, however, the ratio of pyruvate to lactate in blood often is found in "normal" or control ranges, thus making diagnosis of this condition difficult by conventional clinical measurements. The following section summarizes my results on this feasibility study for the differential diagnosis of the lactic acidemias. The results of this study were presented at the *International Symposium om Mass Spectrometry in the Health Sciences*, Barcelona, Spain. A manuscript is in preparation and is the focus of the following chapter.

# Chapter 7: Investigation of Cell Metabolism Using Labelled Glucose

### Introduction

Studies of metabolic disorders collectively known as the organic acidemias have revealed the molecular mechanisms of more than 50 heritable disorders and an explanation for accumulated metabolites. Differential diagnoses have been made, generally, by detecting abnormal concentrations of specific organic acids in either plasma or urine. The most widely used and accepted approach for identifying these metabolic disorders has been to combine gas chromatography with mass spectrometry (GC-MS). 4,43

Lactic acidemia is a syndrome of several of the most frequently diagnosed metabolic disorders. The identification of these disorders by GC-MS has been achieved by detecting excessive levels of lactic, and in some cases, 2-hydroxybutyric acids in urine. 14,138 The lactic acidemias have been a particularly intriguing class of genetic diseases due to the diverse enzyme defects that are responsible for the excessive buildup of lactate in physiological fluids. This condition has been reviewed extensively by Matsumoto et al. 15 who suggest that more than 15 enzyme deficiencies may lead to congenital lactic acidosis.

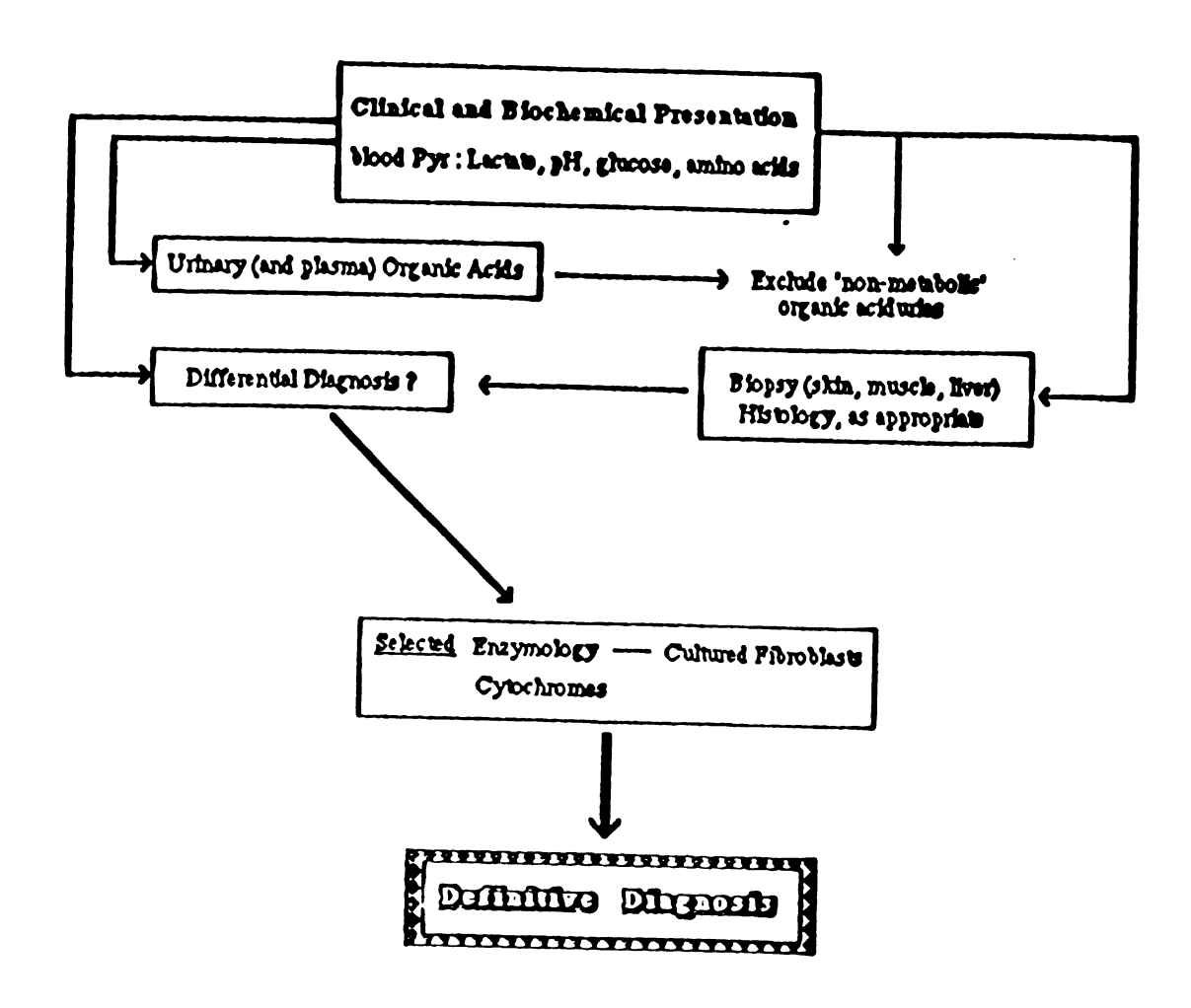
Differential diagnosis of the lactic acidemias has been especially difficult since several enzyme defects may give rise to clinically indistinguishable urinary metabolic profiles. Chalmers presented data which suggest that congenital lactic acidoses may be differentiated upon evaluation of the respective urinary organic acid profiles. However, conditions in which uninherited and/or other acquired causes of lactic acidosis could occur were excluded from these studies; inclusion of these factors which could lead to increased excretion of lactate would make differential diagnoses

more difficult. Therefore, a more conclusive method for differentiating these enzyme deficiencies, which produce nearly identical clinical states, is required.

Two enzyme defects associated with lactic acidemia are pyruvate dehydrogenase and cytochrome oxidase deficiencies. Pyruvate dehydrogenase (PDH) deficiency has been the subject of intensive study. 141 In general, lactic acid accumulation is a consequence of total pyruvate accumulation. In conditions in which there is a partial PDH deficiency, the conversion of pyruvate to acetyl-CoA is blocked and a concomitant increase in both lactate and pyruvate is observed. However, blood lactate/pyruvate ratios remain nearly equivalent to those for age-matched controls, making clinical recognition of the enzyme defect difficult. Cytochrome oxidase deficiency has been described in patients with a wide variety of symptoms, the majority of cases being reported with neurodegenerative disease with a pathology typical of Heights disease. Like pyruvate dehydrogenase deficiency, cytochrome oxidase deficiency also is characterized by grossly elevated levels of lactate in urine. As a consequence, differential diagnosis of these enzyme deficiencies has been difficult when based solely on the comparison of urinary organic acid profiles. A general scheme for definitive diagnoses of the congenital lactic acidoses is shown in Figure 64. The protocol for the identification and differentiation of the lactic acidemias is quite extensive. As mentioned, the presentation of the disease-state can often be masked by what appears to be "normal" blood pyruvate/lactate concentrations. Since differential diagnosis is difficult to make based on the concentrations of urinary organic acids, enzymological approaches are needed for the definitive diagnosis.

Chalmers has suggested that in vivo experiments involving labelled substrates may be well-suited for the differential diagnosis of the congenital lactic acidoses.

Both cytochrome oxidase and PDH deficiencies involve intermediates of glucose



reproduced from J. Inher. Metab. Dis. Suppl. 7 Vol. 1 1984 (with permission from author)

Figure 64. Scheme for the clinical and biochemical investigation of patients with suspected congenital lactic acidoses

metabolism, with channeling of either pyruvate or an intermediate of the electron transport system through the energy-generating pathways. Applications of GC-MS for stable isotopically labelled tracer experiments include investigations of the intermediates of the TCA cycle, and others. 142-145

However, few studies involving labelled tracers have been performed for distinguishing between enzyme defects. Most recently, Lapidot et al. 146 used [U-13C]-glucose for studying glucose-6-phosphatase deficiency in patients suffering from glycogen storage disease (Type 1). The scope of these studies has been limited, however, due perhaps, to the high cost associated with performing such an experiment in vivo. This report describes the feasibility of stable isotope tracer experiments for differentiating between several of the more commonly occurring enzyme deficiencies associated with the lactic acidemias. The utility of [U-13C]-glucose metabolism in cultured fibroblasts for distinguishing between cytochrome oxidase and PDH deficiencies is the focus of the investigation. Differences in 13C-turnover in various metabolite pools are presented for the two enzyme defects; the results suggest that these two deficiencies may be readily differentiated.

# Experimental

Fibroblasts of one infant with PDH deficiency and one infant with cytochrome oxidase deficiency and those of age-matched controls were isolated following procedures outlined by Robinson et al. Fibroblasts were grown to a concentration of 105 cells / 25 cm<sup>2</sup> petri dish in culture medium ( $\alpha$ -MEM). The medium was then removed and replaced by a medium ( $\alpha$ -MEM with no added glucose) to which [U- $^{13}$ C]-glucose (concentration = 1.0mM) was added for a

"pulsing" period of three hours. Following the "pulsing" period, medium containing labelled glucose was removed and replaced with fresh medium containing unlabelled glucose (1mM) and incubated for a "chase" period of 12 to 15h.

Cells were extracted with Triton X-100 and collections of extracts were made during the [U- $^{13}$ C]-glucose pulse period (t=0.5, 1, 2, 3h for PDH and control lines; t = 3h for cytochrome oxidase line) and the "chase" period (t = 0, 3, 6, 9, 12, 15h for cytochrome oxidase and control lines; t = 0, 1, 3, 7, 15h for PDH line). In addition, collections of cultured medium were made at times identical to those for the cell extracts.

Cell extracts and cultured medium were lyophilized and cell metabolites were solubilized in pyridine and extracted from excess detergent. Subsequent derivatization of the components and cell medium was made using bis(trimethylsilyl)trifluoroacetamide (BSTFA) and pyridine (4:1) and solutions were heated at T = 80 °C for t = 1h. Resultant derivatized organic acids and amino acids were sealed in capillary tubes and kept refrigerated until the analyses were performed.

All analyses were performed using an HP5985 GC/MS/DS. A 25m DB-1 megabore column (0.52 mm i.d., purchased from J&W Sci., Inc.) equipped with oncolumn injection was temperature programmed from 55 - 75 °C at 5 °C/min then from 75 - 255 °C at 10 °C/min for all analyses. Mass spectra were acquired by electron ionization (EI)-MS (electron energy = 70eV, emission current = 300 mA, and ion source temperature, T = 150 °C), and chemical ionization (CI)-MS (ammonia pressure = 300-400 mtorr, electron energy = 115eV, emission current = 325mA, and T = 150 °C). Selected ion monitoring (SIM) of MH<sup>+</sup> and MNH<sub>4</sub> <sup>+</sup> ions was performed for determining the extent of label enrichment into various metabolite pools.

# Results and Discussion

Shown in Figure 65 a-c are the reconstructed total ion current (TIC) profiles for the metabolites found in control, cytochrome oxidase, and PDH deficient cells, taken at the third hour of <sup>13</sup>C-glucose "pulsing" period. Evaluation of the metabolic profiles of the cell extracts reveal only subtle differences. Although slight differences in relative amounts of metabolites are observed, differential diagnosis based on the respective organic acid patterns would be difficult. Table 8 summarizes the identified organic acids and amino acids from experimentally obtained EI and NH<sub>3</sub>-CI data, and from available literature EI mass spectra. Glycine (tri-TMS) is relatively abundant in the PDH fibroblasts, but is relatively less abundant in the cytochrome oxidase and control fibroblasts; however, at later times throughout the "chase" period, glycine abundances vary slightly. The significance, though, of these results cannot be evaluated until additional cell lines have been examined to determine whether this behavior is characteristic and unique to the PDH deficiency.

Cultured medium of the respective cell lines were also analyzed by GC-MS. Shown in Figure 66 a-c are the reconstructed TIC chromatograms of the metabolites secreted into control, cytochrome oxidase, and PDH cultured medium. The amino acid and organic acid profiles shown correspond to the onset of the "pulsing" period. Striking similarities are observed between the amounts, and number of metabolites secreted into the control and PDH medium. A slightly greater number of metabolites are secreted into the cytochrome oxidase medium at early onset of the "pulsing" period, but this result tends not to be a consistent one throughout the entire collection periods. The metabolites identified in the cultured medium also are summarized in

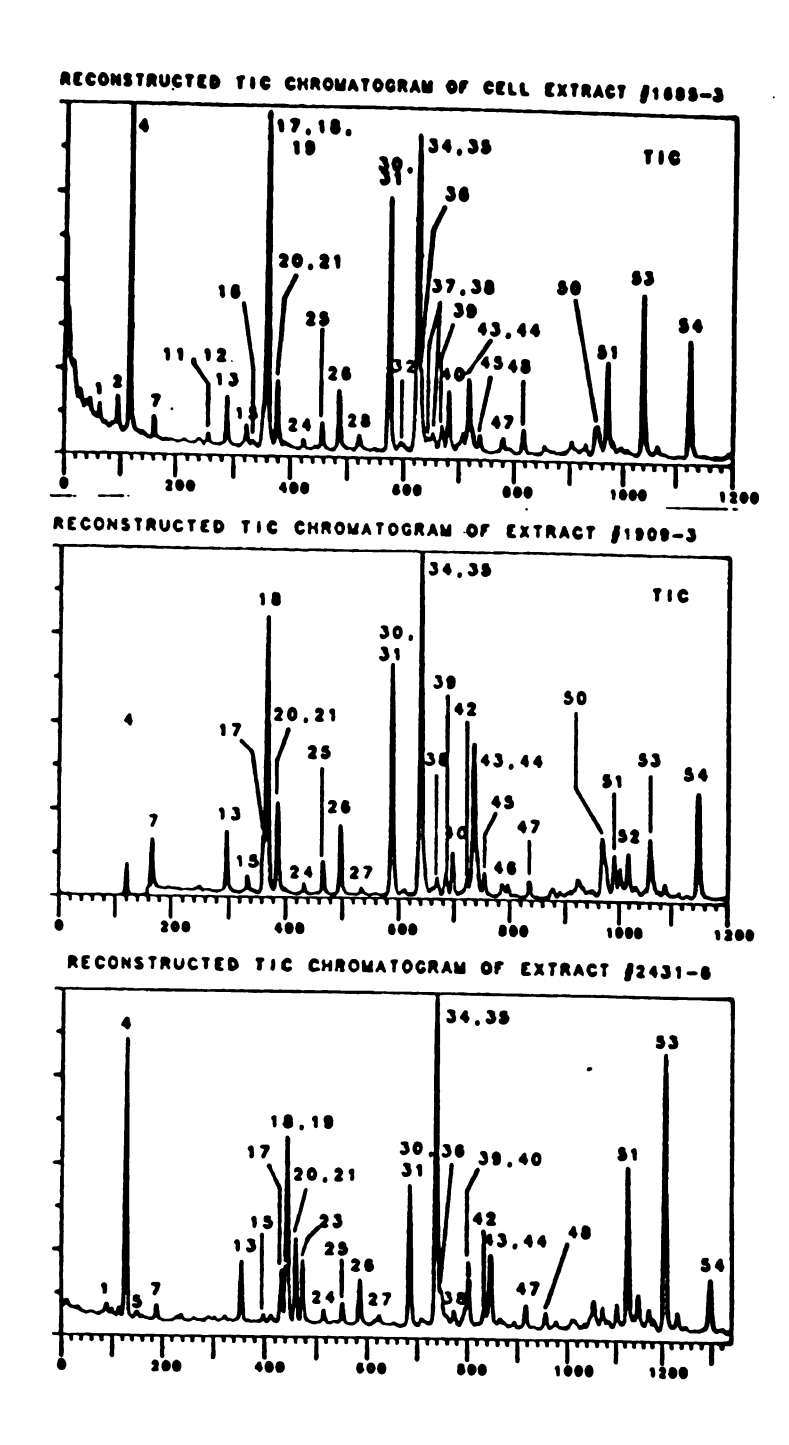


Figure 65. GC-EI-MS TIC profiles of metabolites found in (a) control, (b) cytochrome oxidase deficient, and (c) pyruvate dehydrogenase deficient fibroblast cells

Table 8. Identified metabolites of both cell fibroblasts and cell medium. Peak number 43-glutamic acid. Peak number 47-unknown (MW=437), believed to be a five-carbon aminoribose sugar

PEAK :	# COMPOUND r	$n/z (MH^+)$	PEAK #	COMPOUND m	<u>z (MH</u> +)
1	Acetic Acid	133	28	Methyladipic	221
2	Unknown #1	122	29	Unknown #6	278
3	Acetylglycine	190	<b>30</b>	Homoserine	336
4	Lactic acid	235	31	Aspartic acid	<b>350</b>
5	Glycolic	221	<b>32</b>	Unknown #7	<b>306</b>
6	Indole	190	33	Pipecolic acid	202
7	Alanine	234	34	Pyroglutamic	274
8	Glycine (di-TMS)	220	35	Unknown #8	<b>350</b>
9	Propionylglycine	204	36	Glutamic (di-TMS)	292
10	Unknown #2	218	37	Malonylglycine	<b>320</b>
11	Propionylglycine	204	38	2-aminoadipic	378
12	3-indoleacrylic	188	39	Threonic acid	425
13	Valine	262	40	N-valerylglycine	304
14	Unknown #3	336	41	2-hydroxycaproic	277
15	Urea	205	42	N-acetylaspartic	<b>392</b>
16	Serine (di-TMS)	250	43	Glutamic (tri-TMS	364
17	Leucine	276	44	Phenylalanine	310
18	Phosphoric acid	315	45	Mannitol-tetraacetate	<b>380</b>
19	3-(4-phenyl)propenoi	c 309	46	Oxaloacetate	349
20	Isoleucine	276	47	<b>AMINOPENTOSE</b>	438
21	Proline Proline	260	48	Unknown #9	452
22	Unknown #4	264	49	Lysine	363
23	Glycine (tri-TMS)	292	50	$\beta$ -Galactofuranoside	540
24	Glyceric acid	323	51	α-D-glucose	540
25	Serine (tri-TMS	322	52	Tyrosine	<b>398</b>
26	Threonine	336	53	β-D-glucose	540
27	Unknown #5	278	54	Inositol (hexa-TMS)	613

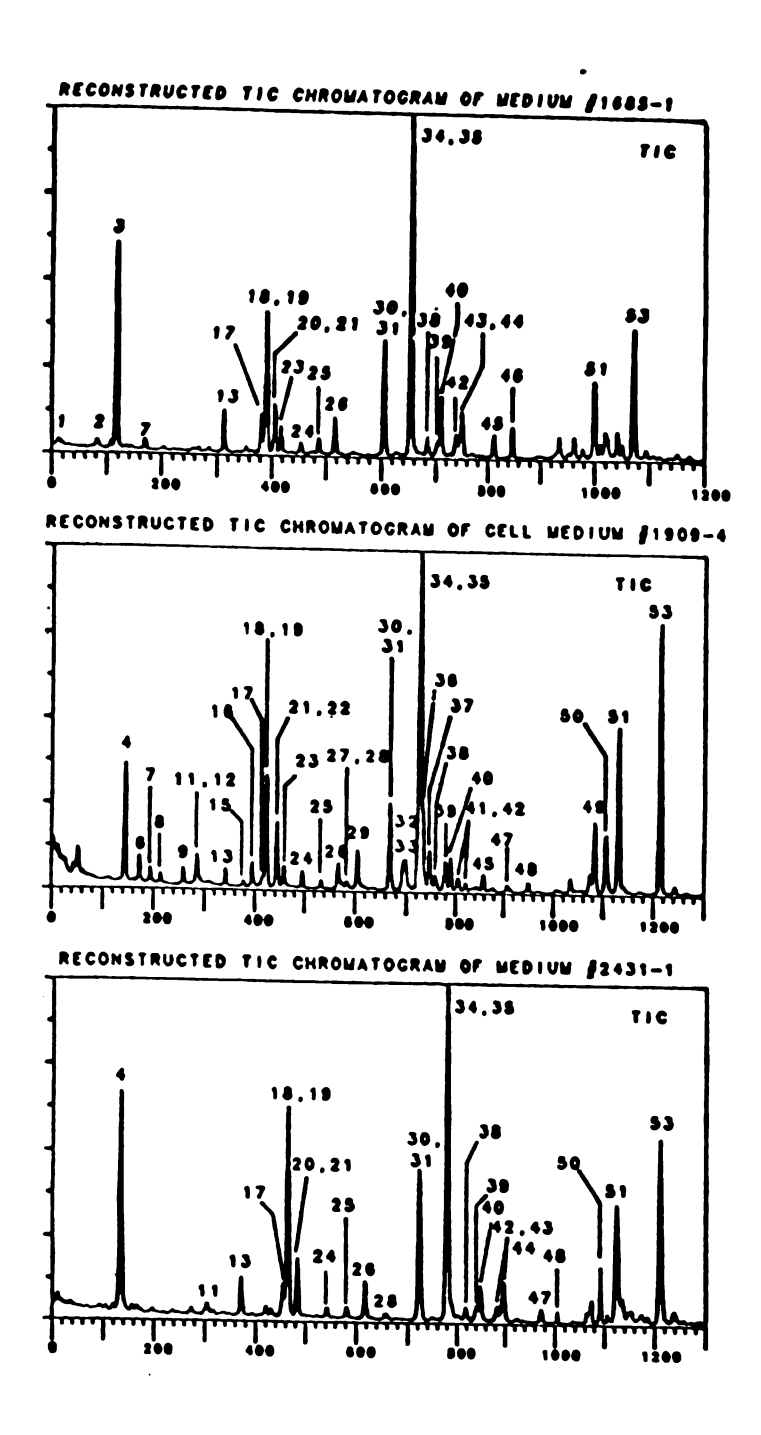


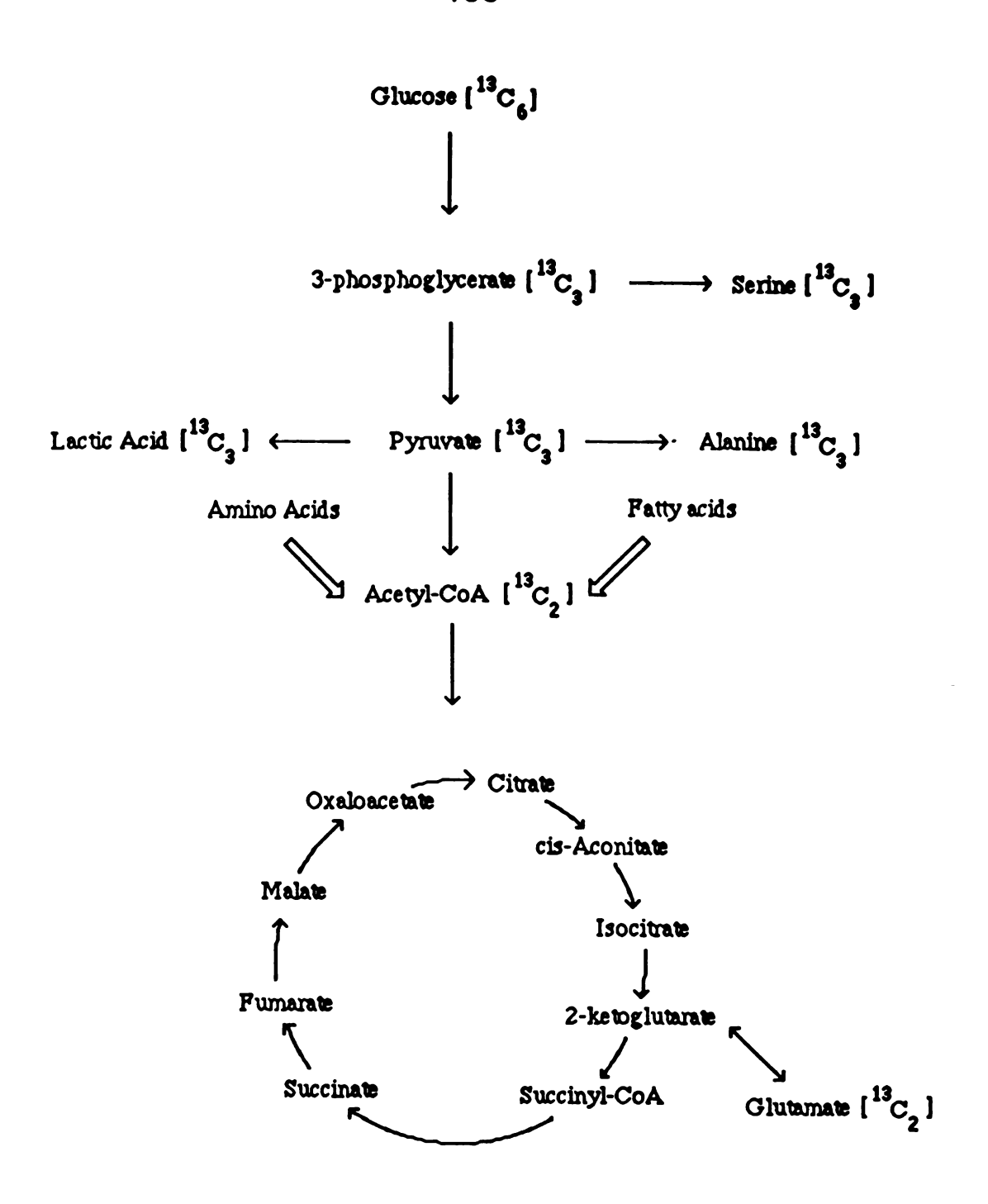
Figure 66. GC-EI-MS TIC profiles of metabolites excreted into (a) control, (b) cytochrome oxidase (CytOx) deficient, and (c) pyruvate dehydrogenase (PDH) deficient cell medium

### Table 8.

The principal organic acid of fibroblasts and in the cultured medium has been identified as lactic acid. Other low molecular weight organic acids are observed, but in only very low abundance. The majority of metabolites observed are amino acids and glycine conjugates. Pyroglutamic acid (peak #34), a major cell and medium metabolite is believed not to be an artifact of cyclization of glutamic acid, which frequently results during gas chromatographic analysis. 149

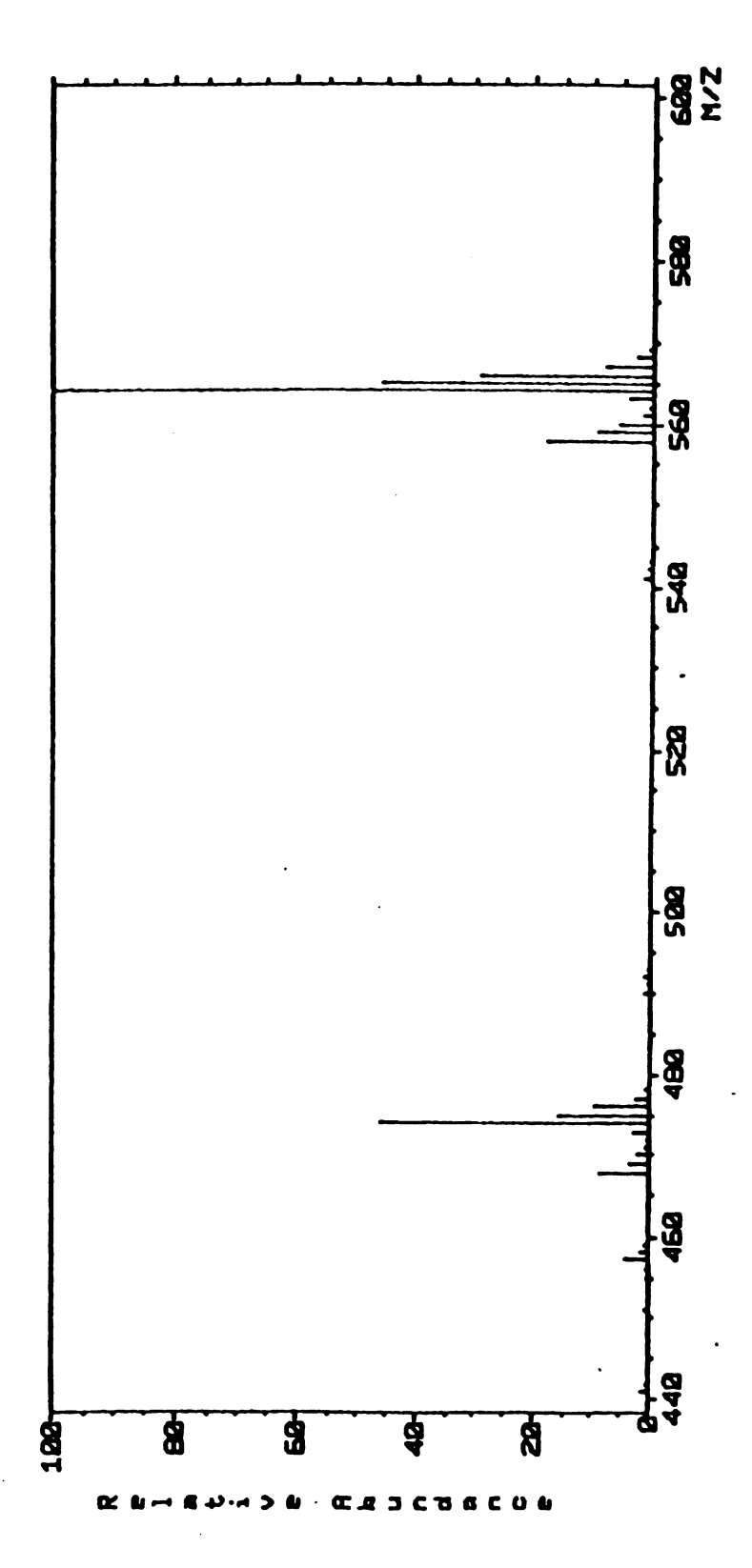
The results from the reconstructed TIC chromatograms suggest that differential diagnosis of these enzyme defects by measurement of pool sizes is difficult, and only very slight differences in the metabolic profiles are observed when comparing patients to age-matched controls. A more useful approach for differentiating these enzyme deficiencies from one another is based on monitoring individual metabolite pools for <sup>13</sup>C label enrichment and/or turnover rates after uptake of [U-<sup>13</sup>C]-glucose.

The pertinent pathways involving glucose consumption are shown in Scheme 5a and 5b. [U-<sup>13</sup>C]-Glucose can enter the glycolytic pathway, thereby generating <sup>13</sup>C-enrichment into glycolytic intermediates, transamination products, etc. (e.g., lactate, alanine, serine). Since only partial PDH and cytochrome oxidase deficiencies are typically observed, a portion of glucose continues to be channeled through the TCA cycle (scheme 4b). Metabolites such as glutamic acid, for example, should experience two <sup>13</sup>C atoms from acetyl-CoA. Shown in Figure 67 is the amount of labelled glucose (enriched at all six carbon atoms) observed at the onset of the pulsing period. Only 80 per cent of fully labelled glucose is observed, suggesting that more than one source of glucose (i.e., from gluconeogenesis and breakdown of glucose-containing carbohydrates) is available to the cells. Enrichment of <sup>13</sup>C-label into various metabolites may be diluted by the presence of these unlabelled sources of glucose.



Scheme 5a and 5b

Summarized in Table 9 are those cell metabolites (and metabolites from cultured medium) that experience <sup>13</sup>C-enrichment (+) and those for which no enrichment (o)



NH3-CI mass spectrum of glucose (penta-TMS) obtained at the onset of pulse-labelling. Isotope enrichment observed at m/z 564 (MNH <sup>+</sup>). Figure 67:

13 C-Enrichment observed into various metabolite pools from fibroblast cells and cell medium for (a) Cytochrom oxidase, (b) Pyruvate Dehydrogenase, and (c) control lines. Table 9:

tor (a) Cytocinom Oxidase, (b) Cytoria Ecciymogenase, and (c) condomines.	YOUND m/z RATIO CYT. OX. PYR.DEHYDROG. CONTROL	: Acid 238 / 235 + + + +	uine 237 / 234 + + + +	ine 293 / 292 0 + + +	eric 326 / 323 + + +	ne 325 / 322 + + +	mic 366 / 364 + 0 0 +	W=437) <sup>‡</sup> 441 / 438 0 +	
	COMPOUND	Lactic Acid	Alanine	Glycine	Glyceric	Serine	Glutamic	UN (MW=437)*	

++ approximately twice the <sup>13</sup>C-enrichment

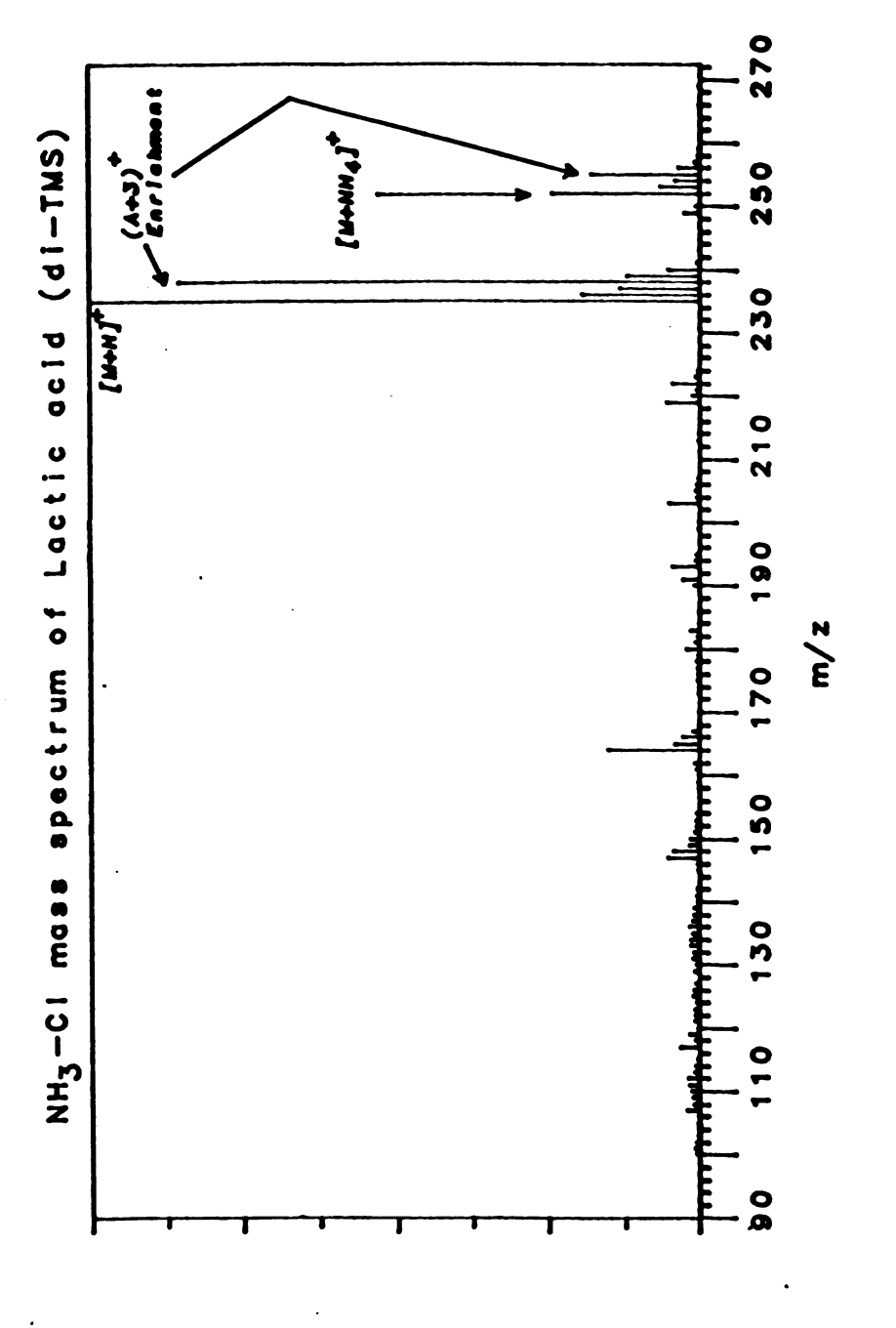
-- insufficient data

# This unknown has been determined to be a polyhydroxy aminoribose sugar based solely on interpretation of mass spectral data.

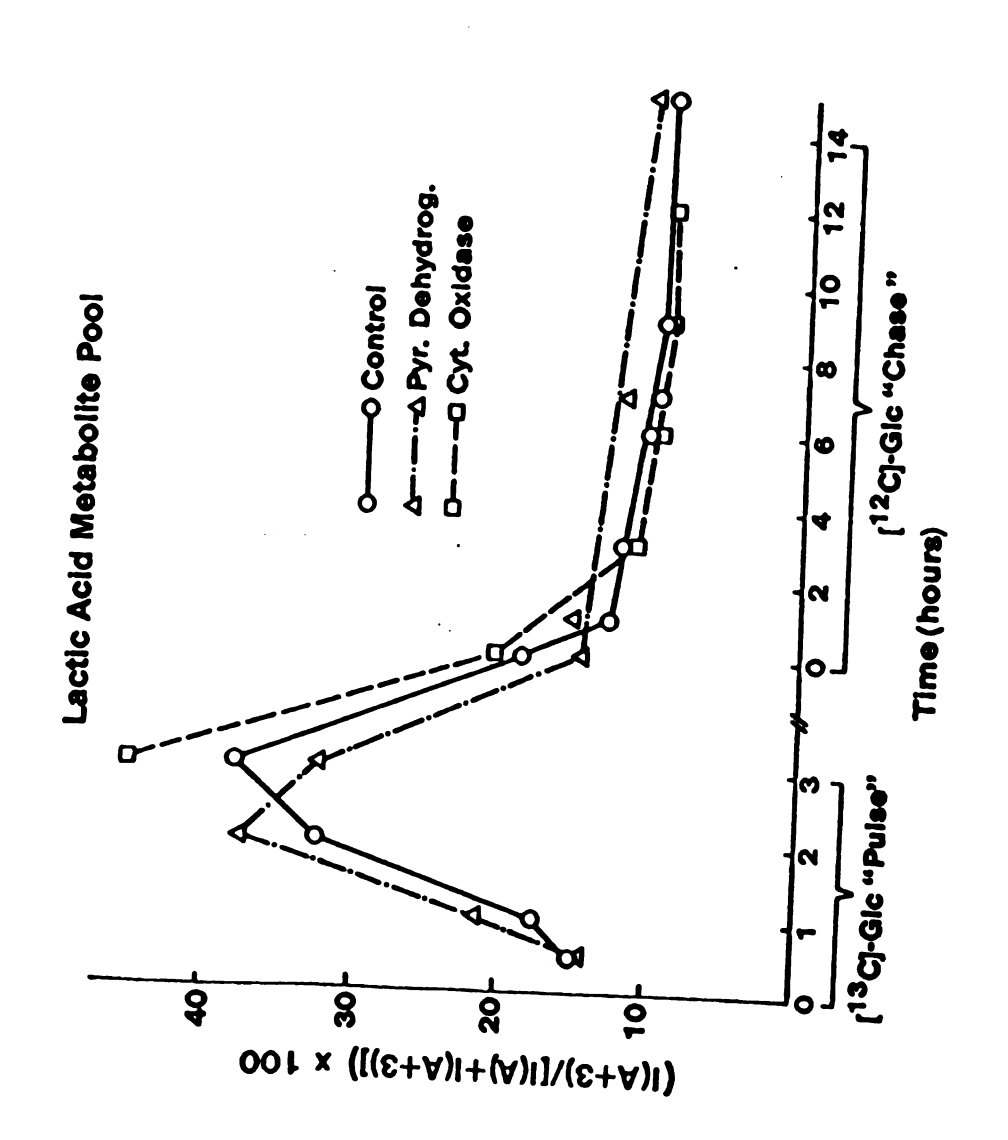
is observed. Compounds such as lactic acid would be expected to incorporate three <sup>13</sup>C atoms from fully labelled glucose. Shown in Figure 68 is the NH<sub>3</sub>-CI mass spectrum of lactic acid. Approximately 40 per cent enrichment is observed at the (A+3)<sup>+</sup> peak for the MH<sup>+</sup> and MNH<sub>4</sub><sup>+</sup> ions. These results suggest that <sup>13</sup>C in lactate is derived from the labelled precursor ([U-<sup>13</sup>C]-glucose).

Table 9 reveals, however, that <sup>13</sup>C enrichment is observed for lactic acid in all three cell lines. A plot of <sup>13</sup>C-enrichment vs. collection time for lactic acid is shown in Figure 69. The maximum in <sup>13</sup>C-enrichment occurs at t = 3 hours during the "pulse" period for the PDH and control cell lines. Collections were not made for the cytochrome oxidase line at times earlier than t = 3h during the "pulsing" period, yet the level of <sup>13</sup>C-enrichment observed for this line suggests there is very little difference in the extent of label enrichment and turnover times for the three cell lines. Therefore, lactic acid cannot be considered useful as a target compound for differentiating these enzyme defects. Similarly, alanine and glycine demonstrate similar behaviors, with nearly equivalent levels of enrichment when comparing the three cell lines.

The pattern of  $^{13}$ C-enrichment of these metabolites is no more revealing than that obtained when the medium is analyzed by GC-MS. In fact, only alanine and lactic acid (in addition to glucose) show any enrichment at all. For lactate secreted into the cell medium, slightly higher levels of enrichment are observed in the PDH line (50 % +/- 3 %) relative to the control and cytochrome oxidase lines (c.a. 44%). Maximum label enrichment occurs at t = 3h during the "pulsing" period for all three cell lines. In the case of alanine, higher levels of enrichment are observed for all three cell lines, with  $^{13}$ C-enrichment at the (A+3)<sup>+</sup> peak exceeding 16 % +/- 2 % for the cytochrome oxidase line and 9% for the control and PDH lines, the former showing nearly a two-



NH3-CI mass spectrum of lactic acid (di-TMS) from control fibroblasts collected during the pulse-labelling period. Figure 68:



Pigure 69: Plot of <sup>13</sup>C-enrichment vs. collection time for lactic acid in control, CyrOx, and PDH fibroblast cells,

fold increase over the levels obtained from the cell extract.

The results shown in Table 9 suggest that  $^{13}$ C-enrichment is observed in the metabolite pool of glutamic acid for the control and cytochrome oxidase lines, but is not observed for the PDH line. Enrichment is found at the  $(A+2)^+$  peak for the MH<sup>+</sup> ion, as expected. The NH<sub>3</sub>-CI mass spectra of glutamate in the cytochrome oxidase and PDH lines, respectively, are compared in Figure 70 a-b. Clearly, enrichment is observed for the cytochrome oxidase line but not for the PDH line when comparing the contribution of  $^{13}$ C-enrichment at the  $(A+2)^+$  peaks for the two species. A plot of  $^{13}$ C-enrichment vs. collection time for the glutamic acid metabolite pool is shown in Figure 71 to further demonstrate this behavior. At t = 3h during the "pulse" period, only a one per cent enrichment (corrected for natural isotopic contribution) is seen in the PDH glutamic acid pool. At the same collection time, though, much higher levels of  $^{13}$ C-enrichment are observed in the control and cytochrome oxidase lines.

Results from Table 9 suggest that an unknown (derivatized MW =437) found in the cell extracts may also be used to differentiate these two enzyme defects. This cell and medium metabolite has been tentatively identified as a 5-carbon aminopentose sugar based on mass spectral interpretations. A literature mass spectrum of the TMS derivative of this compound has not been available. A structural assignment has been proposed, therefore, on the basis of experimentally obtained NH<sub>3</sub>-CI and EI mass spectra for the TMS [Si(CH<sub>3</sub>)<sub>3</sub>] and d<sub>9</sub>-TMS [Si(CD<sub>3</sub>)<sub>3</sub>] derivatives. Listed in Table 10 are the observed ions from both ammonia-CI and EI analyses on the TMS and d<sub>9</sub>-TMS derivatives of this compound. From the d<sub>9</sub>-TMS experiment, it is possible to determine the number of TMS groups associated with each fragment ion, as shown in the third column of Table 10. Furthermore, these experiments have revealed that the

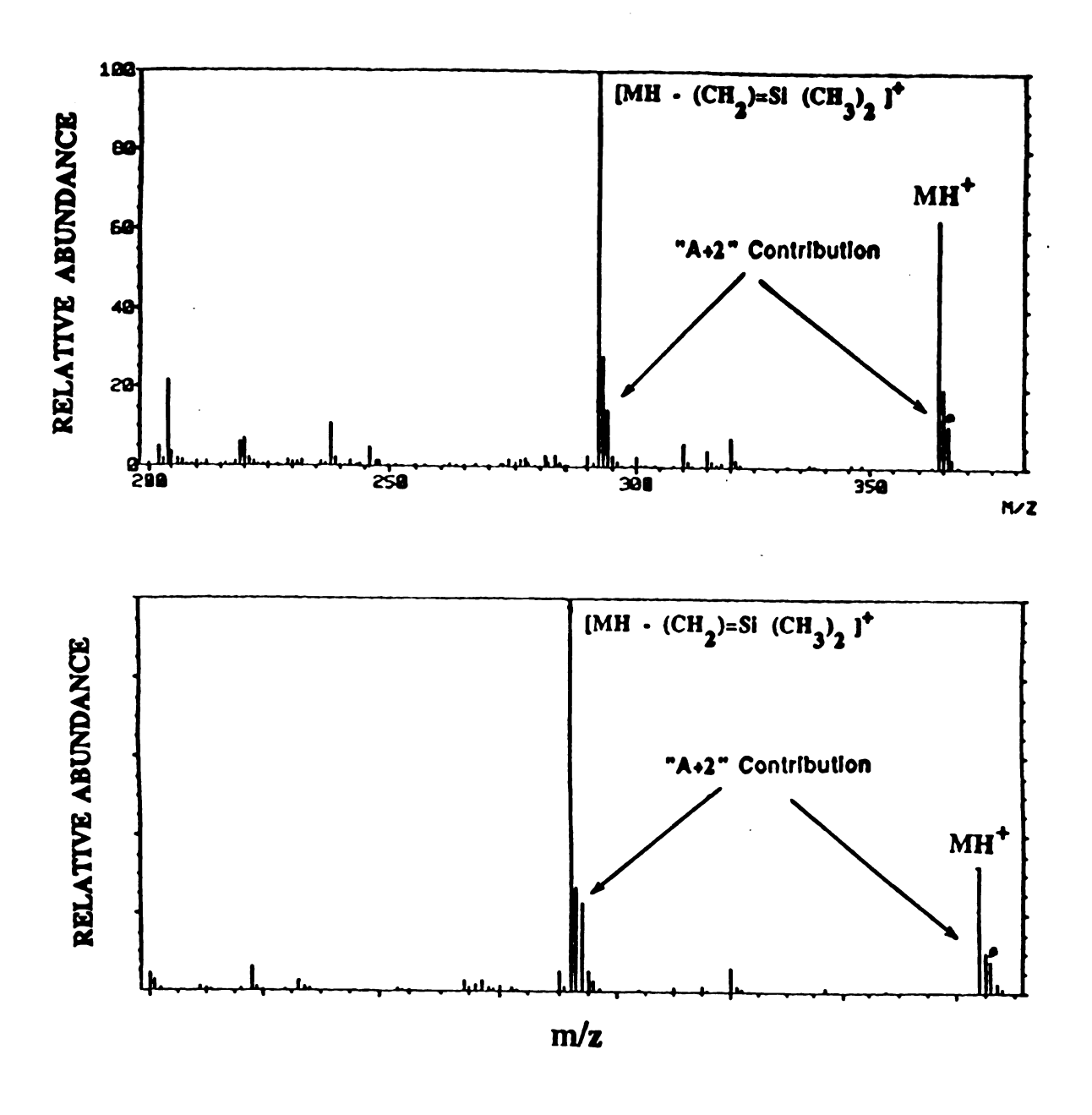
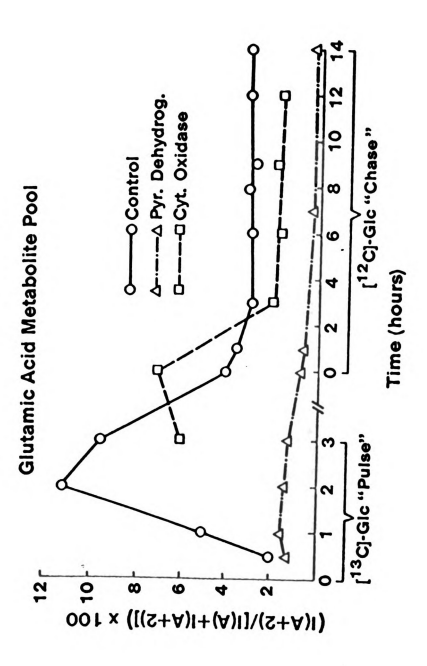


Figure 70. NH<sub>3</sub>-CI mass spectrum of glutamic acid from (a) cytochrome oxidase, and (b)pyruvate dehydrogenase fibroblasts



Plot of  $^{13}\mathrm{C-enrichment}$  ws. collection time for glutamic acid in control, CyrOx, and PDH fibroblast cells, Figure 71:

Fragment ions observed and number of trimethylsilyl groups associated with each fragment from the electron impact ionization mass spectrum of the do-TMS and do-TMS derivatives of Unknown (MW=437). Table 10.

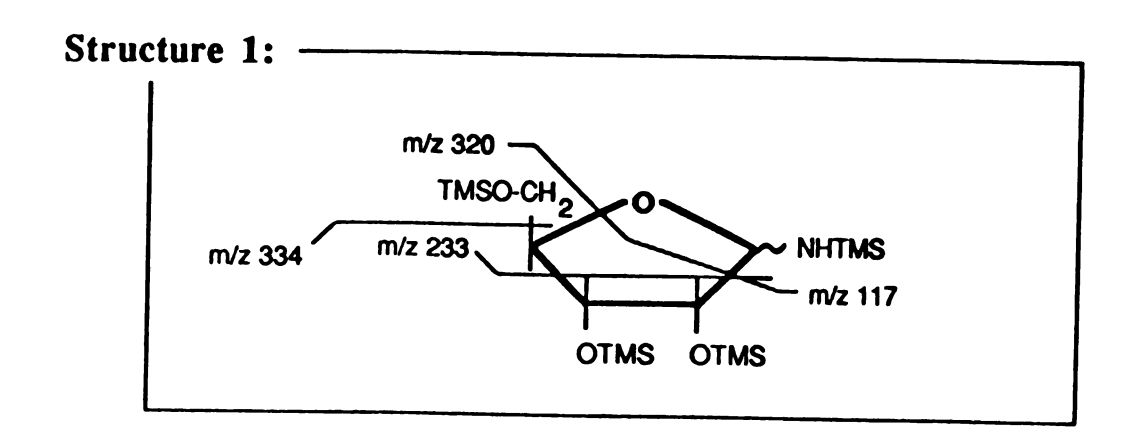
# **BESULTS OF AMMONIA-CI ANALYSIS**

# TMS	4	က		ETMS	•	1	m	က	က	•	8	~	<b>÷</b>	:
lon Designation	[M+H]*	[M+H - 72 U] <sup>+</sup>		ion Designation	÷	[M-CH <sub>3</sub> ] <sup>+</sup>	[M-CH2OTMS]	[M-OCHNHSI(Me_)]	:	[m/z 320 - CH2=C=O]	[M - 2 CHOTAS]	[m/z 320 - HOSKCH <sub>3</sub> ) <sub>3</sub> ] <sup>+</sup>	•	[(CH <sub>3</sub> ) <sub>2</sub> -Si=0-Si(CH <sub>3</sub> ) <sub>3</sub> ] <sup>+</sup>
do-IMS	438	366	LANALYSIS	dTMS	437	422	334	320	290	278	233	230	217	147
lon Designation	[M+H]	[M+H - 81 u] <sup>+</sup>	RESULTS OF ELANALYSIS	lon Designation	÷=	[M-CD <sub>3</sub> ] <sup>†</sup>	[M-CH2OTMS]	[M-OCHNHSI(Me3)3]	•	[m/z 347 - CH2=C=O]	[M - 2 CHOTMS]	[m/z 347 - HOSI(CD3)3]	•	[(CD <sub>3</sub> ) <sub>2</sub> -SI=O-SI(CD <sub>3</sub> ) <sub>3</sub> ] <sup>+</sup>
d,-IMS	474	393		do-IMS	473	455	361	347	317	305	251	248	232	162

derivatized molecular weight of the unknown is 437u. In addition, the parent structure is found to consist of four TMS groups, as the molecular weight of the deuterated analog was found to be 473 u, suggesting the replacement of four Si(CH<sub>3</sub>)<sub>3</sub> groups with four Si(CD<sub>3</sub>)<sub>3</sub> groups. Schoots and coworkers recently reported on the trimethylsilyl derivatives of carbohydrates and organic acids retained in uremic serum, <sup>150</sup> however, no amine-containing carbohydrate (MW=437) was observed. A possible organic acid analog of this unknown, 2-deoxyerythropentonic acid (tetra-TMS, MW = 438), was reported, however, and chromatographic elution times between this compound and the unknown were similar, lending support to the unknown being an aminopentose sugar derivative.

Figure 72 gives two proposed structures for this compound and the origins of the fragment ions. Structure 1, ribosylamine, must be considered since a number of fragment ions can be rationalized from common ring-cleavages. This structure is consistent with known five-carbon ring structures, yet no literature mass spectrum for this compound has been available. However, a number of fragment ions are difficult to explain fully from analysis of this ring structure. An important ion observed in the EI mass spectrum is found at m/z 278, and the d<sub>Q</sub>-TMS experiment has revealed that the fragment contains three timethylsilyl groups. The only plausible explanation for such an ion is a result of migration of a TMS group in its formation. Migration of trimethylsilyl groups in carbohydrate molecules have been reported previously. 151 This ion might arise through elimination of ketene (CH<sub>2</sub>=C=O) from the [M-117]<sup>+</sup> ion, as shown in the proposed mechanism of Figure 72 (structure 2). Structure one is not readily able to undergo such an elimination reaction, whereas structure II appears to be capable of such a rearrangement due to the presence of the unhindered C-4 position. GC-MS-MS analyses are currently being evaluated to verify this precursordaughter relationship.

# Proposed structures and fragment ions for Unknown (MW=437)



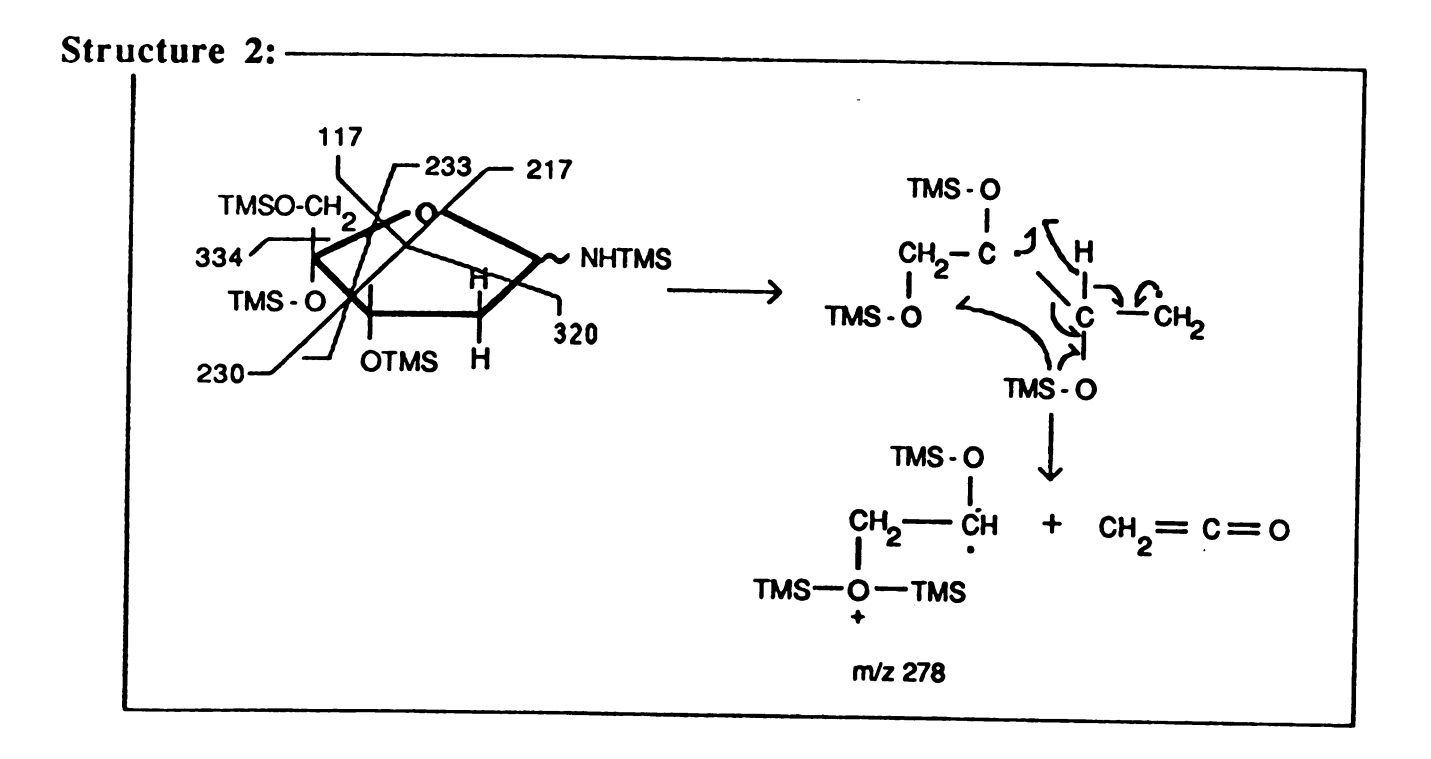
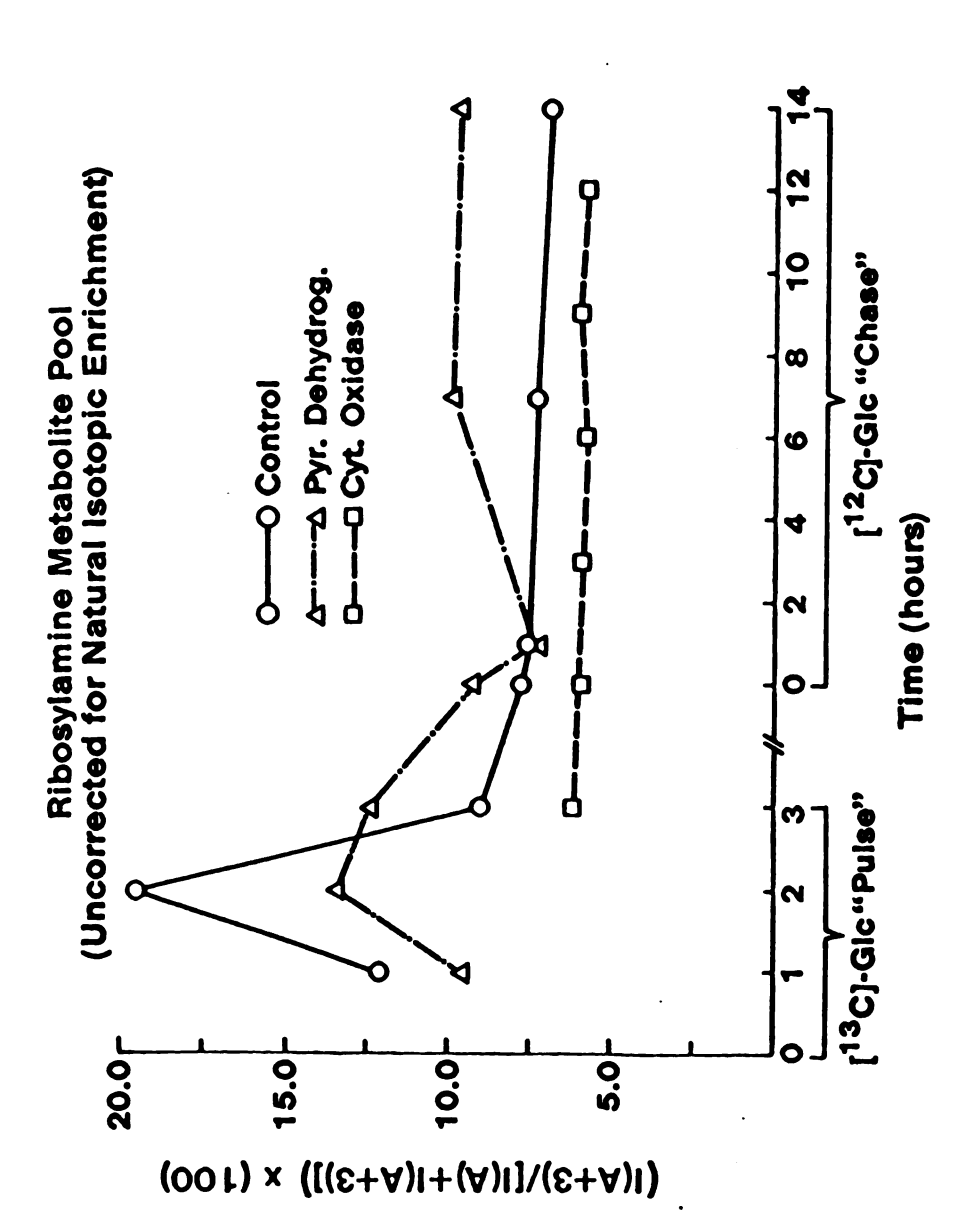


Figure 72. Proposed structure and fragment ions for unknown (MW =437) presumed to be an aminoribose sugar metabolite

Regardless of the identity of this compound at present, it is of special interest because, unlike the case for glutamic acid, <sup>13</sup>C-enrichment is observed in the PDH and control lines, but not in the cytochrome oxidase line. Enrichment at the (A+3)<sup>+</sup> peak for the MH<sup>+</sup> species is observed (c.a. 15 % above the natural isotopic contribution for similar compounds ciontaining four TMS groups). A plot of <sup>13</sup>C-enrichment vs. collection time for this compound shown in Figure 73 suggests that these two enzyme defects may be differentiated from measurements of <sup>13</sup>C-flux into this metabolite pool.

Of interest, too, are the metabolites serine and glyceric acid. Glyceric acid is an intermediate in the interconversion of serine and 2-phosphoglyceric acid. The levels of <sup>13</sup>C-enrichment incorporated into serine are nearly equivalent for the two enzyme deficient lines (c.a. 8%), though a two-fold increase in label incorporation is observed for the control line. The higher levels of label observed in the control line for the serine metabolite pool is based on the fact that in the two deficient lines, there is more heavy reliance on the glycolysis pathway to provide ATP. Because of this, the concentration of 2-phosphoglyceric acid is lower in the deficient lines and as a result, is not available for shunting into the serine metabolite pool. For all three cell lines, maximum label enrichment is observed well into the "pulse" labelling period (t = 3h), The results on glyceric acid indicate that this metabolite, like glutamic acid and the aminopentose sugar metabolite, may be used to differentiate the enzyme defects. Interestingly, the <sup>13</sup>C-turnover rates into the glyceric acid pool differ significantly from the serine metabolite pool. Unlike serine, glyceric acid experiences maximum label enrichment at the onset of "pulse" labelling (collection times, t = 0.5h and 1h). After two hours, nearly all of the <sup>13</sup>C-label has been consumed by the cell. Explanations for this behavior are under investigation. Nearly five % enrichment is



Plot of <sup>13</sup>C-enrichment vs. collection time for Unknown (MW =437) in control, CytOx, and PDH fibroblast cells. Figure 73:

observed for the  $(A+3)^+$  peaks of the MH<sup>+</sup> and MNH<sub>4</sub><sup>+</sup> ions in both the control and PDH lines. However, results for the cytochrome oxidase line are unavailable at this time since collections were only made at times, t = 3h during the "pulse" period. Thus, determining whether this rapid turnover of glyceric acid occurs in the cytochrome oxidase deficient line is not presently possible.

# Conclusions

This feasibility study suggests that turnover rates are superior to pool size assessment by conventional GC-MS profiling for distinguishing between some of the lactic acidemias. For some metabolites, differences in <sup>13</sup>C-turnover rates and levels of enrichment are only slight. However, we have shown that some important metabolites may be used as target compounds for such feasibility studies. The results for glutamic acid are not surprising. Partial PDH deficiency results in diminished channeling of glucose through the TCA cycle. Since induction of glycolysis was the principal pathway through which glucose was metabolized, this PDH deficiency results in the buildup of the intermediates pyruvate, lactate, and amino acids, such as alanine in fibroblasts. Since the enzyme block occurs in the conversion of pyruvate to acetyl-CoA, the amount of labelled glucose available to enter the TCA cycle will be severely diminished, therefore resulting in low levels of label enrichment in metabolites such as glutamic acid.

Results on the tentatively assigned amino pentose sugar metabolite are not nearly as easily interpreted and explanations for the observed <sup>13</sup>C-enrichment can not be made until unequivocable identification of the unknown is made. This five-carbon sugar shows label enrichment into three carbon atoms, for both the control and

cytochrome oxidase lines, but <sup>13</sup>C-enrichment is absent in the pyruvate dehydrogenase line. The results suggest that this five carbon carbohydrate may be derived exlusively from a 3-carbon metabolite of glucose.

The differential diagnosis of cytochrome oxidase and PDH deficiencies is therefore possible based on the flux of <sup>13</sup>C from glucose through these specific metabolites. The explanation for the difference in the five carbon carbohydrate enrichment may lie in the different redox state of the cells. In cytochrome oxidase deficiency there is a more reduced NADH/NAD<sup>+</sup> state and also probably a more reduce NADPH/NADP<sup>+</sup> state. This would restrict entry of glucose-6-phosphate into the hexose monophosphate shunt pathway in the cytochrome oxidase deficiency but not in the control or PDH deficiency.

The goals of this feasibility test were to determine whether enzyme deficiencies could be differentiated based on the use of labelled substrates for <u>in vitro</u> studies. Antoshechkin <u>et al.</u> 152 in a similar investigation, concluded that metabolites excreted by fibroblasts may be reflected by the activity of various metabolic processes <u>in vitro</u>. In hereditary organic acidurias, those pathological metabolites arising from enzyme defects are typically excreted by cells from many tissues, including fibroblasts.

As a feasibility study, there appears to be the potential for extending this method to the differential diagnosis of other heritable enzyme deficiencies associated with congenital lactic acidosis. Experimental parameters such as the amount of labelled precursor, length of "pulse" time, and periodicity of collection time will be evaluated to optimize the conditions for future experiments. Theoretically, experiments of this kind may be employed using other fully-labelled precursors. However, the availability and cost of other labelled precursors may preclude their routine use. The low cost associated with the use of uniformly-labelled glucose (nearly 100 per cent

enriched) makes these <u>in vitro</u> studies attractive for future investigations. The preliminary results obtained from <u>in vitro</u> analyses of cultured cells suggest that stable-isotopes might also be used <u>in vivo</u> to differentiate between various enzyme defects that are clinically indistinguishable.

As mentioned, the future of this study is to extend this stable-isotope approach to the investigation of several enzyme disorders, in addition to those associated with the lactic acidemias. The goal is to determine whether metabolites, either from cell extracts or those excreted into the cell medium may be associated with individual metabolic conditions. <sup>13</sup>C-label enrichment into the metabolite pools such as lactate, alanine, serine, and others are not useful for differential diagnoses since they are not unique to one particular condition. The goal, then is to determine whether specific metabolites may be targeted for in selected ion monitoring experiments in order to determine whether label enrichment is experienced in their metabolite pools. From these results on a wide number of enzyme disorders it may be possible to correlate specific metabolites with a particular enzyme disorder.

The long-term goal of this feasibility test, as stated, is to apply these tracers for in vivo analysis. To this point, the cost associated with purchasing uniformly labelled glucose far exceeds the economic feasibility of such experiments. For the in vitro studies, only 10-20 mg of uniformly labelled glucose were required per cell line (a releatively low cost). However, to attain the same levels of enrichment into various metabolite pools from in vivo analysis would require in excess of 1g [U-13C]-glucose to be ingested by the subject. The cost per experiment would thus not be practical for the differentiation of these organic acidurias. Differential diagnosis could be attained through approaches utilizing molecular biology at a much reduced cost, but at the expense of time and training of qualified personnel.

Lapidot and coworkers have done some elegant work in the area of in vivo

analysis using labelled substrates. In their most recent work, they developed an in vivo assay for various metabolites using [U-<sup>13</sup>C]-glucose on patients suffering from Glycogen Storage Disease (GSD). Not only were they interested in the flux of carbon into various metabolite pools, such as glutamic acid, but were also interested in the carbon recycling nature of these metabolites. They showed that for glutamic acid, only specific position in this five-carbon amino acid metabolite are directly involved in glucose metabolism. In order to determine the position of labelling in these metabolites, it was necessary to use exclusively EI ionization for mass spectrometric analysis.

The initial experiments conducted in our laboratory for the differential diagnosis of lactic acidemias were geared solely to targeting those metabolite pools which did or did not experience <sup>13</sup>C-enrichment. A great wealth of information may become apparent, though, if we are not only to look at the extent of label incorporation, but as well, the position of label incorporation into these various metabolite pools. These kinds of results may uncover various subtleties in the operative metabolic pathways of these enzyme deficient conditions.

# Chapter 8: ECNI-MS w/ CCl pretreatment

# Introduction

Negative chemical ionization (NCI) is a recent addition to the plethora of ionization methods that now exist in the area of mass spectrometry. This ionization method is analogous to positive chemical ionization for gas phase ion molecule reactions. Negative reagent ions are produced upon bombardment of reagent gas contained at high pressure in the ion source by high energy electrons. Ionization to form negative ion reagent ions typically proceeds through dissociative electron attachment reactions, as shown in eq. 18 below:

$$e^- + MX - M^+ + X^-$$
 (18)

Stable reagent ions for negative ions reactions include the superoxide,  $O_2^-$ , ion, <sup>153</sup> methanolate (OCH<sub>3</sub><sup>-</sup>) ion, <sup>154</sup> and hydroxyl ion. <sup>155-156</sup> In addition, the chloride ion has found use as a reagent ion. <sup>157</sup> Under conditions of negative chemical ionization, one of two reactions dominate, those being (a) association reactions and (b) proton transfer reactions. For the negative ion molecule reaction to proceed exothermically, as shown in eq. 19 below,

$$X^{-} + Y \longrightarrow XH + (Y-H)^{-}$$
 (19)

the gas-phase acidity of YH must be greater than the gas-phase acidity of XH. This is analagous to what was described earlier for positive ion-molecule reactions.

Attachment reactions in the negative ion mode, on the otherhand, are analogous to

those reactions most commonly observed under positive ammonia chemical ionization conditions (i.e., the formation of the [M+reagent ion]<sup>+</sup> adduct. Negative ion adduct ion formation requires a third-body for stabilization. Most association reactions observed in NCI-MS have been found to involve the chloride anion. Reactions of Cl<sup>-</sup> with polychlorinated molecules typically result in [M+ Cl<sup>-</sup>] adduct ion formation 158-159 Under conditions such as those described above, negative ion detection offers no dramatic enhancement in the selectivity or sensitivity that may already be achieved using positive ion detection.

The real strengths for negative ion mass spectrometry are realized when the mass spectrometer is operated under conditions for electron capture negative ionization (ECNI). A high concentration of near thermal energy electrons are generated under high pressure conditions into the source of the mass spectrometer. These near-thermal electrons are produced when methane, for example, is introduced (c.a. 1 torr) to the mass spectrometer ion source and subjected to electron ionization. Actually, these low energy electrons may be produced regardless of whether methane, or some other reagent gas (which does not participate in subsequent ion-molecule reactions) is used.

Methane, as mentioned, has been chosen most frequently as this necessary high pressure stabilizing gas for electron capture negative ion mass spectrometry. Recall, as these near thermal energy electrons are produced, so to are a high flux of positive ions (see eqn.'s 5-8). Recently, Hunt showed the strengths of a method called pulsed positive ion -negative ion (PPINI)-MS. <sup>160</sup> This technique has shown enormous potential and is available on many commercial instruments today. The instrument is capable of operating in both the positive and negative ionization modes. In some instances, ammonia has been used as the reagent gas to provide a greater amount of

selectivity in positive ion analysis.

The bombardment of methane (or other non-reactive gas, such as N<sub>2</sub>, NH<sub>3</sub>) by a high energy electron generates an excited methane molecule. The energy of the primary electron is reduced approximately 40 per cent with each ionization event<sup>79</sup>. Secondary ions of much lower energy are formed as a consequence of this ionization event. The "slowed" primary electrons are typically of sufficient energy to participate in a second ionization event. These electrons, and the secondary electrons generated are further stabilized through subsequent collisions with reagent gas until a high flux of near-thermal electrons is produced.

The analytical utility of such a situation is that reactions involving these near-thermal electrons and analyte molecules proceed at relatively high rates. When the analyte molecule exhibits a suffficiently positive electron affinity and high cross-section for electron capture very low detection limits can be observed. It is the electrophilicity of the analyte molecule that determines to what extent electron capture ionization occurs. The processes which the initially formed anion competes with is autodetachment, as shown in eq. 20, below.

$$MX + e^{-}$$
 ---->  $[MX^{-*}]$  ----->  $MX + e^{-}$  (20)

The molecular anions formed by electron attachment will undergo autodetachment unless stabilize through collisional deactivation. For significant collisional stabilization at CI operating pressures, the lifetime of the  $[MX^{-*}]$  species should be greater than 1  $\mu$  sec. Those species with positive electron affinites tyically exhibit sufficiently long lifetimes to be collisionally stabilized to the molecular anion<sup>78</sup>.

The sensitivity of this method lies in the fact that rate constants for electron capture can be approximately 400 times larger than corresponding ion-molecule

reactions (in both the positive and negative ionization modes). These rate constants vary to a much greater extent than the positive ion counterparts, though. This is due to the fact that electron capture cross-sections are strongly structure-dependent. As a consequence, ECNI-MS is often found to be a very selective and sensitive technique. In fact, detection limits as low as 25 femtograms (fg) have been reported under conditions of ECNI-MS. This is the case since ECNI mass spectra typically contain very little fragment ion information and is a result of the low-energy process associated with electron capture ionization.

# A novel ionization method for EC-NI mass spectrometry

The manuscript on threonine metabolism in conditions of Type 1 diabetes discusses the use of ECNI for the analysis of plasma amino acids. It was of interest to determine the amount of uniformly labelled threonine that was actually present in the plasma of the animal under study. This information was of importance because the rate of infusion of the labelled precursor did not occur over a "pulsed" period, as desired, but was administered as a bolus injection, at the onset of the experiment. The result was lower levels of <sup>13</sup>C-enrichment into various organic acid metabolite pools than originally anticipated and there was a desire to correlate these levels of label enrichment with the the amount of labelled precursor present in plasma.

Procedures outlined by Duffield and coworkers <sup>160</sup> for the isolation and derivatization of amino acids from plasma were employed. Literature mass spectra of these types of amino acid derivatives were typically devoid of molecular weight information. ECNI-MS appeared to be a reasonable alternative to EI since these derivativized amino acids contained highly electrophilic moieties.

# Experimental

Initial analyses on the isolated and derivatized amino acids by mass spectrometry were uninformative since only very small ion signals were achieved for the components of the mixture. Gas chromatographic analysis using electron capture detection (ECD) revealed that the amino acids were present, and of relatively high abundance in the mixture. The poor sensitivity of the mass spectrometer was determined to be a result of poor tuning and calibration of the instrument. Typically, perfluorotributylamine (PFTBA) is used as the calibrant in both the positive and negative ionization modes. Under negative ion conditions, though, PFTBA yields only high mass ions (e.g., m/z = 633, 595, 452) under electron capture conditions. The ECNI mass spectrum of PFTBA is devoid of intense ions below m/z =414.

Tuning by PFTBA on these high mass ions yielded what appeared to be "sensitive" tuning files. However, subsequent analyses of the derivatized amino acids showed very poor sensitivities. The possibility that the quadrupole mass spectrometer was being tuned for preferential high mass ion transmission was investigated. In order to test this hypothesis, a calibrant mixture containing equimolar PFTBA and CCl<sub>4</sub>, the latter being used to ensure the production of low molecular weight ions (i.e., Cl<sup>-</sup>), was utilized. Initial results indeed suggested preferential transmission of high mass ions through the quadrupoles and subsequent tuning adjustments allowed for generation of not only PFTBA ions but also Cl<sup>-</sup>, CCl<sub>2</sub><sup>-</sup>, and CCl<sub>3</sub><sup>-</sup> ions. Following these tuning "adjustments", the amino acid mixture was once again analyzed by ECNI mass spectrometry and this time, the compounds were easily detected. However, close inspection of the ECNI mass spectra of these amino acids revealed some very unique ions.

This chapter describes a novel ionization method based on carbon tetrachloride

ion source pretreatment for electron capture negative ion (ECNI) mass spectrometry. The utility of this method resides in improved detection capabilities for selected classes of compounds (e.g., amino acids) over conventional electron capture detection while providing molecular weight information which is generated independent of useful structural information available on the compounds by convnetional ECNI-MS. Adduct ions of the form [M+Cl'] are formed from reactions of analyte molecules on ion source surfaces that have been "pre-conditioned" with chlorine-containing compounds such as methylene chloride, chloroform, or carbon tetrachloride. An [M+ Cl'] radical intermediate appears to exhibit an enormous crosssection for electron capture which facilitates in abundant ion formation. Analyte molecules not participating in these surface reactions undergo conventional electron capture ionization, yielding the types of ions observed under conditions in which the mass spectrometer is not pretreated. A manuscript entitled "Utility of Ion Source Pretreatment with Chlorine-Containing Compounds for Enhanced Performance in Gas Chromatography/Negative Ionization Mass Spectrometry " has recently been accepted for publication in Analytical Chemistry. The manuscript, in its entirety may be found in Appendix III.

# Results and discussion on simple mixtures

Compounds not exhibiting high cross-sections for electron capture under conventional ECNI conditions may be (as described in this paper) capable of forming a radical intermediate that readily undergoes electron attachment to form the stable molecular adduct ion, of the type [M+Cl]. This technique may find use in that compounds previously considered unlikely to yield stable molecular anions or pseudomolecular anions by electron capture, can, following CCl<sub>4</sub> pretreatment of the ion source, produce intense negative ion mass spectra. The results of such an analysis are shown in Figure 74. The reconstructed TIC chromatogram of an equimolar mixture of TMS derivatives of organic acids obtained under electron ionization (positive ion mode) conditions are shown in Figure 74a. Shown in Figure 74b is the convenetional ECNI mass spectrum of this same mixture. Not surprising is that the majority of derivatized organic acids do not form detectable anions since the trimethylsilyl groups imparts no additional electrophilicity to organic acids upon derivatization.. Surprisingly, maleic acid exhibits a relatively high cross-section for electron attachment, due to its highly conjugated system. When the ion source of the mass spectrometer was pretreated with CCl<sub>4</sub> and the organic acid mixture reanalyzed by ECNI, the reconstructed TIC chromatogram in Figure 74c is observed. In this case, several of the organic acids now exhibited sufficiently high cross-sections for electron capture that molecular anions are observed. In fact, the TIC "counts" for many of these compounds in the negative ion mode equal those obtained using EI. These results are an excellent example of the strengths of this pretreatment method. Compounds not previously considered amenable to negative ion analysis might now be detected under the appropriate conditions.

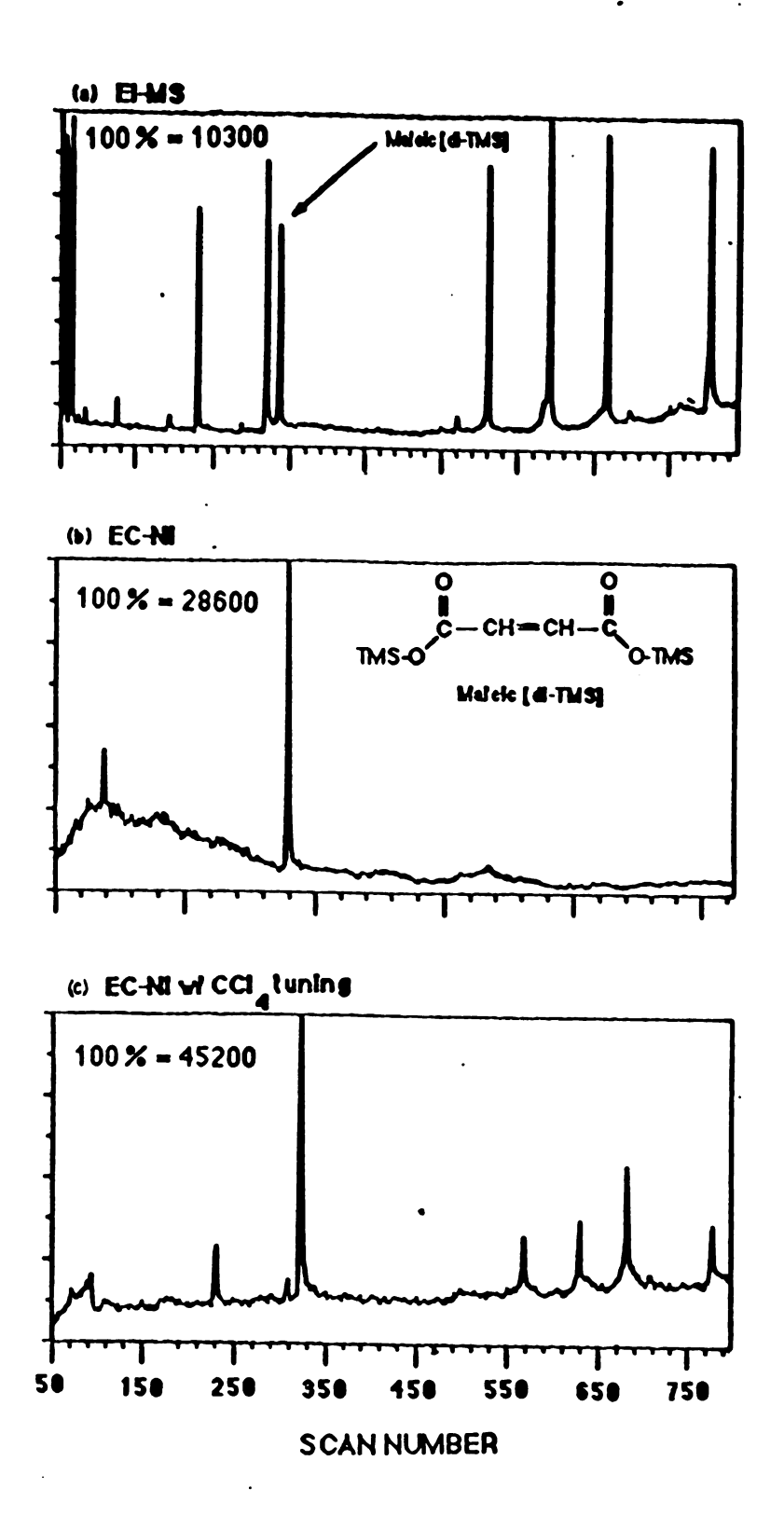


Figure 74. TIC profile of the trimethylsilyl derivatives of a synthetic mixture of organic acids obtained using (a) EI-MS, (b) conventional ECNI-MS, and (c) carbon tetrachloride "pretreatment" prior to ECNI analysis

Another example demonstrating the strengths of this pretreatment procedure is illustrated in Figure 75 for the analysis of a mixture of fatty acid methyl esters. Under conventional ECNI conditions, the signals for these compounds are almost indistinguishable from background (see Figure 75a). Following CCl<sub>4</sub> pretreatment, however, these species are found to yield ion signals that are easily discerned from the background noise (Figure 75b). These results suggest that surface reactions within the ion source of a mass spectrometer can occur readily and alter the ionization efficiency of certain molecules to such an extent that unique chemistry can be observed. Formation of these radical intermediates through ion source surface reactions can be considered as derivatization reactions, in situ. Future work in this area might involve the desorption of other "reactive" gases onto the ion source walls in order to investigate any "unique" chemical behavior and selectivity that might be exploited.

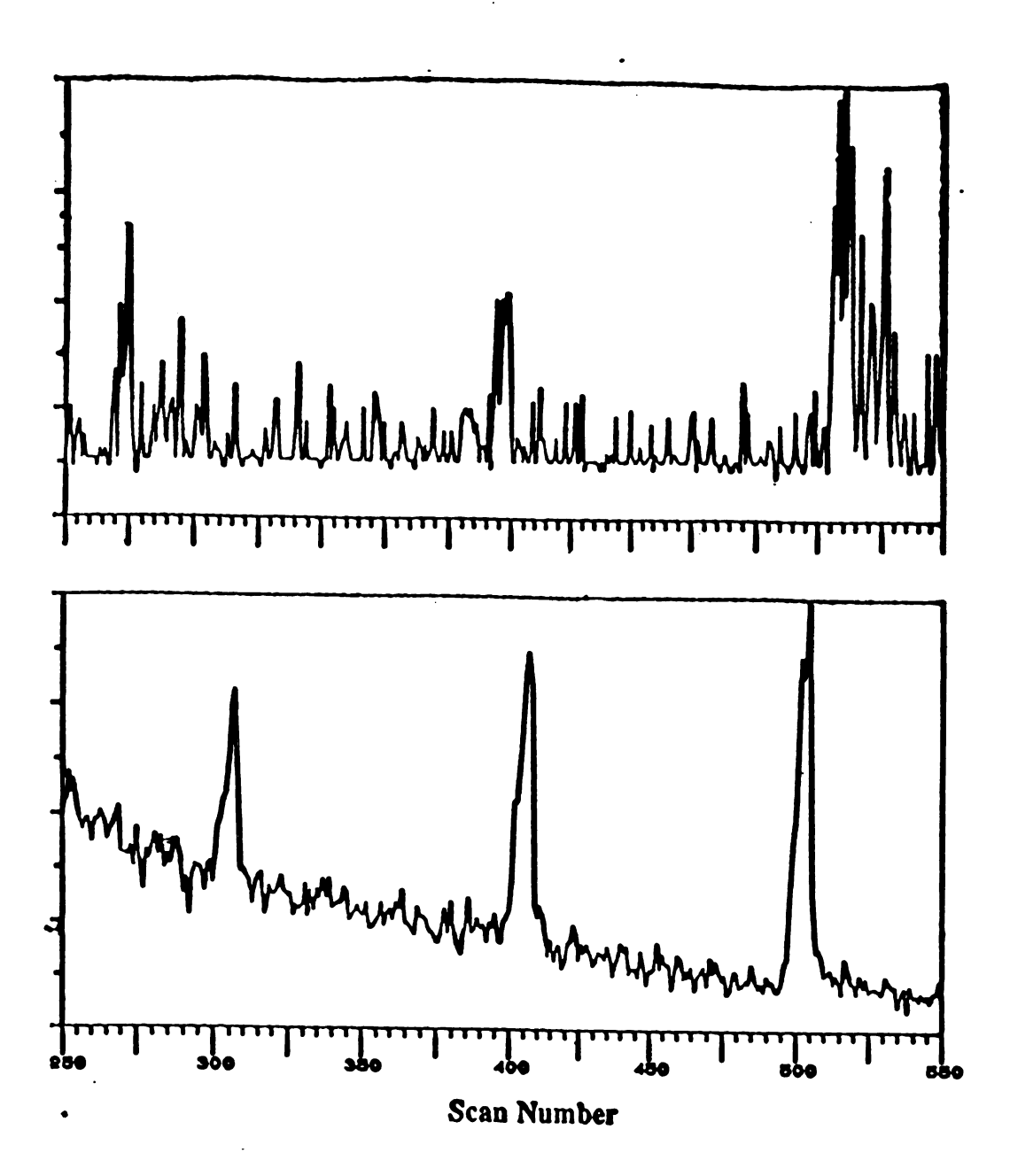


Figure 75. Comparison of TIC profiles of an equimolar mixture of three fatty acid methyl esters, (C-14, C-16, and C-18) obtained using (a) conventional ECNI-MS, and (b) ECNI-MS following ion source pretreatment with CCl<sub>4</sub>

# Final Remarks

The utility and limitations of a number of novel and existing ionization methods for complex mixture analysis have been evaluated. This thesis demonstrated that the type and amount of information derived in metabolic profiling analyses was enhanced dramatically when existing ionization methods, such as ammonia-CI were used in conjunction with conventional electron impact ionization mass spectrometry. The ammonia-CI mass spectra of derivatized physiological metabolites readily provide molecular weight information and the overall sensitivity of this technique is comparable to EI ionization. These strengths were exploited for those metabolic profiling analyses in which precursor-metabolite relationships were being evaluated through the use of stable-isotope labelled tracers. In addition, combining the strengths of ammonia-CI and EI is in general, quite useful for identifying unknowns present in complex mixtures.

The novel technique of CCl<sub>4</sub> pretreatment for ECNI mass spectrometric analysis was shown to be capable of lowering detection limits substantially for selected classes of compounds. More importantly, this study has led to a better understanding of processes important in negative ion mass spectrometry. The prevalence of surface reactions and their effect on the formation of highly electrophilic species capable of readily undergoing electron attachment were also studied. Much interest in the area of reactions between species on mass spectrometer ion source surfaces has been generated in the past few years. The unique chemistry that might occur between analytes presented to an intentionally "contaminated" mass spectrometer can be an attractive and useful feature under controlled conditions.

The novel desorption/ionization method, K<sup>+</sup>IDS, has been shown to be capable of

yielding both quantitative and qualtitative information on mixtures of organic acids from urine. The implementation of a new, dual-filament probe design for the K<sup>+</sup>IDS experiment has resulted in a dramatic increase in sensitivity of the technique, making it more competitive with other existing desorption/ionization (DI) methods in terms of sample size requirements. The K<sup>+</sup> ionization method is free from chemical interference, unlike the technique of FAB, which suffers from severe matrix effects.

The quantitative strengths of the technique have been shown in the analysis of urinary organic acids, for the purpose of providing as a <u>rapid</u> "screening" technique in the identification of disease-states, without the need for extensive sample work-up and sample derivatization. The results obtained from analyses of these mixtures as well as others presented suggest that this method might be an attractive alternative to other DI methods when quantitative information is sought. Additionally, K+IDS has been found to be nearly universal in the types of compounds that are amenable to the method. Analyses of steroids, carbohydrates, polymers, peptides and organic salts, and marginally volatile compounds, such as amino acids and fatty acids, to name only a few, have been successful by K+IDS. The technique also might find utility as a rapid method for determining the purity of compounds (e.g., synthetic drugs, stable-isotope labelled species, etc.), since the K+DS mass spectra are, in general, free from interferences.

The real limitation of this technique to date lies in the fact that most experiments have been performed using a low resolution, low mass quadrupole mass spectrometer, which does not offer features that would be desirable for K<sup>+</sup>IDS analyses of mixtures. This technique should find a great deal of success when utilized on higher resolution, high mass instruments, such as the JEOL HX-110 or the Finnigan TQMS. Implementation of K<sup>+</sup>IDS on either of these instruments will allow for MS/MS studies to be performed, which in reality are essential for mixtures containing isobars

and isomers. The TQMS will offer the advantage of speed in data acquisition, a necessary prerequisite for K<sup>+</sup>IDS experiments in which only small sample sizes are utilized. The high resolution capabilities of the JEOL HX-110, on the otherhand, offers the advantges of both high mass and high resolution capabilities. Implementation of the K<sup>+</sup>IDS technique on either instrument will require modifications to existing probes so as to maximize the sensitivity of the technique, keeping it competitive with other DI methods.

# APPENDIX I

Reprinted from Analytical Chemistry, 1984, 52, 1676.
Copyright © 1986 by the American Chemical Society and reprinted by permission of the copyright ewner.

Utility and Limitations of Electron Ionization and Chemical Ionization for the Determination of Position and Extent of Labeling for <sup>18</sup>O- and <sup>13</sup>C-Containing Permethylated Alditols by Gas Chromatography/Mass Spectrometry

Daniel B. Kassel and John Allison\*

Department of Chemistry, Michigan State University, East Lansing, Michigan 48824

The strengths and weaknesses of a variety of ionization methods are discussed in the context of GC/MS analyses of <sup>18</sup>C- and <sup>16</sup>O-labeled permethyl alditols. The goals were to determine the position of the label and the extent of label Incorporation. Electron lonization mass spectra were useful in determining the location of the label, however, the rates of dissociative lonization from both halves of these "symmetric" molecules appear to be different, resulting in erroneous extent-of-labeling determinations. Isobaric ion interferences in methane and isobutane chemical ionization (CI) mass spectra require that the extent of labeling calculation be performed by solving a quadratic equation that has two roots, i.e., suggests two values for label enrichment. Ammonia CI mass spectra are shown to accurately reflect the extent of label incorporation, which exceeded 97% for the compounds investigated here.

Stable isotopes, or tracers, have frequently and successfully been used for studying metabolic pathways in biological systems. Typically in such studies, labeled precursors (containing <sup>13</sup>C, <sup>18</sup>O, etc.) are presented to a biological system. These labeled species lead to the production of metabolites containing the stable isotope. Once the label is incorporated, an analytical method is required to monitor one or more metabolites and determine the extent of label incorporation as well as where in the metabolite the label appears.

Gas chromatography/mass spectrometry (GC/MS) has been extremely useful for studying metabolic pathways involving stable isotopes. Electron ionization (EI) has frequently been used in such studies due, predominantly, to the reproducibility and extensive fragmentation, i.e., structural information, associated with the technique. However, recently a number of problems associated with the technique have been

identified, which frequently make it inadequate for such analyses. Since El does produce extensive fragmentation, the resulting mass spectra frequently carry no molecular weight information. This also becomes a problem when determining the extent of label incorporation since the major fragment ions may not contain the labeled atom.

GC/chemical ionization (CI)-MS, however, has been found to be valuable for both structural and extent-of-labeling studies. Abundant protonated molecules are frequently produced by the CI method, and these ions are found to be ideal for determining the amount of the label present. The GC/CI-MS technique has been successfully applied to the study of stable isotopes in the analyses of amino acids in urine and serum (1-3), stariods (4, 5) and fatty acids (6) in urine and in many other areas.

Of particular importance is the use of stable isotopes of sugars for studying carbohydrate metabolism (7-10). Invahuable information regarding how labeled glucose is utilized when subjected to a variety of metabolic pathways is attainable. Labeled sugars have been used for studying aspects of the citric acid cycle (11) and other metabolic pathways.

We report here the results of GC/MS studies on sugars for the purpose of determining the extent of <sup>13</sup>C and <sup>13</sup>O enrichment—not as products of a specific metabolic process but as products of a new method developed for preparing sugars that are nearly 100% labeled in the position of choica. Documented here are the strengths and weaknesses associated with GC/EI-MS and several types of CI-MS for determining both the position and extent of labeling in these synthesized permethylated acyclic sugars. EI-MS is found to be valuable for determining the position of the label in these alditols but yields erroneous results for extent-of-labeling determinations, as do some forms of CI. Ammonia CI is suggested to be the method of choice for this class of compounds for extent-of-labeling determinations.

# EXPERIMENTAL SECTION

All experiments were performed on an HP-5985 GC/MS/DS quadrupole instrument. The GC inlet was modified so that capillary columns could be used. A descrivated, nonvitreous capillary transfer line (40 cm long, 0.11 mm i.d., Scientific Instruments Services, Inc.) was used as the GC interface, which was maintained at 280 °C. A wide bore (55 m, 0.32 mm i.d.) capillary GC column (J and W Scientific) was used for all experiments. Isolated, derivatized alditols were introduced on column; the column was temperature programmed from 50 to 250 °C at a rate of 20 °C/min.

For electron ionization, the source temperature was held at 200 °C, electron energies used were 70 eV and 18 eV. Emission current was maintained at 300  $\mu$ A. For CI experiments, source temperature was maintained at 150 °C, electron energy was 150 eV, and emission current was 300  $\mu$ A. Methane (~200-300 mtorr), isobutane (~250 mtorr), and ammonia (~300 mtorr) were used as CI reagent gases. Source pressures were measured by placing a hollow solids probe attached to a thermocouple gauge directly against the CI source volume.

Selected ion monitoring (SIM) was used to integrate peak areas of designate ions for determinations of the extent of labeling. For abort-term replications of experimental determination of extent-of-labeling, there was good precision. The average standard deviation for EI was 6.6%. The extent of label enrichment determined by NH<sub>2</sub> CI was 97 ± 1.1%.

# RESULTS AND DISCUSSION

1. 78-eV Electron Ionization. The first method used to determine the position and extent of labeling in the four-six carbon permethylated alditols was 70-eV EI-MS. In this discussion, we will focus on a particular set of labeled sugars, the permethyl sorbitols. Selected ion monitoring (SIM) was utilized to produce accurate integrated intensities of designate ions for the label enrichment determinations. Shown in Figure 1a is the 70-eV EI mass spectrum of unlabeled permethyl

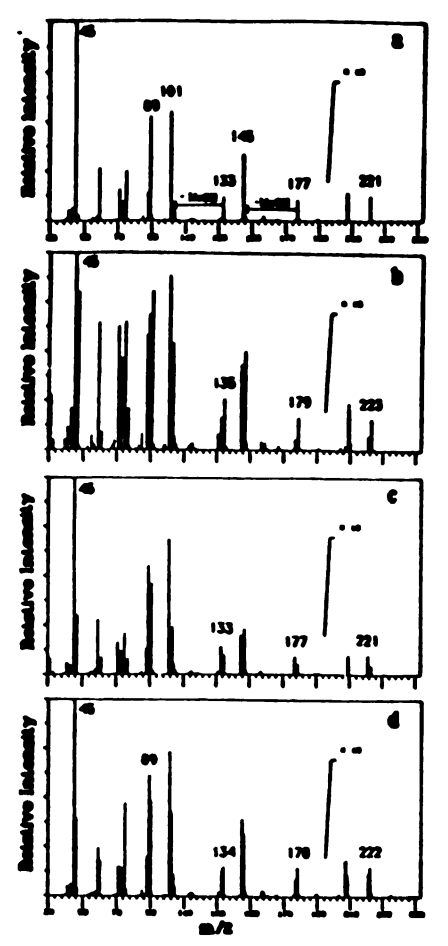


Figure 1. 70-eV electron lonization mass spectra of (a) nonlabeled, (b) [1-40]-, (c) [6-4-0]-, and (d) [1-40]-permethylactrists.

# PERMETHYL SORBITOL OF CH 2 OCH 3 HC-OCH 3

Figure 2. Designate ions formed by electron lonization on permethylecrolitics.

sorbitol ( $C_{12}H_{22}O_6 = M$ ). No molecular ion (M\*) is observed; the highest mass ion in the spectrum, m/z 221, corresponds to loss of the neutral (-CH<sub>2</sub>OCH<sub>2</sub>). A number of pairs of ions that appear to correspond to simple C-C bond cleavages (primary fragments) throughout the carbon skeleton are also observed, as shown in Figure 2. These were chosen as the designate ions for determining the extent of labeling.

Table L Position of Label from Designate Ione

# MO-Labeled Sugare

condition	label at position		
I(A+2)/I(A) > natural isotopic ratio A = m/s 133 A = m/s 177 A = m/s 221	l or 6 x x x	i or 5 X X	3 or 4 X
<sup>18</sup> C-Labeled Sug	200		

condition	label at position		
I(A+1)/I(A) > natural isotopic ratio	1 or 6	2 or 5	3 or 4
A = m/z 133	*	×	×
A = m/s 177	×	×	
A = m/z 221	×		

Deuterated analogues of these straight chain alditols have been studied extensively by Golovkina et al. (7). Their results suggest that both -OCH<sub>3</sub> and -H groups can scramble, complicating the mechanisms through which some of the ions in the mass spectrum can be formed. However, they suggested that the designate ions in Figure 2 should be formed in the straightforward processes shown, except for m/z 45, (C<sub>2</sub>H<sub>2</sub>O)\*.

The EI mass spectrum of unlabeled permethyl sorbitol suggests that the larger primary fragment ions decompose further by loss of methanol; that is, the ions of m/z 221, 177, and 133 eliminate methanol (32 u) to form m/z 189, 145, and 101, respectively.

On the basis of Figure 1a, EI-MS appears to be well suited for both the determination of position and extent of labeling in permethyl alditols. Take as an example [1-18O]permethylsorbitol. Golovkina suggests that such molecules may be regarded as symmetrical structures and that their stereochemistry has no effect on their mass spectra. Furthermore they suggest that cleavage of C-C bonds between atoms of equal distance from both ends of the carbon skeleton can be regarded as equivalent. Assuming that the compounds under study are close to 100% labeled (as will eventually be shown), we would expect that m/2 47 (CH<sub>2</sub><sup>12</sup>OCH<sub>3</sub>)\* would be an intense as m/2 45, the <sup>16</sup>O analogue (after correcting for naturally occurring 18O), since for [1-18O]permethylsorbitol half of these ions would be produced from the labeled end and half from the unlabeled end. For the fragmentations presented in Figure 2, we would also expect to see m/z 223 equal in intensity to m/z 221, as would be the case for the labeled/ unlabeled ion pairs 179/177, 135/133, and 91/89.

The presence/absence of the label in the designate ions will depend on the location of the label. For a sorbitol molecule labeled with 180 on C2, there should be no enhancement of the m/z 47; i.e., the label should never appear in this ion if it were only formed as shown in Figure 2. Conversely, there should be no m/z 221; the entire ion current for this fragment ion would shift to m/z 223; i.e., this ion should always contain the label for the 2-18O-labeled sugar. The ion pairs m/z 89/91, 133/135, and 177/179 should still be formed with ratios of unity. Similar arguments can be made for a permethyl sorbitol molecule labeled with 18O at the C3 position. For any isotopic enrichment of a particular skeletal C or O. the position of the label should be apparent from the designate ions as shown in Table L. In addition, these designate ions should be useful to determine the extent of label enrichment in molecules of this type. For extent of labeling determinations, SIM is used and the following equation should be valid for any designate ion (A), of intensity I:

% label enrichment = 
$$\frac{I(A + n)}{I(A)} \times 100$$
 (1)

Table II. Extent-of-Labeling Implications from Designate Iona

		% labeling	
compound	m/s 221	m/s 177	m/s 135
	70-1		
1-10-M	134	151	196
6. <sup>11</sup> O.M	72		70
	119	155	100
	18 •7	7 <b>m</b>	
1-140-M	131	212	187
€ <sub>n</sub> o.M	70		73
1-14C-M	119	114	97
•M = permethyle	orbitel.		

In this equation n = 1 for <sup>12</sup>C-labeling n = 2 for <sup>14</sup>C-labeling studies. I(A + n) is the intensity of the isotopic peak minus the intensity due to the natural isotopic abundance.

Shown in Figure 1b is the 70-eV EI mass spectrum of the (nearly 100% labeled) [1-16O] permethylsorbitol. It is important to note that we can use the appearance of the label in the designate fragment ions to confirm its position as suggested in Table I. However the ratios of the labeled: unlabeled designate ion peaks (with intensity I) are not at all what was expected, e.g., I (223) > I(221). Table II shows the results of the attempts to determine the extent of labeling based on the integrated peak intensities for the ion pairs with m/z 135/133, 179/177, and 223/221. Peak integration based on SIM gives values for extent of labeling greater than 100%. The values vary for the three sets of designate high mass fragment ions. Note also, that the ratio of m/z 45/47 implies less than 100% label incorporation.

The extent of labeling calculations suggest that, in the car of [1-16O] permethylsorbitol, dissociative ionization from the "bottom" of the molecule (as shown in Figure 2) is occurring to a greater extent than from the top. A number of possible explanations may be proposed to explain this behavior. One possibility is that isotope effects may play an important role. However, we would not expect isotope effects to be operative over long ranges but would be most apparent in fragmentations involving bonds to the labeled atom. A more reasonable explanation may be that the sorbitol molecule is not in fact symmetric, as Golovkins suggests. The O1 is not in exactly the same chemical environment as O6; the same is true for O2 and O5, etc. Therefore, the probability for ionization at O1 may be slightly different than that for O6, as well as the unimolecular decomposition rates for processes occurring at both ends of the molecular ion. Wheatever the cause of the preferential ionization/fragmentation occurring at the bottom of the molecule, the 70-eV mass spectra cannot be used to determine the true extent of labeling by EL

The 70-eV mass spectrum of essentially 100% enriched [6-18O] permethylsorbitol is shown in Figure 1c. The isotopic distribution of the high mass designate ions is consistent with the proposal that products due to cleavage of, e.g., the C5-O8 bond are occurring to a greater extent than those due to cleavage of the C1-C2 bond. What is observed is an inversion of the results found for the [1-160]permethylsorbitol. The preferential fragmentation from the "bottom" of the molecule in [6-14O]permethylsorbitol produces more intense unlabeled designate ions relative to their labeled counterpart. The designate ions and the extent of labeling results for each (calculated by eq 1) are summarized in Table II. The results are in contrast to those for the 1-18O compound, with the exception of the ions at m/z 45 and 47. However, these ions are produced by a number of processes, not only by the simple C-C cleavage shown in Figure 2.

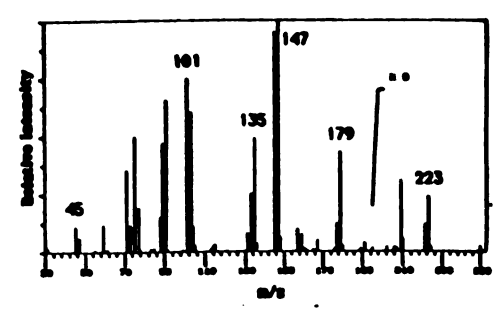


Figure 3. Low-energy (18 eV) electron lonization mass spectrum el [1-190]permethylsorbilist.

A similar trend is observed for the <sup>12</sup>C-labeled alditola. Shown in Figure 1d is the 70-eV EI mass spectrum of [1
<sup>12</sup>C]permethylsorbitol. Again, the location of the label can be confirmed based on the presence of labeled designate iona. Secondly, enrichment appears to exceed 100%, as shown in Table II, indicating further that, indeed, both ends of the molecule do not behave in a chemically identical manner.

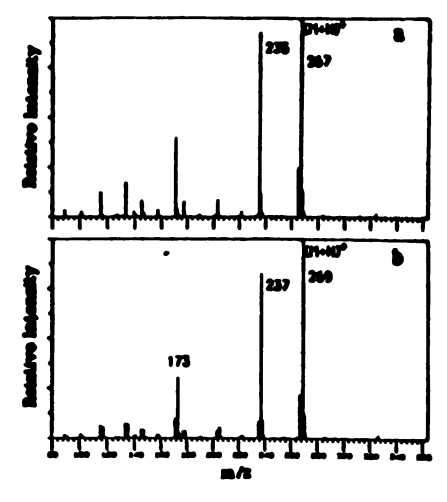
Table I suggests that the 70-eV mass spectra could be used to distinguish between a [1-14O]sorbitol and [2- or 3-14O]sorbitol, but not between the 1- and 6-labeled species. However, we have shown here that it is possible to differentiate each one, due to the asymmetry of the system. However, determinations of extent of label enrichment cannot be performed due to preferential dissociative ionization from the bottom of the molecule.

A truly accurate measure of the label enrichment using these designate ions is further complicated by the fact that their intensities (relative to the total ion current (TIC)) are so small. However, the ion statistics in these experiments should not be the source of such large errors, continually skewed in the same direction.

Another possible explanation for the observed behavior is that the mass spectral fragmentation mechanisms for these molecules are much more complex than those previously described. Extensive rearrangements may be occurring following 70-eV electron ionization and the fragment ions may have structures much different than what is suggested by the simple model in Figure 2. Thus, low-energy (18 eV) El was chosen as a possible solution to the problem. Frequently, at lower ionization energies there is less fragmentation and scrambling; also a larger fraction of the TIC may appear as higher mass ions, possibly improving ion statistics.

2. Low-Energy Electron Ionization. The 18-eV mass spectrum of [1-18O]permethylsorbitol is shown in Figure 3. As expected, the relative intensities of the high mass designate ions have increased in comparison to the 70-eV spectrum. There is a decrease in the abundance of the m/z 45 ion, which may be expected for a lower ionizing energy. The designate ion pairs observed in the 70-eV EI spectrum are present and the ratios of labeled-unlabeled species are essentially the same in the low and high energy spectra—i.e., the low energy spectra still lead to calculated extent-of-labeling values greater than 100%, which are not unlike the values obtained from the 70-eV spectra.

The extent of labeling determinations from the low-energy EI experiments for the [1-12C]- and [1-12O]- and [6-12O] permethylsorbitols are presented in Table II. Since they parallel the 70-eV EI results, this may suggest that scrambling is probably not the problem in the electron ionization spectra and may support the proposal in which dissociative ionization does not occur for the "top" and "bottom" of the molecule to the same extent.



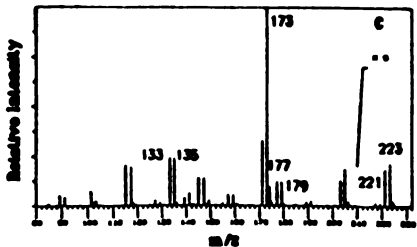


Figure 4. Methane chemical ionization mass spectra of (a) nonlabeled and (b) [1-10] permetry/sorbitol. (c) Magnification of the designate ion rection of the spectrum in 48

Since electron ionization did not yield meaningful extent of labeling information, a variety of chemical ionization experiments were performed. Proton transfer reagents should produce (M + H)\* ions that contain the intact sugar, thus the extent of labeling should be apparent.

3. Methane and Isobutane Chemical Ionization. Methane CI-MS has been used successfully for the analysis of a wide variety of biologically related compounds (12-14). It has been successfully used for extent-of-labeling studies. For polar compounds such as permethylated sugars, protonation and fragmentation are expected.

The methane CI mass spectrum of the nonlabeled permethylsorbitol is shown in Figure 4a. The base peak is the protonated molecule (M + H)+ at m/z 287. The loss of methanol following protonation is a prominent process leading to the (M + H - CH,OH) ion at m/z 235. These intense high mass ions should be useful for determining the extent of label incorporation. The methane CI mass spectrum of [1-180]permethylsorbitol is shown in Figure 4b. SIM results of integrated peak intensities for the ions m/z 287 and 269 suggest low levels of enrichment, approximately 70%. Note that in Figure 4a, there is a peak at m/z 265, (M + H - H<sub>2</sub>)\*. This fragment ion is an isobaric interferent in the molecular ion region of the mass spectrum of the 1-14O-labeled compound. The ion at m/z 267 not only consists of the nonlabeled protonated parent but is also the labeled (M + H - H<sub>2</sub>)\*. It is not possible to deconvolute the information in this region of the spectrum for the labeled compound based on relative ion intensities in the nonlabeled spectrum since the ratio of the ions (M + H)\* and ((M + H - H<sub>2</sub>)\* is pressure dependent. Therefore, in the protonated molecular region of the spectrum of the labeled compound, two ions are present that yield three peaks (l, labeled; nl, nonlabeled): m/z 265, [M(nl) + H - H<sub>2</sub>]\*;

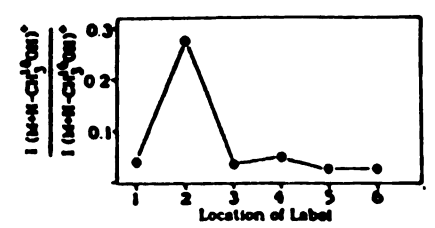


Figure 8. (M  $\pm$  H - CH<sub>2</sub>CH) $^{+}$  lone indicate that O2 is preferentially protonated.

m/z 267, [M(1) + H - H<sub>2</sub>]<sup>+</sup> + [M(m) + H]<sup>+</sup>; m/z 269, [M(1) + H)<sup>+</sup>.

Attempts to determine the extent of labeling by deconvoluting the intensities of these three ions involve the solution of a quadratic equation that has two roots. In Figure 4b the relative intensities for the three ions are I(265):I(267):I(267):I(267)=0.35:21.81:100. The extent of labeling that would yield these results could be 96.16% or 85.65%. Therefore, due to the (M + H - H<sub>2</sub>)\* interferent, this portion of the methane CI spectrum cannot be used for determining the extent of label incorporation. (The ion labeled (M + H - H<sub>2</sub>)\* may also be written as (M - H)\*, which could be formed directly in a hydride transfer reaction with the ethyl cation.)

The methane CI spectra of permethylated alditols also contain a number of fragment ions. The designate ions at m/z 133, 177, and 221 are present in these spectra. These are shown in more detail in Figure 4c. Here these ions are formed following protonation, not as the result of electron ionization. It is interesting to note that the ion pairs 133/135, 177/179, and 221/223 appear (for the 18O-labeled species) with ratios very close to unity, suggesting close to 100% label incornoration. Unfortunately, these ions are only minor CI products, and the ion statistics are insufficient to be relied upon for accurate determinations of extent of labeling, although SIM data on these ion pairs suggests 90 ± 5% label incorporation. Apparently, on protonation, the asymmetry of the system in reduced and the simple assumptions in the El discussion are accurate (for these designate ions)-i.e., these results imply that the processes leading to these ions following protonation occur at sites on the bottom and the top of the molecule to the same extent (or, that decomposition processes are simply less complex in CI than in EI).

Since proton transfer from CH<sub>8</sub><sup>+</sup> to such molecules is an exothermic process in which fragmentation frequently follows, other CI reagents for which proton transfer would be less exothermic were investigated. Isobutane was chosen as the next CI reagent for study. The isobutane CI mass spectra of permethylated additols contain less fragment ions but contain both the (M + H)<sup>+</sup> and (M + H - H<sub>2</sub>)<sup>+</sup> ions—thus the same problems exist for isobutane CI as for methane CI in that region of the spectrum. It should also be noted that the sensitivity of isobutane CI appeared to be less than that for methane CI in the analysis of these compounds.

A third CI reagent with a higher proton affinity than methane and isobutene was next chosen, ammonia. However, before the results of ammonia CI are discussed, an interesting feature of the methane and isobutane CI experiments merits discussion. In addition to the (M + H)<sup>4</sup> and (M + H - H<sub>2</sub>)<sup>4</sup> ions formed, there is also loss of methanol following protonation of permethylsorbitol forming (M + H - CH<sub>2</sub>OH)<sup>4</sup>. Presumably methanol elimination occurs by inductive cleavage following protonation. The interior oxygens (positions 2-5) are attached to more highly branched carbons, which can more readily stablize the positive charge than positions 1 and 6. Thus, the interior oxygens may be expected to exhibit slightly more basic character and hence be protonated more exten-

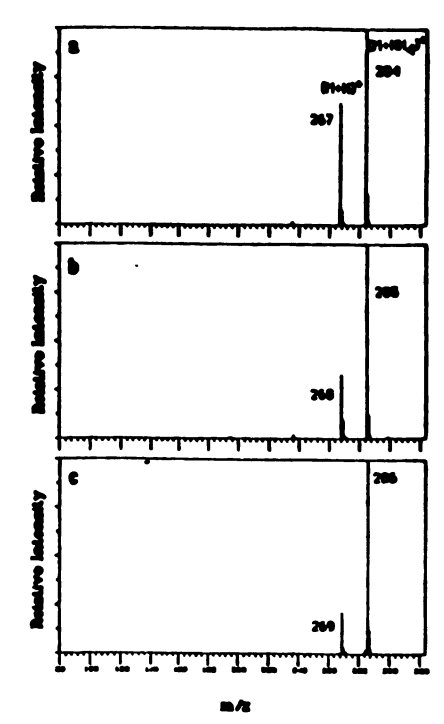


Figure 6. Ammonia chemical ionization mass spectra of (a) nonisbeled, (b) [1-10]-, and (c) [1-10] permethylaorbitol.

sively than the terminal ether oxygens. Our CI results for the [1- through 6-16O] permethylsorbitols suggest that the oxygen at the 2 position is preferentially protonated. This conclusion is based on the data presented in Figure 5. The [2-16O]-permethylsorbitol shows an enhanced loss of labeled methanol relative to the other 16O-labeled compounds. The isomer permethylmannitol behaves in a similar way. We are currently investigating possible explanations for this behavior.

4. Ammonia Chemical Ionization. A great deal of work has appeared in the literature in which ammonia CI-MS has been used for the analysis of both underivatized and (MegSi) derivatized sugars (15-19). The predominant ions formed are typically the adduct ions (M + H)\* and (M + NH,)\*. Since less energy is involved in the proton transfer from ammonia than from methane, less fragmentation is observed. Furthermore, ammonia CI has been used for determining the extent of label incorporation in studies of organic acids in type 1 diabetic patients (20).

The ammonia CI mass spectra of permethyl alditols show the expected  $(M + H)^*$  and  $(M + NH_s)^*$  ions as the predominant species. Figure 6 shows the ammonia CI mass spectra of nonlabeled,  $[1^{-n}C]_r$ , and  $[1^{-12}C]_permethylsorbitol.$  Note that, in the nonlabeled compound, there is no  $(M + H - H_s)^*$  interferent, only the protonated molecule at m/z 267 and the ammonium adduct at m/z 284. Since the spectra are simple and the sugar molecules remain intact, the determination of the extent of labeling is straightforward. An analysis of the data in Figure 6, parts b and c, reveal that the percent label enrichment is  $97 \pm 1\%$  for both molecules, confirming the assumption made at the beginning of the text that these permethyl alditols were essentially 100% labeled from the new synthetic route that was used to make them. The extent of labeling determined from the  $(M + H)^*$  and  $(M + NH_s)^*$  peaks is the same.

Therefore, ammonia CI is the method of choice for determining the extent of labeling of compounds of this type. It is important to note that the problems associated with using El for determining isotopic enrichment were obvious since essentially pure labeled compounds were used. However, M this were a metabolism study in which the extent of label enrichment was small (typically <20%), the EI results would have suggested an extent of labeling that was too high, and it would be difficult to realize that this value was incorrect. Therefore, El data of labeled compounds must be interpreted with great care in such quantitative determinations.

# CONCLUSIONS

The above discussion focused on the mass spectrometric behavior of labeled permethylsorbitola. Electron ionization was a useful tool for structure determination; however, the rates of dissociative ionization from both ends of the molecule appear to be different, which leads to difficulties in determining the extent of label incorporation based on simple assumptions.

Both El and NH<sub>2</sub> Cl have been used for similar analyses of permethylribitol, arabinitiol, erythritol, and mannitol. Ammonia CI confirmed that the label incorporation exceeded 97% for all of these synthesized sugars.

Again, it must be emphasized that great care must be exercised in using El mass spectral data for extent-of-label incorporation calculations on molecules such as these. Depending on the position of the label, results could consistently be high or low due the unique chemical environments at the two ends of acyclic sugars.

Ammonia CI is a useful method for label-enrichment determinations since >95% of the total ion current is carried in the protonated molecule and the ammonium adduct. However, CI alone is insufficient to determine the position of the label. While ammonia CI was useful for such studies of 12C- and 18O-labeled compounds, this may not be true for deuterated sugars, since H/D scrambling between the analyte and CI reagent may occur.

# ACKNOWLEDGMENT

The authors wish to thank Brian Musselman for helpful discussions, and R. Clark, Jr., for making available the labeled compounds.

Registry Ne. <sup>10</sup>O, 14797-71-8; <sup>10</sup>C, 14762-74-4; permethylsorbitol, 20746-36-6; [1-<sup>10</sup>O]permethylsorbitol, 101860-67-7; [6-<sup>10</sup>O]permethylsorbitol, 101977-08-4; [1-<sup>10</sup>C]permethylsorbitol, 101916-21-4

# LITERATURE CITED

- Frinyson, P. J.; Christophy, R. K.; Duffield, A. M. Blomed. Mace Spectrom. 1988, 7, 486.
   Robrecom, J. R.; Sarsel, A. M.; Schlahefie, E. E. Blomed. Mace Spectrom. 1978, 8, 646.
   Robret, J. J.; Seculer, B.; Kozlel, J. Dibette 1966, 54, 67.
   Cambert, P.; Lakmard, C.; Archambad, A. J. Chromatoy. 1978,
- Carnost, P.; Laternari, G.; Archemball, A. J. Gromatogr. W78, 162. 1.
   Lincherg, C.; Johnsson, B.; Hedner, P.; Christifiasson, A. Clin. Chem. (Wriston: Salaes, N.C.) 1982, 39, 174.
   Wilson, D. M.; Burlingama, A. L.; Crotholm, T.; Sjovel, J. Blochem. Biophys. Rev. Commun. 1974, 59, 828.
   Goovidna, L. B.; Yufbon, N. B.; Chichor, O. B. Zh. Gry. Rhim. 1986, 428.

- 4. 737.

- 4, 737.
  (8) Caprioll, R. M.; Ritarberg, D. Blochemistry 1969, 8, 2376.
  (9) Caprioll, R. M.; Selflert, W. E., Jr. Blochtm. Blophys. Acts 1973, 297, 213.
  (10) Clark, E., Jr.; Ph.D. Theels, Michigan State University, 1965.
  (11) Weinhouse, S.; Medes, G.; Floyd, N. F. J. Blot. Chem. 1946, 1965,
- (12) Wison, M. S.; Dzidle, I.; McCloskey, J. A. Blochim. Biophys. Acts

- Whon, M. S.; Dade, I.; McCloskey, J. A. Blochim. Biophys. Acta 1971, 240, 823.
   Mursta, T.; Taluhashi, S.; Takeda, T. Anal. Chem. 1978, 47, 573.
   Hooghion, E.; Tesla, P.; Dumasla, M. C.; Welby, J. K. Blomed. Mass Spectrom. 1982, 9, 489.
   Horton, D.; Wander, J. D. Carbortydr. Res. 1984, 36, 75.
   Hogg, A. M.; Naposhrushan, T. L. Telrahedron Lett. 1972, 47, 4827.
   Deubong, E. G.; Heerma, W.; Scherer, C. Blomed. Mass Spectrom. 1978, 9, 242.
   Dougherty, R. C.; Roberts, J. D. J. Org. Chem. 1974, 39, 461.
   Rossel, D. B.; Martin, M.; Schell, W.; Sweeley, C. C. Blomed. Mass Spectrom., in press.

RECEIVED for review December 4, 1985. Accepted February 14, 1986. This work was made possible through the financial support of the National Institutes of Health (NIH Grant No. RR00480-16).

# Urinary Metabolites of L-Threonine in Type 1 Diabetes Determined by Combined Gas Chromatography/Chemical Ionization Mass Spectrometry

D. B. Kassel

Department of Chemistry, Michigan State University, East Lansing, Michigan 48824-1319, USA

M. Martin

Department of Biochemistry, Michigan State University, East Lansing, Michigan 48824-1319, USA

W. Schall

Department of Veterinary Medicine, Michigan State University, East Lansing, Michigan 48224-1319, USA

C. C. Sweeleyt

Department of Biochemistry, Michigan State University, East Lansing, Michigan 48824-1319, USA

Metabolic profiling of urinary organic acids from patients with juvenile-onset (Type 1) diabetes mellitus have revealed significantly elevated levels of 2-hydroxybutyric and 4-deoxythreonic acids. To test the hypothesis that these metabolites, as well as 4-deoxyerythronic acid, are derived from L-threonine, stable isotope-labeled threonine was infused into an insulin-deficient dog and the incorporation of <sup>13</sup>C into these metabolites was monitored by gas chromatography/mass spectrometry. Electron louization was relatively insensitive, but positive chemical ionization with ammonia as the reactant gas gave both protonated molecules and [M+NH<sub>d</sub>]\* ions, which could be analysed by selected ion monitoring. The isotope-labeled species of 2-hydroxybutyric, 4-deoxyerythronic and 4-deoxythreonic acids were observed, but <sup>13</sup>C was not incorporated into other organic acids. Thus, it is proposed that L-threonine is a precursor of these metaboliten.

# INTRODUCTION

Juvenile-onset (Type 1) diabetes mellitus is caused by the persistent deficiency of insulin, accompanied by a large excess of glucagon. Several metabolic disorders are associated with the disease, including increased hepatic gluconeogenesis, elevated levels of blood and urinary glucose, and excessive mobilization of free fatty acids (derived frm adipose triglycerides) with a concomitant susceptibility to ketoacidosis. Electrolytic imbalances frequently accompany the ketoacidotic state.<sup>1-3</sup>

One method for exploring the metabolic status of an individual is to monitor acidic metabolites of urine. This is the basis of 'metabolic profiling' and numerous papers have been published in which combined gas chromatography/mass spectrometry (GC/MS) is used to identify and quantitate the urinary organic acids.

Diabetics who are under poor insulin control may have increased levels of urinary 3-hydroxybutyric acid, derived from increased oxidation of free fatty acids. Lactic acid is also increased in the urine under some circumstances. We have monitored approximately 200 organic acids of morning-fasting urine specimens of 20 patients with Type 1 diabetes and of 17 age-matched control subjects by computer-assisted GC/MS. Of particular interest was the finding that the diabetic patients excreted consistently higher amounts of 2-hydroxy-butyric acid (than age-matched controls) as well as

† Author to whom correspondence should be addressed.

enhanced levels of 4-deoxythreonic acid and several other metabolites. The levels of urinary 3-hydroxybutyric and lactic acids were elevated in some but not all patients.

The metabolic origins of 4-deoxythreonic, 4-deoxyerythronic and 2-hydroxybutyric acids have not been previously studied. It has been reported, however, that 2-hydroxybutyrate may be found in urine when there is a large excess of excreted lactic acid, a consequence perhaps of an elevated NADH/NAD\* ratio.\*

It can be postulated that 2-hydroxybutyric acid may be derived from threonine by threonine dehydratase (Scheme 1). The four-carbon metabolites, 4-deoxyerythronic and 4-deoxythreonic acids, may also be postulated to be products of threonine reactions involving both threonine deaminase and reductase (Scheme 1). The ramifications of this dependency would be significant, if true, since these metabolites might then be important measures of protein catabolism in skeletal muscle and other insulin target cells, when deprived of glucose. To test this hypothesis, we have determined the stable isotopic abundance of 2-hydroxybutyric, 4deoxyerythronic, 4-deoxythreonic and other organic acids following the intravenous administration of [U-<sup>13</sup>C]-threonine to an insulin-deficient dog with clinical symptoms similar to human Type 1 diabetes.

# **Experimental**

Reagents. Highly enriched [U-13C]-threonine (>99% labeled species) was provided by the Los Alamos Stable

Received 4 October 1985 Accepted 10 March 1986

0887-6134/86/100535-06 \$05.00 © 1986 by John Wiley & Sons Lad

Scheme 1

Isotope Resource, bis(trimethylsilyl)-trifluoroacetamide (BSTFA) was purchased from Regis Chemical Co., and trifluoroacetic anhydride was purchased from Supelco, Inc. HPLC-grade n-butanol was utilized for derivatization.

Equipment. A HP-5985 quadrupole gas chromatograph/mass spectrometer was operated in both the positive and negative chemical ionization (CI) modes. A modification of the instrument was made for fused-silica capillary GC experiments with a 60-m DB-1 wide-bore capillary column, purchased from J&W Sci., Inc.

GC conditions. All injections were made on-column. The oven was temperature-programmed from 55 °C to 300 °C at a rate of 5 °C min<sup>-1</sup>. Carrier gas was helium (flow rate = 2.5 ml min<sup>-1</sup>). An open-split interface consisting of deactivated, non-vitreous capillary tubing (purchased from S.G.E.) was maintained at 280 °C, and the split was determined to be approximately 3:1.

MS conditions. CI was employed for the analysis of urinary organic acids, using ammonia as the reactant gas in the positive ion chemical ionization (PICI) mode. Source pressure was held constant at 0.3-0.4 Torr to ensure maximum sensitivity. Source temperature was maintained at 150 °C for all analyses. Filament electron energy was set at 175 eV. PICI and negative ion chemical ionization (NICI) experiments were performed on the plasma amino acid samples. Methane was used as the reactant gas (pressure = 190 mTorr) in the NICI analyses. Source temperature was held constant at 135 °C. Filament electron energy was maintained at 150 eV. Selected ion monitoring (SIM) experiments were simultaneously performed on the protonated molecule and molecular adduct ion species.

Infusion of labeled threoalne. Hyperglycemia was induced in the diabetic dog by hypoinsulinization one day prior to infusion of labeled threonine. Just prior to infusion of the [\frac{13C\_4}-threonine, insulin was administered to the dog in order to restore normal blood glucose levels. A control urine was collected at this time. Infusion occurred over a period of 20 min. Due to the rapid delivery of [\frac{13C\_4}-threonine into the animal, urine specimens were collected hourly at times just following infusion. After 5 h collections were made at longer intervals for the remainder of the 48-h collection period. A

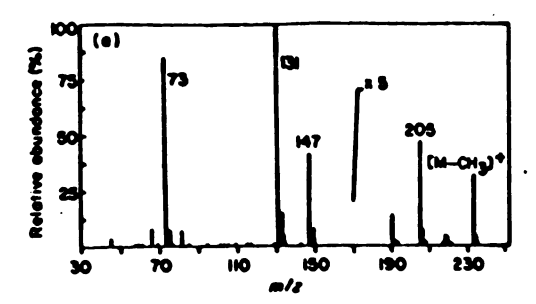
blood sample was drawn just after completion of the infusion.

Formation of derivatives. Organic acids were isolated from urine specimens as described in an earlier paper by Sweeley and Gates. Trimethylsilyl (TMS) derivatives of the organic acids were made by reaction with BSTFA in pyridine (4:1) at 80 °C for 1 h. The resultant mixture of derivatized organic acids was sealed in capillary tubes and stored in a refrigerator until introduction into the gas chromatographic/mass spectrometric system. Plasma samples were deproteinized and the amino acids were derivatized following the procedures outlined by Kingston and Duffield. Amino acids in a protein-free filtrate of plasma were separated from neutral substances on a Dowex ion-exchange column. The N-trifluoroacetyl-n-butyl esters were then formed and the resultant derivatives were sealed into capillary tubes.

# **RESULTS**

# Organic acids in urine

Attempts were made to determine 13C isotopic abundance in the organic acids of interest by conventional electron impact mass spectrometry (EIMS) of the TMS derivatives. To obtain accurate determinations of enrichment, it was necessary to have relatively abundant molecular ions or high-molecular-weight fragment ions. The predominant ions observed in the analyses of the derivatized organic acids by EIMS were related to the fragmentation of the TMS derivative and provided no information about the relative enrichment of 13C in the species being analysed (see Fig. 1(a)). Furthermore, in general, very little or no molecular weight information was available from the EI mass spectra of these organic acids. In addition, the results of the analyses by EIMS showed significant variations from one run to the next, due to the low intensities of the high-mass ions monitored. To overcome the problems associated with EIMS, alternative ionization methods were employed for determining 13C enrichment in urinary organic acids. Ammonia CI has previously been successfully used to determine the isotopic enrichment of 18O and 13C in labeled permethylated sugars,12 since only molecular ions were observed in the mass spectrum. Similarly,



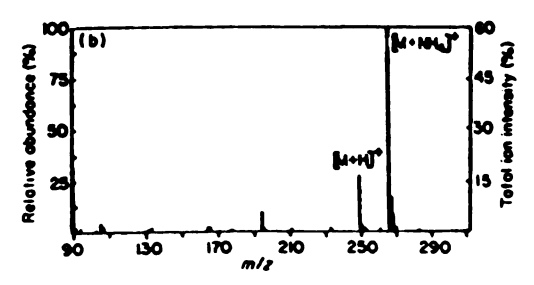


Figure 1. (a) Et mass spectrum of 2-hydroxybutyric acid di-TMS from a urine specimen collected at the 2nd h after onset of labeled-threonine infusion.(b) Ammonia CI mass spectrum of 2-hydroxybutyric acid (di-TMS) from the same urine specimen. Source pressure = 300 mTorr.

organic acids produce intense molecular ions by ammonia CI. It was concluded that this ionization method would be suitable for the enrichment studies.

The ammonia CI mass spectrum of the bis(trimethylsily) derivative of 2-hydroxybutyric acid is shown in Fig. 1(b). Molecular weight information is apparent in the form of the protonated molecule and molecular adduct ion species. The [M+NH<sub>a</sub>]\* ion comprised approximately 60% of the total ion intensity (TII), and was ideal for the <sup>13</sup>C isotope enrichment studies. Enhancement of the (A+4) peaks, at m/z 253 and 270, was observed for both the [M+H]\* and [M+NH<sub>a</sub>]\* ions, respectively.

SIM was performed on both molecular species and their isotope-labeled species (+4 u) from 2-hydroxybutyric acid in order to obtain the best ion statistics. Similar experiments were performed for 4-deoxythreonic, 3-hydroxybutyric and 4-deoxyerythronic acids. The ions chosen for the analyses are summarized in Table 1. All ions were monitored simultaneously, and the most abundant ion [M + NH<sub>4</sub>]\* was given the shortest dwell time (100 ms). In performing the SIM analyses,

Table 1. Molecular adduct ion and protonated molecules of 2and 3-hydroxybutyric, 4-deoxyerythronic and 4deoxythreonic acids for SIM using ammonia CIMS

it was noted that urinary 3-hydroxybutyric acid could

Organic sold	lon(s) monitored	
2-Hydroxybutyric	249, 263, 266, 270	
3-Hydroxybutyric	249, 253, 266, 270	
4-Deoxyerythronic	337, 341, 364, <b>368</b>	
4-Deoxythreonic	337, 341, 364, 368	

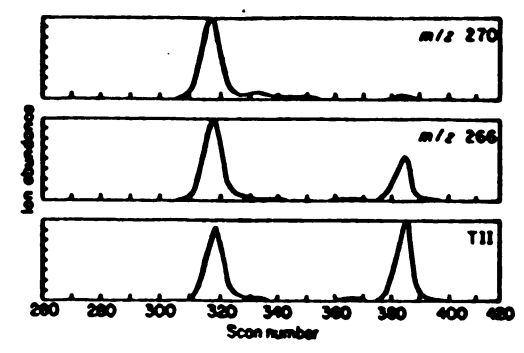


Figure 2. The use of STM under ammonia CI conditions to detect low levels of <sup>15</sup>C enrichment in 2-hydroxybutyric adic (di-TMS) and 3-hydroxybutyric acid (di-TMS); the peaks at scan 318 are from 2-hydroxybutyric and those at scan 355 are from 3-hydroxybutyric and

be used as an internal reference (or check) for the  $^{13}$ C isotopic enrichment in 2-hydroxybutyric acid observed in urine samples collected following [U- $^{13}$ C]-threonine administration. Conveniently, since the two acids are isomers and eluted from the GC column within a narrow retention time span, the same four ions were monitored in the same gas chromatographic run. The small ion intensity observed in the (A+4) peaks of 3-hydroxy-butyric acid (at m/z 253 and 270) was due solely to naturally occurring isotopic contributions, primarily due to silicon (Si) isotopes (i.e. no  $^{13}$ C enrichment was observed). This [A+4] $^{+}$  ion intensity was used to correct for 'background' isotopic content of 2-hydroxybutyric acid. True label enrichment for 2-hydroxybutyric acid was thus obtained, and provided accurate results since run-to-run variations were assumed to be the same for both acids.

The SIM results for the ion pair at m/z 266 and 270 for 2- and 3-hydroxybutyric acids are shown in Fig. 2. An enrichment of <sup>ID</sup>C for 2-hydroxybutyric acid was clearly observed, relative to that of 3-hydroxybutyric acid. For 4-deoxythreonic and 4-deoxyerythronic acids, no internal reference was available; hence, isotopic enrichment was obtained by subtraction of a control urine mixture (collected just prior to labeled-threonine infusion).

SIM analyses were performed on the control urine and the samples that were collected serially for 48 h following the onset of infusion. Figure 3 shows the per cent of labeled species observed for 2-hydroxybutyric, 4-deoxyerythronic and 4-deoxythreonic acids, as a function of urine collection time (after corrections were made for the naturally occurring isotopic contributions, as described earlier). For 2-hydroxybutyric and 4-deoxyerythronic acids, maximum 13C incorporation from threonine occurred between the 2nd and 6th h following infusion. The peak maximum for 4-deoxythreonic acid was observed at later times, following infusion (between the 6th and 10th h). However, it was determined that when the per cent labeled species of 4-deoxythreonic acid was normalized for the different pool sizes (from the urine specimens collected serially), a shift in the 4-deoxythreonic curve resulted, so that it was coincident with both the 2-hydroxybutyric and 4deoxyerythronic acid curves.

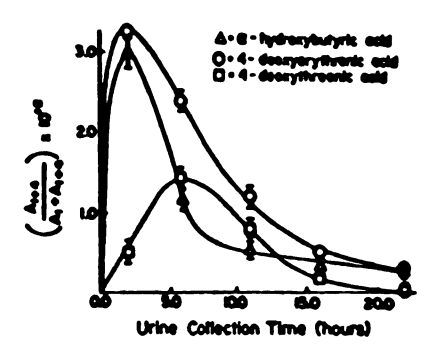


Figure 3. Extent of label enrichment of 2-hydroxybutyric (di-TMS), 4-deoxyerythronic and 4-deoxythreonic acids (tri-TMS) determined over a 24-h collection period using ammonia CIMS; ammonia wee maintained at constant pressure (P = 325 mTorr) for all experiments.

Label enrichment was observed to be 2.83 ± 0.41% at the peak maximum for 2-hydroxybutyrate. For 4-deoxythreonic acid, maximum <sup>13</sup>C enrichment was 1.1± 0.15%. Interestingly, maximum 13C enrichment observed for 4-deoxyerythronic acid was 3.25 ± 0.40%. Runs showed excellent reproducibility over a wide range of source pressures, with standard deviations frequently calculated to be as small as ±0.085% No 13C enrichment was observed for any of the other organic acids. Figure 4 is the reconstructed TII plot of the organic acids found in the urine sample collected just following infusion. Peaks labeled 1-23 are identified, and per cent label enrichment for the acids, prior to and just following (U-13C)threonine infusion, are summarized in Table 2. Ion intensity was observed for most organic acids at the [A+4]\* peaks. However, this intensity was not due to <sup>13</sup>C enrichment, but resulted, for the most part, from the natural isotopic contribution of silicon, from the TMS derivatives of the organic acids. As expected, 13C enrichment was observed only for 2-hydroxybutyric, 4-deoxyerythronic and 4-deoxythreonic acids.

# Threonine in plasma

The somewhat low enrichment of <sup>13</sup>C observed for the urinary organic acids led us to suspect that the per cent of labeled threonine in plasma might have been some-

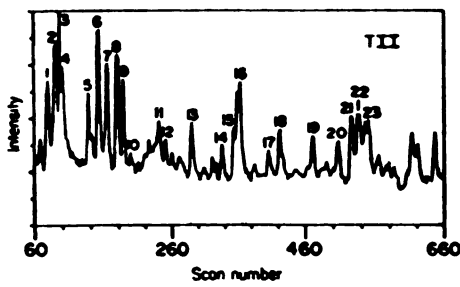


Figure 4. Reconstructed TII plot of organic acids excreted in the diabetic dog urine collected between the 2nd and 6th h following (U-13C)-threonine infusion. Ammonie CI reagent gas pressure = 300 mTorr.

Table 2. <sup>12</sup>C earichment measurements for the major organic metabolites of the diabetic dog urino, collected prior to and following influsion

		N+4, pre prompts		
Produ	Organia sald	Control 1	Une 4	
1	Unknown	0.10	0.14	
2	2-Hydroxypropensis	0.00	0.00	
3	2-Hydroxyleobutyrle	0.14	0.10	
4	Glycolie	0.0	44	
8	Oxalic	0.24	1.25	
•	2-Hydroxybutyrie	9.40	1.25	
7	2-Aminobutyris	0.26	0.24	
	3-Hydroxybutyris	0.40	0.40	
•	Pyruvic oxime		4.0	
10	Diabetic 11	44	0.0	
11	Methyl malonic	0.22	0.20	
12	2-Ketobutyric oxime	0.0	M	
13	2-Methyl-3-hydroxybutyrle	0.10	0.11	
14	Glyceric	0.08	0.11	
15	4-Deoxyerythronic	0.00	3.85	
16	4-Deoxythreonic	0.70	2.36	
17	3-Deoxytetronic	0.46	0.50	
18	2-Deoxytetronic	0.48	0.41	
19	Adipie	0.0	0.0	
20	Unknown (mol. wt = 329)	0.60	0.82	
21	Erythronic	0.86	0.90	
22	Threonic	0.90	0.96	
23	Tropic (internal standard)	0.20	0.17	

what lower than originally anticipated. Analyses of the isotopic enrichment of <sup>13</sup>C-labeled species of threonine in plasma were therefore carried out on the *N*-trifluoracetyl-n-butyl esters of the plasma amino acids. Literature El mass spectra of these derivatives showed that relatively little molecular weight information is available by this method.<sup>13</sup>

Since the derivative is strongly electrophilic, it seemed reasonable that CI would yield molecular-type ions by electron capture NICI mass spectrometry EC/NICI/MS. EC/NICI/MS has been found to produce abundant molecular ions through the capture of near-thermal-energy electrons. 14 The NICI mass spectrum in the molecular ion region for the threonine derivative is shown in Fig. 5. The predominant ion in the

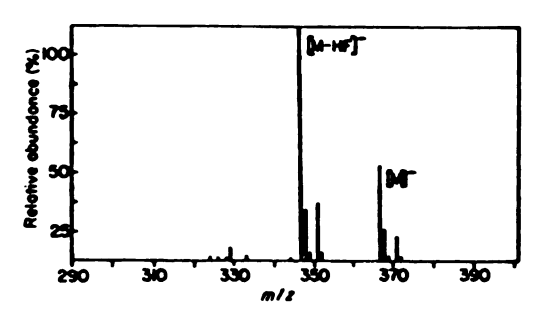


Figure 8. EC/NICI/MS of the molecular ion region of the Ntrifluoroacetyl-n-butyl ester of threonine from a plasma specimen collected just following infusion of labeled threonine into the dog (reactant gas, methane; pressure, 190 mTorr).

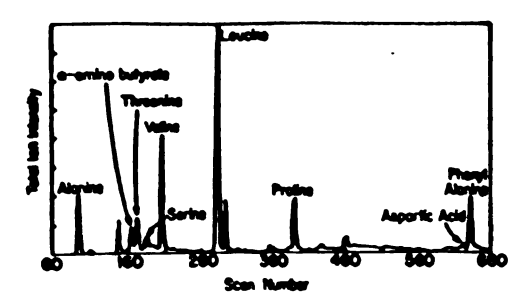


Figure & Reconstructed TII plot of the major emino acids found in the diabetic dog plasma, by ammonie CIMS; pressure = 300 mTerr.

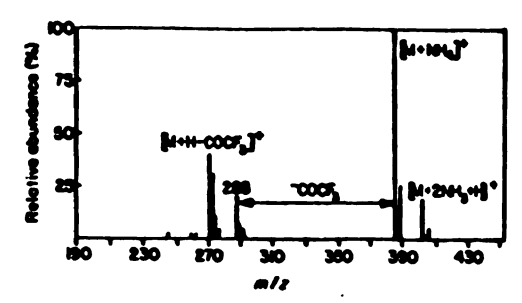


Figure 7. Ammonie CI mass spectrum of the N-trifluoroacetyl-abutyl aster of threonine.

spectrum resulted from protonation of the threonine molecule, followed by elimination of HF. Very little fragmentation was observed for the amino acid. Ion pairs used for determining the <sup>13</sup>C enrichment of the plasma threonine pool were the [M]<sup>-</sup> and [M-HF]<sup>-</sup> species, occurring at m/z 367 and 371 and at m/z 347 and 351, respectively. Another adduct ion, at m/z 480, corresponding to [M+CO<sub>2</sub>CF<sub>3</sub>]<sup>-</sup>, also showed a labeled species at m/z 484. SIM analyses were performed on all three sets of ions; the plasma threonine pool contained 25.0±0.5% of the <sup>13</sup>C<sub>4</sub>-labeled species (average enrichment in the three ions).

To confirm the results obtained by EC/NICI/MS, the plasma amino acids were also analysed by ammonia CI. The reconstructed mass chromatogram for the major amino acids found in the dog plasma is shown in Fig. 6. Ammonia CI on the amino acids produced atypicallooking mass spectra. Due to the low proton affinities of the derivatized amino acids with respect to the ammonia reactant ions, no protonated molecules were observed. For threonine, the two ions dominating the mass spectrum were the molecular adduct ions, in which one and two ammonium ions were electrophically attached to the molecular species (Fig. 7). These ions, and their isotopes at +4 u, were monitored by SIM. The results of the ammonia CI experiments on threonine were in agreement with the results obtained by EC/NICI/MS. The amount of labeled threonine in plasma was determined to be 24.6 ± 2.3%.

# DISCUSSION

There are several reports concerning the excretion of 2-hydroxybutyric acid in the urine. In addition to those conditions where large amounts of lactic acid are excreted, 2-hydroxybutyric acid has been associated with a rare methionine malabsorption syndrome called Oasthouse disease and has been induced in a 65-year-old man by 3 days of total fasting (C. C. Sweeley and S. Fajans, unpublished results).

The excretion of 4-deoxythreonic and 4-deoxyerythreonic acids has not previously been ascribed to any particular disorder. An obvious approach to determine whether these metabolites are products of threonine metabolism would involve the use of a stable isotope tracer experiment in a Type 1 diabetic patient. However, due to the pool size of threonine in humans, the amount of labeled threonine needed for verification would far surpass the economic feasibility of such an experiment, and analysis of low levels of enrichment might be difficult. Fortunately, we found that 4-deoxythreonic, 4-deoxythronic and 2-hydroxybutyric acids are excreted by Golden Retriever dogs. In normal dogs, their levels are low, but evidence suggests that the levels of these metabolite are significantly elevated in urine of dogs with a disease that is clinically indistinguishable from human Type 1 diabetes. 16

As a result, we were able to introduce [13C4]-threonine in vivo and monitor the stable iosotpic enrichment of the three organic acids, and others. Since it was postulated that threonine derived from skeletal muscle protein might be the primary source of these metabolites, promotion of protein anabolism was made during the onset of infusion, subjecting the dog to deliberate blood glucose elevation by hypoinsulinization for 24 h directly prior to the experiment. Insulin injections were made immediately prior to the threonine infusion, so that blood glucose levels could be restored to normal, and protein anabolism would parallel the time period of maximum levels of labeled threonine in the plasma. Finally, it was hoped that insulin deprivation after the infusion might induce protein catabolism and the excretion of labeled metabolites from threonine.

Our results indicated enrichment of <sup>13</sup>C in 2-hydroxybutyric, 4-deoxythreonic and 4-deoxyerythronic acids, but only in the initial few hours following infusion of the labeled threonine. Thus, it cannot be claimed that the threonine was derived from a protein pool, in which a peak of <sup>13</sup>C incorporation should have resulted at later times. However, the experimental evidence certainly supports our hypothesis about the origin of these metabolites. This is a significant finding, and suggests the need for further studies of the metabolism of threonine in Type 1 diabetic patients.

# Acknowledgements

This research was supported in part by Research Grant RR-00490 to the NIH/MSU Mass Spectrometry Facility. The authors are grateful to the Los Alamos Stable Isotope Laboratory for the gift of [12Ca]-threonine; support by NIH(RR-02231) is acknowledged.

# REFERENCES

- 1, A. I. Winigrad and R. S. Clements, Med. Clin. North Am. 55 860
- A. I. Winigrad and N. S. Clements, Med. Clin. North Am. 55 555 (1971).
   J. D. McGerry, and D. W. Foster, Metabolism 21, 471 (1972).
   T. D. R. Hockaday and K. G. M. N. Alberti, Clin. Educrinol. Metab. 1, 751 (1972).

- 1, 751 (1972).
  4. C. C. Sweeley and J. Vrbanac, Biomed. Mass Spectrom 8, 438, 8. S. C. Gates, and C. C. Sweeley, Anal. Chem. 80, 433 (1978).
  8. S. C. Jeffum, J. Chromatogr. 143, 427 (1977).
  7. P. K. Bondy and W. L. Bioom, J. Cin. Invest. 28, 1126 (1948).
  8. C. C. Sweeley, in 11th Meet. Jpn. Biomed. Mass Spectrom. Symp. 72 pp. (extended abstract). Hakone, Japan (1984).
  9. J. E. Petterson, and S. Landaas and L. Eldjarn, Clin. Chim. Aces. 48, 213 (1973).

- C. C. Sweeley and S. C. Gates, Clin. Chem. 24, 1674 (1978).
   E. E. Kingston and A. M. Duffield, Blomed. Mess Spectrum. 9(11), 459 (1982).
   D. B. Kassel and J. Allison, Anal Chem. (In press).
   K. R. Lierner, R. H. Rice and C. W. Gherta, J. Chrometogr. 141, 121 (1977).
   D. F. Hunt and F. W. Crow, Anal. Chem. 80, 1761 (1978).
   A. J. Smith and L. B. Strang, Arch. Dis. Child. 33, 109 (1988).
   M. D. Williams, R. Gregory, W. Schall, V. Gossain, R. Bull and G. Padgetti, Proc. Fed Am. Soc. Exp. Biol., 740 pp. (abstract) (1981) pp. 749.

# UTILITY OF ION SOURCE PRETREATMENT WITH CHLORINE-CONTAINING COMPOUNDS FOR ENHANCED PERFORMANCE IN GAS CHROMATOGRAPHY/NEGATIVE IONIZATION MASS SPECTROMETRY

Daniel B. Kassel, Kathleen A. Kayganich, J. Throck Watson<sup>1</sup>, and John Allison<sup>e</sup>

Department of Chemistry

Michigan State University

East Lansing, MI, 48824

<sup>&</sup>lt;sup>1</sup>Also Department of Biochemistry

# Abstract:

Dramatic variations in the electron capture negative ion (ECNI) mass spectra of several classes of compounds can occur if the ion source is exposed to CCI<sub>4</sub> prior to their analysis. This ion source pretreatment method results in enhancements in detectability for several compounds over that achieved by conventional ECNI analysis. Abundant pseudomolecular ions of the type [M+CI] are observed which are useful as molecular weight indicators for unknowns. The [M+CI] ions formed in the ECNI analysis following ion source pretreatment with CCI<sub>4</sub> are not a result of direct CI attachment in the gas phase, but are presumed to occur through surface reactions. Investigations into the "universality" of this method for enriching ECNI mass spectra are presented and possible mechanisms for [M+CI] ion formation are discussed.

This article describes an unconventional approach to effecting electron capture negative ionization (ECNI) mass spectrometry (MS) which has the potential for enhanced performance in the analysis of selected classes of compounds. For ECNI analysis, the analyte should have sufficiently high electrophilicity to capture near-thermal electrons and produce intense negative ion currents(1,2). The extent to which a molecule will produce an appreciable negative ion signal depends on its electron capture cross-section(3). Electron capture cross sections for different molecules vary by many orders of magnitude, in contrast to the cross-sections for positive ion formation by electron impact ionization (EI) which differ little(4,5), and as a result, extraordinary, but variable, detection limits often are realized among these compounds under conditions for negative ion formation.

Derivatization of an analyte may be performed to increase the cross section for electron capture. Highly fluorinated derivatives, such as pentalluorobenzyl (PFB) and trifluoroacetyl (TFA) derivatives are most useful for improving the response of a compound in ECNI-MS. Depending on the derivative chosen and the structure of the analyte, the types of negative ions formed may differ considerably. The PFB derivatives of most organic acids, for example, typically produce the carboxylate anion as the major negative ion(6). In contrast, TFA derivatives have been found to produce, in addition to molecular weight information (in the form of M\*, [M-H]\*, or [M-HF]\*), abundant fragment ions for several classes of compounds. Thus, the extent to which negative ion mass spectra can be used for providing molecular weight and structural information can vary significantly between compound classes and with the choice of derivative.

In contrast to the ECNI experiment in which a gas such as methane is introduced into the ion source to participate in the generation of thermal electrons for negative ion formation, there is the technique of negative chemical ionization (NCI)-MS in which the analyte is ionized by interaction with an anion(7,8). Methylene chloride NCI-MS(9,10), for example, has been shown to produce abundant molecular adduct ions, [M+CI]. However, few fragment ions are observed, limiting the utility of this method for analyses requiring structural information.

We report here an approach to negative ion MS which yields substantial benefits in the analysis of certain classes of dompounds. When conventional ECNI-MS is performed following pretreatment of the ion

source with a chlorine-containing species such as CH<sub>2</sub>Cl<sub>2</sub> or CCl<sub>4</sub>, substantial differences in the spectra of analytes are observed compared to those obtained with an untreated source. This method frequently yields an abundant [M+Cl] ion. Furthermore, and more importantly, structurally-significant ions such as those seen in ECNI are not lost at the expense of this [M+Cl] ion formation, which contrasts with NCl mass spectra in that fragment ions are typically not observed. In addition, substantial enhancements in the response to ECNI-MS is frequently observed for selected compound classes following this pretreatment procedure. Examples of analyses that were significantly improved by ion source pretreatment, and possible mechanisms for formation of the observed ions are presented here.

# **EXPERIMENTAL SECTION**

Pretreatment Procedure: CCL was introduced into the mass spectrometer source at a pressure of approximately 0.1 torr for 4-5 minutes. Methylene chloride and chloroform also were used successfully. During treatment, the electron filament need not be "on." The temperature of the ion source was maintained between 100° and 130°C.

MS Conditions: All experiments were performed on an HP 5985 GC/MS/DS which was modified for the detection of negative ions. The ion source temperature was maintained at 130°C. ECNI experiments were performed using methane at pressures on the order of 0.4-0.5 torr, as measured at the ion source using a Hastings gauge and a thermocouple gauge. A constant pressure of methane was maintained throughout the experiments using a Granville-Phillips 216 Pressure/Flow controller and servo driven valve assembly. Electron energies were 110 eV, with emission currents of 300µA. Tuning of the instrument in the negative ion mode was achieved using an equimolar mixture of perfluorotributylamine and CCl4.

GC Conditions: An HP-5 (cross-linked 5% phenyl methyl silicone) 30m megabore capitlary column (0.53mm i.d. x .88µm film thickness, Hewlett-Packard Co., Palo Alto, CA) was temperature programmed from 70-300°C at 15°C per minute for all analyses. Hellium flow rates were approximately 5 ml/min. A 40-cm piece of deactivated vitreous silica capitlary tubing, maintained at 285°C, was used as the GC/MS interface.

Derivatization Procedures: The N-trifluoroacetyl n-butyl ester (TAB) derivatives of amino acids were prepared following procedures outlined by Duffield et al.(11), in which trifluoroacetic anhydride (TFAA) and 1.25 N HCI in n-butanol were used. The trimethylsityl (TMS) derivatives of organic acids were prepared following the procedures of Sweeley et al.(12) Pentafluorobenzyl (PFB) esters of organic acids and TFA derivatives of alcohols were prepared according to procedures described in the 1986-87 Pierce Handbook and General Catalog (p. 198-201).

Reagents: Common reagents, such as organic acid, fatty acid, and amino acid standards were obtained from either Nutritional Biochemical Corporation, Cleveland, OH or Sigma Chemical Company, St. Louis, MO. Carbon tetrachloride was purchased from the Aldrich Chemical Company, Milwaukee, WI. Ultra high purity methane was purchased from Matheson Gas Products, Chicago, IL. The derivatizing reagents, trifluoroacetic anhydride and N,O-bis(trimethylsilyl)trifluoroacetamide (BSTFA) were obtained from the Pierce Chemical Company, Rocklord, IL and Regis Chemical Company, Morton Grove, IL, respectively.

# **RESULTS AND DISCUSSION**

The effects of source pretreatment with CCI<sub>4</sub> were discovered after investigating the utility of a PFTBA/CCI<sub>4</sub> calibrant for the production of high- and low-mass negative ions (e.g., m/z 633 from PFTBA and m/z 35 from CCI<sub>4</sub>). Results from a number of analyses by conventional ECNI-MS following exposure of the ion source to CCI<sub>4</sub> were quite surprising. Mass spectra of the trifluoroacetyl-n-butyl ester (TAB) of aspartic acid obtained under ECNI (CH<sub>4</sub>) conditions, without and with CCI<sub>4</sub> source pretreatment, are shown in Figures 1a and 1b, respectively. The only difference in the two analyses was that the ion source had been exposed to CCI<sub>4</sub> prior to obtaining the spectrum in Figure 1b. The negative ion mass spectrum in Figure 1a shows an [M-H]\* peak at m/z 340 of relatively low intensity, comprising less than 4.0% of the total ion current (TIC = 8500 counts). Several other fragment ion peaks are observed. The base peak in the mass spectrum represents the [M-NH<sub>2</sub>COCF<sub>3</sub>]\* ion at m/z 228.

The mass spectrum in Figure 1b was obtained from the same quantity of aspartic acid-TAB as was used for Figure 1a; it shows some strikingly different features. The base peak in the mass spectrum is no longer at m/z 228, but at m/z 376 which represents the [M+CI] ion. This ion proves useful as a molecular weight

indicator, with the incorporation of chlorine being apparent due to the distinct isotopic peak intensity pattern. A significant increase in TiC (to 80,000 counts from 18,200 counts) is observed upon going from Figure 1a to 1b. There is an approximate 5-fold increase in the integrated area of the TiC for aspartic-TAB following a brief exposure of the source to CCl<sub>4</sub>. In Figure 1a, the ion which is most representative of the intact compound is the [M-H] ion, while in Figure 1b, it is the [M+Ci] ion. Selected ion monitoring (SiM) of these two pseudomolecular ions shows an enhancement in detectability by a factor of 40 after pretreatment of the source. Also note that the fragment ions and their relative abundances, observed in Figure 1a, are essentially unchanged in Figure 1b. Modest changes in peak intensity ratios may be attributed to small fluctuations in source pressure from one run to the next. Note also that absolute fragment ion abundances following CCl<sub>4</sub> pretreatment increase 1-5 fold over those from conventional ECNI. The results are summarized in Table I.

Another unique feature of the spectrum in Figure 1b is that only a very small Cl peak is observed. In fact, if the ion source is briefly exposed to CCl<sub>4</sub>, and then allowed to stand free of further exposure for one hour, the ECNI-MS analysis of aspartic-TAB still shows a very intense [M+Cl] peak. These results are also summarized in Table 1. After this one-hour period, only minor amounts of Cl are observed, comprising approximately 0.1% of the TIC, yet the [M+Cl] is still the most intense peak in the mass spectrum. In direct Cl negative ionization (NCl), the base peak always results from Cl (at m/z 35). In addition, depletion in the Cl ion abundance is observed as the analyte elutes from the GC column, indicating that the Cl ions in the gas phase are directly involved in the formation of the [M+Cl] ion during NCl. In the data observed after CCl<sub>4</sub> pretreatment, no depletion in the Cl ion abundance is observed as the analyte elutes from the GC column.

The results above suggest that the [M+CI] ion and the other ions observed after source pretreatment (Figure 1b) are not formed by direct CI attachment(10,13). To investigate this further, the reagent gas was changed from methane to CCI4, creating conditions for NCI with CI as the chemical ionization reagent ion. The NCI mass spectrum of aspartic-TAB is shown in Figure 1c. There are obvious differences between the spectra in Figures 1b and 1c. In the latter spectrum, no fragment ions are observed. Low-mass ions such as CI2 and CCI3 are primary products of electron attachment to CCI4. In the CI-NCI analysis, SIM shows that CI ions are consumed as the derivatized amino acid elutes from the column. This observation is in contrast to that

described above for the experiment following source pretreatment; thus, formation of [M+CI] following source pretreatment apparently does not involve ion/molecule interactions in the gas phase.

It was of interest to determine whether the unusual features observed in the CCI<sub>4</sub>-source pretreatment ECNI mass spectra of aspartic acid-TAB would also be observed for other compounds. The trifluoroacetyl derivative of myristyl alcohol, CH<sub>3</sub>(CH<sub>2</sub>)<sub>12</sub>CH<sub>2</sub>OCOCF<sub>3</sub>, was analyzed by both conventional ECNI-MS and ECNI-MS following CCI<sub>4</sub>-pretreatment of the ion source. Although the TFA group imparts some electrophilic character to the compound, it does not significantly increase the cross section for electron attachment to produce a signal that is easily discernible from background under conventional ECNI conditions. In fact, the only peak observed well above background was for the OCOCF<sub>3</sub> ion at m/z 113. This behavior is not unique; frequently, negative ion mass spectra provide no molecular weight or structural information, producing only ions indicative of the derivatizing agent. When this compound is analyzed following the CCI<sub>4</sub>-pretreatment procedure, a substantial response is observed. The [M+CI] ion is represented by the base peak in the mass spectrum, Figure 2, and fragment ions are still present. Thus, for some compounds that respond poorly in ECNI-MS analyses, CCI<sub>4</sub>-pretreatment of the source may lead to lower detection limits, and at least provide molecular weight information for unknowns.

Pretreatment of the ion source with CCI<sub>4</sub> does not <u>always</u> affect the response of a compound in ECNI-MS. Figure 3 shows the negative ion mass spectrum of maleic acid (di-TMS ester) obtained following the CCI<sub>4</sub>-pretreatment method. In the conventional ECNI mass spectrum, the major peak represents the M<sup>+</sup> ion, comprising over 95% of the TIC. In the mass spectrum obtained following pretreatment, the same situation is observed. No [M+CI] ion is observed, prompting the question of why this compound is unaffected by the source pretreatment that can lead to such dramatic changes for other compounds. Maleic acid (di-TMS ester) differs from the compounds that show good response to the pretreatment method in that it shows an intense M<sup>+</sup> peak in its ECNI spectrum, while aspartic-TAB and the TFA derivative of myristyl alcohol do not. These latter compounds exhibit an [M-H] ion instead. This observation suggested a possible correlation between the stability of the molecule as an intact anion (under conventional ECNI conditions), and the lack of response to source pretreatment (i.e., the lack of a tendency to form [M+CI] in a CCI<sub>4</sub>-pretreated ion source).

The TAB derivative of the amino acid L-proline (L-Pro-TAB) is interesting in that, under conventional ECNI conditions, the compound forms both M° and [M-H] lons. Figures 4a and 4b show the ECNI mass spectra of L-Pro-TAB under conventional conditions and following CCl<sub>4</sub> source pretreatment, respectively. The response observed upon source pretreatment is intermediate to that observed in the extreme cases of aspartic-TAB and maleic acid (di-TMS ester). L-Pro-TAB shows approximately a 4-fold enhancement of ion production under ECNI conditions following source pretreatment (Figure 4b). In this case, the [M+Cl] ion is not the base peak in the mass spectrum, but carries a smaller portion of the TIC relative to the response for compounds such as aspartic acid-TAB.

Table II summarizes the responses of several derivatized compounds under conditions in which the pretreatment procedure was employed, in comparison to responses observed in conventional ECNI analyses. Compounds that respond similarly in both ECNI methods, i.e., compounds that do not yield different mass spectra following source pretreatment, are those that produce abundant M ions in their negative ion mass spectra. In contrast, compounds that typically exhibit a small (or no) M peak also exhibit enhanced responses following source pretreatment with CCI<sub>4</sub>.

Table III summarizes the responses of a number of compounds to ECNI with CCI<sub>4</sub>-pretreatment. While a favorable response does not require that the compounds be as highly functionalized as those presented, it appears that at least one site of unsaturation is required. Compounds such as dodecane are essentially unresponsive under ECNI-MS with or without CCI<sub>4</sub> pretreatment. Ketones, even as simple as acetone, do produce abundant [M+CI] ions, with improved detection limits following the pretreatment procedure.

Duration of "pretreatment" effect: The results presented above were obtained from the analysis of pure compounds. This prompts the question of whether the CCI<sub>4</sub>-pretreatment method is suited for complex mixture analysis. Experience with analyses of simple mixtures and for sequential injections of simple mixtures, shows that the signal enhancements and the formation of [M+CI] ions described here will occur for at least one hour following source pretreatment, without completely depleting the source of chlorine atoms. Figure 5 shows the results of such a study. The ion source was pretreated, and the compound aspartic-TAB was injected several times over a one-hour period. The experiment was repeated at various ion source temperatures. The

data show that the chlorine in the source persists for over an hour, being lost more rapidly at higher source temperatures. Figure 5 shows that the response will decrease by a factor of approximately two over a one hour time period. Thus, if this technique is to be used for lengthy GC/MS mixture analyses, the time dependence must be well understood for the particular instrument being used. One option that could be used to maintain the response throughout a mixture analysis is to constantly provide a small amount of CCl<sub>4</sub> to the ion source (following pretreatment, as the analysis is being performed). This could be done by using a CCl<sub>4</sub>/CH<sub>4</sub> mix, instead of pure CH<sub>4</sub> as the reagent gas. However, care must be taken to supply a constant, but exceedingly small amount of CCl<sub>4</sub>. If this is not done, the concentration of anions such as CCl<sub>3</sub> may dominate the chemistry in the ion source, instead of the chemistry described in this work.

Mechanism of [M+CI] formation: Having fuled out a conventional chemical ionization (NCI) mechanism for the formation of [M+CI] from a CCI<sub>4</sub>- pretreated ion source, i.e., a gas phase ion/molecule mechanism of the type

$$C\Gamma + M + A \rightarrow [M+CI]\Gamma + A$$

(where A=third body), mechanisms in which the <u>incorporation</u> of CI and the <u>ionization</u> process occur in two separate steps must be considered. Reactions such as

$$M' + Cl_{(Q,S)} \rightarrow [M+CI]'$$

where  $Cl_{(g,s)}$  represents some form of chlorine either in the gas phase or on a surface, can be dismissed since there is no evidence for a sufficiently long-fived M<sup>\*</sup> species for most of the molecules investigated. The most reasonable mechanisms involve incorporation of Cl into the molecule followed by electron attachment, presumably to the resulting radical. The incorporation of Cl could occur on a surface or in the gas phase.

Any proposed mechanism must be consistent with the experimental observations. Those considered to be relevant here include: 1. [M+CI] is observed when the CI ion abundance is very small; 2. The [M+CI] ions are observed for more than an hour after source pretreatment; 3. There is a temperature dependence to

this behavior, with the chlorine being depleted from the ion source more rapidly at higher temperatures; 4. An increase in the Cl peak intensity is actually observed when some compounds elute from the GC into the ion source; 5. At least one site of unsaturation is required for [M+Cl] ion formation to occur; 6. The effect is most dramatic for compounds that do not exhibit an M ion under conventional ECNI conditions.

The experimental observations are consistent with storage of chlorine in some form on the inner walls of the ion source. The binding of halogen-containing compounds to metal surfaces has been reported in the literature, for iron and aluminum surfaces(14,15). In these studies, the surface population of halogen atoms can be decreased by heating. The fact that the chlorine remains for long periods of time, and the apparent displacement of CI from the surface by some compounds such as benzene is clear evidence that the halogen atoms are stored on the surface. The question remains whether an analyte molecule collides with the surface, incorporates a CI and desorbs; or whether a gas phase CI atom bonds to the analyte. In either case, a gas phase [M+CI]- radical would be formed, which then presumably captures an electron.

Both mechanisms may be operative. Since CI atoms appear to be stored on the surface, molecules that collide with the source walls could react. On the other hand, the CI present in the source does disappear with time, and, thus, must go into the gas phase in an atomic or molecular form at some point. Could the source have a substantial concentration of CI atoms present in the gas phase following pretreatment? One might assume that this would not be the case due to the negligible signal due to CI at m/z 35. However, the cross section for electron capture for an atomic species should be low since collisional stabilization would be required; this phenomenon would explain the low signal at m/z 35.

A stronger argument against the involvement of free  $Cl_{(g)}$  atoms is supported by the fact that the gas phase reaction (1)

$$Cl + CH_4 \rightarrow HCl + CH_3$$
 (1)

has been observed to occur with a rate constant of  $k \sim 3 \times 10^{-13}$  cm<sup>3</sup> molecule<sup>-1</sup> sec<sup>-1</sup>(16). Thus, at the pressures of CH<sub>4</sub> used in the ion source, CI atoms (if any were present) would be consumed rapidly. The CI then would be converted into HCI, which does not capture thermal electrons(17). In addition to these

considerations, Grimsrud et al.(18) have developed a detailed kinetic model for the high pressure electron capture ion source, with an extensive discussion on the possible origin of unusual and unexpected ions such as those which we observe here. Their work strongly suggests that surface-assisted reactions may support the behavior that we report, while a gas phase radical mechanism may not.

Further insights into the mechanism may be gained by considering the thermodynamics of the formation of an [M+CI]- radical in the gas phase and from a surface. For the reaction (2)

$$M(q) + Cl(s) \rightarrow [M+Cl] \cdot (q)$$
 (2)

to occur in which the CI is available on the surface, there are two thermochemical considerations: the energy required to cleave the CI-surface bond, and the energy involved in forming the [M+CI]- radical (a process which could be endothermic or exothermic). In contrast, if the reaction occurs in the gas phase, reaction (3),

$$M_{(Q)} + Cl_{(Q)} \rightarrow [M+Cl]_{(Q)}$$
(3)

the breaking of the CI-surface bond need not be involved in the overall reaction; i.e., the formation of CI-(g) must occur spontaneously before the reaction occurs. Consider a simple molecule with one site of unsaturation, formaldehyde (CH<sub>2</sub>O). If a CI- is added to this molecule, a C-CI or an O-CI bond may be formed.

$$CI + CH_2O \rightarrow CI - CH_2 - O$$
 (4)

Are reactions (4) and (5) endothermic or exothermic? The  $\Delta H_1$ 's of  $Cl_{(g)}$  and  $CH_2O_{(g)}$  are 29.1 kcal/mol and -28 kcal/mol, respectively. Using group equivalence tables(19), the radical product of reaction (4) has a  $\Delta H_1$  of approximately -5.9 kcal/mol. The same approach gives a value of -3.2 kcal/mol for the  $\Delta H_1$  of the radical product of reaction (5). Using  $\Delta H_1(CH_2CIOH) = -49.4$  kcal/mol, and assuming that the H-O bond energy is 100 kcal/mol,  $\Delta H_1$  of the product of reaction (4) would be kcal/mol. Such numbers suggest that both reactions (4) and (5) would be exothermic, but by less than 10 kcal/mol. Thus, they could occur spontaneously

in the gas phase. However, for these reactions to occur on a surface in an exothermic process, the C1-surface interaction would have to be less than 10 kcal/mol, which is rather weak. (However, if C1 atoms can desorb from the surface thermally, this may reflect a weak C1-surface bond.) Therefore, one cannot rule out either mechanism based on these considerations for formaldehyde. If similar calculations are performed for acetone, the situation becomes more complex. We estimate that reactions (6) and (7)

$$CI + (CH_3)_2 C=O \rightarrow (CH_3)_2(CI)C-O$$
 (6)

$$\rightarrow \text{-C(CH}_3)_2 \text{-O-Cl} \tag{7}$$

are both endothermic by approximately +40 kcal/mol. Thus, if more energy is required in a surface reaction to cleave a surface-Cl bond, reactions (6) and (7) should not occur. These calculations led to two additional possible explanations for the observed results. The first is that energy may be released when a Cl- is abstracted from the surface. For example, if S is a metal atom or atoms on the surface, and species of the type S-CCl<sub>3</sub> are on the surface, the surface chlorination reaction may be written as

$$S-CCl_3 + M \rightarrow S=CCl_2 + MCl$$
 (8)

Reaction (8) may be exothermic for cases such as when M is acetone, due to the strength of the S=C bond that is formed. It has been reported that the triple bond in acetylene can be cleaved when this alkyne bonds to nickel and iron surfaces at temperatures as low as 400 K(20,21). This suggests that the metal surface - C bond energies can be substantial. Thus, reactions such as (8) could be exothermic due to the formation on carbene- or carbyne-like species. If reaction (8) represents the pathway by which chlorination of the analyte occurs, the reaction may lead to various S-CCI<sub>n</sub> species on the surface. It may be expected that such a reaction could result in a modified surface. However, it has been reported that when CCI<sub>4</sub> is adsorbed on an iron surface and the surface chlorine coverage is depleted, the carbon that remains appears to diffuse into the bulk metal at temperatures as low as 444 K, leaving the surface clean(14).

A second possible explanation for the observed results is that surface chlorination does not lead to a radical at all, but to a dichlorinated product. We estimate that reaction (9), in which two chlorine atoms are added to acetone is exothermic.

$$2CI \cdot + (CH_3)_2C = O \rightarrow (CH_3)_2(CI)C - O - CI$$
(9)

We note that the ECNI mass spectra of many chlorinated compounds show an [M-CI] ion as the peak of highest mvz, thus the neutral that is formed on the source walls (MCI<sub>2</sub>) may not actually be observed--only the the fragment corresponding to loss of CI. However, it seems unlikely, for the variety of compounds studied in this work, that if an MCI<sub>2</sub> species were being formed, it would never be observed. Also, no such species are seen when the source is chlorinated and positive EI spectra are obtained. The important conclusion is that the CI is stored on the source walls, and is available for addition to unsaturated compounds for a period of time that is potentially useful in negative ionization mass spectrometry.

Additional experimental results support the surface mechanism. Figure 6a shows the reconstructed TIC profile for serine-TAB with data obtained with an ion source that had been cleaned, and was free from any chlorine contamination. Representation of the chromatography is typical and acceptable. Following source exposure to CCl<sub>4</sub>, reconstruction of the profile from newly acquired data shows a dramatically different peak shape (Figure 6b). After baking the ion source for one hour, the sample was reanalyzed; reconstruction of the original peak shape from newly acquired data (Figure 6a) was achieved. Thus, degradation of the peak profile shown in Figure 6b is not attributable to any chromatographic effect, but may reflect an intermediate chemical step, i.e., conversion of M to [M+Cl]. The tailing may occur due to the reaction of, and subsequent slow desorption of, species from the source walls. Similar behavior has been observed in thermionic GC detectors, in which degradation of peak profiles can occur due to surface reactions within the detector(22,23).

Once the [M+CI] radical is formed, electron capture occurs. If the source is pretreated with CCI<sub>4</sub>, and positive ion (EI) mass spectra are obtained from these compounds, no evidence for such a species is observed. The implication is that only a small fraction of the analyte undergoes CI-attachment. Thus, the resulting radical must have a very large electron capture cross section. For molecules such as maleic acid (di-

TMS ester), the CI attachment may still occur, however, upon electron attachment, the CI is lost to form the stable M<sup>-</sup> species, reaction (10).

$$[M+CI] \cdot + e^{-} \rightarrow [M+CI]^{-e} \rightarrow M \cdot + CI$$
 (10)

For molecules that have conjugated double bonds such as 2-buten-3-one, the formation of the stable [M-H]\* ion dominates over the [M+CI]\* ion.

Since only a small fraction of the analyte is converted into the [M+CI] radical species, the unreacted molecules M can still react by electron capture to form the fragment ions observed in conventional ECNI. For some molecules, the ion current corresponding to the fragment ions is enhanced with their relative abundance distribution being retained. This may suggest a second pathway for formation of fragment ions via the [M+CI] intermediate and the stable [M-H] ion as follows:

id the stable [M-H] ion as follows:
$$[M+CI]^{-} \leftrightarrow [M+CI]^{-} \rightarrow [M+H]^{-} + HCI$$

$$\longrightarrow [m+CI]^{-} \leftrightarrow [m+H]^{-} + HCI$$

Therefore, based on these preliminary results, when an ion source is exposed to chlorine-containing compounds, such as CCI<sub>4</sub>, CHCI<sub>3</sub>, or CH<sub>2</sub>CH<sub>2</sub>, the source walls become covered with CI in some form. The chlorine slowly desorbs. On the surface, unsaturated molecules can react to form [M+CI]- radicals. These radicals capture thermal electrons to form predominantly the [M+CI]<sup>-</sup> anion. The exceptions are molecules whose molecular anions are stable. Further experiments are underway to provide other insights into the mechanism. It should be noted that, in ECNI mass spectrometric studies, there have been other reports suggesting that a variety of species can be stored on ion source walls for reaction with analyte molecules. The capture of H(18,24) and O(25) atoms by molecules has been implied by ECNI experiments, in which surface chemistry has been suggested prior to the electron-capture step. Thus, such studies may lead to a variety of methods in which species with high electron capture cross sections may be generated in an ion source.

#### **CONCLUSIONS**

An understanding of the mechanism through which [M+CI] ions are formed in ECNI studies in an ion source pretreated with CCI<sub>4</sub> is important, since it may lead to the development of new methodology. Meanwhile, empirical analytical advantages can be realized from this technique. For many molecules ECNI-MS with a pretreated ion source may give improved detection limits. Also, when unknowns are detected in GC-ECNI-MS, it can be difficult to derive molecular weight information because the peak at the highest m/z could represent [M-HF], [M+H], or some other fragment anion. Such questions frequently can be resolved by the chlorine pretreatment method because the [M+CI] ion, if formed, is easy to recognize from the isotope peak intensity pattern.

With the large number of ionization methods available for the formation of positive and negative ions from analytes, one can, in many cases, provide the necessary qualitative and quantitative information for selected components of a mixture by combining the results of a few approaches (such as EI and NCI). The method presented here makes the ECNI methodology responsive to a larger number of compound classes, which may be advantageous in the analysis of mixtures when conventional ECNI is the ideal method for only some of the components of interest.

#### Literature Cited

- 1. Hunt, D. F.; Crow, F. W. Anal. Chem. 1978, 50, 1781.
- 2. Jennings, K. R. "Mass Spectrometry," Vol. 4, R.A.W. Johnstone, Ed. The Chemical Society, Burlington House, London, Chapter 9, 1977.
- 3. Pellizzari, E. D. J.: Chromatogr. 1974, 98, 323.
- 4. Harrison, A. G. "Chemical Ionization Mass Spectrometry," CRC Press, Inc. Boca Raton, Florida, Chap. 2, 1986.
- 5. Christophorou, L. G. Chem. Rev. 1976, 76, 409.
- 6. F. K. Kawahara. Anal. Chem. 1968, 40, 1009 and 2073.
- 7. Roy, T. A.; Field, F. H.; Lin, Y. Y.; Smith, L. L. Anal. Chem. 1979, 51, 272.
- 8. Schlunegger, U. P.; Lauber, R. Org. Mass Spectrom. 1986, 21, 401.
- 9. Stemmler, E. A.; Hites, R. A. Anal. Chem. 1985, 57, 684.
- 10. Tannenbaum, H. P.; Roberts, J. D.; Dougherty, R. C. Anal. Chem. 1975, 47, 49.
- 11. Kingston, E. E.; Duffield, A. M. Biomed. Environ. Mass Spectrom. 1982, 9, 459.
- 12. Gates, S. C.; Dendramis, N.; Sweeley, C. C. Clin. Chem. 1978, 24, 1674.
- 13. Dougherty, R. C. Anal. Chem. 1981, 53, 625A.
- 14. Jones, R. G. Surface Science 1979, 88, 367.
- 15. Dowben, P. A.; Jones, R. G. Surface Science 1979, 89, 114.
- 16. Kondratiev, V. N. "Rate Constants of Gas Phase Reactions," U.S. Department of Commerce, NBS, Office of Std. Ref. Data, 1972.
- 17. Adams, N. G.; Smith, D. J. J. Chem. Phys. 1986, 84, 6728.
- 18. Sears, L. J.; Campbell, J. A.; Grimsrud, E. P. Biomed. Environ. Mass Spectrom. 1987, (in press).
- 19. Franklin, J. L.; Dillard, J. G.; Rosenstock, H. M.; Draxl, K.; Field, F. H. Nat. Stand. Ref. Data Ser., Nat. Bur. Stand. 1969, 26.
- 20. Lehwald, S.; Ibach, H. Surface Science 1979, 89, 425.
- 21. Erley, W.; Baro, A. M.; Ibach, H. Surface Science 1982, 120, 273.
- 22. Bombick, D. D. Ph. D. Thesis, Michigan State University 1986.
- 23. Burger, B. V.; Prelorius, P. J. J. Chromatogr. Sci. 1987, 25, 118.
- 24. McEwen, C. N.; and Rudat, M. A. J. Amer. Chem. Soc. 1979, 101, 6470.

25. Buchanan, M. V. and Rubin, I. B. 35th Annual Conference on Mass Spectrometry and Allied Topics, Denver, CO 1987, Presentation #MOB1000.

#### Credit:

This work was performed with instruments in the MSU Mass Spectrometry Facility supported by a grant (5P41-DRR-00480-19) from the Division of Research Resources of NIH and various units of Michigan State University.

### Acknowledgements:

The authors are grateful to Prof. Eric Grimsrud for his suggestions regarding this work and for making ref. 18 available to us during the review of this manuscript.

#### Legends

#### Figure 1

- a) Conventional ECNI mass spectrum 200 ng of aspartic acid-TAB (methane pressure equal to 0.4 torr). Base peak at m/z 228 corresponds to (M-H-NHCOCF<sub>3</sub>). Integrated peak area (TIC) = 18,200.
- b) ECNI mass spectrum of the same compound following ion source preatreatment with CCI<sub>4</sub>. Base peak at m/z 376 corresponds to (M+Ci)'. Integrated peak area (TIC) = 80,000.
- c) NCI mass spectrum of the same compound (CCI<sub>4</sub> reagent gas, pressure = 0.4 torn). (M+CI) base peak at m/z 376. Integrated peak area (TIC) = 18,300.

#### Figure 2

Conventional ECNI mass spectrum of the trifluoroacetyl derivative of myristyl alcohol (MW = 310) following ion source pretreatment with CCl<sub>4</sub>. The base peak is (M+Cl), observed at m/z 345; m/z 213 corresponds to (M-COCF<sub>3</sub>); m/z 113 corresponds to (CO<sub>2</sub>CF<sub>3</sub>).

#### Figure 3

ECNI mass spectrum of the maleic acid (di-TMS ester) following CCl<sub>4</sub> pretreatment (methane pressure = 0.4 torr). No (M+Cl) ion is observed; m/z 260 corresponds to the stable molecular anion, (M).

#### Figure 4

- a) Conventional ECNI mass spectrum of L-Pro-TAB under conditions in which the ion source was free from CCI<sub>4</sub> exposure. Both (M) and (M-H) are observed at m/z 267 and 266, respectively. The following ions have been identified: m/z 211, (M-C<sub>4</sub>H<sub>8</sub>); m/z 191, [M-C<sub>4</sub>H<sub>8</sub>-HF]; m/z 163, [M-C<sub>4</sub>H<sub>9</sub>CO<sub>2</sub>H-H<sub>2</sub>F; m/z 143, [M-C<sub>4</sub>H<sub>9</sub>(O<sub>2</sub>H-H<sub>2</sub>-HF)].
- b) ECNI mass spectrum of the same compound following ion source preatreatment with CCI<sub>4</sub>. The only new ion observed in the mass spectrum is found at m/z 302, corresponding to the (M+CI) ion. An approximate 4-fold enhancement in detectability is observed.

#### Figure 5

A measure of chlorine depletion over time for various ion source temperatures is shown. As the peak elutes, the integrated areas of the (M+CI) ion,  $A_{M+CI}$ , relative to the integrated total ion current,  $A_{TC}$ , is shown as a function of time. Intensities of the (M+CI) ion for aspartic acid-TAB decrease over time, and the intensity of signal decreases more rapidly at high source temperatures.

#### Figure 6

- a) Reconstructed TIC profile for serine-TAB generated from conventional ECNI analysis. The profile represents acceptable chromatographic behavior.
- b) Reconstructed TIC profile for serine-TAB, same sample size, following ion source preatreatment with CCl<sub>4</sub>. Surface interactions result in severe tailing and poor chromatographic peak shape.

TABLE 1:

ECNI results for aspartic acid-TAB obtained prior to and after CCI4 source pretreatment.

# (a) Conventional EC-NI (I.e., without CCI4 exposure)

m/z (Assignment)	% of m/z = 228	Ion Abundance	Integrated Area
183 (M · CO <sub>2</sub> C <sub>4</sub> H <sub>9</sub> · C <sub>4</sub> H <sub>9</sub> ).	55.4	1100	2350
228 (M - H - COCF3NH)	100. <b>0</b>	2000	5270
539 (M - H - CO2C4H2).	76.3	1520	3450
267 (M - H - OC <sub>4</sub> H <sub>9</sub> )*	23.6	470	1080
321 (M - HF)"	8.7	170	470
340 (M - H)	18.8	370	800
TIC		8500	18200

# (b) EC-NI results directly following CCI<sub>4</sub> exposure

m/z (Assignment)	% of m/z = 228	Ion Abundance	Integrated Area
35 (CI) <sup>-</sup>	36.1	1650	-
183 (M - CO <sub>2</sub> C <sub>4</sub> H <sub>9</sub> - C <sub>4</sub> H <sub>9</sub> )*	90.3	3750	8550
228 (M · H · COCF3NH)*	100.0	4160	8950
239 (M - H - CO <sub>2</sub> C <sub>4</sub> H <sub>9</sub> )	89.1	3700	8450
267 (M · H · OC <sub>4</sub> H <sub>9</sub> )*	26.2	1100	2550
321 (M - HF)*	6.2	260	700
340 (M - H)-	18.0	750	1580
376 (M + CI)-	400.	16600	41600
TIC		34300	80000

## (c) EC-NI results following a period of > 1 hr following ion source exposed to CCI4

m/z (Assignment)	% of m/z = 228	Ion Abundance	Integrated Area
35 (CI) <sup>-</sup>	0.6	25	-
183 (M - CO <sub>2</sub> C <sub>4</sub> H <sub>9</sub> - C <sub>4</sub> H <sub>9</sub>	) <sup>-</sup> 36.2	1420	3000
228 (M · H · COCF <sub>3</sub> NH)	100.0	3920	8990
239 (M · H · CO <sub>2</sub> C <sub>4</sub> H <sub>9</sub> ) ·	70.4	2760	6980
267 (M - H - OC <sub>4</sub> H <sub>9</sub> )*	39.3	1540	3650
321 (M · HF)-	8.0	310	790
340 (M · H)	19.8	780	1470
376 (M + CI)	158.	6180	12500
TIC		21500	49100

TABLE 2: Comparison of response for several analytes by EI, ECNI (conventional), and ECNI (source pretreatment).

Compound	1 A(EC-NCIVA(ED	ALEC WICCLIVALED	ALEC WICCLIVALEC-NOI
Valine - TAB	0.18	1.9	10.9
Aspartic - TAB	0.34	3.3	9.9
Myristyl - TFA	0.002	0.1	66.8
Glutamic - TAB	0.94	4.0	4.2
L-Proline - TAB	0.03	0.1	4.2
Cystine - TAB	19.5	25.4	1.3
Serine - TAB	9.1	12.2	1.3
Maleic (di-TMS)	7.6	8.4	1.1
Lauric - PFB	16.1	16.4	1.0

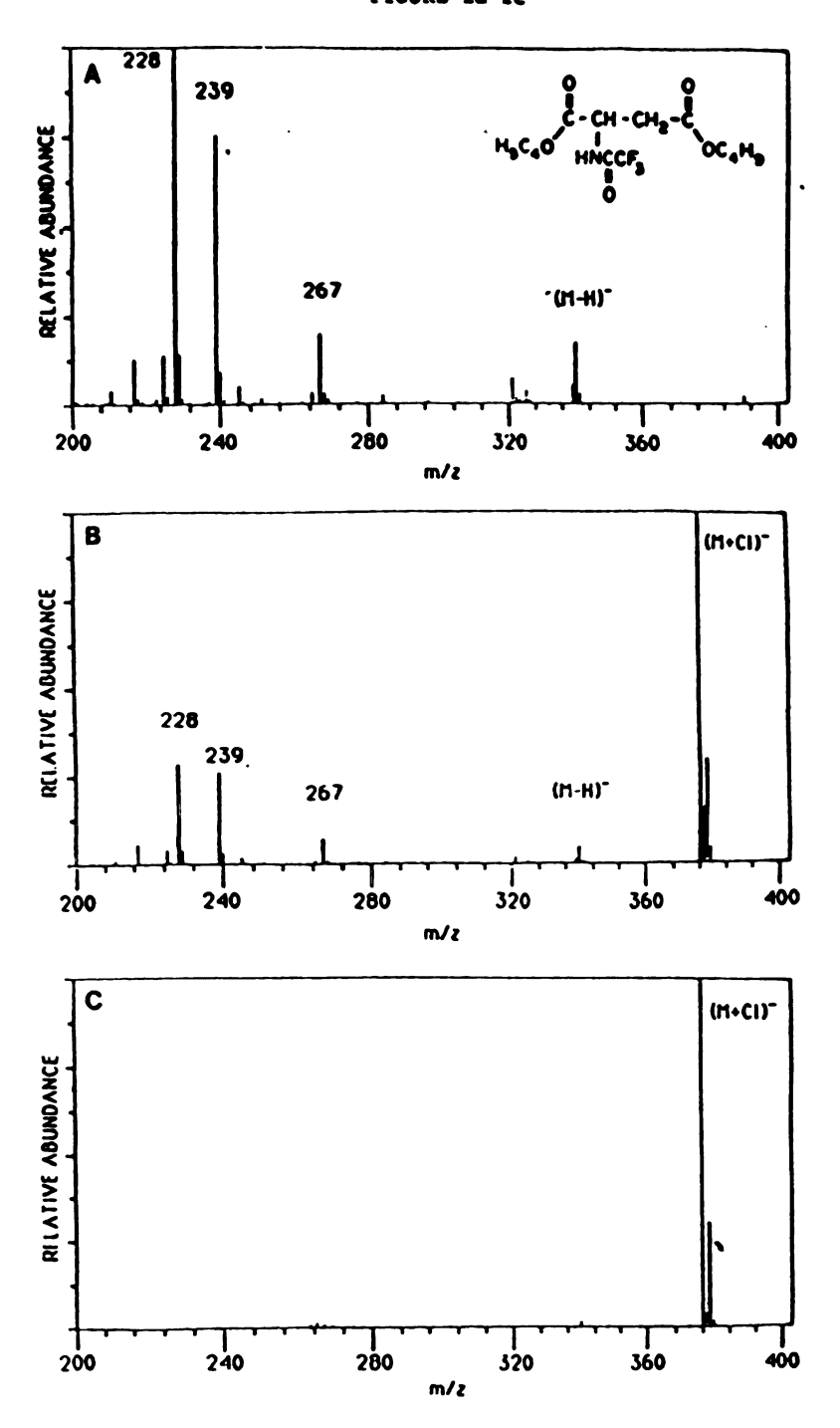
<sup>†</sup> A = integrated areas

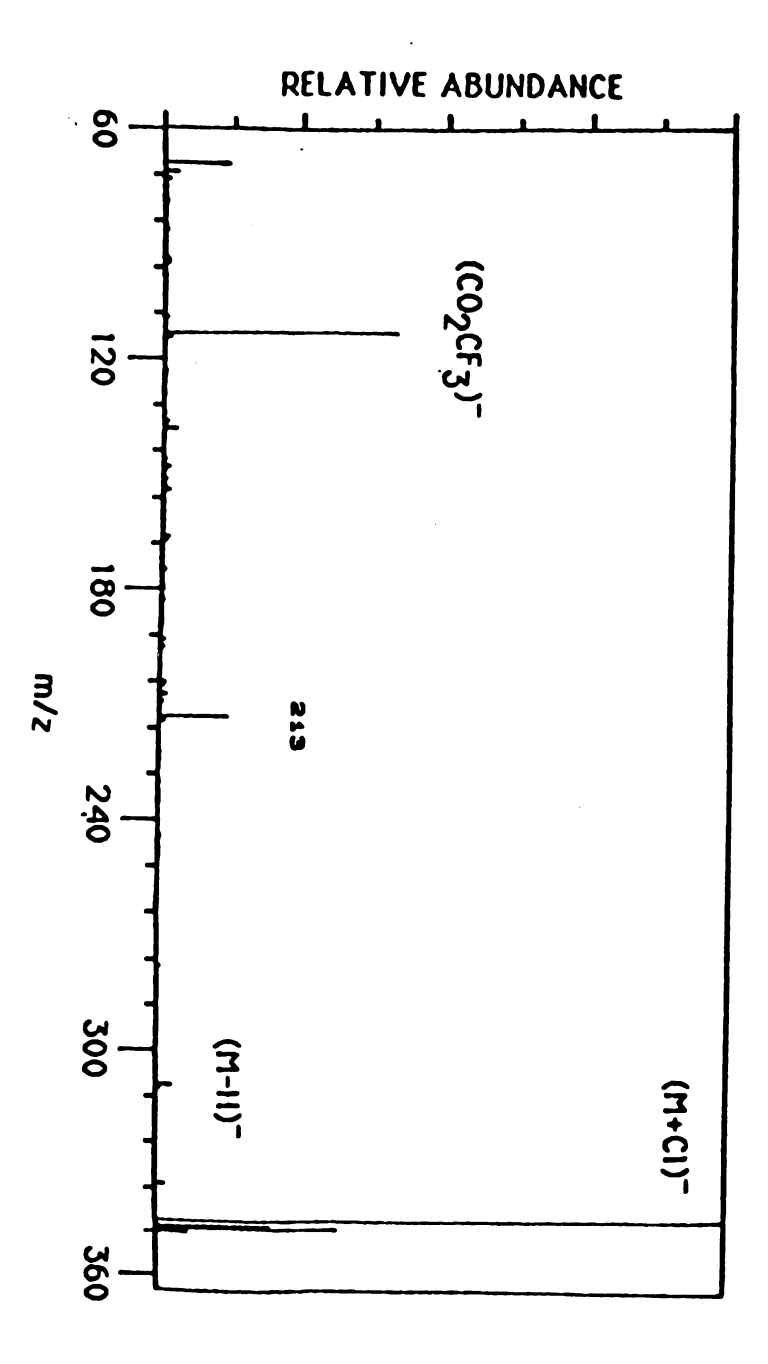
Table 3: Survey of the effect ion source pretreatment has on various compound classes.

<u>Compound</u>	Base Peak	†Enhancement
Organic Acids (TMS):		
- 2-hydroxybutyric	[M-TMS]	•
- Oxalic	[M].	0
Mal <del>ei</del> c	[M].	0
- Malic	[M-TMS]	•
- Adipic	[M+CI].	•
- M-hydroxybenzoic	[M+CI]-	+
- P-hydroxybenzoic	[ M - TMS ] -	<b>+</b>
Organic Acids (PFB esters)	[M-PFB]-	+
Fatty Acids (methyl esters)	[M+CI] -	<b>+</b>
Alcohols (TFA ethers)	[M+CI] -	<b>+</b>
Amino Acids (TAB esters)	Va	aries (see Table 2)
Heptane nitrile	[M+CI] -	+
Acetone	[M+CI] -	+
Pyridine	[M+CI] -	<b>+</b>
3-butene-2-one	`[M-H]-	0
Anisole	None	0
p-Xylene	[M-H] -	0
Dodecane .	None	0
Benzene	[M-H]-	•

<sup>† (+)</sup> indicates an enhancement in detectability using our method over conventional ECNI-MS. (0) indicates <u>no</u> enhancement in detectability using the CCl<sub>4</sub> source pretreatment ECNI-MS method. \*

FIGURE la-le





TGURE 2

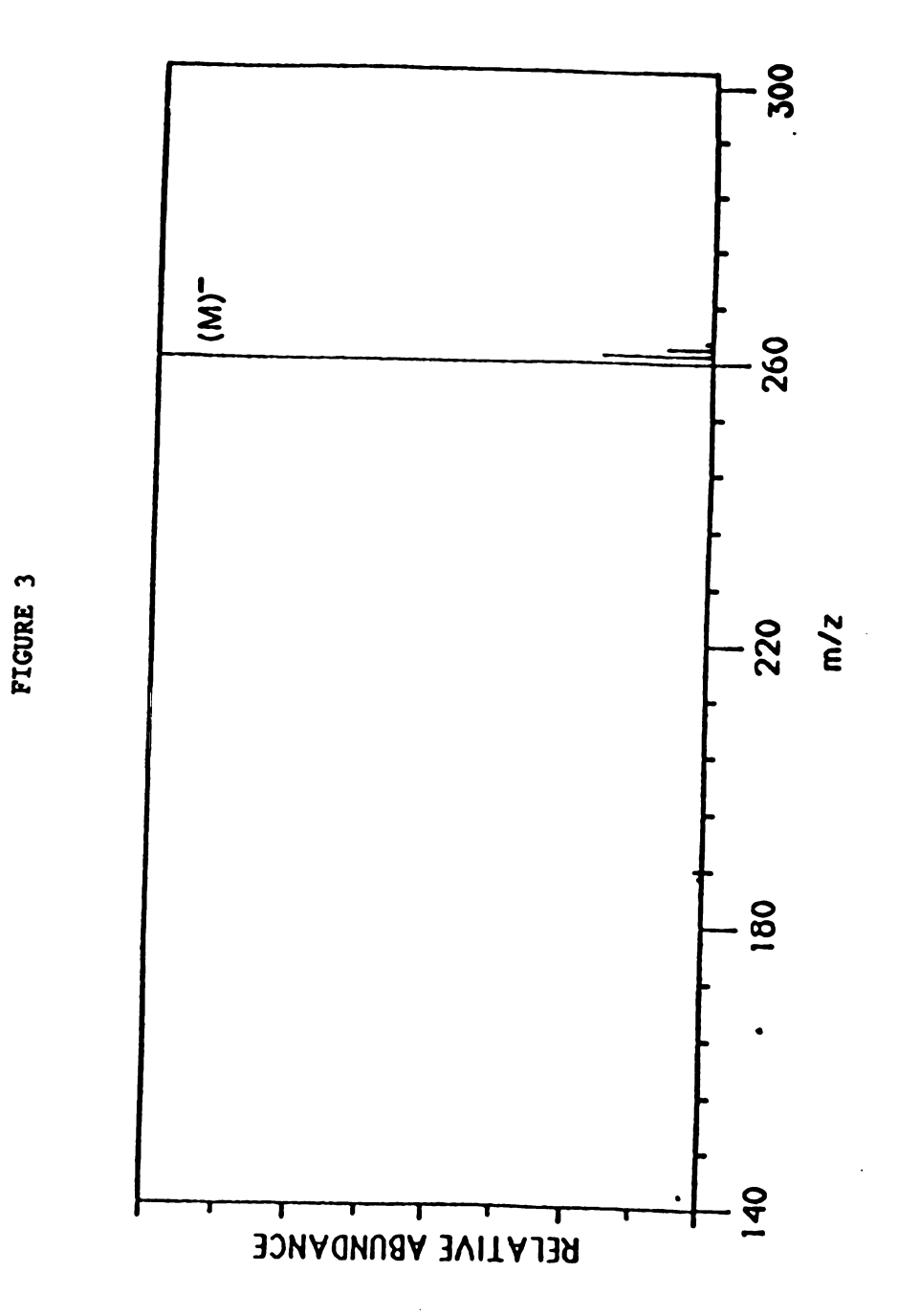
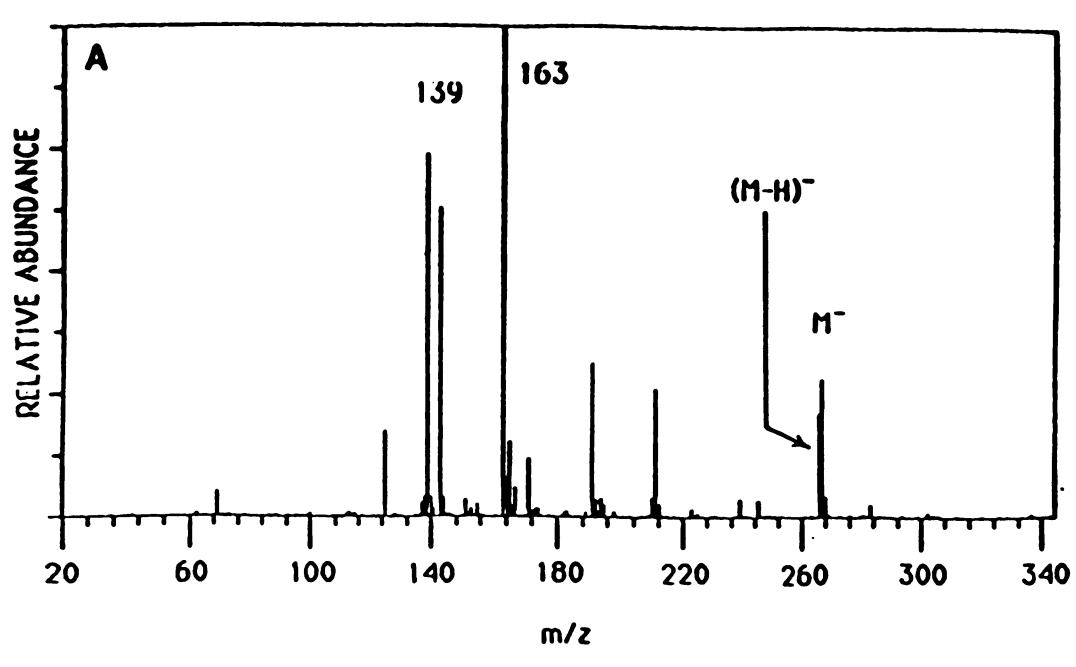
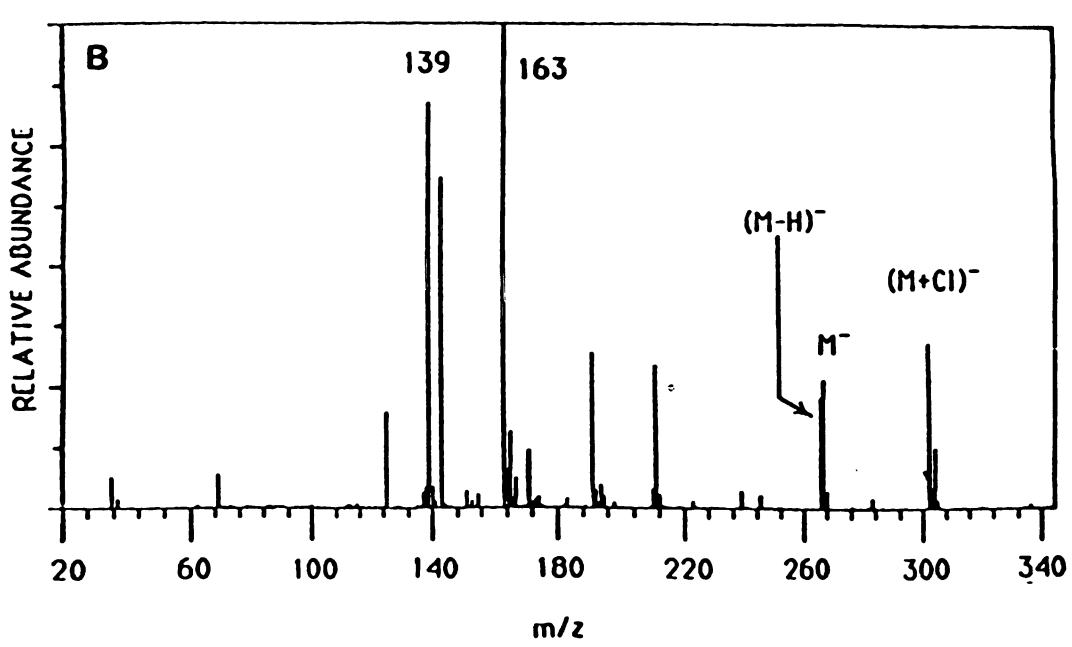


FIGURE 4





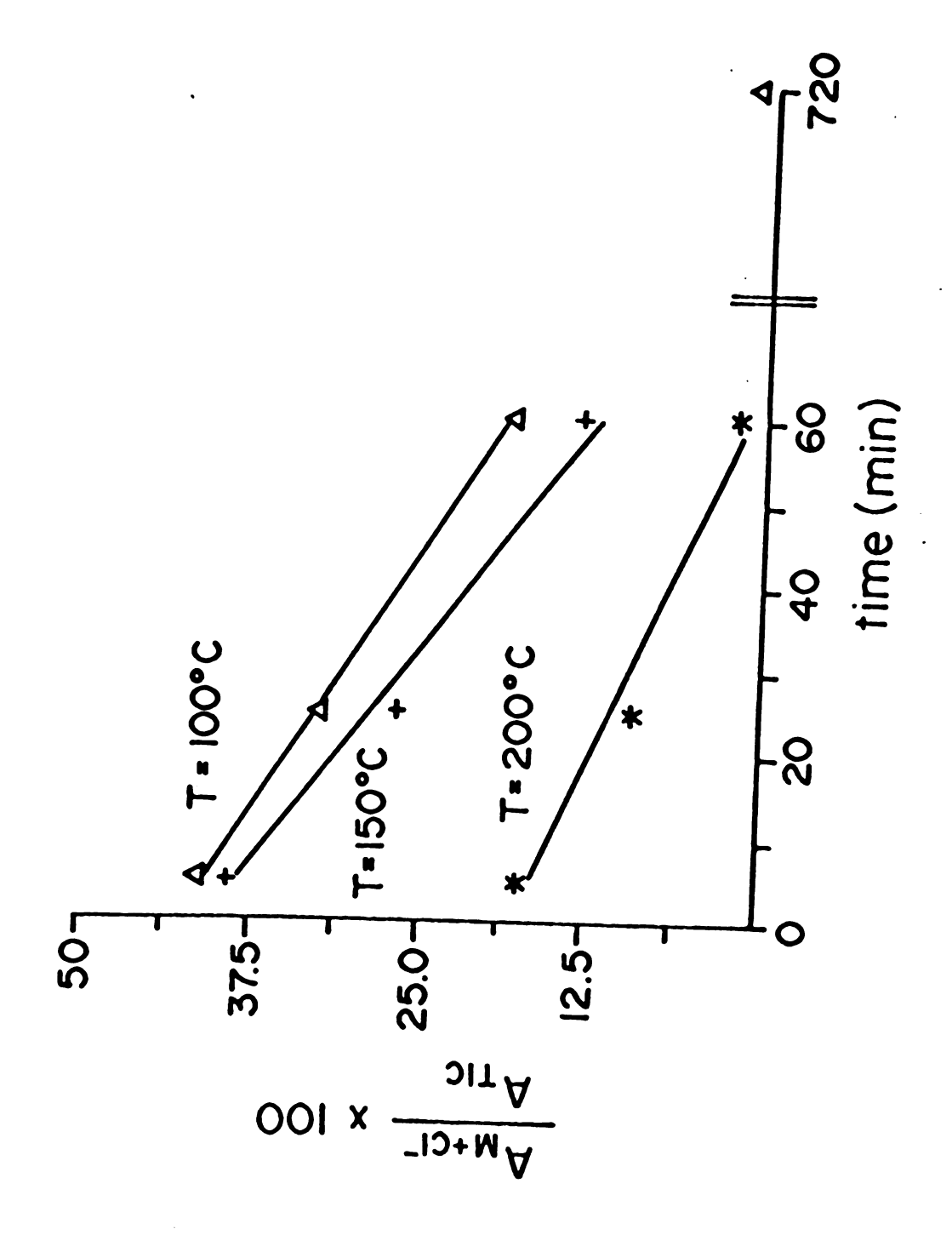
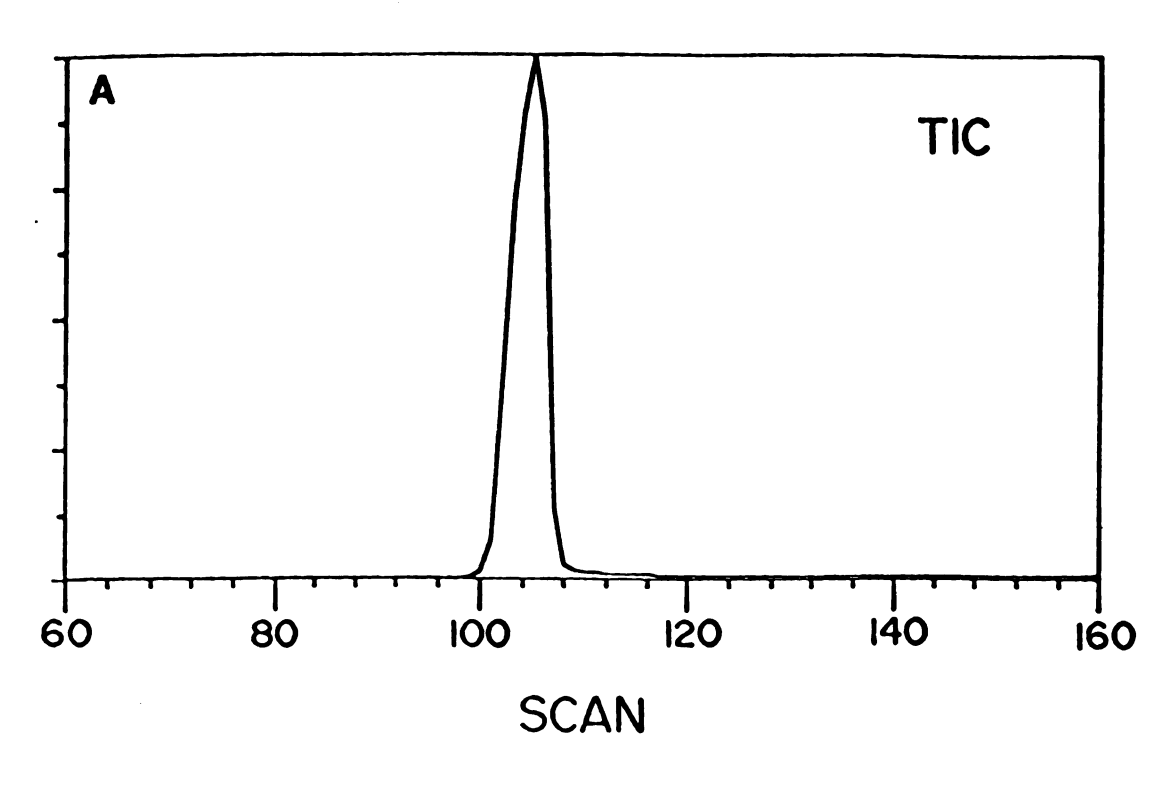
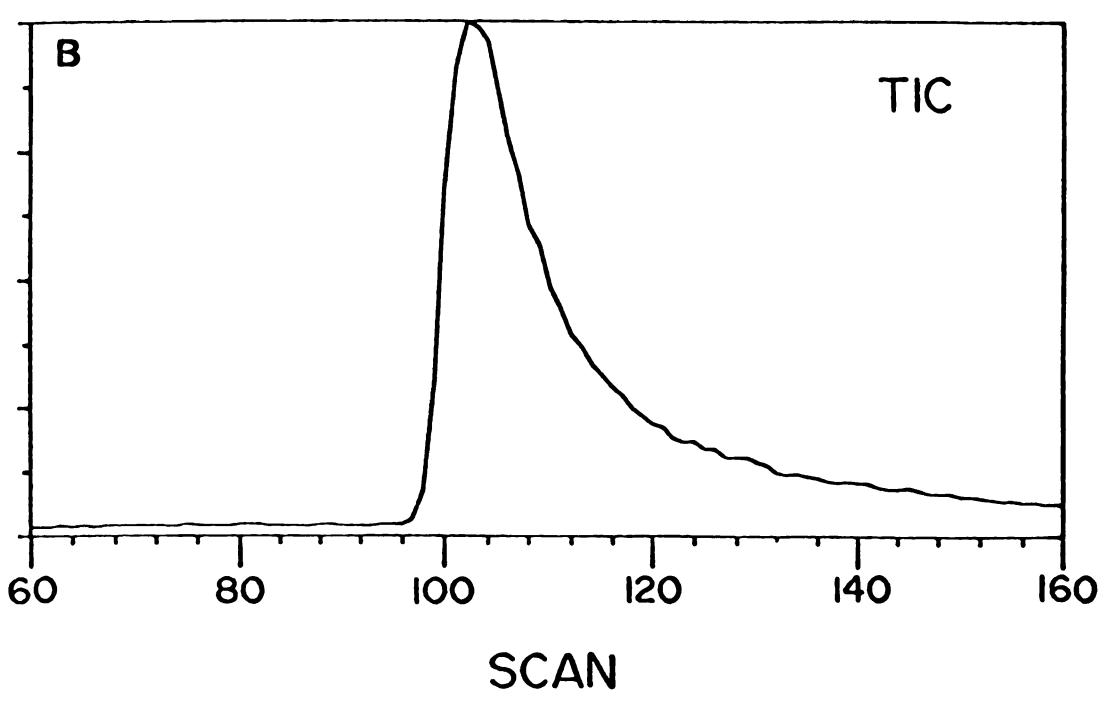


FIGURE 5

FIGURE 6





### APPENDIX II

This appendix (Appendix II) gives molecular weight information on some organic acids observed in the methylmalonic acidemia disease condition for which no molecular weight information has previously been reported. Analyses by GC-only have verified the presence of many of these unknowns and their retention times and indices are documented. However, these species have yet to be identified from EI and/or NH<sub>3</sub>-CI analysis.

Some of the unknowns whose molecular weights have been determined may be useful for disease-state identification since some are observed at concentrations significantly elevated to many of the metabolites identified for this disease-state. The presence of some of these unknowns at such elevated levels may suggest certain metabolic errors and perhaps with identification of these unknowns, a better understanding of the disease condition will be obtained. In addition, the determination of the molecular weights for these unknowns might also be useful for obtaining "true" simulated molecular weight profiles of complex mixtures of organic acids which will be useful for comparison to those molecular weight profiles that are obtained experimentally utilizing the K + IDS technique.

The derivatized and underivatized molecular weights of a number of unknown organic acids (whose concentrations are such that they gave rise to ion signals by GC-MS analysis) and identified organic acids isolated from a methylmalonic acidemia urine sample are reported in Table 1. Retention indices and times for both identified organic acids and the unknowns have been obtained from triplicate GC analyses using a DB-1 50 meter narrow bore capillary column. Concentrations of unknowns and identified organic acids have been obtained based on calculation of creatinine levels in the subject patient and use of the internal standard, tropic acid.

Table 1. Molecular weight determinations on a number of unknowns whose concentrations are above the detection limits of the HP5985 quadrupole GC-MS system.

Compound	Ret. Index	Ret. time	amount <sup>‡</sup>	Deriv. MW	Underiv. MW
Unk 924.9	936.76	9.458	15.53	331	115
Lactic	1012.60	10.218	236.12	234	90
Glycolic	1055.00	10.642	125.35	. 220	76
Unk 1094.0	1091.50	11.007	146.70	232	88
Glyoxylic oxime	1217.19	12.264	28.70	233	89
2-hydroxybutyric	1217.19	12.2641	28.70	248	104
Oxalic	1231.69	12.409	114.22	234	90
3-hydroxypropionic	1261.90	12.712	49.79	234	90
3-hydroxyisobutyri	c 1268.18	12.775	52.41	138	104
Pyruvic oxime	1288.91	12.983	22.06	185	
3-hydroxybutyric	1313.14	13.226	34.76	248	104
Sulfuric	1320.02	13.295	20.02	242	98
3-OH-2-Me-butyri	c 1424.30	14.341	15.56	262	118
3-hdyroxyisovaleri	c 1457.40	14.673	46.92	262	118
Methylmalonic	1478.61	14.886	920.69	262	118
Unk 1568.4	1569.93	15,802	81.05	278	134
Phosphoric	1660.56	16.707	278.59	314	98

Succinic	1757.90	17.679	101.30	262	118
L-Glyceric	1827.54	18.376	300.46	322	106
4-deoxyerythronic	1868.50	18.786	32.08	336	120
Unk 1881.9	1882.82	18.924	10.04	350	134
4-deoxythreonic	1896.00	19.051	38.60	336	120
2-OH-2-Me-malonio	: 1944.68	19.541	23.15	350	134
Glutaric	2008.77	20.186	15.30	276	132
3-deoxytetronic	2051.89	20.620	26.55	336	120
2-deoxytetronic	2105.29	21.154	161.43	336	120
Unk 2168.4	2169.69	21.798	200.50	364	148
2-ketoocatanoic	2221.69	22.318	20.49	302	158
Malic	2248.10	22.582	72.73	350	134
Unk 2256.1	2255.30	22.654	50.94	260	116
Adipic	2277.30	22.874	34.16	290	146
Salicylic	2293.40	23.035	18.99	282	138
Pyroglutamic	2327.30	23.374	21.44	273	119
Pyroglutamic Methyladipic	2327.30 2354.80	23.374 23.649		273 304	119 160
•			21.44		160
Methyladipic	2354.80	23.649	21.44 21.15	304	160
Methyladipic Unk 2384.0	2354.80 2386.00	23.649 23.961	21.44 21.15 26.66	304 did not obser	160 ve
Methyladipic Unk 2384.0 Erythronic	2354.80 2386.00 2415.30	23.649 23.961 24.254	21.44 21.15 26.66 284.53	304 did not observa	160 ve 136
Methyladipic Unk 2384.0 Erythronic Threonic	2354.80 2386.00 2415.30 2458.89	23.649 23.961 24.254 24.690	21.44 21.15 26.66 284.53 441.67	304 did not observ 424 424	160 ve 136 136
Methyladipic Unk 2384.0 Erythronic Threonic 2-hydroxyglutaric	2354.80 2386.00 2415.30 2458.89 2471.80	23.649 23.961 24.254 24.690 24.820	21.44 21.15 26.66 284.53 441.67 32.47	304 did not observa 424 424 364	160 ve 136 136 148

Unk X 2615	2614.64	26.248	35.18	378	162
2-deoxyribonic	2689.90	26.999	69.21	438	150
Unk 2707.60	2708.23	27.183	41.82	311	167
Vanillic	2904.60	29.154	110.76	312	168
Gentisic	2945.61	29.563	124.44	370	154
m-methoxycinnan	nic			220	148
Ribonic	2956.14	29.668	91.84	526	166
Arabinonic	2990.43	30.010	66.90	526	166
Hippuric				323	179
Citric	3060.61	30.710	551.87	480	192
Isocitric				480	192

#### REFERENCES

- 1. Williams, R.J. Biochemical Institute Studies IV. Individual Metabolic Patterns and Human Disease, Univ. of Texas Publication No.5109, Univ. of Texas, Austin, TX 1951, Ch.1.
- 2. Holmes, J.C. and Morrel, F.A. Applied Spectrosc. 11, 86 (1957).
- 3. Horning, E.C. and Horning, M.G. Clin. Chem. <u>17</u>, 802 (1971).
- 4. Holland, J.F., Leary, J.J. and Sweeley, C.C. *J. Chromatogr.* Suppl. Vol. <u>52</u> 3- 26 (1986).
- 5. Horning, E.C. and Horning, M.G. Clin. Chem. 17, 802 (1971).
- 6. Tuchman, M., Bowers, L.D., Fregien, K.D., Crippin, P.J., and Krivit, W. J. Chromatogr. Sci. 22, 198 (1984).
- 7. Sweeley, C.C.; Holland, J.F.; Towson, D.S. and Chamberlin, B.A. J. Chromatogr. 399, 173 (1987).
- 8. Gates, S.C., Smisko, M.L., Ashendel, C.L., Young, N.D., Holland, J.F., and Sweeley, C.C. Anal. Chem. 50, 433 (1978).
- 9. Hagenfeldt, L. and Hagenfeldt, K. Clin. Chim. Acta 42, 219 (1972).
- 10. Nicholls, T. Hahnel, R., Wilkinson, S. and Wysocki, S. Clin. Chim. Acta 69 (1976).
- 11. Waterbury, L.D. and Pearce, L.A. Clin. Chem. 18, 259 (1972).
- 12. Ward, M.E., Politzer, I.R., Laseter, J.L. and Alam, S.Q. Biomed. Mass Spectrom. 3, 77 (1976).
- 13. Brooks, J.B., Kellogg, D.S., Alley, C.C., Short, H.B., Handsfield, H.H. and Huff, B. *J. Infect. Dis.* 129, 660 (1974).
- 14. Chalmers, R.A. J. Inher. Metab. Dis. Vol. 1 Suppl. 7, (1984).

- 15. Matsumoto, I. Kuhara, T. Mass Spectrom. Rev. 6, 77 (1987).
- 16. Tuchman, M. and Ulstrom, R.A. Adv. Pediatr . 32, 469 (1985).
- 17. Chalmers, R.A. and Lawson, A.M. "Organic Acids in Man," University Press, Inc., Cambridge, @ 1982.
- 18. Harrison, A.G.; Jones, E.G.; Gupta, S.K. and Nagy, G.P. Can. J. Chem. <u>44</u>, 1967 (1966).
- 19. Munson, M.S.B. and Field, F.H. J. Amer. Chem. Soc. 88, 2621 (1966).
- 20. Levsen, K. "Selected Topics in Mass Spectrometry" 45, 897 (1983).
- 21. Beckey, H.D. Int. J. Mass Spectrom. and Ion Processes 2, 883 (1969).
- 22. Beuhler, R. J., Flanigan, E., Greene, L.J., and Friedman, L. J. Amer. Chem. Soc. 96, 3990 (1976).
- 23. Barber, M.; Bordoli, R.S.; Sedgwick, R.D. and Tyler, A.N. J. Chem Soc. Chem. Commun. 325 (1981).
- 24. Roepstorff, P.; Hjrup, P. and Moller, J. Biomed. Mass Spectrom. 12, 181 (1985).
- 25. Boyle, P.D.; Johnson, B.J. and Alexander, B.D. J. Amer. Chem. Soc. 26, 1346 (1987).
- 26. Rollgen, F.W. and Schulten, H.-R. Z. *Naturforsch* <u>30</u>, 1685 (1975).
- 27. Rollgen, F.W. and Schulten, H.-R. Org. Mass Spectrom. 10, 660 (1976).
- 28. Giessmann, U. and Rollgen, F.W. Org. Mass Spectrom. 12, 539 (1977).
- 29. Stoll, R. and Rollgen, F.W. Org. Mass Spectrom. 16, 72 (1981).
- 30. Ackermann, B.L.; Watson, J.T. and Holland, J.F. Anal. Chem. <u>57</u>, 2656 (1985).
- 31. Caprioli, R.M.; Fan, T. and Cotrell, J.S. Anal. Chem. <u>58</u>, 2949 (1986).
- 32. Tsarbopoulos, A.; Liberato, D.J. and Jardine, I. 35th ASMS Conference on Mass Spectrom. and Allied Topics, Denver, CO pp.80-81.

- 33. McNeal, C.J. and Macfarlane, R.D. J. Amer. Chem. Soc. 103, 1609 (1981).
- 34. Blewett, J.P. and Jones, E.J. J. Phys. Rev. <u>50</u>, 464 (1936).
- 35. Melton, C.E. "Principles of Mass Spectrometry and Negative Ions", Marcel Dekker, NY, pp.68 (1970).
- 36. Kelsoo, J.F., Pantano, C.G. and Garofalini, S.H. Surf. Sci. 134, L543 (1983).
- 37. Bombick, D.D. Doctoral Dissertation, Michigan State University (1986).
- 38. Bombick, D.D., Pinkston, J.D. and Allison, J. Anal. Chem. <u>54</u>, 396 (1984).
- 39. Day, R.J.; Unger, S.E. and Cooks, R.G. Anal. Chem. <u>52</u>, 458 (1987).
- 40. Bombick, D.D. and Allison, J. Anal. Chem. <u>59</u>, 458 (1987).
- 41. Nakata, H., Hoshino, Y., Takeda, N. and Tatematsu, A. Organic Mass Spectrom. 20 (7), 467 (1985).
- 42. Schmelzeisen-Redeker, G.; Geismann, U. and Rollgen, F.W. Org. Mass Spectrom. 20, 303 (1985).
- 43. Goodman, S.I. and Markey, S.P., "Diagnosis of the Organic Acidemias by Gas Chromatography-Mass Spectrometry" Liss, Inc. NY (1981).
- Van Biervliet, J.P.G.M.; Bruinvis, L., VanderHeiden, C; Ketting, D.; Wadman, S.K., Willems, J.L. and Monnens, L.A.H., Dev. Med. Child Neurol. 19, 392 (1977).
- 45. Page, T. and Nyhan, W.L., Int. J. Biochem. 19, 713 (1981).
- 46. Rhead, W. and Tanaka, K., Proc. Nat'l. Acad. Sci. 77, 480 (1980).
- 47. Dancis, J. and Levitz, M. "The Metabolic Basis of Inherited Disease" McGraw-Hill, Co., NY pp. 397-410 (1978).
- 48. Gates, S.C. and Sweeley, C.C. Clin. Chem. <u>10</u>, 1663 (1978).
- 49. Bencsath, F.A. and Field, F.H., 35th ASMS Conference on Mass Spectrom. and Allied Topics, Denver, CO pp. 29-30 (1987).
- 50. Isacchar, D. and Yinon, J. Biomed. Mass Spectrom. 6, 47 (1979).

- 51. Iles, R.A.; Hind, A.J. and Chalmers, R.A., Clin. Chem. 22, 1795 (1985).
- 52. Shackleton, G.J.L. and Mitchell, F.L., Steroids 10, 359 (1967).
- 53. Hunt, D.F.; Giordani, A.B.; Rhodes, G. and herold, D.A. Clin. Chem. 28, 2387 (1982).
- 54. Gates, S.C., Dendramis, N. and Sweeley, C.C., Clin. Chem. 24, 1674 (1978).
- 55. Chamberlin, B.A. and Sweeley, C.C. Clin. Chem. 33/4, 572 (1987).
- 56. Lin, S-T and Klabunde, K.J. *Langmuir* 1, 600 (1985).
- 57. Munster, H., Budzikiewicz, H. and Schroder, E. Org. Mass Spectrom. 22, 384 (1987).
- 58. Light, K.L. unpublished results.
- 59. Jocelyn-Pare, J.R.; Lafontaine, P.; Belanger, J.; St, W-W.; Jordan, N. and Loo, J.C. J. Pharm. Biomed. Anal. 5, 131 (1987).
- 60. Komori, T.; Kawasaki, T. and Schulten, H-R. Mass Spectrom. Rev. 4, 255 (1985).
- 61. Schulten, H-R.; Komori, T. and Kawasaki, T. Tetrahedron 33, 2595 (1977).
- 62. Games, D.E.; McDowall, M.A.; Levson, K.; Schafer, K.H.; Dobberstein, P. and Gower, J.L. *Biomed. Mass Spectrom.* 11, 87 (1984).
- 63. Shomo, R.E.; Chandrasekaran, A.; Marshall, A.G.; Reuning, R.H. and Robertson, L.W. Biomed. Environ. Mass Spectrom. 14, 0 (1987).
- 64. Costello, C. 35th ASMS Conference on Mass Spectrom. and Allied Topics, Denver, CO (1987), pp.xxx.
- 65. Light. K.L.; Kassel, D.B. and Allison, J. in preparation.
- 66. Martin, S.A. and Biemann, K. Mass Spectrom Reviews 6, 1(1987).
- 67. Rose, K.; Baroch, A. and Offord, R.E. J. Chromatogr. <u>268</u>, 197 (1983).
- 68. McLafferty, F.W. "MassSpectrometry-MassSpectrometry", Elseveir

- Publishing Co., NY © 1983.
- 69. Roepstorff, P. and Fohlman, J. Biomed. Mass Spectrom. 11, 601 (1984).
- 70. Stults, J.T.; Martin, S.; Biemann, K. and Watson, J.T. Biomed. Environ. Mass Spectrom. (in press).
- 71. Munster, H.; Theobald, F.; Budzikiewicz, H. and Schroder, E. Int'l. J. Mass Spectrom. and Ion Processes 79, 73 (1987).
- 72. Musselman, B.D.; Cheng, C.J. and Watson, J.T. Anal. Chem. <u>6</u>, 1277 (1985).
- 73. Dempster, A.J. Phil Mag. 31, 438 (1916); Smyth, H.D. Phys. Rev. 25, 452 (1925).
- 74. Munson, M.S.B. and Field, F.H. J. Amer. Chem. Soc. 88, 2621 (1966).
- 75. Aue, D.H. and Bowers, M.T. "Gas Phase Ion Chemistry", M.T. Bowers, Ed., Academic Press, New York, 1979.
- 76. Bohme, D.K., Mackay, G.I., and Schiff, H.I. J. Chem. Phys. 73, 4976 (1980).
- 77. McMahon, T.B. and Kebarle, P. Can. J. Chem. 63 3160 (1985).
- 78. Harrison, A.G. in "Chemical Ionization Mass Spectrometry," CRC Press, Inc. © 1982.
- 79. Klotz, C.E. "Fundamental Processes in Radiation Chemistry," P. Ausloos, Ed., John Wiley and Sons, Inc. New York, pp. 40 (1968).
- 80. McLafferty, F.W. in "Interpretation of Mass Spectrometry," 3rd Edition, © 1983, pp. xxx.
- 81. Clow, R.P. and Futrell, J.H. J. Amer. Chem. Soc . <u>94</u>, 3748 (1972).
- 82. Munson, M.S.B. and Field, F.H. J. Amer. Chem. Soc. 89, 1047 (1967).
- 83. Ichikawa, H. and Harrison, A.G. Org. Mass Spectrom. 13, 389 (1978).
- 84. Clemens, D. and Munson, B. Org. Mass Spectrom . 20, 368 (1985).
- 85. Cairns, T. and Siegmund, E. Org. Mass Spectrom. 20, 58 (1985).
- 86. Budzikiewicz, H.; Laufenberg, G.; and Brauner, A. Org. Mass Spectrom. 20, 65

- (1985).
- 87. Hunt, D.F. "Finnigan Spectra" 6, (1) (1976).
- 88. Houle, F.A. and Beauchamp. J.L. J. Am. Chem. Soc. 101 4067 (1979).
- 89. Mcloughlin, R.G. and Traeger, J.C. J. Am. Chem. Soc. 101 5791 (1979).
- 90. Bohme, D.K. and Fehsenfield, F.C. Can. J. Chem. <u>47</u>, 2715 (1969).
- 91. Keough, T. and DeStefano, A.J. Org. Mass Spectrom. 16, 527 (1981).
- 92. Westmore, J.B. and Alauddin, M.M. Mass Spectrom. Rev. 5, 381 (1986).
- 93. Lin, L-Y and Smith Biomed. Environ. Mass Spectrom. 5, 604 (1978).
- 94. Nakata, I. Org. Mass Spectrom. 20, 467 (1985).
- 95. Kebarle, P. Ann. Rev. Phys. Chem. 28 445, (1978).
- 96. Hatch, F. and Munson, B. Anal. Chem. <u>49</u>, 731 (1977).
- 97. Hatch, F. and Munson, B. J. Phys. Chem. 82, 2362 (1978).
- 98. Carroll, T.X., Smith, S.R. and Thomas, T.D. J. Amer. Chem. Soc. <u>98</u>, 659 (1975).
- 99. Mills, B.E., Martin, R.L., and Shirley, D.A. *J. Amer. Chem. Soc.* 98, 2380 (1976).
- 100. Benoit, F.M. and Harrison, A.G. J. Amer. Chem. Soc. 99, 3980 (1977).
- 101. Hvistendahl, G. and Uggerud, E. Org. Mass Spectrom. 20, 541 (1985).
- 102. Karabatsos, G.J.; Sonnichsen, G.C>; Papaioannou, C.G.; Scheppele, S.E. and Shone, R.L. J. Amer. Chem. Soc. 89, 463 (1967).
- 103. Millard, B.J. "Quantitative Mass Spectrometry," Heyden and Son, London (1978).
- 104. Munson, B. Anal. Chem. 49 772A (1977).
- 105. Langevin, P.M. Ann. Chim. Phys. 5, 245 (1905).

- 106. Henglein, A. "Molecular Beams and Reaction Kinetics," Schlier, C. ed., Academic Press, New York, 1970.
- 107. Moran, T.F. and Hamill, W.H. J. Chem. Phys. 39, 1413 (1963).
- 108. Su, T. and Bowers, M.T. Int. J. Mass Spectrom. and Ion Processes 12, 347 (1973).
- 109. Field, F.H.; Franklin, J.L.; and Lampe, F.W. J. Amer. Chem. Soc. 79, 2419 (1957).
- 110. Miles, J.M.; Haymone, M.; Nissen, S. and Gerich, J. J. Clin. Invest. 71, 1554 (1983).
- 111. Mayes, P. and Felts, J. Biochem. J. 102, 230 (1967).
- 112. Page, T. and Nyhan, W.L. Int. J. Biochem. 19, 713 (1987).
- 113. Johansson, E.; Ohlsson, A.; Lindgren, J.E.; Agurell, S.; Gillespie, H. and Hollister, L.E. Biomed. Environ. Mass Spectrom. 14, 495 (1987).
- 114. Young, J.W.; Veenhuizen, J.J.; Russell, R.W. Fed. Proceed. 46, 295 (1987).
- 115. Samuelsson, B.; Hamberg, M. and Sweeley, C.C. Anal. Biochem. 38, 301 (1970).
- 116. Mamer, D.A.; Laschic, N.S. and Scriver, C.R. Biomed. Environ. Mass Spectrom. 13, 553 (1986).
- 117. Clutter, W.E., Bier, D.M., Shah, S.D., and Cryer, P.E. J. Clin. Invest. 66, 94 (1980).
- 118. Wolfe, R.R., Wolfe, M.H. and Shulman, G. In "Stable Isotopes in Nutrition", Turnlund, J.R. and Johnson, P.E., Eds. ACS Symposium Series pp.175 (1984).
- 119. Wong, W.W., Cabrera, M.P., and Klein, P.D. Anal. Chem. <u>56</u>, 1852 (1984).
- 120. Mathews, D.E., Ben-Galim, E. and Bier, D.M. Anal. Chem. <u>51</u>, 80 (1979).
- 121. Irving, C.S., Thomas, M.R., Malphus, E.W., Marks, L., Wong, W.W., Boutton, T.W. and Klein, P.D. *J. Clin. Invest*. <u>77</u>, 1321 (1986).

- 122. Weinhouse, S.; Medes, G. and Floyd, N.F. J. Biol. Chem. 166, 691 (1946).
- 123. Murrat, S.; Waddell, K.A. and Davies, D.S. Biomed. Environ. Mass Spectrom. 8 (10), 500 (1981).
- 124. Keller, U., Cherrington, A. and Liljenquist, J. Amer. J. Physiol. E, 238 (1978).
- 125. Balasse, E. Metabolism 28, 41 (1979).
- 126. Miles, J.M., Haymond, M., Nissen, S., and Gerich, J. J. Clin. Invest. 71, 1554 (1983).
- 127. Penman, A.D. and Wright, I.A. Biomed. Environ. Mass Spectrom. 14, 339 (1987).
- 128. Schoeller, D.A. and Klein, P.D. Biomed. Environ. Mass Spectrom. 5, 29 (1979).
- 129. Hachey, D.L., Wong, W.W., Boutton, T.W. and Klein, P.D. *Mass Spectrom*. *Rev.* 6, 289 (1987).
- 130. White, E.V., Welch, M.J. and Sun, T. Biomed. Mass Spectrom. 2, 395 (1982).
- 131. Siekmann, L. J. Clin. Chem. Clin. Biochem. 23, 129 (1985).
- 132. Patterson, D.G., Patterson, M.B., and Culbreth, P.H. Clin. Chem. 30, 619 (1984).
- 133. Takatsu, A. and Nishi, S. Clin. Chem. 33, 1113 (1987).
- 134. Stellaard, F., Sackmann, M., Berr, F. and Paumgartner, G. Biomed. Environ. Mass Spectrom. 14, 609 (1987).
- 135. Hofmann, A.F. and Hoffman, N.E. Gastroenterology 67, 314 (1974).
- 136. Hofmann, A.F. and Cummings, S.A. in "Bile Acids in Gastroenterology", ed. Barbara, L., Dowling, R.H., Hofmann, A.F. and Roda, E. pp.75 MTP Press, Lancaster, England(1983).
- 137. Boulton, A.A. and Davis, B.A. Biomed. Environ. Mass Spectrom. 14, 207 (1987).
- 138. Noren, B., Stromberg, S., Ericsson, O., Olsson L-I. and Moses, P. Biomed. Mass Spectrom. 12, 367 (1985).

- 139. Shigematsu, Y.; Sweeley, C.C; Schall, W.D. and Gossain, V. (submitted).
- 140. Robinson, B.H. and Sherwood, W.G. J. Inher. Metab. Dis. 7, Suppl. 1, 69 (1984).
- 141. Blass, J.D. "Inherited Disorders of Carbohydrate Metabolism," Burman, D.; Holton, J.B.; Pennock, C.A., Eds. MTP Press Ltd. Lancaster, pp. 238-68 (1980).
- 142. Kapetanovic, I.M.; Yonekawa, W.D. and Kupferberg, H.J. J. Chromatogr. 414, 265 (1987).
- 143. Kalhan, S.C.; Ricanati, E.S.; Tserng, K-Y and Savin, S.M. Metabolism 32, 1155 (1983).
- 144. Yudkoff, M.; Nissim, I.M.; Schneider, A. and Segal, S. Metabolism 30, 1096 (1981).
- 145. Ford, G.C.; Cheng, K.N. and Halliday, D. Biomed. Environ. Mass Spectrom. 12 (8), 432 (1985).
- 146. Lapidot, A.; Kalderon, B.; Korman, S.; and Gutman, A. Bookof Abstracts, Int'l. Sympos. Appl. Mass Spectrom, Health Sci., Barcelona, Spain p. 151 (1987).
- 147. Robinson, B.H., MacMillam, H., Petroru-Benedict, R. and Sherwood, W.G. J. Pediatr. 111, 525 (1987).
- 148. Markey, S.P.; Urban, W.G. and Levine, S.P. "Mass Spectra of Compounds of Biological Interest," U.S. Atomic Energy Commission, Vol. 2 Parts 1 and 2, © 1982.
- 149. Oberholzer, V.G.; Wood, C.B.S.; Palmer, T. and Harrison, B.M. Clin. Chim. Acta 62, 299 (1975).
- 150. Schoots, A.C. and Leclercq Biomed. Mass Spectrom. 6, 210 (1979).
- 151. DeJongh, D.C.; Radford, T.; Hribar, J.D.; Hanessiam, S.; Bieber, M.; Dawson, G. and Sweeley, C.C J. Amer. Chem Soc. 91, 1728 (1969).
- 152. Antoshechkin, A.G.; Tatur, V.Yu; Perevezentseva, O.M. and Maximova, L.A. Anal. Biochem. (in press), 1987.
- 153. Dzidic, I., Caroll, D.I., Stillwell, R.N. and Horning, E.C. *Anal. Chem*. <u>47</u>, 49 (1975).

- 154. Hunt, D.F.; Stafford, G.C.; Crow, F.W. and Russell, J.W. Anal. Chem. 48, 2098 (1976).
- 155. Smith, A.L.C. and Field, F.H. J. Amer. Chem. Soc . 99, 6471 (1977).
- 156. Berger, E.A. and Dougherty, R.C. Biomed. Mass Spectrom. 8, 238 (1981).
- 157. Dougherty, R.C.; Dalton, J. and Biros, F.J. Org. Mass Spectrom. 6, 1171 (1972).
- 158. Dougherty, R.C. Anal. Chem. <u>53</u>, 625A (1981).
- 159. Stemmler, E.A. and Hites, R.A. Anal. Chem. <u>57</u>, 684 (1985).
- 160. Hunt, D.F.; Stafford, G.C. and Crow, F.W. Anal. Chem. 49, (1977).
- 161. Hunt, D.F. and Crow, F.W. Anal. Chem. <u>50</u>, 1781 (1978).
- 162. Kingston, E.E. and Duffield, A.M. Biomed. Mass Spectrom. 9 (11), 459 (1982).